Secondary Metabolites from *Calophyllum nodosum* and their Antibacterial Activity

by

Yiizamy bin Suffian
(24020087)

Presented to the
FACULTY OF RESOURCE SCIENCE AND TECHNOLOGY
in Fulfillment of the Requirement for the Degree of

MASTER OF SCIENCE
(Chemistry)

2026

UNIVERSITI MALAYSIA SARAWAK

DECLARATION

I hereby declare that the work presented in this thesis was conducted in full compliance with the regulations of Universiti Malaysia Sarawak (UNIMAS). Except where proper acknowledgment is given, this work is solely the effort of the author. This thesis has not been accepted for the award of any other degree and is not being **concurrently** submitted for any other academic qualification.

Signature 

Student Name: Yiizamy bin Suffian

Matric No: 24020087

Date: 8 June 2026

Faculty of Resource Science and Technology
Universiti Malaysia Sarawak (UNIMAS)

ACKNOWLEDGMENT

Allah. Alhamdulillah. Looking back, I realised that You have shaped this path in a way that was best for me, even when I could not understand it at the time. Dr. Hisam, thank you for pushing me beyond limits I never knew I could cross, yet always knowing when I needed space to breathe. You listened to every rant and chaos that came along with my research like 3-in-1. You protected us and opened countless opportunities that shaped my growth. Thank you for being the "firefighter" who ran into every blaze I was in. Dr. Ainaa, you were the warmth that made even the hardest days bearable. Our connection never faded despite responsibilities and distance. The effort we put into the direct PhD meant a great deal, and even when the outcome wasn't what we had hoped for, your positivity never wavered. You are a light in every room you enter, and I hope you continue being that youthful, inspiring version of yourself—while being "teased" in badminton, of course. AP Dr. Vivien Jong, thank you for shaping my growth while I was at UiTM. Despite your demanding schedule, you guided me with kindness and ensured I stayed on track. The chocolates you brought back from your travels always brightened my day (and yes, I still blame them for making me fat). You made UiTM feel safe and fair—although Mas and Sheril kept bullying me anyway. My family, Yii Wei Yang, Chan Kim Nue, Suffian, and Nur Yiizzaty@Yii Lee Ping. Thank you for supporting me patiently, even when you didn't understand the weight of my journey. Thank you for giving me space, listening to my frustrations, and believing in me. My siblings, Yiizzan, Yiisham, and Yiizhazy. Thank you for the stories, the late-night rants, and the comfort of knowing I always had someone on my side. You kept me grounded and sane when everything else felt overwhelming. Irdina Zulaika, thank you for the companionship throughout the years. You have grown, healed, and done better than before. I pray that you continue shining and find the companionship you deserve. Mas Atikah, my backbone in UiTM. Thank you for sharing your knowledge without hesitation and sacrificing your time and energy. You taught me patience, kindness, and forgiveness. Thank you for walking with me through every hardship and becoming a witness to the work I poured into this thesis. Kai Wei, Bob, Totoro family (Jessica, Joanna, Karen, Willy, Jordan I, and Sean), thank you for bringing joy and balance during a time drowning in deadlines. My gPBL friends, Liza, Aisyah, Athirah, Dzikri. Ivan, Jordan T, Anisa, Amilin, Davyle, Alia, Azmeer, Filicia, Farah, Ivy, LiangLin, Dayini, Sheril, Maya, Fazlin and others. Thank you for the shared frustration and laughter, even if our paths may never cross again. To those unlisted, it is not because you were unimportant; too many have left a mark or scar on this journey. Science officers, thank you for guiding and keeping the lab safe. UNIMAS Basketball Club, Spartans PJ, and badminton circle, thank you for keeping me mentally and physically alive when this master journey tried to turn me into a zombie. And to those who tested my patience—thank you. You motivated me in a different way; you strengthened me. Your chaos sharpened my discipline and reminded me of who I must never become. You taught me lessons about life. My sincere appreciation goes to MyBrainSc for funding my master's studies and lifting a tremendous weight off my shoulders. It would be an honour to continue my PhD under this scholarship, and I truly hope for that opportunity. Lastly, to everyone who crossed paths with me, thank you. If I have ever hurt you knowingly or unknowingly, I sincerely apologise. To those who hurt me, I may never forget, but I have forgiven. These experiences taught me about life and shaped the person I am today. Yes, it was heavy and chaotic, but it was also beautiful, exhausting, and unforgettable. Thank you to every soul who made it meaningful. Your name will forever remain a part of this master's work and of my story. And with that, another chapter comes to an end. "Mamba Out" — Kobe Bryant.

Secondary metabolites from *Calophyllum nodosum* and their antibacterial activity

ABSTRACT

Utilising natural resources to discover compounds with antibacterial potential is crucial in addressing the growing threat of antibiotic resistance. The *Calophyllum* genus has gained attention for its diverse secondary metabolites, particularly xanthones with notable pharmacological activities. This study aimed to investigate the phytochemical profile and antibacterial potential of *Calophyllum nodosum* stem bark, given the well-documented therapeutic potential of the genus in antibacterial activity. The dried, ground stem bark was extracted using a maceration technique with different solvents of *n*-hexane, chloroform, and methanol sequentially, followed by filtration to obtain respective extracts. The compounds were isolated and purified using various chromatographic techniques and characterised through 1D and 2D nuclear magnetic resonance (NMR), Fourier-transform infrared spectroscopy (FT-IR), mass spectrometry (MS), ultraviolet-visible spectroscopy (UV-Vis), and melting point analysis. Seven compounds were successfully isolated, including nodosuxanthone (**89**), a newly undescribed xanthone, trapezifolixanthone (**20**), caloxanthone C (**5**), 1-hydroxy-7-methoxyxanthone (**27**), canumolactone (**90**), friedelin (**71**), and stigmasterol (**70**). The antibacterial activity of the extracts and isolated compounds was evaluated against Gram-positive bacteria and Gram-negative bacteria (*Acinetobacter baumannii, Staphylococcus aureus*, *Klebsiella pneumoniae, Pseudomonas aeruginosa,* and *Escherichia coli*) using the well-diffusion method, followed by minimum inhibitory concentration (MIC) and minimum bactericidal concentration (MBC). Caloxanthone C (**5**) and canumolactone (**90**) exhibited the most potent antibacterial activities as both compounds demonstrated comparable activity with ampicillin against *A. baumannii* and *E. coli* (MIC = 0.025 mg/mL; MBC = 0.05 – 0.1 mg/mL). Notably, both compounds demonstrated strong activity against *P. aeruginosa*, surpassing the inhibitory effect of ampicillin under the tested conditions. As for the extracts, the *n*-hexane extract displayed moderate activity (MIC = 0.25 mg/mL) against *A. baumannii*, *E. coli*, and *K. pneumoniae* with MBC values of 1.0 mg/mL, 1.0 mg/mL, and 0.5 mg/mL against the three bacterial strains, respectively. Remarkably, this study reports the first natural occurrence of nodosuxanthone (**89**), contributing to the

growing knowledge of *Calophyllum*-derived bioactive compounds and supporting the potential of *Calophyllum* species as a valuable source for novel antibacterial candidates.

Keywords: *Calophyllum nodosum*, secondary metabolites, isolation, nodosuxanthone, antibacterial.

Metabolit sekunder daripada Calophyllum nodosum dan antibakteria

ABSTRAK

Penggunaan sumber semula jadi dalam penemuan sebatian yang berpotensi sebagai agen antibakteria adalah penting dalam menangani ancaman rintangan antibiotik yang semakin meningkat. Genus Calophyllum *telah mendapat perhatian kerana kepelbagaian metabolit sekundernya, terutamanya xanton yang menunjukkan aktiviti farmakologi yang ketara. Kajian ini bertujuan untuk menyiasat profil fitokimia dan potensi antibakteria kulit batang* Calophyllum nodosum*, selaras dengan potensi terapeutik genus ini yang telah didokumentasikan dalam aktiviti antibakteria. Kulit batang kering yang telah dikisar diekstrak secara berperingkat menggunakan teknik maserasi dengan pelarut n-heksana, kloroform dan metanol, diikuti dengan penapisan untuk mendapatkan ekstrak masing-masing. Sebatian-sebatian telah diasingkan dan ditulenkan menggunakan pelbagai teknik kromatografi serta dicirikan melalui spektroskopi resonans magnet nuclear (NMR) satu dimensi dan dua dimensi, spektroskopi inframerah transformasi Fourier (FT-IR), spektrometri jisim (MS), spektroskopi ultraungu-nampak (UV-Vis) dan analisis takat lebur. Sebanyak tujuh sebatian berjaya diasingkan, termasuk nodosuxanton (**89**), iaitu xanton baharu yang belum pernah dilaporkan sebelum ini, bersama trapezifolixanton (**20**), kaloxanton C (**5**), 1-hidroksi-7-metoksixanton (**27**), canumolakton (**90**), friedelin (**71**) dan stigmasterol (**70**). Aktiviti antibakteria ekstrak dan sebatian terasing telah dinilai terhadap bakteria Gram-positif dan Gram-negatif (*Acinetobacter baumannii*, Staphylococcus aureus*, Klebsiella pneumoniae*, Pseudomonas aeruginosa dan* Escherichia coli*) menggunakan kaedah peresapan telaga agar, diikuti dengan penentuan kepekatan perencatan minimum (MIC) dan kepekatan pembunuhan minimum (MBC). Kaloxanton C (**5**) dan canumolakton (**90**) menunjukkan aktiviti antibakteria yang paling poten apabila kedua-dua sebatian tersebut memperlihatkan aktiviti yang setanding dengan ampisilin terhadap* A. baumannii *dan* E. coli *(MIC = 0.025 mg/mL; MBC = 0.05 – 0.1 mg/mL). Selain itu, kedua-dua sebatian ini turut menunjukkan aktiviti yang kuat terhadap* P. aeruginosa*, melebihi kesan perencatan ampisilin di bawah keadaan ujian yang dijalankan. Bagi ekstrak pula, ekstrak n-heksana menunjukkan aktiviti sederhana (MIC = 0.25 mg/mL) terhadap* A. baumannii*,* E. coli*, dan* K. pneumoniae *dengan nilai MBC masing-masing sebanyak 1.0 mg/mL, 1.0 mg/mL, dan 0.5*

*mg/mL terhadap ketiga-tiga strain bakteria tersebut. Penemuan nodosuxanthone (**89**) sebagai sebatian semula jadi baharu menyumbang kepada pengembangan kepelbagaian kimia genus* Calophyllum *serta menyokong potensi spesies ini sebagai sumber sebatian antibakteria baharu.*

Kata Kunci: Calophyllum nodosum*, metabolit sekunder, pengasingan, nodosuxanthon, antibakteria*.

TABLE OF CONTENTS

LIST OF TABLES

LIST OF FIGURES

LIST OF APPENDICES

LIST OF ABBREVIATIONS

^{13}C	Carbon-13
1D	one dimensional
1H	Proton
^{1}J	One-Bond Coupling Constant
2D	two dimensional
AMR	Antimicrobial Resistance
ANOVA	One-way analysis of variance
AI	Artificial Intelligence
ATR	Attenuated Total Reflectance
CFU	Colony Forming Units
COSY	Correlation Spectroscopy
DEPT	Distortionless Enhancement by Polarization Transfer
DMSO	Dimethyl Sulfoxide
FT-IR	Fourier Transform Infrared Spectroscopy
GC-MS	Gas Chromatography Mass Spectrometry
HIV	Human immunodeficiency viruses
HMBC	Heteronuclear Multiple Bond Correlation
HSQC	Heteronuclear Single Quantum Coherence
IBM SPSS	IBM Statistical Package for the Social Sciences
IUPAC	International Union of Pure and Applied Chemistry
LC-MS	Liquid Chromatography Mass Spectrometry
MBC	Minimum Bactericidal Concentration
MDR	Multidrug-Resistant
MHA	Mueller Hinton Agar
MHB	Mueller Hinton Broth
MIC	Minimum Inhibitory Concentration
MD	Molecular Dynamics
MS	Mass Spectrometry
NMR	Nuclear Magnetic Resonance
QSAR	Quantitative Structure-activity Relationship
TLC	Thin Layer Chromatography
TMS	Tetramethylsilane
UiTM	University Teknologi MARA
UNIMAS	University of Malaysia Sarawak
UV-Vis	Ultraviolet-Visible
VRE	Vancomycin-Resistant Enterococci

CHAPTER 1:

INTRODUCTION

1.1 Background of Study

Plants have long been the foundation of life on Earth, providing essential resources such as shelter, habitat, food, oxygen, and raw materials for various industries. Apart from their ecological and economic value, plants also play a pivotal role in human well-being. This can be seen especially since mankind relies on natural organisms like plants to treat diseases, injuries, and ailments, leading to the development of current pharmaceutical discoveries (Sezer et al., 2024). Plants are commonly used in traditional medicinal systems worldwide. As a country that is rich in plant biodiversity, Malaysia has more than 2000 plant species that are known to have medicinal properties (Bakar et al., 2018). For instance, *Labisia pumila*, also known as *Kacip Fatimah*, is commonly used in the puerperium (Wang et al., 2025). The volatile oils of *Cinnamomum verum* exhibit potent antimicrobial and anti-inflammatory properties, which make it useful for treating infections, dyspepsia, and bronchitis (Al-Mijalli et al., 2023). Another example, *Andrographis paniculata,* has also been traditionally used for treating fever, infections, and sore throat (Rahmatullah et al., 2024).

The presence of such beneficial medicinal plants, along with the advancement of science and technology, has allowed their potential to be explored and widened, which further contributes to the development of the pharmaceutical industry. Some of the examples of natural products that are widely used in the pharmaceutical industry include paclitaxel from the *Taxus brevifolia* plant, which is useful as an anticancer drug (Zein et al., 2019). Other than that, there is also artemisinin from *Artemisia annua* for malaria treatment, and aspirin derived from willow bark, which revolutionised pain management in pharmaceutical science. (Newman & Cragg, 2020). Given that, one genus from the Calophyllaceae family, *Calophyllum,* is well-known for its phytochemical diversity. Some examples of classes for the bioactive compounds that were isolated previously from the *Calophyllum* genus include

xanthones, coumarins, chromanone acids, and triterpenoids. These isolated compounds were evaluated for their biological properties of antibacterial, anticancer, and anti-inflammatory activity (Lee et al., 2018). Among them, a coumarin derivative, calanolide A, was isolated for the first time as an undescribed compound from *Calophyllum lanigerum* in the early 90s, which has been reported as a novel anti-HIV inhibitor (Kashman et al., 1992), further highlighting the pharmaceutical promise of the genus.

The rising challenge of antimicrobial resistance (AMR) makes such discoveries especially relevant, as AMR has rendered common infections harder to treat, largely due to the overuse and misuse of antibiotics, which have accelerated the emergence of multidrug-resistant (MDR) pathogens like *Escherichia coli*, *Staphylococcus aureus*, *Pseudomonas aeruginosa*, and *Klebsiella pneumoniae* (Kilari et al., 2024). While synthetic drugs remain an option, the associated side effects following their consumption are undeniable (Nisar et al., 2018). For example, liver toxicity from paracetamol (Tanne, 2006), renal failure in children linked to ibuprofen (Moghal et al., 2004), which emphasises the need for safer alternatives. In this regard, the secondary metabolites from plants played a pivotal role in the discovery of new antibacterial agents. This is especially true for the *Calophyllum* genus, as previous research has highlighted its potential as a source for new antibacterial agents due to its rich content in xanthones (Heilman et al., 2023) and coumarins (Mah et al., 2019), making them an interesting candidate for further investigation.

Despite the extensive phytochemical investigations on several *Calophyllum* species such as *C. inophyllum* and *C. lanigerum*, limited information is available regarding the chemical composition and antibacterial potential, an endemic species in Sarawak. Thus, the study aims to investigate the phytochemical constituents of *Calophyllum nodosum* and evaluate their antibacterial activity.

1.2 Problem Statements

Numerous studies have reported prenylated xanthones and coumarins from various *Calophyllum* species with demonstrated antibacterial activity. However, these investigations are largely focused on a limited number of extensively studied species, leaving other members of the genus comparatively underexplored. *Calophyllum nodosum*, although endemic to Sarawak, has not undergone comprehensive phytochemical characterisation nor systematic antibacterial evaluation against clinically relevant bacterial pathogens.

Although specific ethnomedicinal documentation for *C. nodosum* remains limited, related *Calophyllum* species have traditionally been used in Southeast Asia for treating skin infections, wounds, and inflammatory conditions. Such traditional applications suggest potential antimicrobial relevance and provide indirect ethnopharmacological justification for further scientific research of this endemic species. Furthermore, previous phytochemical studies on other *Calophyllum* genus members have consistently revealed the isolation of bioactive secondary metabolites, supporting the rationale of chemotaxonomic potential of the genus as a reservoir of antibacterial compounds. Given the urgent global need for a novel antibacterial agent and the established biosynthetic capacity of the *Calophyllum* genus, the absence of phytochemical and antibacterial data on *C. nodosum* represents a significant knowledge gap that warrants systematic investigation.

1.3 Objectives of Study

1. To extract and isolate secondary metabolites from *C. nodosum* stem bark using sequential maceration followed by column chromatography (CC), gel filtration chromatography, and radial chromatography (RC), with purification monitoring by thin-layer chromatography (TLC).

2. To characterise the isolated compounds with spectroscopic techniques of NMR, MS, FTIR, UV-Vis, and melting point.

3. To evaluate the antibacterial activity of the crude extracts and the compounds isolated against selected Gram-positive and Gram-negative bacterial strains by using the agar well diffusion method, followed by MIC and MBC determination.

1.4 Scope of Study

This study focused on the extraction, isolation, and characterization of secondary metabolites from the stem bark of *Calophyllum nodosum*, an endemic species found in Sarawak. Sequential maceration extraction was carried out by using solvents of *n*-hexane, chloroform, and methanol to obtain crude extracts of increasing polarity. The isolation and purification of compounds were performed using chromatographic techniques, including silica gel column chromatography, gel filtration chromatography (LH-20), and radial chromatography, with monitoring by TLC. Structural elucidation of the isolated compounds

was conducted using spectroscopic analysis, namely 1D and 2D NMR, MS, FT-IR, UV-Vis, and melting point determination.

The antibacterial activities of crude extracts and the isolated compounds were evaluated in vitro against selected Gram-positive and Gram-negative bacterial strains using the agar well diffusion method, followed by MIC and MBC assays. This study was limited to laboratory-scale extraction and in vitro antibacterial assessment. Mechanistic studies, cytotoxicity evaluation, in vivo experiments, and other pharmacological investigations were beyond the scope of this research and were recommended for future research.

1.5 Significance of Study

This study is significant as it provides the first comprehensive phytochemical investigation of *Calophyllum nodosum*, an underexplored endemic species in Sarawak. Through systematic extraction and chromatographic isolation, the study expands the chemical knowledge of the species by identifying and characterising the isolated secondary metabolites, including a newly reported xanthone. This contributes to the chemotaxonomic understanding of the *Calophyllum* genus and highlights the biosynthetic potential of this species.

Furthermore, the evaluation of antibacterial activity of both crude extracts and isolated compounds against Gram-positive and Gram-negative bacterial strains provides scientific evidence regarding its antibacterial potential. The identification of compounds exhibiting activity comparable to the standard antibiotics strengthens the prospect of *C. nodosum* as a potential source of lead molecules for antibacterial drug development.

Overall, this research bridges the existing knowledge gap on *C. nodosum*, supports future natural product-based drug discovery efforts, and reinforces the pharmaceutical relevance of Malaysia's plant biodiversity.

1.6 Organisation of Study

This thesis is divided into five chapters.

Chapter 1 provides the introduction, including the research background, problem statement, objectives, scope, and significance of the study.

Chapter 2 reviews the relevant literature on the genus *Calophyllum*, its phytochemical contents, and its antibacterial activity of extracts and secondary metabolites.

Chapter 3 describes the materials and methods used for extraction, isolation, characterization, and antibacterial testing.

Chapter 4 presents and discusses the results from phytochemical analysis and antibacterial evaluation.

Chapter 5 concludes the study with a summary of findings and recommendations for future research.

CHAPTER 2:

LITERATURE REVIEW

2.1 Introduction

There are two types of metabolites from natural products, namely primary and secondary metabolites, which are useful in living organisms. Primary metabolites are essential organic compounds directly involved in living organisms' growth, development, and reproduction, which include amino acids, lipids, and nucleic acids (Alamgir, 2018). On the other hand, the secondary metabolites are not essential for the basic life processes of living organisms, but they are very crucial in the ecological function, especially in plant defence mechanisms against pathogens and environmental stresses (Anjali et al., 2023; Elateeq et al., 2023). Due to that, the secondary metabolites are often species-specific, as each species faces a different environment (Li et al., 2020). These include a diverse array of compounds like alkaloids, phenolics, and terpenoids, whereby they differ in structure and have a variety of biological properties (Abegaz & Kinfe, 2019). These properties make them useful for the advancement in modern medicine, as those biologically active compounds can offer potential in drug discovery.

2.2 *Calophyllum* genus

The Malpighiales order consists of many families, which include Hypericaceae, Clusiaceae, Bonnetiaceae, Podostemaceae, and Calophyllaceae (Trad et al., 2021). Among them, the Calophyllaceae family is noticeable as it consists of 460 species distributed across 14 different genera (Cabral et al., 2021). Members of this family are predominantly cultivated across tropical regions, particularly in countries like Asia, Africa, and South America (Zailan et al., 2022).

Previously, the *Calophyllum* genus was classified under the Clusiaceae family, which was formerly known as the Guttiferae family. Until recently, in 2016, the genus was reassigned to the reinstated family of Calophyllaceae (Zailan et al., 2022) because of

molecular phylogenetic and morphological evidence proving that the present *Calophyllum* is evolutionarily different from Clusiaceae (Chase et al., 2016). This genus consists of around 190 species distributed all around the world, particularly within the tropical and warm regions (Raj et al., 2022). It is an evergreen broad-leaved tree that is endemic to the coastal regions of Southeast Asia, such as Singapore, India, Sri Lanka, including Malaysia (Gupta & Gupta, 2020).

Morphologically, the plants from the *Calophyllum* genus are a low-branching and slow-growing tree, which can grow from shrubs to large trees, approximately 30 meters in height (Hogarth, 2004). The *Calophyllum* genus can easily be identified through its physical characteristics, such as its oppositely arranged leaves with different parallel veins interspersed with latex canals (Chinthu et al., 2023). The flowers are normally actinomorphic (radially symmetrical), bisexual, or unisexual, and commonly found in white or cream colours. The inflorescences may occur as racemes, cymes or solitary flowers. The stamens are abundant, with the anthers often containing oil glands at their tips, and the ovary is superior, typically consisting of 2–5 carpels (Li et al., 2007). The fruits are generally drupes or capsules, which often contain lipophilic compounds such as essential oils and resins, sometimes with promising medicinal and industrial applications (Cabral et al., 2021; Pessoa et al., 2021). Not only that, but its fissured bark, which features different hues from greyish-brown to yellowish brown, its axillary or terminal inflorescences and the number of stamens can also become the taxonomic traits that give important clues to make them easily identifiable (Rojas-Sandoval, 2023).

2.3 *Calophyllum nodosum* Species

Calophyllum nodosum Vesque is an evergreen tree or shrub indigenous to regions of Peninsular Malaysia, across Borneo, including Sabah, Sarawak, Brunei, and Kalimantan. This species thrives in kerangas forests characterised by acidic, often sandy soils, and can be found at elevations reaching up to 1,900 meters (Damit et al., 2024). Figure 2-1 shows the herbarium voucher collected by Mr. Tinjan Anak Kuda and deposited in the Faculty of Applied Sciences, UiTM Samarahan (Voucher No. UiTM 3050).

Figure 2-1:
The Herbarium Voucher Specimen of *C. nodosum*

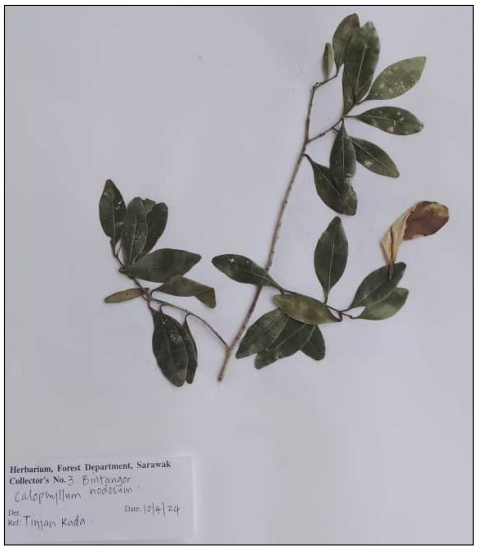

C. nodosum typically attains heights up to 40 meters tall, with trunk diameters reaching up to 47 centimetres (Damit et al., 2024). The tree produces a colourless, white, or yellow latex. Its leaves are arranged oppositely, featuring petioles with leathery blades borne, and distinctive narrow parallel veins that alternate with its resin canals. The inflorescence is a cyme or thyrse emerging from leaf axils or terminal branches, comprising flowers with sepals and petals arranged in whorls, and numerous stamens (Malaysia Biodiversity Information System, n.d.). While the ethnobotanical applications of *C.* nodosum have not been documented in the available literature, the species has nevertheless been recognized for its practical utility, particularly as a source of durable timber (Damit et al., 2024). Table 2-1 shows the taxonomic classification of *Calophyllum nodosum*.

Table 2-1:
The taxonomic framework of the *Calophyllum nodosum (World Flora Online, 2025)*

Kingdom:	Plantae
Division:	Tracheophyta
Class:	Magnoliopsida
Order:	Malpighiales
Family:	Calophyllaceae
Genus:	*Calophyllum*
Species:	*nodosum Vesque*

Source: World Flora Online (2025)

2.4 Phytochemical Studies of *Calophyllum* Species

Phytochemicals, largely represented by secondary metabolites, are compounds that help plants adapt to environmental stress and defend against biotic or abiotic threats, while also playing regulatory roles in growth and reproduction (Molyneux et al., 2007). Over the years, many phytochemical investigations on the *Calophyllum* genus have been carried out, verifying the presence of several biologically active chemicals. Among them are chemical classes of triterpenes, chromanones, coumarins, and xanthones (Gupta & Gupta, 2020). The most frequently obtained class of phytochemicals in this genus is xanthones (Aparamarta et al., 2018). It has been well established that this class of compounds shows notable pharmacological effects, including antimicrobial activity (Elsaman et al., 2020). Coumarins are also another class of chemicals that are equally acknowledged for their antibacterial properties (Ee et al., 2011). Both chromanones and triterpenes also contributed to the therapeutic action of the *Calophyllum* genus (Lemos et al., 2012; Li et al., 2010).

2.4.1 Xanthones

Xanthones are oxygenated heterocyclic aromatic compounds known as 9H-xanthen-9-one. The defining structural characteristics of xanthones are a bicyclic structure from a benzene base, where a gamma-pyrone, oxygen-containing ring connects the two benzene rings (Salman et al., 2019). The described structure resulted in the molecular makeup of xanthone, which is represented by the general formula, $C_{13}H_8O_2$, as shown in Figure 2-2 (Pinto et al., 2021). "Xanthone" was derived from the Greek word "Xanthos" for its yellow hue characteristic. (Klein-Júnior et al., 2020). The first described xanthone, gentisin, was from the *Gentiana lutea* plant back in 1821 (Badiali et al., 2023).

Figure 2-2:
General xanthone skeleton

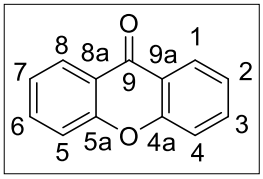

Earlier research has shown that the genus *Calophyllum* is a great source of xanthone chemicals, as several xanthone derivatives were successfully extracted from various sections of the plant species (Lizazman et al., 2022). From the phytochemical investigation of *C. tetrapterum*, xanthone derivatives like calotetrapterin A (**1**), calotetrapterin B (**2**), and

calotetrapterin C (**3**) were obtained (Tanjung et al., 2021). Another xanthone derivative, namely macluraxanthone (**4**), was also isolated from both *C. inophyllum* (Bolagun et al., 2019) and *C. andersonii* (Sichaem et al., 2018). While caloxanthone C (**5**) was obtained from the root of *C. inophyllum* and stem barks of *C. andersonii*, globuxanthone (**6**) and symphoxanthone (**7**) also came from *C. elatum* (Tee et al., 2018). Figure 2-3 shows the structure of xanthone derivatives isolated from the *Calophyllum* genus.

Figure 2-3:
Xanthones isolated from *Calophyllum* genus

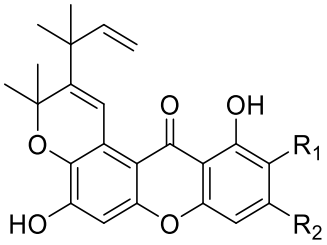

	R_1	R_2
(**1**)	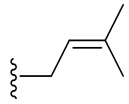	OH
(**2**)	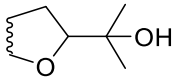	-
(**3**)	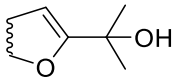	-

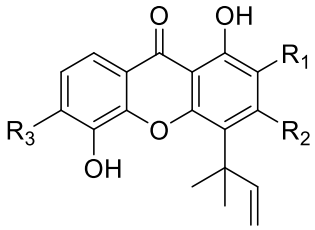

	R_1	R_2	R_3
(**4**)	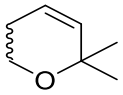	-	OH
(**5**)	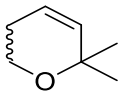	-	H
(**6**)	OH	H	H
(**7**)	OH	H	OH

Prenylated xanthones form a unique subcategory of the wide class of xanthones due to their being isolated from the species of *Calophyllum* (Genovese et al., 2016), making them serve as useful chemotaxonomic markers in the *Calophyllum* genus (Ribeiro et al., 2019). Prominent prenylated xanthones from *Calophyllum* include α-mangostin (**8**), of which two prenyl units are incorporated into its molecular structure, and were derived from the bark of *C. pseudomolle* and stems of *C. tetrapterum* (Tanjung et al., 2021, 2022). Meanwhile, a derivative known as *β*-mangostin (**9**) was found to be derived from the stem bark of *C. teysmannii* (Lee et al., 2018). Additionally, 8-deoxygartanin (**10**) and isogarciniaxanthone E (**11**) have been noted as unique substances extracted from stems of *C. macrocarpum* bark and the roots of *C. elatum*, respectively (Karunakaran et al., 2022). Figure 2-4 shows the prenylated xanthones that were isolated from the *Calophyllum* genus.

Figure 2-4:
Prenylated xanthones isolated from the *Calophyllum* genus

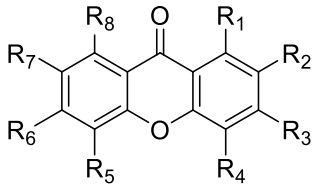

	R_1	R_2	R_3	R_4	R_5	R_6	R_7	R_8
(**8**)	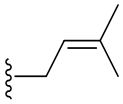	OCH_3	OH	H	H	OH	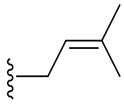	OH
(**9**)	OH	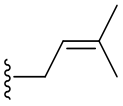	OCH_3	H	H	OH	OCH_3	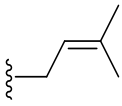
(**10**)	OH	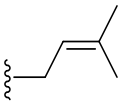	OH	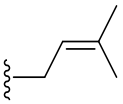	OH	H	H	H
(**11**)	OH	H	OH	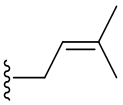	OH	OH	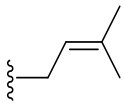	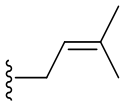

Pyranoxanthone is another xanthone derivative found within the *Calophyllum* genus, where two pyranoxanthones, namely calotetrapterin D (**12**) and calotetrapterin E (**13**), were obtained from the stem bark of *C. pseudomolle* (Tanjung et al., 2021). Besides that, two angular pyranoxanthones, named as ananixanthone (**14**), were derived from the stem bark of *C. hosei*, *C. depressinervosum*, as well as *C. buxifolium* (Zamakshshari et al., 2019), while rheediaxanthone A (**15**) was isolated from the roots of *C. elatum* (Ito et al., 2018). Apart from that, ananixanthone (**14**) was also found in other *Calophyllum* species such as *C. macrocarpum* (Karunakaran et al., 2022) and *C. teysmannii* (Lee et al., 2018). Linear pyranoxanthones such as osajaxanthone (**16**) and 7,9,12-trihydroxy-2,2-dimethyl-2H, 6H-pyrano [3,2-b]xanthen-6-one (**17**) were reported from the isolation study on *C. hosei* and the roots of *C. elatum* (Daud et al., 2021; Ito et al., 2018). Figure 2-5 shows the pyranoxanthones isolated from the *Calophyllum* genus.

Figure 2-5:
The structure of pyranoxanthone isolated from the *Calophyllum* genus

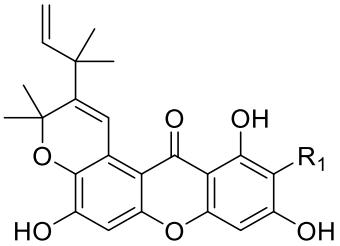

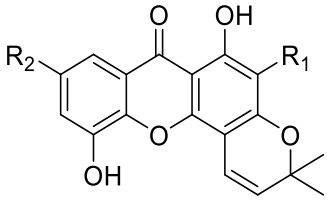

	R_1
(**12**)	H
(**13**)	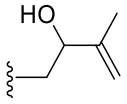

	R_1	R_2
(**14**)	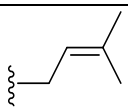	H
(**15**)	H	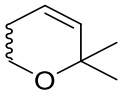

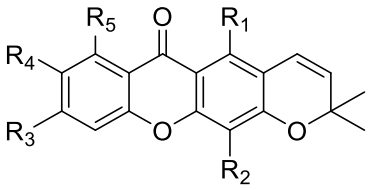

	R_1	R_2	R_3	R_4	R_5
(**16**)	OH	H	H	OH	H
(**17**)	H	OH	OH	H	OH

Furthermore, bigger structures of pyranoxanthones like pyranojacareubin (**18**) and caloxanthone I (**19**) was also identified from *C. tetrapterum*, *C. andersonii*, *C. depressinervosum*, and *C. buxifolium* stem bark (Tanjung et al., 2021; Tee et al., 2018; Zamakshshari et al., 2019). Not only that, but another xanthone derivative, prenylpyranoxanthone, has been reported to be found in the *Calophyllum* species. This includes trapezifolixanthone (**20**), one of the most identified compounds in the *Calophyllum* genus, along with its derivative, trapezifolixanthone A (**21**), 9-hydroxycalabaxanthone (**22**), dombakinaxanthone (**23**), caloxanthone A (**24**), caloxanthone J (**25**), and xanthochymon B (**26**) (Taher et al., 2021). Figure 2-6 shows the bigger pyranoxanthone structure isolated from the *Calophyllum* genus.

Figure 2-6:
Bigger pyranoxanthone derivatives isolated from *Calophyllum* genus

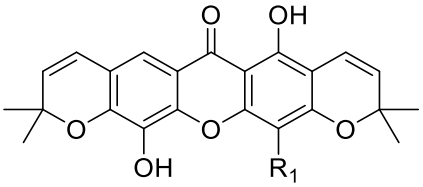

	R_1
(**18**)	H
(**19**)	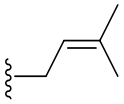

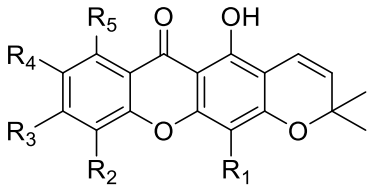

	R_1	R_2	R_3	R_4	R_5
(**20**)	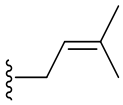	OH	H	H	H
(**21**)	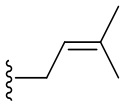	H	OH	H	H
(**22**)	H	H	OH	OCH_3	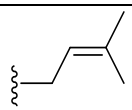
(**23**)	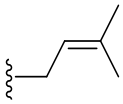	H	H	OH	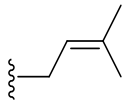
(**24**)	H	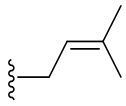	OH	OH	H
(**25**)	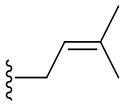	OH	OH	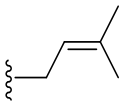	H
(**26**)	H	H	OH	H	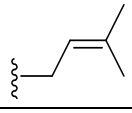

Another xanthone derivative, which is similar to hydroxyxanthone, has also been discovered in the *Calophyllum* genus. This includes compounds like 1-hydroxy-7-methoxy-9H-xanthen-9-one (**27**), 1,3,5,6-tetrahydroxyxanthone (**28**), and euxanthone (**29**), which were isolated from the stem bark of both *Calophyllum ferrugineum* and *Calophyllum*

castaneum (Lim et al., 2019; Noh & Jong, 2020). In addition, the extraction from *C. inophyllum* also yielded 1,5-dihydroxyxanthone (**30**), 1,6-dihydroxy-7-methoxyxanthone (**31**), 4-hydroxyxanthone (**32**), 2-hydroxyxanthone (**33**), 3-hydroxy-4-methoxyxanthone (**34**), and 3-hydroxy-2-methoxyxanthone (**35**) (Sichaem et al., 2018). Figure 2-7 shows the simple xanthone derivatives isolated from the *Calophyllum* genus.

Figure 2-7:
Simple xanthone derivatives isolated from the *Calophyllum* genus

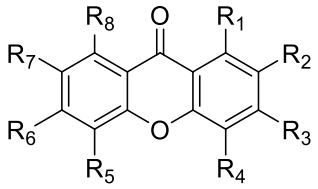

	R_1	R_2	R_3	R_4	R_5	R_6	R_7	R_8
(**27**)	OH	H	H	H	H	H	OCH_3	H
(**28**)	OH	H	OH	H	OH	OH	H	H
(**29**)	OH	H	OH	H	H	H	OH	H
(**30**)	OH	H	H	H	OH	H	H	H
(**31**)	OH	H	H	H	H	OH	OCH_3	H
(**32**)	H	H	H	OH	H	H	H	H
(**33**)	H	OH	H	H	H	H	H	H
(**34**)	H	H	OH	OCH_3	H	H	H	H
(**35**)	H	OCH_3	OH	H	H	H	H	H

A recent research work of Taher et al. (2021) discovered a new derivative of xanthone known as dimeric xanthone, named biscalaxanthone (**36**) from *C. canum* stem bark. Additionally, furanoxanthones like caloxanthone B (**37**) were found in a few *Calophyllum* species, including *C. hosei*, *C. depressinervisum*, and *C. inophyllum* (Daud et al., 2021; Sichaem et al., 2018; Zamakshshari et al., 2019). In line with this finding, another furanoxanthone, dulciol E (**38**), was obtained from the roots of *C. elatum* by Ito et al. (2018). Figure 2-8 shows the structure of dimeric xanthone and furanoxanthones isolated from the *Calophyllum* genus.

Figure 2-8:
The dimeric and fluranoxanthone derivatives isolated from the *Calophyllum* genus

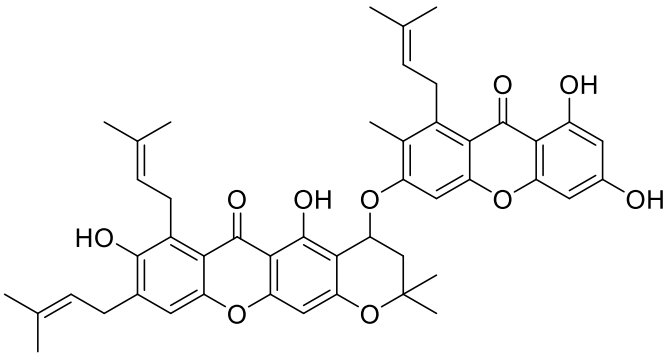

(**36**)

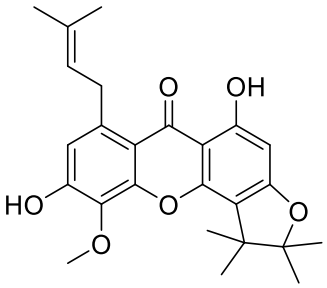

(**37**)

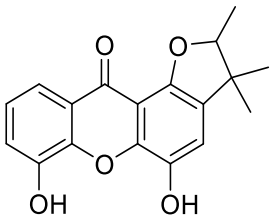

(**38**)

The *Calophyllum* genus is particularly rich in structurally diverse xanthones, especially prenylated and pyranoxanthone derivatives that are likely to enhance lipophilicity and membrane interaction. While many xanthone derivatives' structure have been reported, consistent quantitative antibacterial comparisons remain limited. Systematic evaluation of isolated xanthones alongside their extracts, as well as other classes of compounds and controls in this study can help establish a stronger understanding between phytochemical diversity and validated antibacterial activity.

2.4.2 Coumarins

Coumarins are another naturally occurring secondary metabolite that are frequently isolated from the *Calophyllum* genus. This compound is known as a benzopyran due to its benzene ring structure fused with an α-pyrone ring, giving it the IUPAC name of 2H-1-benzopyran-2-one, as shown in Figure 2-9 (Joshi, 2021). This compound class is frequently found in the *Calophyllum* genus and other plant families like the Rutaceae and Umbelliferae (S. Mishra et al., 2020). The term "coumarin" originates from the term "coumarou", which refers to a Tonka bean (*Dipteryx odorata*) from the Fabaceae family, in which the name was given due to it being first isolated from this species (Pavela et al., 2021).

Figure 2-9:
General coumarin skeleton

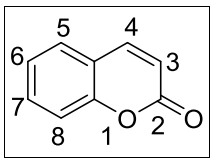

The phytochemical investigation performed on the *Calophyllum* species has led to the discovery of various coumarin derivatives. One of the examples includes apetalolide (**39**) and methyl inophyllum P (**40**), from *C. dioscurii* (Tjahjandarie et al., 2021). Other than that, another coumarin derivative, isocalanone (**41**), was also isolated from *C. ferrugineum* by Noh & Jong (2020). Pyranocoumarin, such as calanolide E1 (**42**), calanolide E2 (**43**), and soulattrolide (**44**) were reported from the isolation of the stem bark of *C. Brasiliense* (Vanegas et al., 2019). The isolation of calophyllolide (**45**) was also documented as one of the major coumarin derivatives that can be obtained from the seed oils of *C. inophyllum* (Herawati & Rakhmawati, 2025). Additionally, the compounds inophyllum D (**46**) and calanone (**47**) were reported from different plant parts of *C. symingtonianum* (Aminudin et al., 2016a). Similarly, a notable furo-pyranocoumarin, inophyllum H (**48**), was also isolated from the same plants. Figure 2-10 shows some of the coumarin derivatives isolated from the *Calophyllum* genus.

Figure 2-10:
Coumarin derivatives isolated from the *Calophyllum* genus

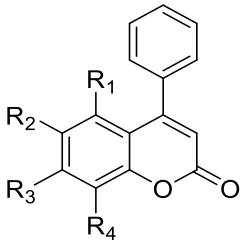

	R_1	R_2	R_3	R_4
(39)	OCH_3	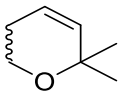	-	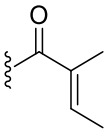
(41)	OH	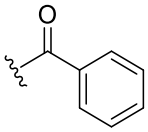	-	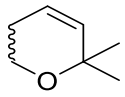
(45)	-	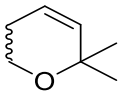	OCH_3	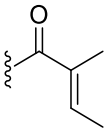
(47)	-	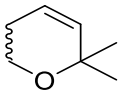	OH	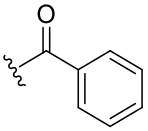

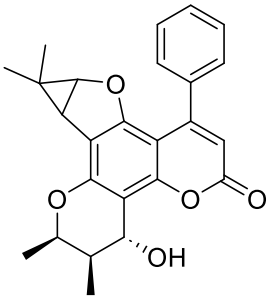

(48)

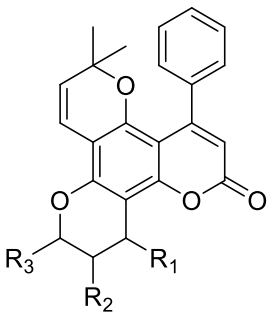

	R_1	R_2	R_3
(40)			
(44)			
(46)			

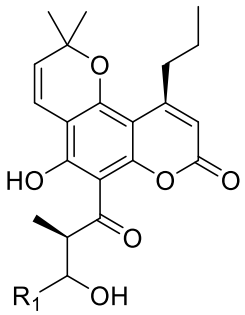

	R_1
(42)	
(43)	

Not only that, but newly undescribed coumarins were also isolated for the first time from *C. incrassatum*. This includes incrassamarin A (**49**), incrassamarin B (**50**), incrassamarin C (**51**), and incrassamarin D (**52**) and (7S,8S)-7,8-dihydro-5-hydroxy-7,8-dimethyl-4 propyl-2H,6H-benzo[1,2-b;5,4-b']dipyran-2,6-dione (**53**), which were isolated by Aminudin et al. (2016b). Hydrocoumarin is also available as one of the derivatives that can be found from the *Calophyllum* species, as compounds like isodispar B (**54**), 5,7-dihydroxy-6-(3-methylbutyryl)-4-phenylcoumarin (**55**), and 5,7-dihydroxy-6-(2-methylbutyryl)-4-phenylcoumarin (**56**) were presented from the phytochemical study of *C. sclerophyllum* (Thiagarajan et al., 2017). Figure 2-11 shows the coumarin derivatives, like hydrocoumarin, isolated from the *Calophyllum* genus.

Figure 2-11:
Coumarin derivatives isolated from the *Calophyllum* genus (continued)

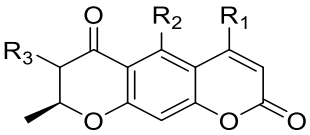

	R_1	R_2	R_3
(**49**)	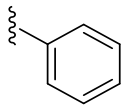	OCH_3	
(**50**)	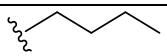	OH	
(**51**)		OH	
(**52**)	CH_3	OH	
(**53**)	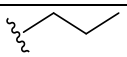	OH	

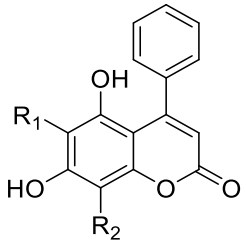

	R_1	R_2
(**54**)	H	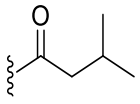
(**55**)	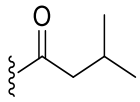	H
(**56**)	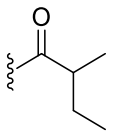	H

In addition to xanthones, coumarins type compounds, especially pyranocoumarins and furo-pyranocoumarins are the recurrent constituents of *Calophyllum* and contribute to its benzopyran-based chemical diversity. Although individual compounds have been reported, comparative and standardized antibacterial evaluations across metabolite classes remain limited. This makes the profiling of coumarins in relation to antibacterial potential in this study able to provide better insight into their functional role within the genus.

2.4.3 Chromanones

Chromanones or chroman-4-ones are heterobicyclic compounds that have the $C_9H_8O_2$ as their molecular formula (Kamboj & Singh, 2021). It is a benzene ring with a 2,3-dihydro-γ-pyranone moiety and is therefore structurally highly akin to the chromones (Diana et al., 2021). The two series vary in their lack of a C2-C3 double bond for the chromanones (Emami & Ghanbarimasir, 2015). Notably, the chromanone structure is comparable to both flavonoids and coumarins, which could be the reason that makes them able to exhibit strong biological properties, just like coumarins (Ma et al., 2024).

Previous studies on phytochemical investigations of the *Calophyllum* genus reported several chromanone derivatives. This includes the isoblancoic acid (**57**) and blancoic acid (**58**), which were obtained by Lim et al. (2019) from the phytochemical study of the stem bark of *C. castaneum*. Furthermore, a study on *C. incrassatum* also gave calofolic acid B (**59**) and apetalic acid (**60**) (Hasanah et al., 2019). As in 2018, Ponguschariyagul et al. reported the presence of caloinophyllin A (**61**) from *C. inophyllum*, followed by another compound, caloinophyllin B (**62**) from its bark, as reported by Sichaem et al. (2018). Figure 2-12 shows some of the chromanone compounds isolated from the *Calophyllum* genus.

Figure 2-12:
Chromanone compounds isolated from the *Calophyllum* genus

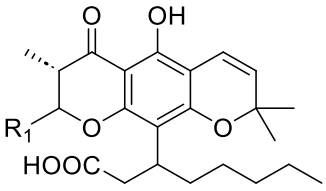

	R_1
(57)	
(58)	

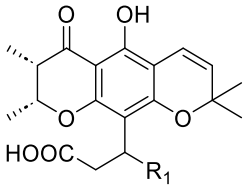

	R_1
(59)	
(60)	

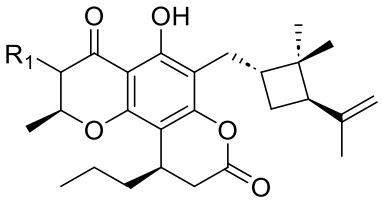

	R_1
(61)	
(62)	

Further investigation on another *Calophyllum* species, *C. scriblitifolium*, also led to the isolation of six structurally distinct compounds: calofolic acid A (**63**), calofolic acid B (**64**), calofolic acid D (**65**), and calofolic acid F (**66**) (Nugroho et al., 2017). Another notable chromanone acid, isocordato-oblongic acid (**67**) was also isolated from *C. symingtonianum* (Aminudin et al., 2016a). Figure 2-13 shows the chromanone compounds isolated from the *Calophyllum* genus.

Figure 2-13:
The chromanone derivatives isolated from the *Calophyllum* genus

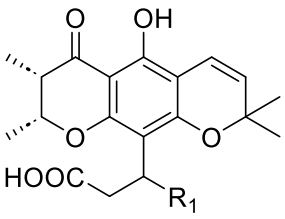

	R_1
(63)	
(64)	
(65)	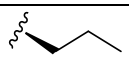
(66)	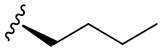

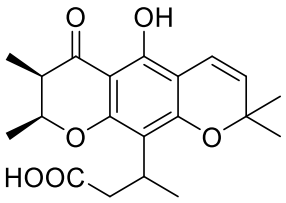

(67)

Chromanones is another class that represents the conserved metabolite class within *Calophyllum*, sharing structural similarities with flavonoids and coumarins suggests potential biological relevance (Ma et al., 2024). However, their antibacterial activity is not extensively evaluated, with most of the studies focusing primarily on their structural elucidation, which is as mentioned above. Therefore, incorporating chromanone-containing fractions into standardized antibacterial assay in this study helps in contributing to their antibacterial profile within the genus.

2.4.4 Triterpenoids

Triterpenoids are the oxygenated derivatives of the class of triterpenes. They are biosynthetically formed by cyclisation of six C5 isoprene molecules, resulting in a C30 molecule of a squalene precursor (Awuchi, 2019; Proshkina et al., 2020). Further cyclisation of squalene results in several triterpenoid skeletons such as steroids, sterols, and saponins (Abe, 2007; Abe et al., 1993). Over 100 triterpenoid skeletons have been reported, of which the most widespread are in tetracyclic as well as pentacyclic form (Ren & Kinghorn, 2019). Triterpenoids are found in various biological kingdoms, ranging from bacteria, animals, to plants (Roy & Saraf, 2006). Triterpenoids were reported in several studies to exhibit a wide spectrum of pharmacological activities, ranging from anticancer (Rascón-Valenzuela et al., 2016), hepatoprotective activities (Xu et al., 2018) to anti-inflammatory (Abdullah et al., 2022).

Several triterpenoids and sterols have been identified in the *Calophyllum* genus. Taher et al. (2021) have reported taraxerone (**68**) and taraxerol (**69**) from the stem bark of *C. canum*. Stigmasterol (**70**) and friedelin (**71**) were also obtained from the *C. macrocarpum* (Karunakaran et al., 2022). Apart from that, lupeol (**72**) and friedelin (**71**) were isolated from *C. ferrugineum* bark during its phytochemical study done by Noh & Jong (2020). Friedelin (**71**), as one of the most common triterpenoids, can be isolated from various other *Calophyllum* species like *C. castaneum* and *C. incrassatum*, reflecting its distribution across the *Calophyllum* genus (Aminudin et al., 2016b; Lim et al., 2019). The continued phytochemical investigation on the leaves of *C. inophyllum* also presented canophyllol (**73**). (Thanh et al., 2019). Another similar triterpenoid of Friedelinol (**74**) was also reported to be isolated from *C. castaneum* (Lim et al., 2019). Figure 2-14 shows the triterpenoid compounds isolated from the *Calophyllum* genus.

Figure 2-14:
The triterpenoid class of compounds isolated from the *Calophyllum* genus

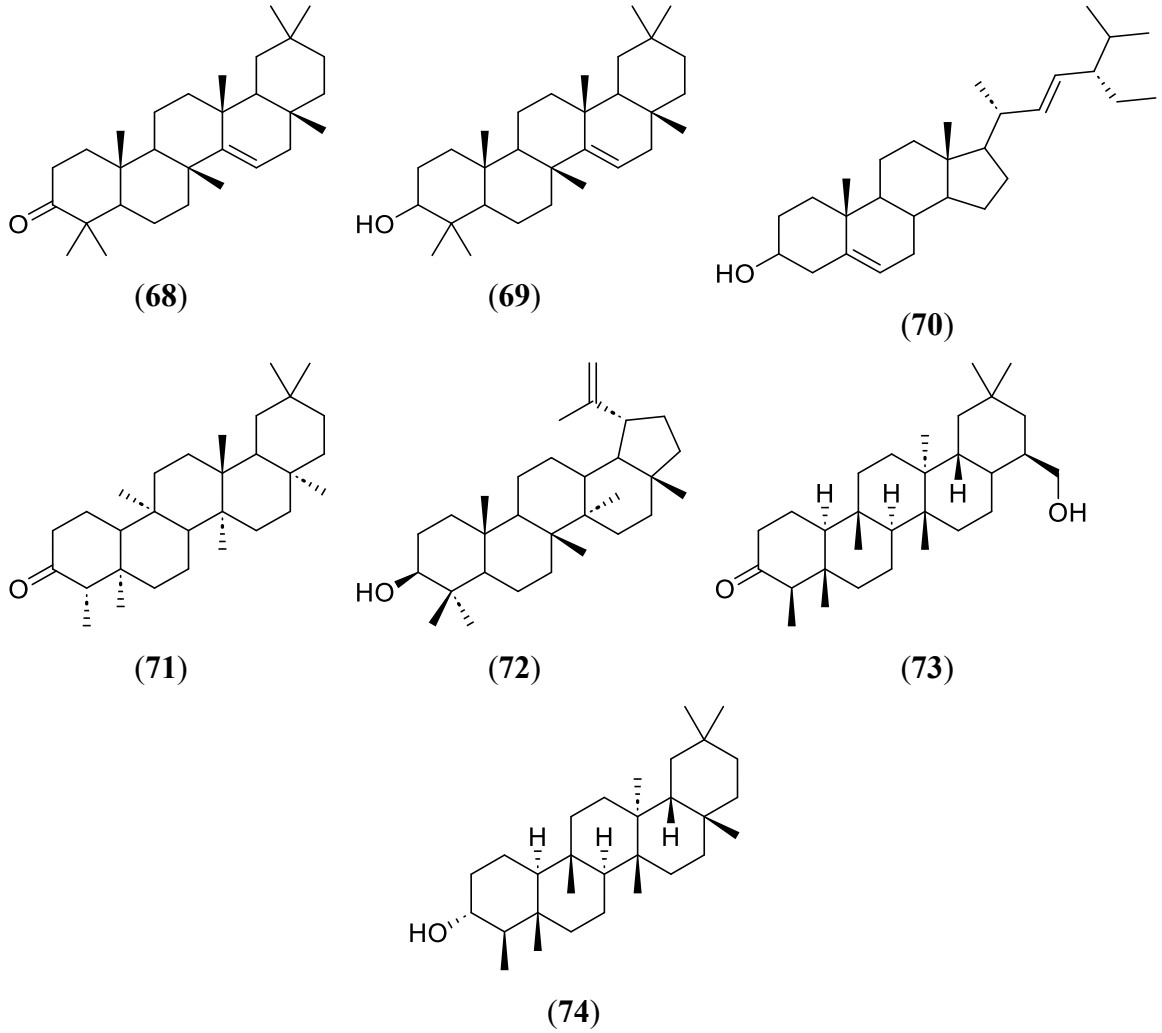

(**68**) (**69**) (**70**)

(**71**) (**72**) (**73**)

(**74**)

Triterpenoids are widely distributed in *Calophyllum*, representing a common core component of the genus' phytochemical profile. Although their reported antibacterial activity is generally moderate compared to xanthones (Hamza et al., 2016), their lipophilic nature may contribute to the membrane interaction and support antibacterial effects. For example, triterpenoids such as friedelin (**70**), and stigmasterol (**71**) have demonstrated measurable antibacterial activity against Gram-negative bacteria strains like *Enterobacter cloacae* (Heilman et al., 2024). Evaluating the triterpenoid-rich fractions which usually are from the hexane extract and isolated compounds in parallel with other classes of metabolites would help in clarifying if triterpenoid functioning as a primary antibacterial agent or as complementary contributors to overall bioactivity.

Collectively, the major classes of compound from the *Calophyllum* genus along with their potential in antibacterial studies have highlighted the importance of exploring the phytochemical and biological data for *C. nodosum.* It is believed that systematic isolation and antibacterial evaluation for this endemic species can fill the important gap within the genus, providing essential species-level validation within the broader chemotaxonomic framework of the genus *Calophyllum*.

2.5 Antibacterial Activity of *Calophyllum* spp.

2.5.1 Antibacterial activity of *Calophyllum* plant extracts

Bacterial resistance to antibiotics can arise through horizontal gene transfer or mutations in the genes (Christaki et al., 2020). Additionally, resistance mechanisms may involve the production of enzymes that degrade antimicrobial agents or alterations in the bacterial cell envelope composition (Aljeldah, 2022). Due to the growing concern over bacterial resistance, there has been increasing interest in identifying novel antibacterial agents from natural sources, especially from medicinal plants (Khan et al., 2013), which includes the *Calophyllum* genus due to its antibacterial properties.

Alkhamaiseh et al. (2011) investigated *C. rubiginosum* bark extracts and discovered that both the hexane along dichloromethane extracts exhibited good antibacterial activity towards *Bacillus cereus* (MIC = 0.0125 mg/mL) and *Staphylococcus aureus* (MIC = 0.1 mg/mL), two prominent Gram-positive bacterial strains. Similar findings were also reported in the investigation on *C. canum*, whereby its stem bark extracts displayed strong inhibitory

activity against the same bacterial strains (Alkhamaiseh et al., 2012). The most potent inhibition was observed in the hexane extract, as its minimum inhibitory concentration (MIC) gives a value of 12.5 µg/mL against *B. cereus*, while the dichloromethane extract exhibited moderate activity against *S. aureus* at 50 µg/mL.

The antibacterial activity of *C. inophyllum* was also investigated, as its chloroform extract displayed moderate inhibition towards bacterial strains of *P. aeruginosa*, *Proteus vulgaris*, and *B. subtilis* (Mishra et al., 2010). Furthermore, the leaf extract of *C. inophyllum* also shows moderate activity against *Clostridium perfringens* and *Listeria monocytogenes*, with an MIC value of 128 µg/mL (Kudera et al., 2017). Other than that, the oil derived from *C. inophyllum* has been utilised for wound healing and treatment of skin diseases due to its antibacterial properties (Dweck & Meadows, 2002). Furthermore, a study reported that C. inophyllum extracts exhibit significant activity against *Mycobacterium smegmatis*, whereas the nonpolar hexane extract effectively inhibits the pathogen by disrupting the mycobacterial membrane (Ha et al., 2009).

The hexane and dichloromethane extract from *C. andersonii* and *C. gracilentum* have also been evaluated for their antibacterial properties using the MIC and MBC assays. The results revealed that extracts from both plants exhibited strong antibacterial activity, with MIC values ranging from 0.25 to 1.00 mg/mL against different types of bacterial strains such as *B. subtilis, B. cereus,* and *E. coli* (Yeap et al., 2017). Among the extracts tested, the methanol extracts specifically demonstrated particularly potent activity, recording an MIC and MBC value of 0.25 mg/mL and 0.50 mg/mL against *Escherichia coli*, further highlighting the importance of exploring the plants from the *Calophyllum* genus and also their potency against Gram-negative bacteria (Yeap et al., 2017).

Similarly, the antibacterial properties of *C. ferrugineum* stem bark extracts have also been investigated, as the dichloromethane extract exhibited potent activity against *B. cereus* and *S. aureus*, with an MIC value of 125 µg/mL (Aminudin et al., 2019). Meanwhile, its chloroform extract demonstrated effective antibacterial activity towards *P. aeruginosa* and *E. coli*, with an MIC value of 112.5 µg/mL (Noh & Jong, 2020). In another study, *C. symingtonianum* was found to possess remarkable antimicrobial potential as its *n*-hexane and methanol extracts exhibited high activity against *Gloeophyllum trabeum*, with MIC values of 50 µg/mL, while their respective MIC values against *Phellinus sanguineus* were 10 µg/mL and 50 µg/mL (Kawamura et al., 2012).

Overall, previous studies indicate that non-polar extracts like hexane and dichloromethane of various *Calophyllum* species frequently demonstrate stronger antibacterial activity, particularly against Gram-positive bacteria. Moderate activity against Gram-negative pathogens was also reported, although comparative evaluations remain inconsistent across species and methodologies. Notably, no systematic antibacterial evaluation has been reported for *C. nodosum*, highlighting the need for species-specific investigations. Table 2-2 summarises the reported antibacterial activity of *Calophyllum* extracts.

Table 2-2:
The reported antibacterial activity of *Calophyllum* extracts.

Species	Plant part	Extract	Bacteria	MIC value	Findings	References
C. rubiginosum	Bark	Hexane	*B. cereus*	0.0125 mg/mL (12.5 µg/mL)	Strong activity (Gram-positive)	Alkhamaiseh et al., 2011
		DCM	*S. aureus*	0.1 mg/mL	Good activity	
C. canum	Stem bark	Hexane	*B. cereus*	12.5 µg/mL	Strong inhibition	Alkhamaiseh et al., 2012
		DCM	*S. aureus*	50 µg/mL	Moderate activity	
C. ferrugineum	Bark	DCM	*B. subtilis* *S. aureus*	125 µg/mL	Moderate activity	Aminudin et al., 2019
		Chloroform	*P. aeruginosa* *E. coli*	112.5 µg/mL	Moderate Gram-negative activity	Noh & Jong, 2020
C. inophyllum	Bark	Chloroform	*P. aeruginosa* *P. vulgaris* *B. subtilis*	Not specified	Moderate inhibition	Mishra et al., 2010
	Leaves	Various extracts	*C. perfringens* *L. monocytogenes*	128 µg/mL	Moderate activity	Kudera et al., 2017
	Oil	-	Skin pathogens	-	Used traditionally for wound healing	Dweck & Meadows, 2002
	-	Hexane	*M. smegmatis*	-	-	Ha et al., 2009
C. andersonii	-	Hexane / DCM	*B. subtilis* *B. cereus* *E. coli*	0.25–1.00 mg/mL	Strong to moderate	Yeap et al., 2017

C. gracilentum	-	Methanol	*E. coli*	0.25 mg/mL (MIC); 0.50 mg/mL (MBC)	Potent Gram-negative activity	Yeap et al., 2017
C. symingtonianum	-	Hexane / Methanol	*G. trabeum*	50 µg/mL	Strong antifungal activity	Kawamura et al., 2012
			P. sanguineus	10–50 µg/mL	High antifungal activity	

2.5.2 Antibacterial activity of the isolated compounds from *Calophyllum* spp.

The antibacterial activity observed in *Calophyllum* extracts has been attributed to the presence of bioactive secondary metabolites, particularly xanthones, coumarins, chromanones, and triterpenoids (Vittaya et al., 2023).

A study done by Pretto et al. (2004) presented that 1,5-dihydroxyxanthone (**30**) was isolated and assessed for antibacterial activity using MIC determination. The compound was tested against multiple pathogenic bacterial strains, including *Bacillus cereus*, *Enterobacter cloacae*, *Escherichia coli*, *Pseudomonas aeruginosa*, *Proteus mirabilis*, *Salmonella typhimurium*, *Staphylococcus aureus*, *Staphylococcus saprophyticus*, and *Streptococcus agalactiae*. The results revealed that 1,5-dihydroxyxanthone (**30**) exhibited moderate activity against Gram-positive bacteria, while no inhibitory effects were observed against Gram-negative bacteria. This disparity in activity is likely due to the presence of the outer phospholipidic membrane of Gram-negative bacteria, which acts as a barrier, preventing the penetration of many antibiotic molecules (Miller, 2016). Furthermore, the periplasmic space of Gram-negative bacteria contains enzymes capable of degrading foreign antimicrobial compounds, thereby limiting their effectiveness (Beacham, 1979; Miller & Salama, 2018).

Compounds isolated from *C. symingtonianum* have been assessed for their antibacterial properties. Notably, rubraxanthone (**75**) displayed potent antimicrobial activity against *G. trabeum*, with a MIC value of 0.080 µg/mL. This potency is attributed to its hydrophobic xanthone core linked to a lipophilic side chain, along with the presence of double bonds on the geranyl moiety and hydroxyl groups at the C-3 and C-6 positions, which are thought to enhance its disruption against microorganisms (Ruan et al., 2017). In addition, 6-deoxyjacareubin (**76**) was highly effective against *P. sanguineus*, showing an MIC of 0.16 µg/mL. Its antimicrobial effect is believed to arise from the structural features of the xanthone scaffold, particularly its phenolic hydroxyl groups and conjugated aromatic system (Muhammad et al., 2019; Zou et al., 2013), which can disrupt microbial cell walls and interfere with membrane integrity, ultimately impairing bacterial survival (Ambarwati et al., 2020).

Moreover, isocordato-oblongic acid (**67**) exhibited strong activity against *Bacillus subtilis*, with a MIC of 62.5 µg/mL, while demonstrating moderate inhibition of *S. aureus*, with an MIC of 125 µg/mL (Kawamura et al., 2012). Subsequent research by Yasunaka et al. (2005) explored the antibacterial activity of extracts from *Calophyllum brasiliense*. Their phytochemical study revealed that two compounds, macluraxanthone (**4**) and

symphoxanthone (**7**), were mainly the reasons for the activity demonstrated by the plant extracts. These compounds exhibited significant inhibition towards *S. aureus* and moderate activity towards *E. coli*. In contrast, another compound isolated, globuxanthone (**6**), showed no antibacterial activity against either strain.

Furthermore, four xanthones namely macluraxanthone (**4**), 1,5-dihydroxy-8-methoxyxanthone (**77**), 1,7-dihydroxyxanthone (**78**), and trapezifolixanthone (**20**) have been investigated for their antimicrobial properties. According to research conducted by Tantapakul et al. (2016), trapezifolixanthone (**20**) exhibited notable inhibitory effects against several bacterial strains, demonstrating promising antibacterial potential. In contrast, macluraxanthone (**4**) displayed only weak antibacterial activity across all tested strains.

Other than xanthone, coumarins isolated from different species within this genus also showed potential in antibacterial activity. One of the most prominent coumarin compounds that is well known for its antibacterial activity is calophyllolide (**45**), isolated from *C. inophyllum,* which was reported to have good inhibition, especially towards Gram-positive bacteria like *S. aureus.* According to Yimdjo et al. (2004), calophyllolide (**45**), inophyllum C (**79**) and E (**80**) were reported to demonstrate significant bacteriostatic activity against Gram-positive bacteria, specifically *S. aureus* at 16.0 mm, 10.0 mm, and 13.0 mm, respectively. These compounds were also isolated by Léguillier et al. (2015) from the nuts of *C. inophyllum,* which complement their activity against Gram-positive bacteria in the study. Léguillier et al. (2015) explained that it could be due to Gram-positive bacteria lacking the protective outer membrane found in Gram-negative bacteria (Miller, 2016).

Inophyllum E (**80**) also reported to inhibit strongly against *S. aureus, S. epidermidis,* and *P. aeruginosa* at MIC values <50 µg/mL. While *E. coli, K. pneumoniae*, and *B. subtilis* were also inhibited by the compound at a 50 µg/mL concentration (Kumar & Garg, 2020). In the same study, inophyllum C (**79**) also showed activity against the mentioned bacterial strains with less efficacy. Inophyllum H (**48**) also exhibited weak activity against *B. subtilis* at 250 µg/mL in a study done by Aminudin et al. (2016a). Moreover, calanolide E (**42**) isolated from *C. wallichianum* also exhibited activity against *B. megaterium, B. cereus, B. pumilus,* and *B. subtilis* with MIC values in the range of 0.25-0.50 mg/mL (Tee et al., 2018).

The same goes for another class of compounds, chromanone acids, whereby some of the compounds isolated show good antibacterial activity. For example, isocordato-oblongic acid (**81**) showed moderate inhibition towards *S. aureus* and *B. subtilis* bacteria at 125 µg/mL

and 62.5 μg/mL, respectively Aminudin et al. (2016a). Similar to coumarins, isocordato-oblongic acid (**81**) was more selective towards Gram-positive bacteria, as no inhibition was observed for Gram-negative bacteria. According to Biagi et al. (1970), this is because of the presence of the pentanoic acid functional group within the chromanone acid structure that increases its lipophilic character, enabling better penetration of the low lipid content of the cell wall in Gram-positive bacteria. Another six more chromanone acids that were isolated from the bark of *C. brasiliense* also showed moderate to strong antibacterial activity against *B. cereus and S. epidermidis*. This is especially true for brasiliensophyllic acid (**82**), isobrasiliensophyllic acid A (**83**), whereas both showed the most activity against the two bacterial strains at 1 μg/mL and 16 μg/mL, respectively (Cottiglia et al., 2004). Coumarin mammea A/B (**84**) also has strong antibacterial activity as Yasunaka et al. (2005) reported that the mammea A/B (**84**) gives MIC values at 1 ug/mL and 2 ug/mL, respectively, for different *S.aureus* bacteria strains. A study done by Quintans et al. (2014) also reported that canophyllic acid (**85**) exhibits bactericidal activity towards *Proteus mirabilis*.

The terpenes and triterpenoids constituents also exhibit antibacterial activity as the triterpene, canophyllol (**86**), showed antimicrobial activity towards *S. aureus*, *Corynebacterium diphtheriae, Klebsiella pneumoniae, and Proteus mirabilis* with inhibition zones of 5.50, 4.53, 3.00, and 3.50 cm, respectively (Ragasa et al., 2015). The antibacterial activity of this compound is attributed to its triterpene nature, as members of this class commonly act by compromising bacterial cell membranes and interfering with vital metabolic pathways (Ragasa et al., 2015). Another pentacyclic triterpenoid, taraxasterol (**87**), also possessed strong activity towards *S. aureus* (Ragasa et al., 2015). Friedelin (**71**), a common triterpenoid that can often be isolated from the genus of *Calophyllum,* also shows antimicrobial properties in the same study, whereby the results were further supported by a previous report in 2024, as compound (**71**) showed bactericidal activity against *Enterobacter cloacae* at an MBC value of 50 μg/mL (Heilman et al., 2024). Both stigmasterol (**70**) and *β*-sitosterol (**88**) are also some of the common triterpenoids that have been studied for their antimicrobial properties. All these studies support that many secondary metabolites isolated from the *Calophyllum* genus can potentially become antibacterial agents.

In overall, isolated compounds from *Calophyllum* spp. demonstrated broad antibacterial potential, with xanthones and prenylated derivatives frequently exhibiting the strongest activity, particularly against Gram-positive bacteria. Coumarins and chromanone acids also contribute to the inhibition while triterpenoids generally display moderate but

measureable antimicrobial effects. These findings collectively highlight that multiple metabolite classes within the genus contribute to the antibacterial profile, thereby supporting the continued species-specific investigations, including the present study towards *C. nodosum*. Table 2-3 summarises the antibacterial activity of isolated compounds from *Calophyllum* spp.

Table 2-3:
The reported antibacterial activity of isolated compounds from *Calophyllum* spp.

Compound	Class	Species	Bacteria	MIC / antibacterial activity	Reference
1,5-Dihydroxyxanthone (**30**)	Xanthone	*C. brasiliense*	Gram-positive bacteria	Moderate activity	Pretto et al., 2004
			Gram-negative bacteria	No activity	
Rubraxanthone (**75**)	Prenylated xanthone	*C. symingtonianum*	*Gloeophyllum trabeum*	0.080 µg/mL	Ruan et al., 2017
6-Deoxyjacareubin (**76**)	Xanthone	*C. symingtonianum*	*Phellinus sanguineus*	0.16 µg/mL	Muhammad et al., 2019
Macluraxanthone (**4**)	Xanthone	*C. brasiliense*	*S. aureus*	Significant	Yasunaka et al., 2005; Tantapakul et al., 2016
Symphoxanthone (**7**)	Xanthone	*C. brasiliense*	*S. aureus*	Significant	Yasunaka et al., 2005
			E. coli	moderate	
Trapezifolixanthone (**20**)	Xanthone	-	Various bacteria	Notable inhibitory activity	Tantapakul et al., 2016
Globuxanthone (**6**)	Xanthone	*C. brasiliense*	*S. aureus*, *E. coli*	No activity	Yasunaka et al., 2005
Calophyllolide (**45**)	Coumarin	*C. inophyllum*	*S. aureus*	Strong inhibition (16 mm)	Yimdjo et al., 2004
Inophyllum C (**79**)	Coumarin	*C. inophyllum*	*S. aureus*	10 mm zone; MIC ~50 µg/mL	Yimdjo et al., 2004; Kumar & Garg, 2020
Inophyllum E (**80**)	Coumarin	*C. inophyllum*	*S. aureus* *S. epidermidis* *P. aeruginosa*	MIC <50 µg/mL	Kumar & Garg, 2020
Inophyllum H (**48**)	Coumarin	*C. symingtonianum*	*B. subtilis*	250 µg/mL	Aminudin et al., 2016a
Calanolide E (**42**)	Pyranocoumarin	*C. wallichianum*	*Bacillus* spp.	0.25–0.50 mg/mL	Tee et al., 2018
Isocordato-oblongic acid (**81**)	Chromanone acid	*C. brasiliense*	*S. aureus* *B. subtilis*	125 µg/mL; 62.5 µg/mL	Aminudin et al., 2016a
Brasiliensophyllic acid (**82**)	Chromanone acid	*C. brasiliense*	*B. cereus*	1 µg/mL	Cottiglia et al., 2004

Isobrasiliensophyllic acid A (**83**)	Chromanone acid	*C. brasiliense*	*S. epidermidis*	16 µg/mL	Cottiglia et al., 2004
Mammea A/B (**84**)	Coumarin	-	*S. aureus*	1–2 µg/mL	Yasunaka et al., 2005
Canophyllic acid (**85**)	Chromanone acid	-	*Proteus mirabilis*	Bactericidal activity	Quintans et al., 2014
Canophyllol (**86**)	Triterpenoid	-	*S. aureus* *C. diphtheriae* *K. pneumoniae* *P. mirabilis*	Inhibition zones 3–5.5 cm	Ragasa et al., 2015
Taraxasterol (**87**)	Triterpenoid	-	*S. aureus*	Strong activity	Ragasa et al., 2015
Friedelin (**71**)	Triterpenoid	-	*Enterobacter cloacae*	MBC 50 µg/mL	Heilman et al., 2024

CHAPTER 3:

RESEARCH METHODOLOGY

3.1 Instrumentation

Both 1D and 2D NMR spectra were acquired using a Bruker AV400III HD 400 MHz spectrometer. It operates at 400 MHz for ^{1}H NMR and 100 MHz for ^{13}C NMR. The 2D NMR consisted of DEPT (45°, 90°, 135°), COSY, HMQC, and HMBC. The chemical shifts were recorded in ppm, while coupling constants (*J*) were in Hertz (Hz). A Shimadzu CBM-20A spectrometer was used to obtain the LC-MS chromatograms, while GC-MS spectra were obtained using a Shimadzu GC-MS-QP 5050A spectrometer. An Agilent Cary 60 spectrophotometer was utilised to obtain the UV-Vis spectra. Using an Elmer Frontier model, the attenuated total reflection (ATR) method was used to obtain the infrared spectra of isolated compounds, which fell between 4000 and 400 cm^{-1}. The melting point apparatus, Stuart SMP3, was used for the melting point determination of crystalline compounds. Crude extracts of the plant were dried using a rotary evaporator (Heidolph LABOROTA 4000 efficient). Using the EYELA autoclave MAC-601, all equipment used in biological test procedures was autoclaved. A Class II Biological Safety Cabinet was used for bioassay operations.

3.2 Materials and Chemicals

All chemicals and reagents (*n*-hexane, dichloromethane, chloroform, ethyl acetate, acetone, and methanol) were of analytical grade and used for the extraction, isolation, and purification process. Gravity column chromatography was done using silica gel Merck 60 (1.07734.1000), silica gel Merck 60 (1.09385.1000), and gel filtration chromatography was performed using Sephadex LH-20 (Sigma Aldrich). The thin-layer chromatography (TLC) was conducted on TLC silica gel Merck 60 F254 (1.05554.0001) aluminium sheets. The radial chromatography was using the silica gel Merck 60 PF254 (1.07749.1000) containing gypsum in 0.5, 1.0, and 2.0 mm thickness. The spots and bands on the TLC and radial

chromatography plate were visualised under UV light at two different wavelengths, 254 nm for shortwave and 366 nm for longwave. Deuterated chloroform ($CDCl_3$) and acetone ($(CD_3)_2CO$) with 99.6 atom % D were used for NMR. The reference standard, tetramethylsilane (TMS), was used for the newly isolated compound. Mueller-Hinton Agar (MHA) and Mueller-Hinton Broth (MHB) were used in this study for the well diffusion assay, MIC, and MBC determination. The positive standard used was ampicillin, while dimethyl sulfoxide (DMSO) was employed as the negative control in this study.

3.3 Isolation and Purification of Secondary Metabolites

3.3.1 Plant materials

The stem bark of *C. nodosum* (Voucher Specimen, No. UiTM3050) was collected from Gunung Santubong, Kuching, Sarawak, and identified by a plant taxonomist. The stem bark was air-dried before being ground with a conventional mill and a waring laboratory blender.

3.3.2 Preparation of crude extracts

The dried and ground stem bark of *C. nodosum* (2.68 kg) was extracted with *n*-hexane for 72 hours using the maceration technique for three times (Zamakshshari et al., 2021). After that, all three extracts were combined and filtered with Whatman No.1 filter paper and concentrated using a rotary evaporator to obtain the crude extract. The crude was kept in a fume hood and consistently weighed until a constant weight was obtained. The extraction process was repeated using different solvents of increasing polarity, from *n*-hexane, chloroform, to methanol, sequentially.

3.3.3 Extraction, isolation and purification of compounds from *C. nodosum*

The stembark of *C. nodosum* (2.68 kg) was successfully extracted using a sequential maceration technique, yielding 229.0 g of *n*-hexane extract, 61.6 g of chloroform extract, and 284 g of methanol extract. The isolation and purification of the *n*-hexane extract identified four xanthones, one lactone, and two triterpenes. Through extensive purification process of the *n*-hexane extract, the following compounds were successfully obtained:

nodosuxanthone (**89**) (18.3 mg), trapezifolixanthone (**20**) (27.5 mg), caloxanthone C (**5**) (43.6 mg), 1-hydroxy-7-methoxyxanthone (**27**) (22.7 mg), canumolactone (**90**) (110.8 mg), friedelin (**71**) (54.2 mg) and stigmasterol (**70**) (28.9 mg). Notably, nodosuxanthone (**89**) is a novel compound that has not been previously reported, marking a significant contribution to the chemical diversity of the *Calophyllum* genus.

The *n*-hexane extract (229.0 g) was pre-adsorbed onto silica gel (1:1, w/w) using the dry loading technique prior to fractionation. The sample was subjected to gravity column chromatography over silica gel 60 (230–400 mesh) as the stationary phase, employing a sequential gradient system of hexane:chloroform, chloroform:ethyl acetate, and ethyl acetate:methanol as the mobile phases. This procedure afforded 19 fractions (CnH1–19).

Fractions CnH1–11 were combined and rinsed with methanol to remove insoluble terpenoid crystals, in which compound **71** was obtained. The methanol-soluble portion (CnH1b) was repeatedly chromatographed on Sephadex LH-20 column chromatography using 100% methanol as the eluent, yielding 12 subfractions (CnH1b3b5e1–12). Subfractions 7–12 were further purified by radial chromatography using hexane:acetone (98:2, v/v), affording six subfractions (CnH1b3b5e7a–f). Subsequent purification of subfraction b (hexane:acetone, 98:2, v/v) led to the isolation of compound **5** (fraction 3) and compound **27** (fraction 6).

Fractions CnH17–19 were combined and subjected to silica gel column chromatography using a hexane:chloroform:acetone gradient system, yielding subfractions a–do. Subfractions v–ah were further fractionated with hexane:chloroform:methanol gradients into 33 fractions. Fractions 4–25 were purified by radial chromatography using chloroform:acetone (99:1, v/v), affording subfractions a–am. Subfractions e–y were subsequently separated on Sephadex LH-20 to yield eight fractions. From these, fractions 3–8 were further purified using hexane:chloroform (2:8, v/v), producing subfractions a–ac. Subfractions o–q were fractionated using hexane:acetone (8:2, v/v), generating four subfractions. Final purification of the second subfraction using hexane:dichloromethane (9:1, v/v) resulted in fraction a and b, whereas fraction a is compound **90**. On the other hand, the purification of the fraction b using hexane:ethyl acetate (8:2, v/v) led to the isolation of compound **20** and **89**. While further purification of compound **20** gives the isolation of compound **70**.

The chloroform extract (61.6 g) was fractionated using a gradient system of hexane:chloroform:methanol, affording 11 fractions (CnC1–11). Fractions CnC3–7 were combined and subjected to Sephadex LH-20 chromatography, yielding subfractions a–o. Subfractions b–f were further purified by silica gel column chromatography using hexane:ethyl acetate (96:4, v/v), producing eight fractions. Radial chromatography of subfractions 1–5 with hexane:ethyl acetate (95:5, v/v) afforded compound **27**. Meanwhile, subfractions 6–7 were subjected to radial chromatography using hexane:acetone (95:5, v/v), yielding five fractions (a–e), of which fraction e afforded compound **5**. Subfractions c–d were further purified using hexane:chloroform (7:3, v/v), providing an additional portion of compound **20**. Figure 3-1 and Figure 3-2 show the flowchart of the isolation and purification processes to obtain all isolated compounds from both *n*-hexane and chloroform extracts.

Figure 3-1:
Simplified flow diagram showing the isolation process of compounds from the *n*-hexane extract of *C. nodosum* stem bark

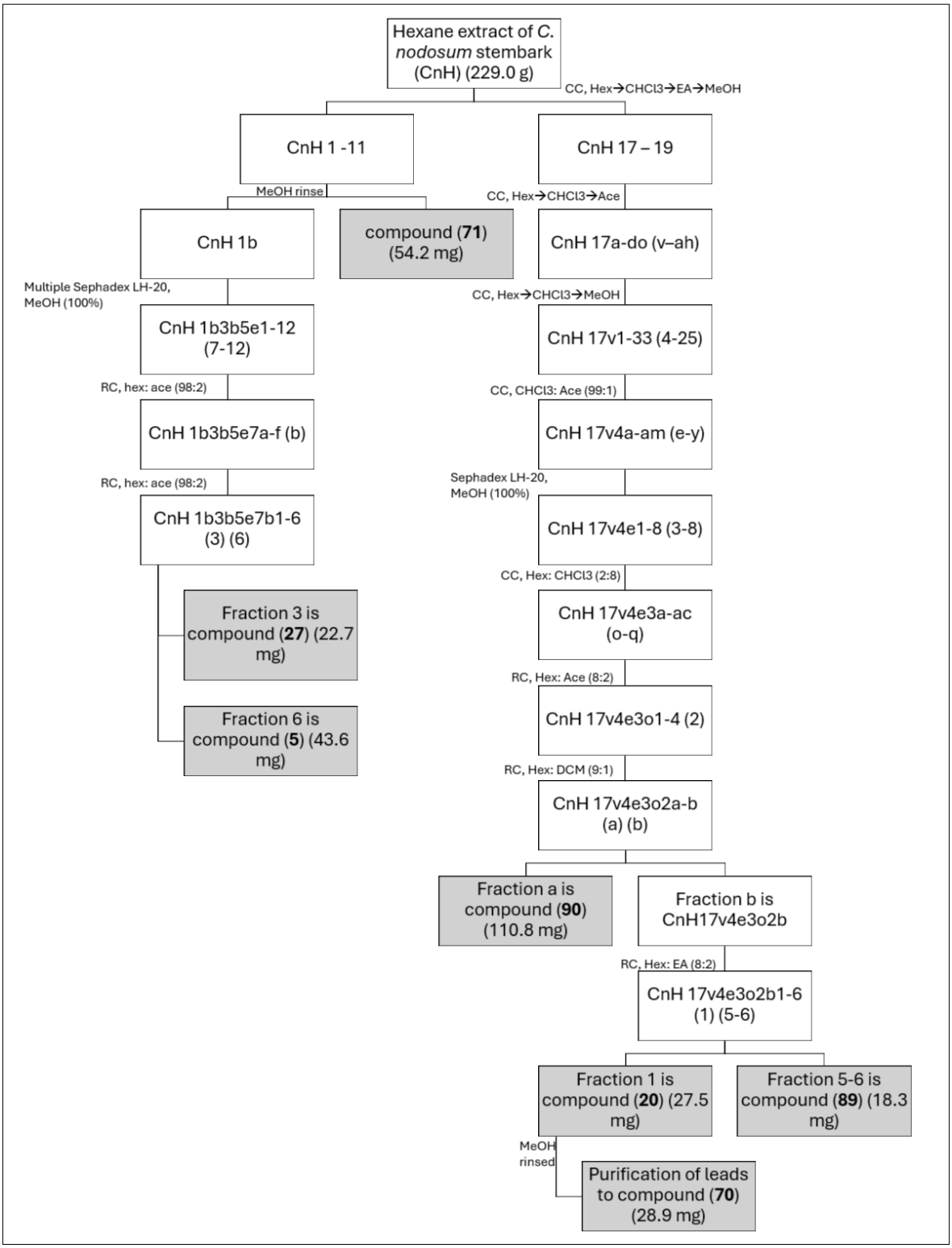

Hex = Hexane; DCM = Dichloromethane; $CHCl_3$ = Chloroform; EA = Ethyl acetate; Ace = Acetone; MeOH = Methanol; CC = Column chromatography; RC = Radial chromatography.

Figure 3-2:
Simplified flow diagram showing the isolation process of compounds from the chloroform extract of *C. nodosum* stem bark

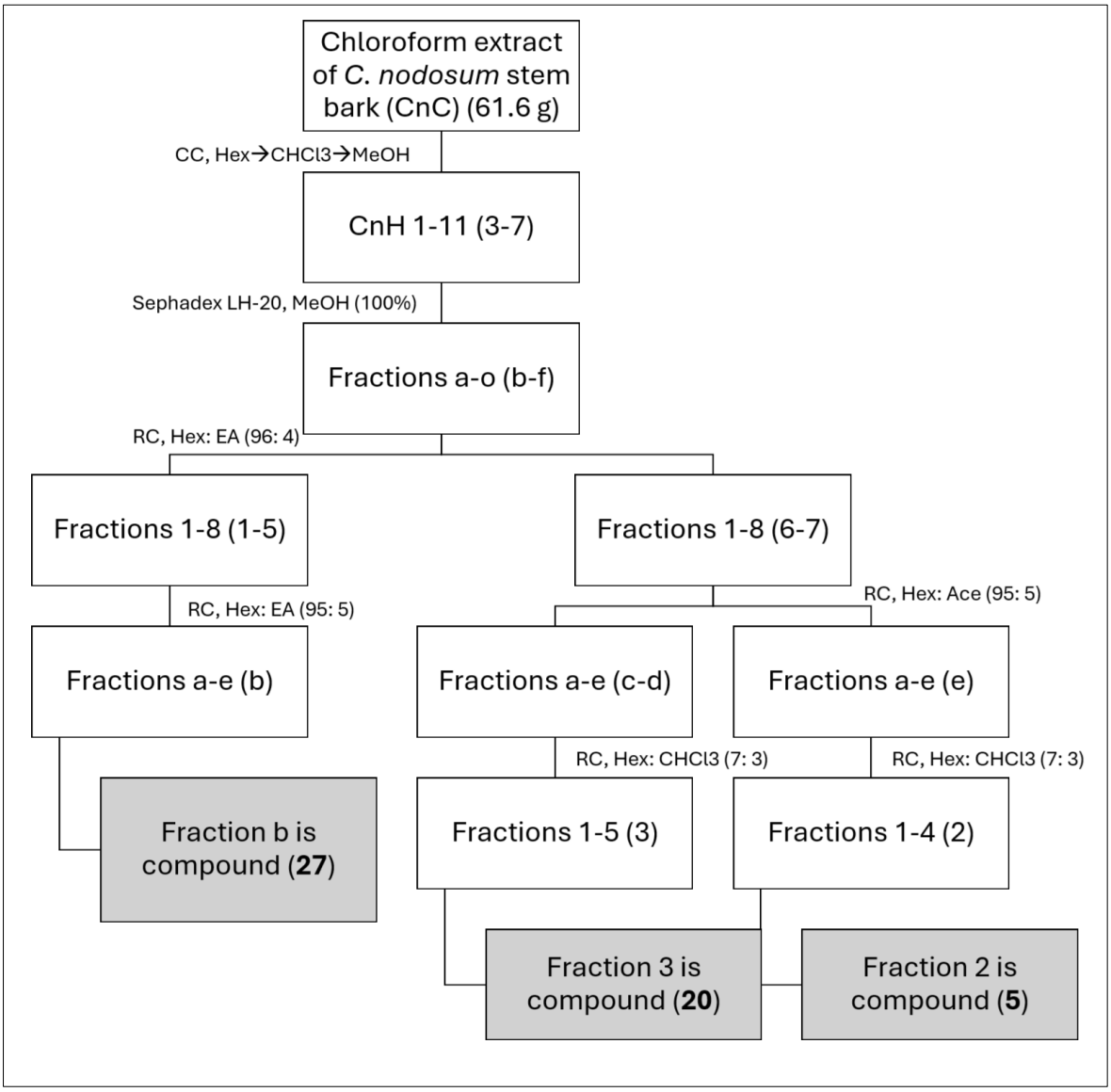

Hex = Hexane; DCM = Dichloromethane; $CHCl_3$ = Chloroform; EA = Ethyl acetate; Ace = Acetone; MeOH = Methanol; CC = Column chromatography; RC = Radial chromatography.

3.3.4 Chromatographic method

Column Chromatography (CC)

Chromatographic techniques are a set of methods used for separating and analysing mixtures of substances. These techniques use the differential interactions between the constituents of a mixture and the stationary phase and the mobile phase. The extracts obtained underwent several chromatography techniques, as column chromatography was used to separate mixtures of different polarities of compounds by using columns packed with silica gel. Two types of column chromatography were used in this study. The first is gravity column chromatography, whereby the mixtures were separated based on their affinity to the stationary phase due to different polarities. The adsorbent used was silica gel, Merck Kieselgel 60 of particle size 0.040-0.063 mm and silica gel Merck Kieselgel PF 252 of particle size 0.063-0.200 mm. The column was being prepared by pouring the Merck Kieselgel 60 or Merck Kiesel gel PF 252 silica gel mixed with *n*-hexane into the column. The silica gel was allowed to settle down and make the solvent flow through it and was packed about 5 times before use. The sample was introduced onto the top of the column by using the dry and wet loading methods. The column was then eluted with suitable solvent systems by increasing the solvent polarity.

Gel Filtration Column Chromatography

Sigma Lipophilic Sephadex LH-20 was utilised as the gel filtration chromatography, which separates based on molecular weights. It is hydrophilic and can only use a polar solvent as a mobile phase, like methanol. The Sephadex silica was mixed with methanol and left overnight before being poured into the column. The sample was subjected to the column by using the wet loading method. The fractions eluted from each column were collected as the fractions were transferred to sample vials and monitored using TLC after obtaining their dry weight.

Thin Layer Chromatography (TLC)

The compound's purity was determined by using analytical TLC before proceeding to other analyses such as NMR, LC-MS, and FTIR. It was done by using aluminium sheets of dimensions 50 mm x 50 mm x 0.25 mm coated with silica gel 60F254 (Merck 1.05735) as their stationary phase, while the mobile phase used was a different ratio of solvents that acted via capillary action. The solvent consisted of nonpolar to polar solvents. The baseline,

expected solvent front, and sample names were marked gently with a pencil. The sample was spotted using a fine glass capillary tube onto the TLC sheets and placed into a closed TLC glass chamber filled with 5 mL of mobile phase. The solvents were allowed to reach the expected solvent front marked 1cm from the top of the plate before removing it. The plates were then visualised under UV light at 254 nm (short wave) and 366 nm. (long wave).

Radial Chromatography (RC)

When multiple spots were observed on the TLC plate, radial chromatography was used to purify the compounds isolated from column chromatography. The silica gel Merck 60 PF254, containing gypsum, was used to prepare the plates in thicknesses of 0.5 mm, 1.0 mm, and 2.0 mm. The sample was dissolved using a suitable solvent and dropped onto the plate. A mobile phase composed of nonpolar to polar solvent mixtures was introduced onto the plates. The radial chromatography spins radially, allowing the compounds to migrate radially outward via capillary action. The plate was covered to prevent solvent evaporation, and separation was monitored under the UV light. Spots and bands on the TLC and radial chromatography plate were visualised under UV light before collecting the separated compounds.

3.4 Spectral Data of the Isolated Compounds from *C. nodosum*

3.4.1 Nodosuxanthone (89)

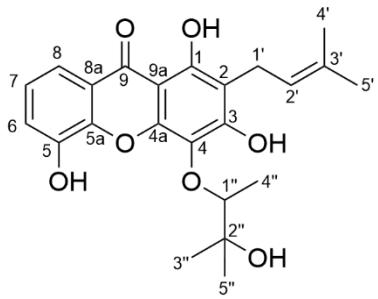

Yellow crystal (18.3 mg). $C_{24}H_{28}O_6$. Melting point: 118-120. IR ν_{max} (cm^{-1}): 3260 (broad, O-H), 3080-3030 (weak aromatic C-H), 2926 (sp^3 hybridisation of C-H stretching), 1647 (C=O, conjugated), 1620 (conjugated C=C stretching), 1580 (aromatic C=C), 1222 (C-O stretching), 1100 (C-O-C stretching). UV (MeOH) λ_{max} (nm): 205, 221, 244, 325. LC-MS (ESI^-) *m/z* = 414.2. ^{1}H NMR (400 MHz, acetone-d_6) δ H: 13.51 (*s*, 1-OH), 9.26 (*s*, 5-OH), 7.69 (1H, *dd*, *J* = 1.5 Hz, 7.9 Hz, H-8), 7.37 (1H, *dd*, *J* = 1.5 Hz, 7.9 Hz, H-6), 7.25 (1H, *t*, *J* = 7.9 Hz, H-7), 5.29 (1H, *t*, *J* = 7.3 Hz, H-2′), 4.61 (1H, *q*, *J* = 6.6 Hz, H-1″), 3.30 (2H, *d*, *J* = 7.3 Hz, H-1′), 1.78 (3H, *s*, H-4′), 1.66 (3H, *s*, H-5′), 1.65 (3H, *s*, H-3″), 1.44 (3H, *d*, *J* = 6.6 Hz, H-4″), 1.36 (3H, *s*, H-5″). ^{13}C NMR (100 MHz, acetone-d_6) δ C: 181.6 (C-9), 165.4 (C-3), 161.9 (C-1), 151.8 (C-4a), 147.1 (C-5a), 146.1 (C-5), 132.2 (C-3′), 124.6 (C-7), 122.7 (C-2′), 122.4 (C-8a), 121.1 (C-6), 116.4 (C-8), 113.3 (C-4), 107.3 (C-2), 104.2 (C-9a), 91.6 (C-1″), 44.9 (C-2″), 25.9 (C-3″), 25.8 (C-5′), 22.3 (C-1′), 21.5 (C-5″), 17.9 (C-4′), 14.7 (C-4″).

3.4.2 Trapezifolixanthone (20)

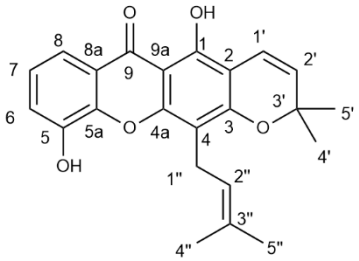

Yellow needle crystals (27.5 mg). $C_{23}H_{22}O_5$. Melting point: 160-162 °C (168-169 °C, Lizazman et al., 2023). IR ν_{max} (cm^{-1}): 3323 (broad, O-H), 3030 – 3070 (weak, aromatic C-H stretching), 2928 (aliphatic C-H stretching), 1651 (conjugated C=O), 1621 (unsaturated C=C), 1580 (aromatic C=C), 1286 (C-O stretching) Karunakaran et al. (2022). GC-MS (*m/z*): 378.0. ^{1}H NMR (400 MHz, acetone-d_6) δ H: 13.45 (*s*, 1-OH), 9.21 (*s*, 5-OH), 7.72 (1H, *dd*, *J* = 7.9 Hz, 1.6 Hz, H-8), 7.39 (1H, *dd*, *J* = 7.9 Hz, 1.5 Hz, H-6), 7.31 (1H, *t*, *J* = 7.9 Hz, H-7), 7.09 (1H, *d*, *J* = 10.0 Hz, H-1′), 5.79 (1H, *d*, *J* = 10.0 Hz, H-2′), 5.26 (1H, *t*, *J* = 7.4 Hz, H-2″), 3.36 (2H, *d*, *J* = 7.4 Hz, H-1″), 1.83 (3H, *s*, H-5″), 1.67 (3H, *s*, H-4″), 1.52 (3H, *s*, H-4′), 1.52 (3H, *s*, H-5′). ^{13}C NMR (100 MHz, acetone-d_6) δ C: 182.2 (C-9), 159.2 (C-3), 156.6 (C-1), 154.9 (C-4a), 147.2 (C-5), 146.4 (C-5a), 131.8 (C-3″), 128.7 (C-2′), 124.8 (C-7), 123.3 (C-2″), 122.1 (C-8a), 121.5 (C-6), 116.3 (C-8), 116.0 (C-1′), 108.6 (C-4), 105.1 (C-9a), 104.0 (C-2), 79.1 (C-3′), 28.5 (C-4′), 28.5 (C-5′), 26.0 (C-4″), 22.0 (C-1″), 18.1 (C-5″). Both the ^{1}H and ^{13}C NMR spectral data correspond with the literature documented by Karunakaran et al. (2022).

3.4.3 Caloxanthone C (5)

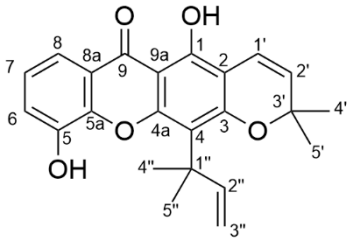

Yellow needle crystal. $C_{23}H_{22}O_5$. Melting point: 214-215 °C (211-213 °C, (Zamakshshari et al., 2016). IR ν_{max} (cm^{-1}): 3438 (broad, O-H), 3052 (weak, aromatic C-H stretching), 2931 (aliphatic C-H stretching), 1649 (conjugated C=O), 1616 (unsaturated alkene C=C), 1498 (aromatic C=C), 1218 (C-O stretching) Lee et al. (2017). GC-MS (*m/z*): 378.0. ^{1}H NMR (400 MHz, acetone-d_6): 13.70 (*s*, 1-OH), 8.95 (*s*, 5-OH), 7.65 (1H, *dd*, *J* = 1.2 Hz, 7.9 Hz, H-8), 7.36 (1H, *dd*, *J* = 1.1 Hz, 7.9 Hz, H-6), 7.26 (1H, *t*, *J* = 7.9 Hz, H-7), 6.72 (1H, *d*, *J* = 10.0 Hz, H-1′), 6.52 (1H, *dd*, *J* = 10.6 Hz, 17.5 Hz, H-2″), 5.74 (1H, *d*, *J* = 10.0 Hz, H-2′), 5.04 (1H, *dd*, *J* = 0.88 Hz, 17.5 Hz, H-3″), 4.88 (1H, *dd*, *J* = 1.0 Hz, 10.6 Hz, H-3″), 1.75 (6H, *s*, H-4″ & H-5″), 1.51 (6H, *s*, H-4′ & H-5′). ^{13}C NMR (100 MHz, acetone-d_6): 181.5 (C-9), 159.3 (C-3), 156.3 (C-1), 155.0 (C-4a), 151.7 (C-2″), 146.4 (C-5), 145.1 (C-5a), 127.7 (C-2′), 124.0 (C-7), 120.1 (C-8a), 120.0 (C-6), 115.4 (C-1'), 115.0 (C-8), 113.5 (C-4), 106.6 (C-3″), 104.9 (C-2), 103.5 (C-9a), 78.4 (C-3′), 40.9 (C-1″), 29.0 (C-4″ & C-5″), 27.2 (C-4′ & C-5′). Both the ^{1}H and ^{13}C NMR spectral data correspond with the literature documented by Lee et al. (2017).

3.4.4 1-hydroxy-7-methoxyxanthone (27)

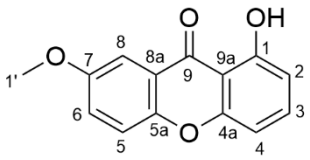

Pale yellow crystal. $C_{14}H_{10}O_4$. Melting point: 121-124 °C (124-126 °C, (Leslie Gunatilaka et al., 1982). IR ν_{max} (cm^{-1}): 3428 (broad, O-H), 3087 (weak, aromatic C-H stretching), 2930 (aliphatic C-H stretching), 1644 (conjugated C=O), 1607 (unsaturated alkene C=C), 1474 (aromatic C=C), 1238 (C-O stretching) Lizazman et al. (2026). ^{1}H NMR (400 MHz, acetone-d_6): 12.71 (*s*, 1-OH), 7.74 (1H, *t*, *J* = 8.4 Hz, H-3), 7.64 (1H, *d*, *J* = 3.1 Hz, H-8), 7.61 (1H, *d*, *J* = 9.2 Hz, H-5), 7.52 (1H, *dd*, *J* = 3.1 Hz, 9.2 Hz, H-6), 7.04 (1H, *dd*, *J* = 1.0 Hz, 8.4 Hz, H-4), 6.81 (1H, *dd*, *J* = 1.0 Hz, 8.2 Hz, H-2), 3.97 (*s*, 7a-OCH3). ^{13}C NMR (100 MHz, acetone-d_6): 182.0 (C-9), 161.8 (C-1), 156.4 (C-7), 154.9 (C-4a), 151.0 (C-5a), 137.0 (C-3), 125.6 (C-6), 120.7 (C-8a), 119.5 (C-5), 109.9 (C-2), 108.3 (C-9a), 107.0 (C-4), 105.1 (C-8), 55.4 (C-7a). Both the ^{1}H and ^{13}C NMR spectral data correspond with the literature documented by Lizazman et al. (2026).

3.4.5 Canumolactone (90)

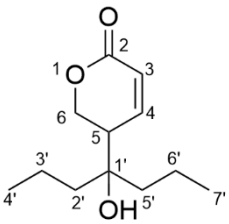

Yellowish orange, oily. IR ν_{max} (cm^{-1}): 2950 (aliphatic C-H stretching), 1725 (C=O stretching), 1603 (unsaturated alkene C=C), 1268 (C-O stretching) Lizazman & Jong (2024). LC-MS (ESI^-) (*m/z*): 212.3. ^{1}H NMR (400 MHz, acetone-d_6): 7.77 (1H, *dd*, *J* = 3.4 Hz, 5.8 Hz, H-3), 7.67 (1H, *dd*, *J* = 3.4 Hz, 5.8 Hz, H-4), 4.23 (2H, *m*, H-6), 1.72 (1H, *m*, H-5), 1.46 (2H, *m*, H-3′), 1.40 (2H, *m*, H-2′), 1.36 (2H, *m*, H-5′), 1.31 (2H, *m*, H-6′), 0.95 (3H, *t*, H-4′), 0.92 (3H, *t*, H-7′). ^{13}C NMR (100 MHz, acetone-d_6): 167.1 (C-2), 132.6 (C-1′), 131.1 (C-4), 128.7 (C-3), 67.4 (C-6), 38.8 (C-5), 30.3 (C-2′), 28.8 (C-5′), 23.6 (C-3′), 22.7 (C-6′), 13.4 (C-7′), 10.4 (C-4′). Both the ^{1}H and ^{13}C NMR spectral data correspond with the literature documented by Lizazman & Jong (2024).

3.4.6 Friedelin (71)

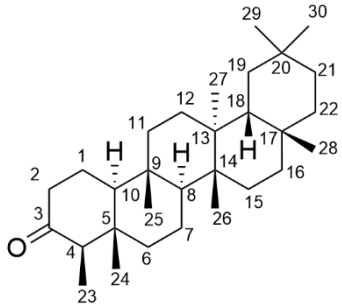

White-needle crystals. $C_{30}H_{50}O$. Melting point: 260-261 °C (263-265 °C, Sunil et al., 2021). IR v_{max} (cm^{-1}): 2925 & 2857 (aliphatic C-H), 1714 (strong non-conjugated C=O), 1460 & 1389 (CH_3 bending) Heilman et al. (2024). GC-MS (*m/z*): 426.0. ^{1}H NMR (400 MHz, $CDCl_3$) δ H: 2.38, 2.27 (2H, *m*, H-2), 2.24 (1H, *q*, 6.8, H-4), 1.96, 1.70 (1H, *m*, H-1), 1.71, 1.28 (2H, *d*, 11.9, H-6), 1.53, 1.35 (2H, *m*, H-16), 1.52 (1H, *m*, H-18), 1.48 (1H, *m*, H-10), 1.50, 1.31 (2H, *m*, H-21), 1.51, 0.96 (2H, *m*, H-22), 1.49, 1.36 (2H, *m*, H-7), 1.45, 1.25 (2H, *m*, H 11), 1.47, 1.27 (2H, *m*, H-15), 1.38 (1H, *t*, 9.2, H-8), 1.37, 1.22 (2H, *m*, H-19), 1.34, 1.32 (2H, *m*, H-12), 1.17 (3H, *s*, H-28), 1.04 (3H, *s*, H-27), 0.99 (3H, *s*, H-26), 0.99 (3H, *s*, H-30), 0.93 (3H, *s*, H-29), 0.88 (3H, *d*, 6.8, H-23), 0.86 (3H, *s*, H-25), 0.71 (3H, *s*, H-24). ^{13}C NMR (100 MHz, $CDCl_3$) δ C: 213.2 (C-3), 59.5 (C-10), 58.2 (C-4), 53.1 (C-8), 42.8 (C-18), 42.1 (C-5), 41.3 (C-6), 41.5 (C-2), 39.7 (C-13), 39.3 (C-22), 38.3 (C-14), 37.4 (C-9), 36.0 (C-16), 35.3 (C 19), 35.6 (C-11), 35.0 (C-29), 32.8 (C-21), 32.4 (C-15), 32.1 (C-28), 31.8 (C-30), 30.5 (C-12), 30.0 (C-17), 28.2 (C-20), 22.3 (C-1), 20.2 (C-26), 18.6 (C-27), 18.2 (C-7), 17.9 (C-25), 14.6 (C-24), 7.0 (C-23). Both the ^{1}H and ^{13}C NMR spectral data correspond with the literature documented by Heilman et al. (2024).

3.4.7 Stigmasterol (70)

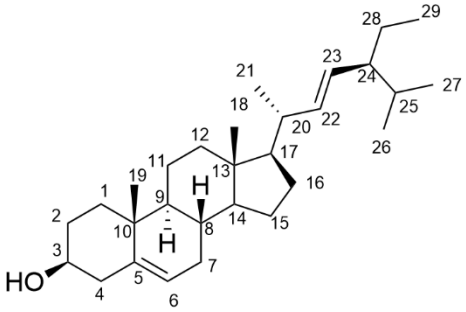

White needle crystal. $C_{29}H_{48}O$. Melting point: 174-175°C (175°C, (Zaine et al., 2024). IR v_{max} (cm^{-1}): 3482 (broad, O-H), 3030 (unsaturated alkene C-H), 2929 & 2868 (aliphatic C-H stretching), 1649 (unsaturated C=C stretching), 1463 & 1382 (CH_3 bending), 1052 (C-O stretching) Marliyana et al. (2021). GC-MS (*m/z*): 412.7. ^{1}H NMR (400 MHz, $CDCl_3$) δ H: 5.37 (1H, *m*, H-6), 5.17 (1H, *m*, H-23), 5.03 (1H, *m*, H-22), 3.54 (1H, *m*, OH-3), 1.03 (3H, *s*, H-18), 0.95-0.83 (12H, *m,* H-26, H-27, H-21, H-19), 0.69 (3H, *s*, H-29). ^{13}C NMR (100 MHz, $CDCl_3$) δ C: 140.9 (C-5), 138.4 (C-22), 129.4 (C-23), 121.8 (C-6), 71.9 (C 3), 56.9 (C-14), 56.2 (C-17), 51.3 (C-24), 50.2 (C-9), 42.4 (C-4), 42.3 (C-13), 40.6 (C-20), 39.8 (C-12), 36.6 (C-10), 36.3 (C-8), 32.0 (C-25), 31.8 (C-1), 29.3 (C-7), 28.4 (C-2), 28.4 (C-16), 25.5 (C-28), 24.5 (C-11), 24.5 (C-15), 19.9 (C-26), 19.5 (C-19), 19.1 (C-27), 18.9 (C-21), 12.2 (C-29), 12.0 (C-18). Both the ^{1}H and ^{13}C NMR spectral data correspond with the literature documented by Marliyana et al. (2021).

3.5 Antibacterial Assay

3.5.1 Well Diffusion Method

The antibacterial activity was done through the well-diffusion method, adapted from Zamakshshari et al. (2024). All seven compounds isolated were tested against five bacterial strains: *Acinetobacter baumannii*, *Klebsiella pneumoniae*, *Staphylococcus aureus*, *Pseudomonas aeruginosa*, and *Escherichia coli*. The bacterial culture was adjusted to the optical density (OD) of 0.5 McFarland standard, which represents 1.5×10^8 CFU/mL by using the spectrophotometers (ranging from 0.08 to 0.12 Abs). The positive control used was ampicillin, and the negative control used was DMSO. A 5 mg extract was dissolved using DMSO to reach a 1 mg/mL concentration for the complexity and lower concentration of active constituents, while the isolated compounds were dissolved to a concentration of 0.1 mg/mL using DMSO, in line with established practices in natural product research on antibacterial studies (Rahman et al., 2022). Wells were punched on the inoculated agar plate and 50 µL of the sample was pipetted into it. Then, the petri dish was incubated for 24 hours at 37 °C. The inhibition zone was determined by measuring the diameter around the punched well where there was no bacterial growth. Each sample was done in triplicate, and all seven compounds, including the *n*-hexane, chloroform, and methanol extracts, were tested.

3.5.2 Minimum Inhibitory Concentration (MIC)

The MIC was defined as the minimum concentration of the antibacterial agent needed to prevent bacterial growth. The compounds and plant extracts that showed moderate to strong activity (≥ 10 mm inhibition zone) were further tested for the MIC and MBC values against each bacterial strain. The MIC values for each compound and its extract were assessed using the broth microdilution technique, as adapted with slight modifications from previous studies (Noh & Jong, 2020; Tee et al., 2018). Mueller-Hinton broth was used as the medium, and DMSO (negative control) was used to dissolve plant extracts before undergoing a two-fold serial dilution to achieve concentrations from 1.0 to 1.95×10^{-3} mg/mL; compounds underwent a two-fold serial dilution to achieve concentrations from 0.1 to 1.95×10^{-3} mg/mL. The bacterial cultures were adjusted to an OD equivalent to the 0.5 McFarland standard, which represents 1.5×10^8 CFU/mL by using the spectrophotometers (ranging from 0.08 to 0.12 Abs). A 100 µL of bacterial suspension was added to 96-well

microplates and 100 µL of each concentration of plant extracts. The plates were then incubated at 37.5 °C for 18 hours to allow bacterial growth in the presence of compounds and extract.

3.5.3 Minimum Bactericidal Concentration (MBC)

The MBC is defined as the minimal concentration of the antibacterial agent needed to kill the bacteria. It was determined using the samples from the MIC investigation that did not show turbidity or any bacterial growth and subcultured them onto a new agar plate in triplicate and incubated at 37.5 °C for another 18 hours. Following the incubation time, the colony development on the subcultured plate was observed to determine its MBC (Abdul Rahman et al., 2022).

3.6 Statistical Analysis

All experimental data were expressed as mean ± standard error of the mean (SEM). Data processing and statistical analysis were performed using IBM SPSS Statistics 27. All experiments were conducted in triplicate. One-way analysis of variance (ANOVA) was employed to assess differences among the tested samples, and it was performed for each bacterial strain. Significant difference between groups were further analysed using Tukey's post-hoc test or Games-Howell post-hoc test. Statistical significance was set at $p < 0.05$.

CHAPTER 4:

FINDINGS AND DISCUSSION

4.1 Overview

Calophyllum nodosum, being an endemic species in Sarawak, has received little attention compared to other *Calophyllum* species. With sustained research interest in discovering novel antimicrobial agents and the known fact that the genus *Calophyllum* is a source of bioactive secondary metabolites, this investigation, specifically on phytochemical constituents and antibacterial potential of *C. nodosum* was initiated. The isolation and purification of the *n*-hexane and chloroform extracts of *C. nodosum* stem bark by utilising various chromatographic techniques have led to the discovery of seven compounds, namely nodosuxanthone (**89**), trapezifolixanthone (**20**), caloxanthone C (**5**), 1-hydroxy-7-methoxyxanthone (**27**), canumolactone (**90**), friedelin (**71**), and stigmasterol (**70**). The antibacterial capability towards several bacterial strains was also discussed.

4.2 Characterisation of Secondary Metabolites from *C. nodosum*

4.2.1 Characterisation of Nodosuxanthone (89)

Figure 4-1:
Structure of nodosuxanthone (89)

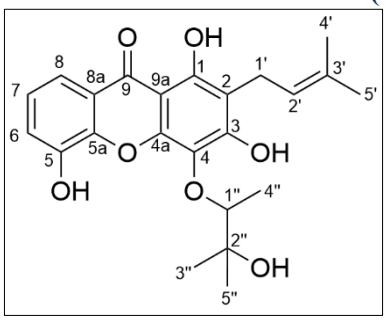

Nodosuxanthone (**89**) is the first xanthone-based, also a newly undescribed compound to be isolated in this study that exhibits this unique structural framework (Figure 4-1). Compound **89** was a yellowish crystal powder (18.3 mg) that was isolated from fraction CnH17o2b5 within the *n*-hexane extract of *C. nodosum*, with a melting point of 118-120 °C. Its LC-MS (ESI^-) chromatogram (Figure 4-2) revealed a molecular ion peak at *m/z* 414.2000, consistent with its proposed molecular formula of $C_{23}H_{26}O_7$.

Figure 4-2:
LC-MS chromatogram of compound 89

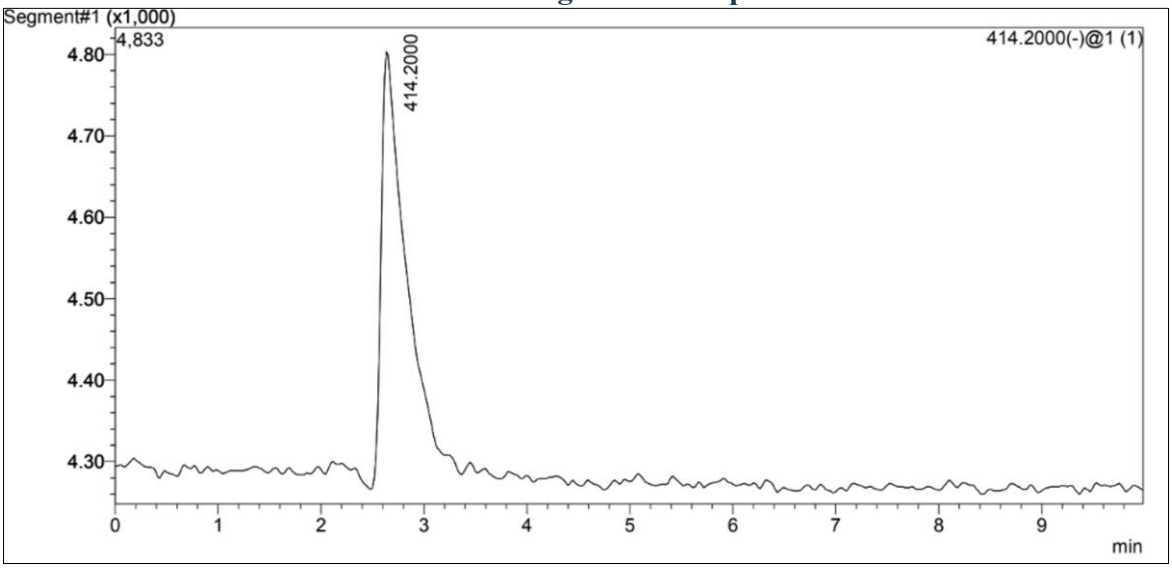

The IR spectrum of compound **89** (Figure 4-3) showed strong absorptions at 3260 cm^{-1} due to the hydroxyl group in the compound (Krysa et al., 2022), 3080 - 3030 cm^{-1} for the stretching of unsaturated C-H (Sun, 2005), 1647 cm^{-1} for the conjugated carbonyl group, 1580 cm^{-1} for the carbon-carbon aromatic groups, 1222 cm^{-1} for its C-O-C stretching, and

1100 for C-O-C stretching. The UV spectrum (Figure 4-4) [λ_{max} (MeOH) 204, 221, 244, and 325 nm] refers to the presence of the xanthone skeleton in nodosuxanthone (**89**) (Kurniawan et al., 2021).

Figure 4-3:
IR spectrum of compound 89

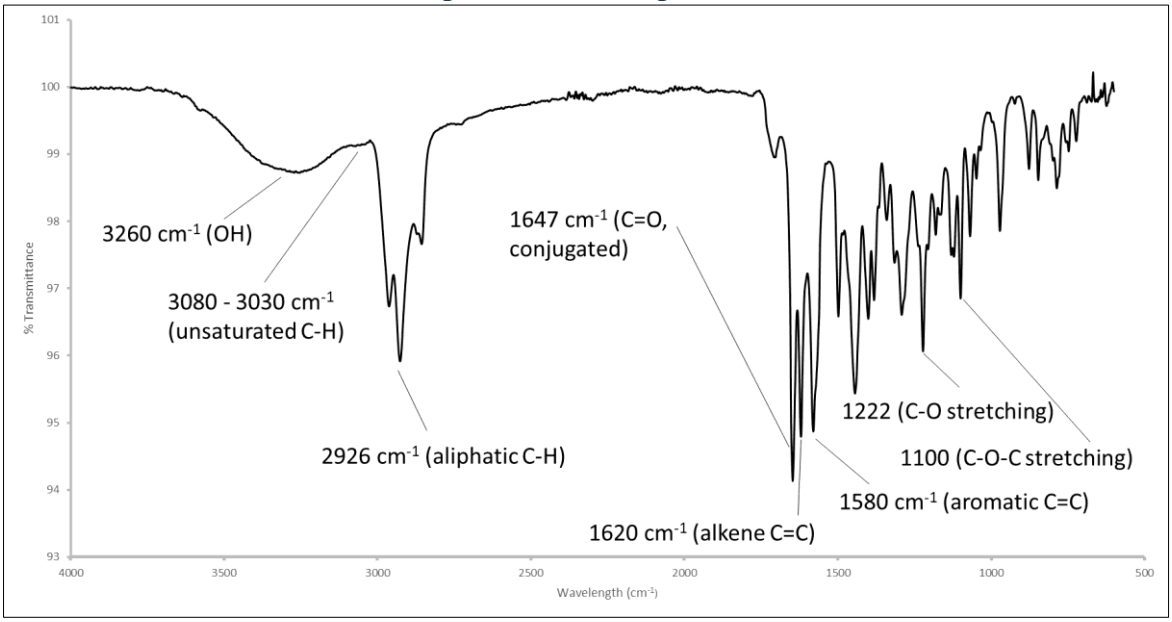

Figure 4-4:
UV-Vis of compound 89

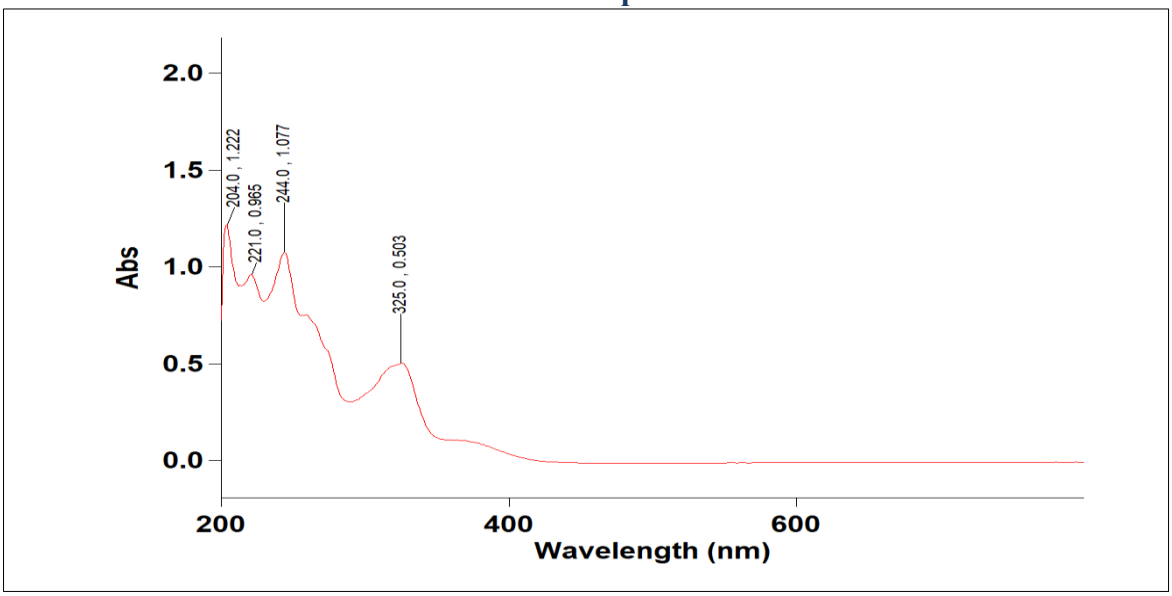

The ^{1}H NMR spectrum (Figure 4-6) displayed a marked downfield resonance at δ_H 13.51 corresponds to a chelated hydroxyl proton, as the strong deshielding effect arises from the intramolecular hydrogen bonding with the adjacent carbonyl group at C-9. This interaction enhances electron withdrawal through both resonance and inductive effects of

the conjugated carbonyl system, stabilizing the hydrogen-bonded form and shifting the proton significantly downfield (Silverstein et al., 2015). Another hydroxyl proton at δ_H 9.26 was less deshielded, indicating a weaker electronic interaction with neighboring substituents.

The protons of δ_H 7.69, 7.37, and 7.25 suggest the presence of three aromatic protons that were in a trisubstituted form within the compound. Furthermore, a doublet (δ_H 3.30) for H-1′, a triplet (δ_H 5.29) for olefinic proton H-2′, and two methyl groups resonating at δ_H 1.78 and δ_H 1.66, is a typical indicator of an isoprenyl group (Hakim et al., 2021; Su et al., 2003). The more downfield position of the methylene proton at H-1′ relative to being a typical aliphatic methylene is due to the inductive deshielding effect of the adjacent oxygen atom and the anisotropic influence of the aromatic ring (Pavia et al., 2015). Meanwhile, the olefinic proton at δ_H 5.29 reflects conjugation within the prenyl moiety and interaction with the aromatic π-system, leading to deshielding through resonance effects (Claridge, 2016).

Moreover, the quartet (δ_H 4.61) that corresponds to methine group, two singlet peaks (δ_H 1.36 and 1.64), and a doublet peak (δ_H 1.44), were all corresponds as methyl protons. The methine proton at δ_H 4.61 is significantly deshielded due to the attachment to an oxygen-bearing carbon, where the strong negative inductive effect of the electronegative oxygen atom reduces electron density around the proton (Fleming & Williams, 2020). The associated methyl resonances reflect electron-donating positive-inductive effects of alkyl substituents, indicating the presence of 3-hydroxy-3-methylbutan-2-yl)oxy chain, as shown in the HMBC analysis (Figure 4-5).

The ^{13}C NMR spectrum (Figure 4-7) of compound **89** exhibited 23 carbons, which were supported by experiments of the DEPT spectrum (Figure 4-8) as five methyls (-CH_3), five methines (-CH-), a methylene (-CH_2-), and twelve quaternary carbons (-C-).

Figure 4-5:
HMBC (^2J and ^3J) ^{1}H-^{13}C correlations and ^{1}H-^{1}H COSY correlations of compound 89

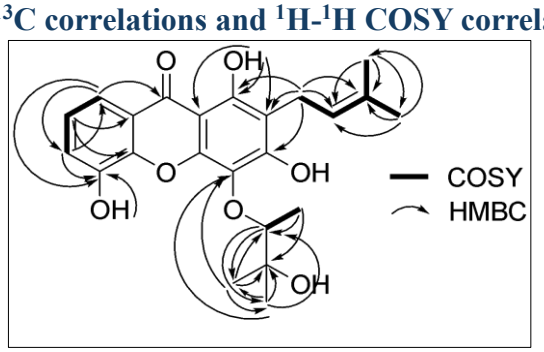

Figure 4-6:
^{1}H NMR spectrum of compound 89

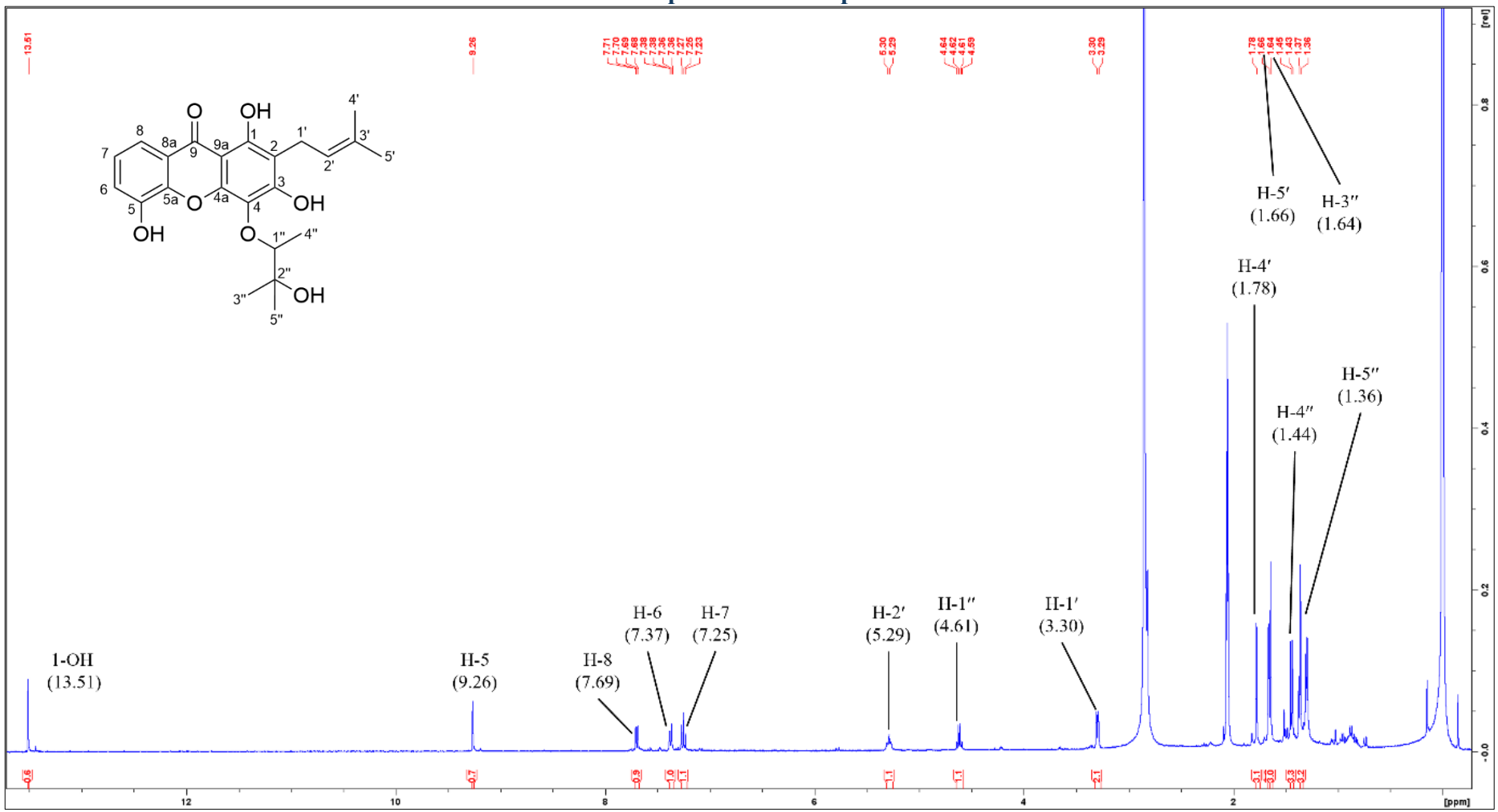

Figure 4-7:
^{13}C NMR spectrum of compound 89

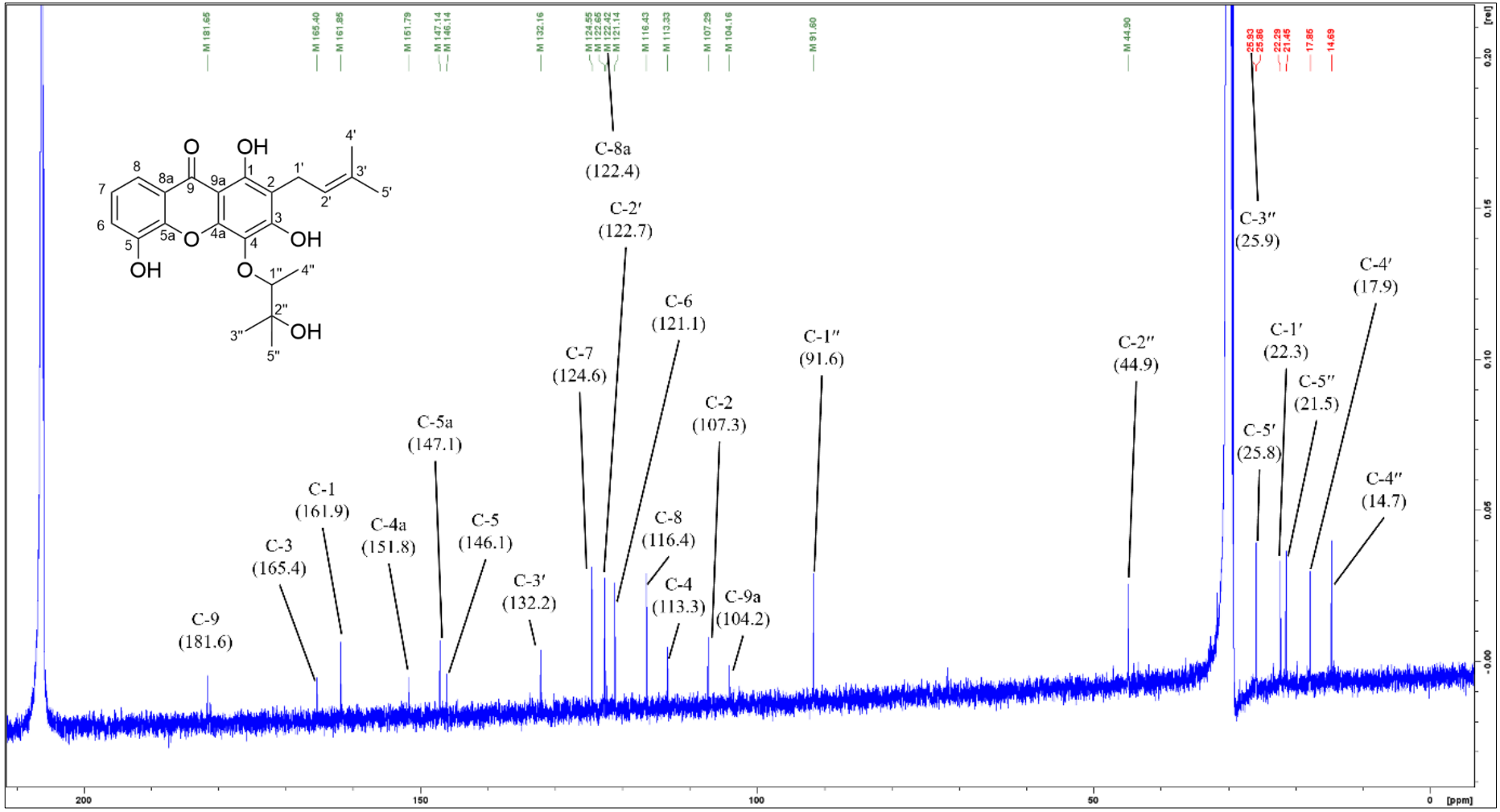

Figure 4-8:
DEPT ^{13}C NMR spectra of compound 89

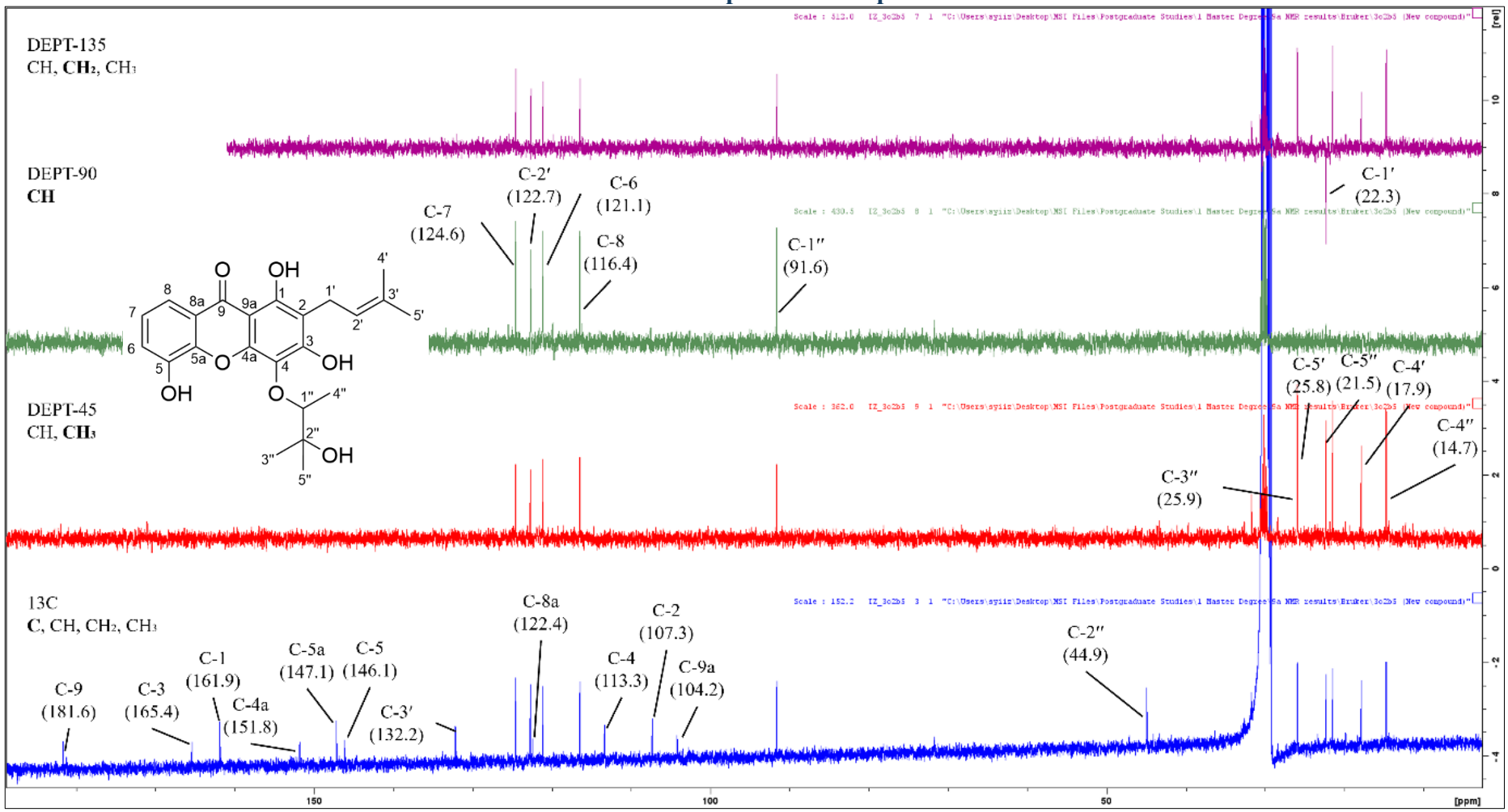

The HSQC and HMBC (Figure 4-9 till Figure 4-15) correlations further confirm the presence of the alkoxy group. The proton signal at δ_H 4.61 exhibits a ^3J correlation with carbon signals at δ_C 21.5 and 25.9. Additionally, the δ_H 1.44 proton shows both ^2J and ^3J correlations with δ_C 44.9 and 91.6, respectively. The δ_H 1.64 proton establishes ^2J to ^5J correlations with δ_C 21.5, 44.9, 91.6, and 113.3. Furthermore, the ^2J and ^3J correlations of δ_H 1.36 with δ_C 25.9, 44.9, 91.6, and 113.3. Meanwhile, the COSY (Figure 4-9) analysis also showed a cross-peak between protons of δ_H 4.61 (H-1″) with δ_H 1.44 (H-4″), further supporting the presence of the alkoxy chain in this compound.

The connectivity of the three-ring system (A-ring, B-ring, and C-ring) is confirmed through HMBC correlations, where the aromatic B-ring protons of δ_H 7.69 exhibit correlations with the carbonyl group of the pyranone C-ring δ_C 181.6 and another proton of δ_H 7.25 exhibits correlations with the carbons at the pyranone C-ring of δ_C 122.4 and 147.1. Additionally, the A-ring connectivity is established by the correlation of the hydroxyl group (δ_H 13.51) with the pyranone C-ring carbon at δ_C 161.9. The COSY spectrum also portrayed the *ortho* and *meta*-couplings of the proton resonating at δ_H 7.69 (H-8) with respective proton peaks at δ_H 7.25 (H-7) and δ_H 7.37 (H-6), suggesting these three protons are within the same ring system, which can be concluded as in the aromatic B-ring.

The structure was further clarified through the analysis of HMBC as the protons were set to their respective direct carbons' bonding based on the HSQC spectrum. The ^2J - ^3J correlation between the chelated hydroxyl proton at δ_H 13.51 with δ_C 161.9 (C-1), δ_C 107.3 (C-2), and δ_C 104.2 (C-9a) has confirmed its position at C-1 (Araya-Maturana et al., 2008). The isoprenyl group's position was deduced at C-2 through the ^2J correlation of protons at δ_H 3.30 with δ_C 107.3 (C-2) and the ^3J correlation of the protons at δ_H 3.30 with δ_C 161.9 (C-1) and δ_C 165.4 (C-3). Moreover, the other OH group at δ_H 9.26 gave the HMBC correlation with the carbon peak at δ_C 146.1, proposing its position at C-5. The long-range correlations of HMBC between protons of δ_H 1.64 (H-3″) and δ_H 1.36 (H-5″) with δ_C 113.3 (C-4) showed that the attachment of (3-hydroxy-3-methylbutan-2-yl)oxy chain is at C-4 (Araya-Maturana et al., 2008). Table 4-1 shows all the assignments of compiled spectra from 1D and 2D NMR.

Therefore, the structure of compound **89** was elucidated as proposed in Figure 4-1 and herein reported as a new xanthone, named nodosuxanthone, isolated for the first time from the *n*-hexane extract of the stem bark of *Calophyllum nodosum* collected in Sarawak, Malaysia.

Figure 4-9:
$^{1}H - {}^{1}H$ COSY spectrum of compound 89

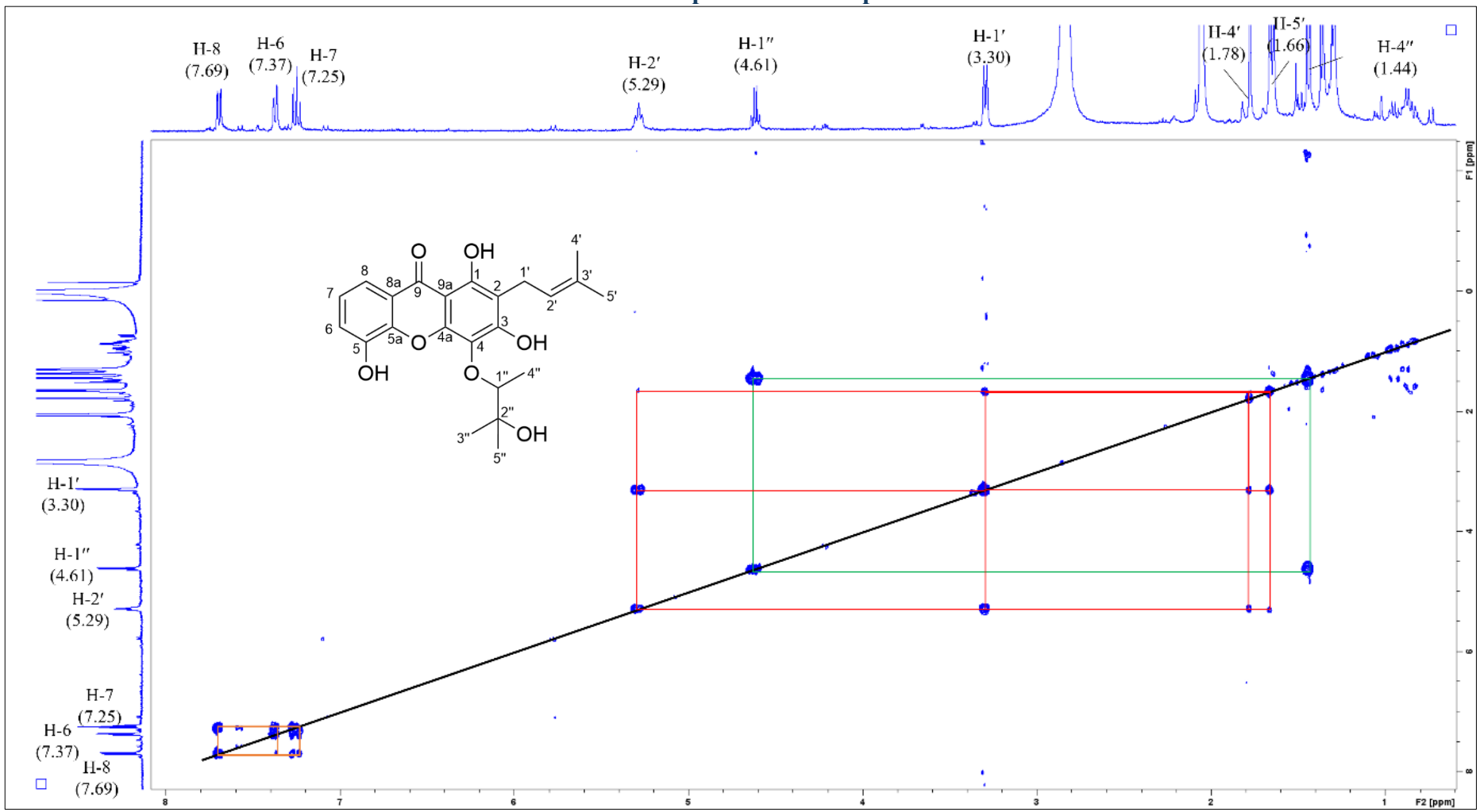

Figure 4-10:
HSQC spectrum of compound 89

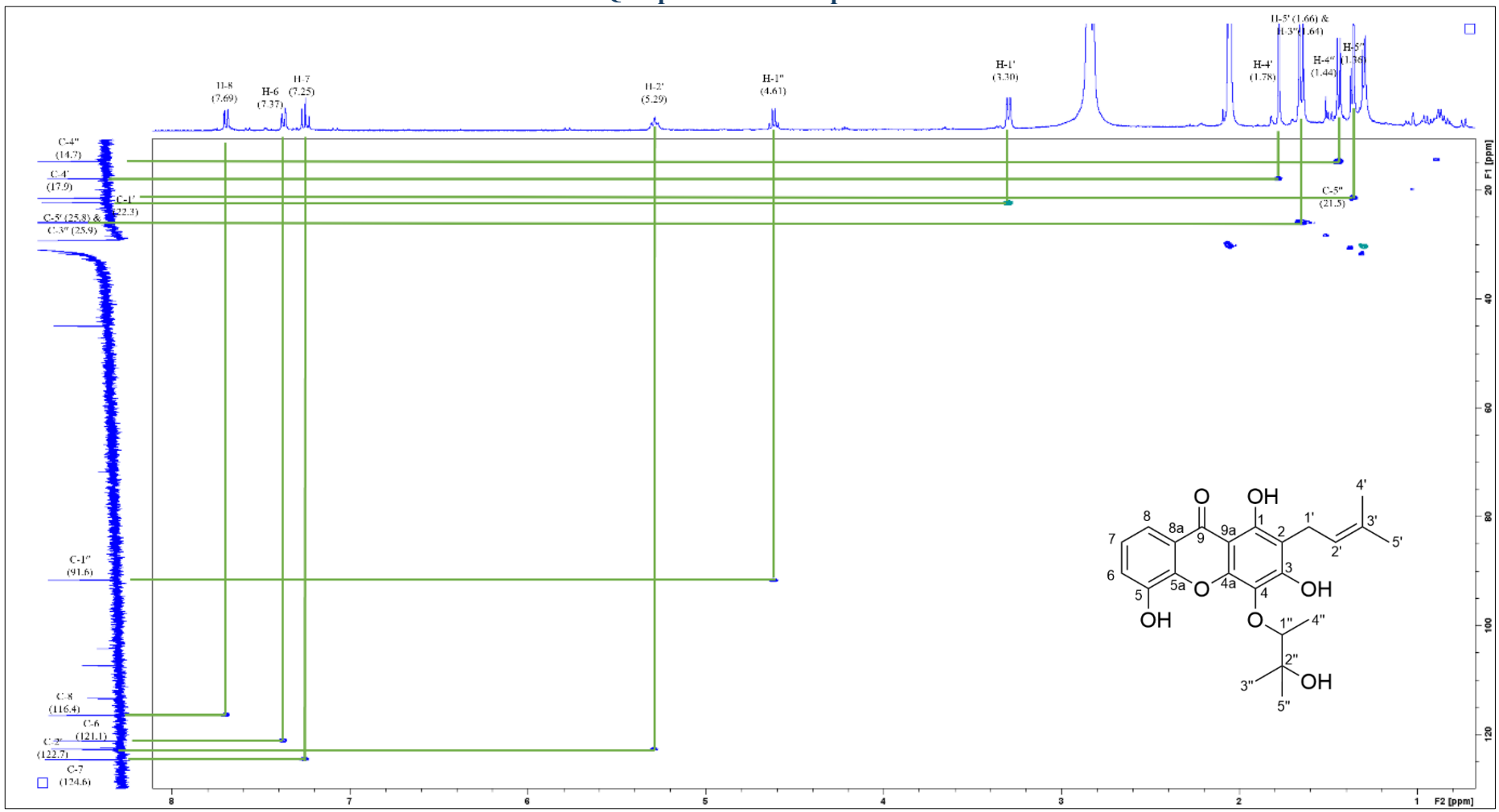

Figure 4-11:
Expanded HSQC spectrum of compound 89 in the 0.0-3.5 ppm region

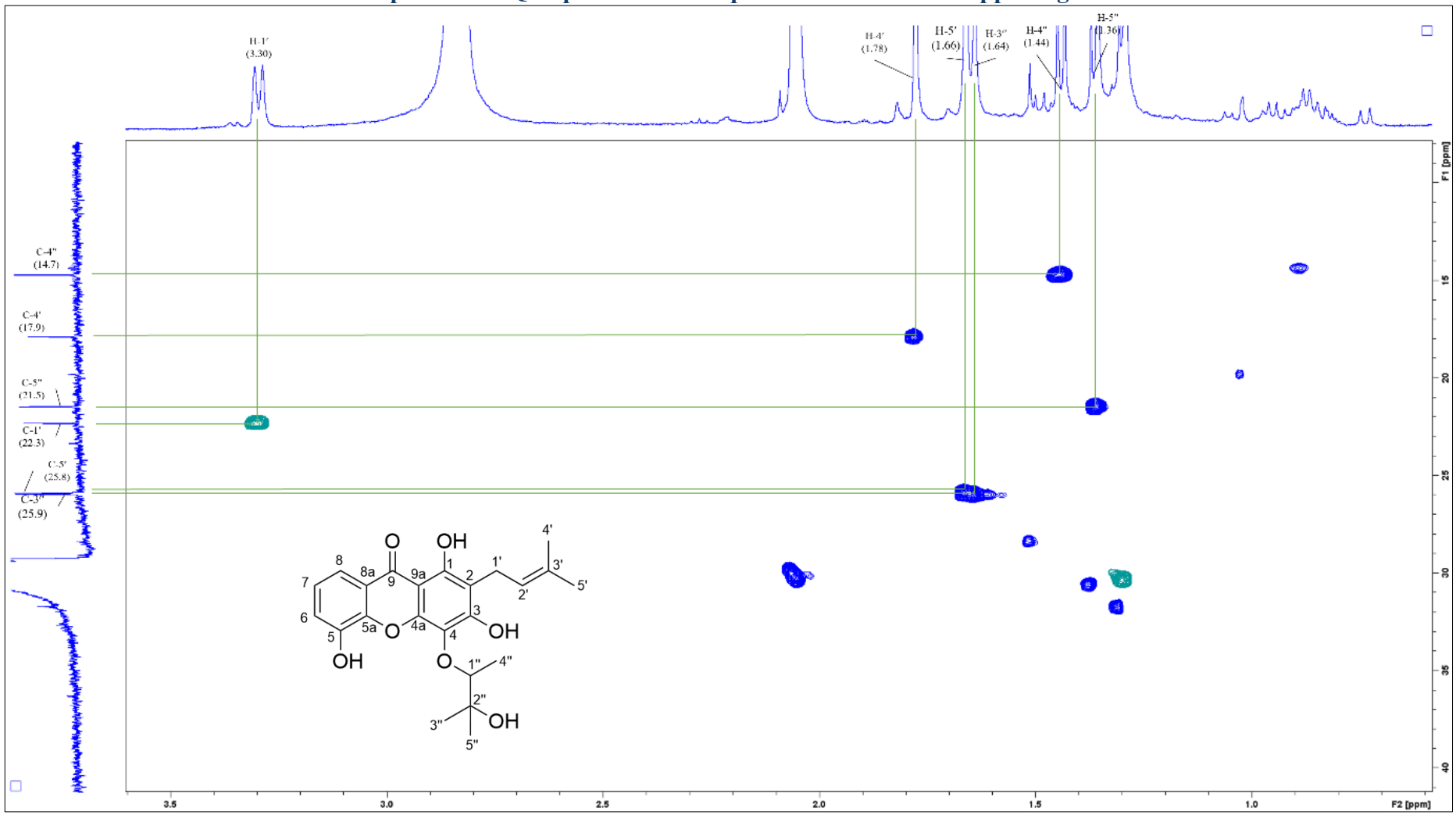

Figure 4-12:
Expanded HSQC spectrum of compound 89 in the 4.4-8.0 ppm region

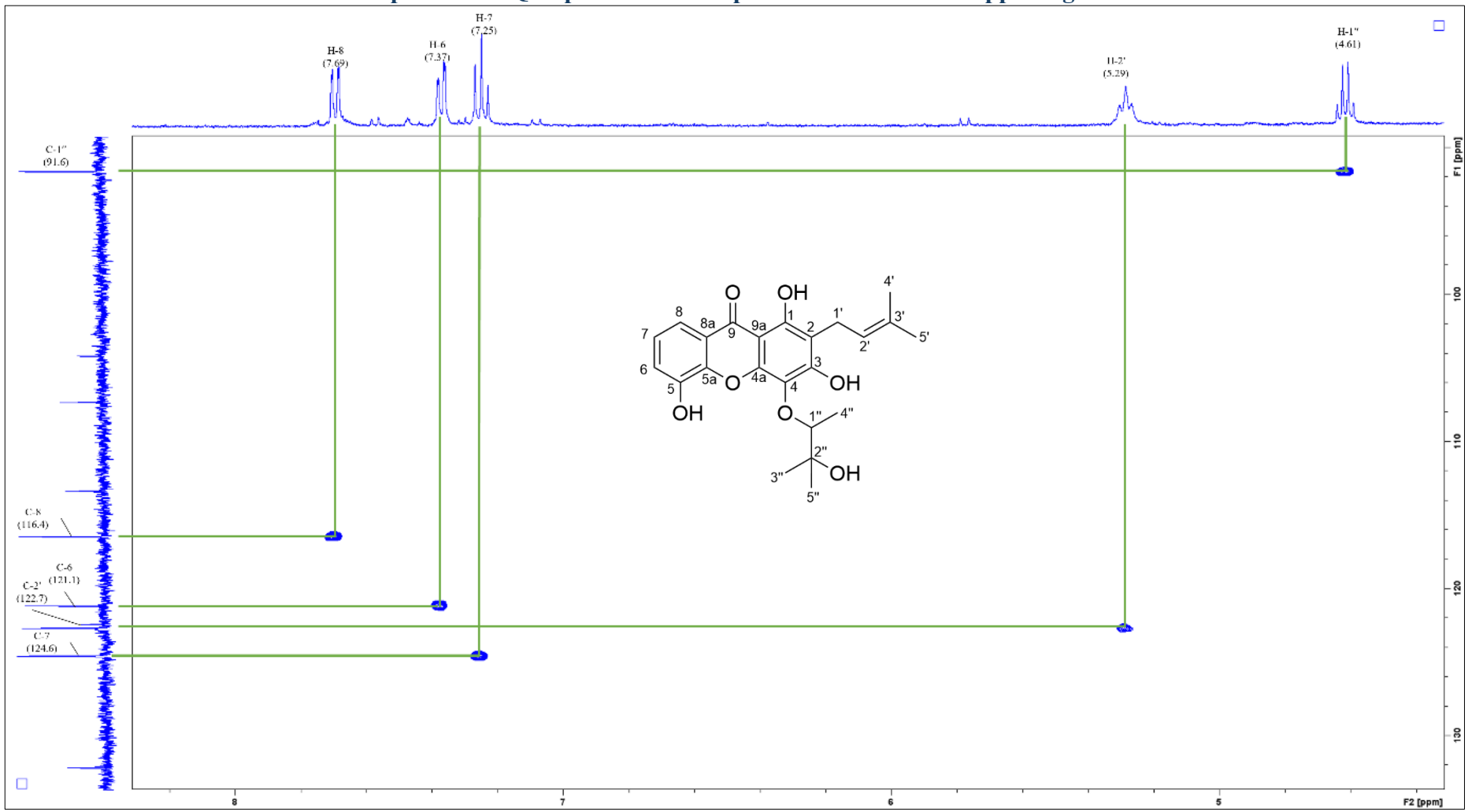

Figure 4-13:
HMBC spectrum of compound 89

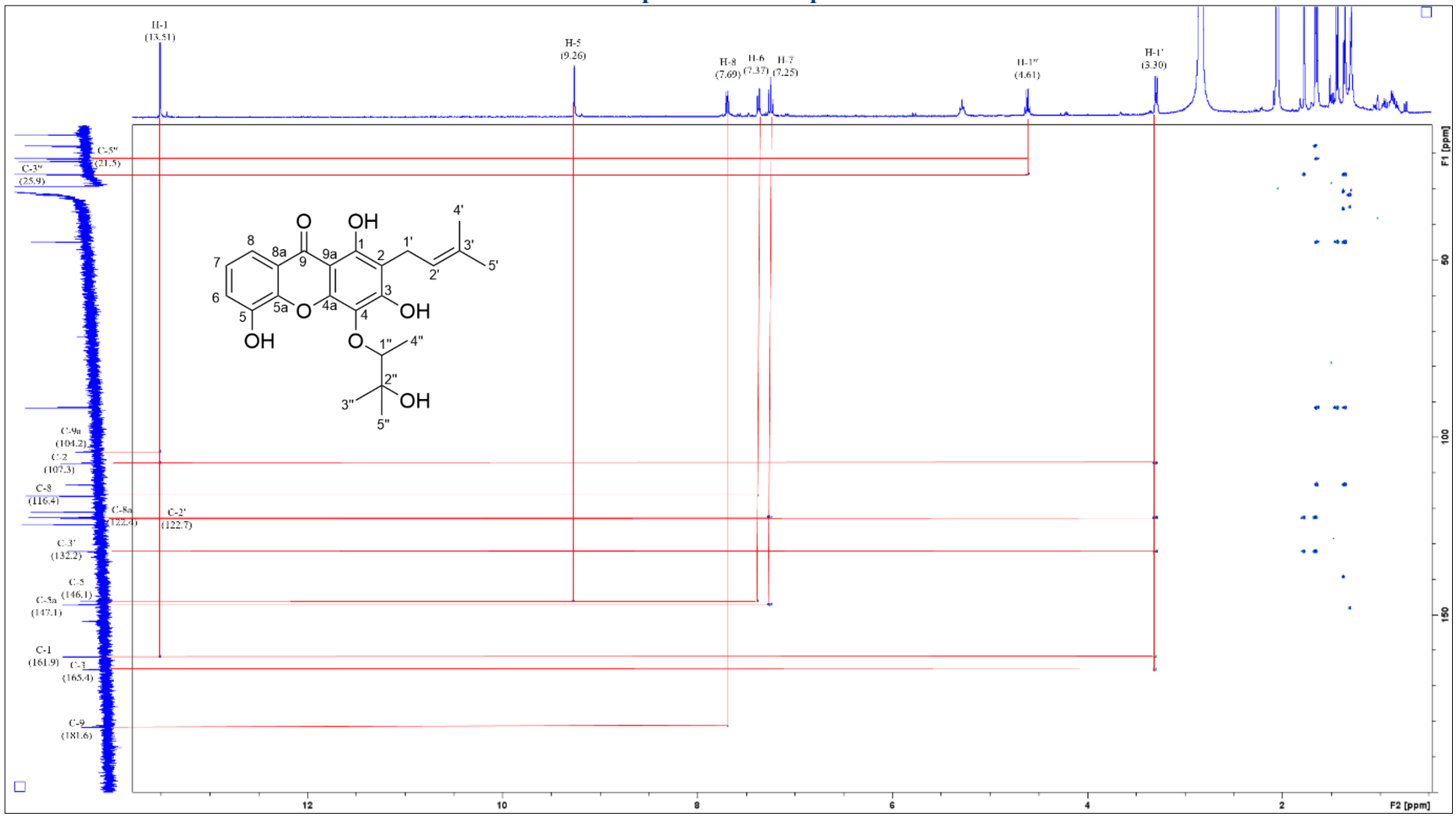

Figure 4-14:
Expanded HMBC spectrum of compound 89 in the 0.0-2.0 ppm region

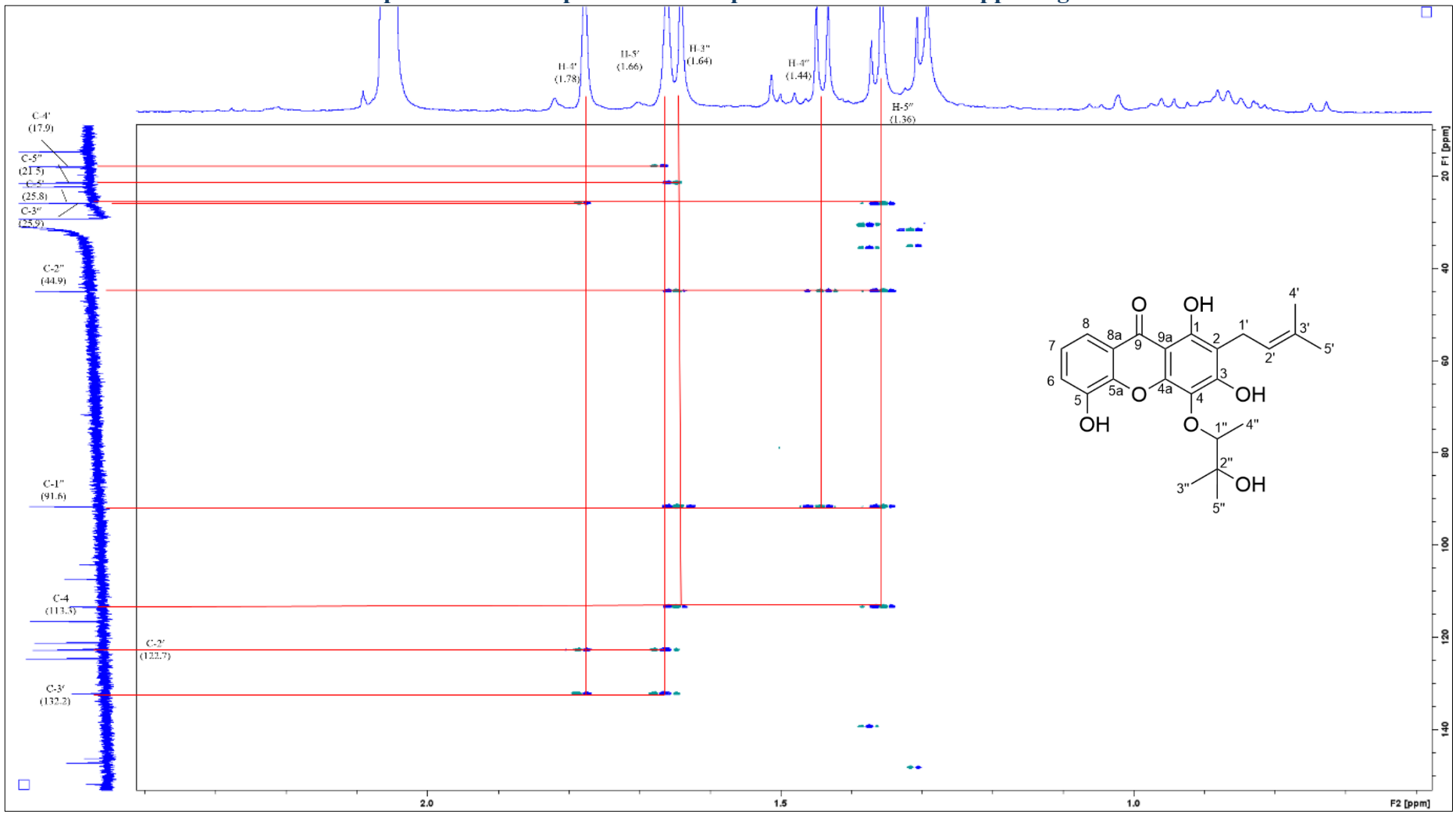

Figure 4-15:
Expanded HMBC spectrum of compound 89 in the 7.0-13.6 ppm region

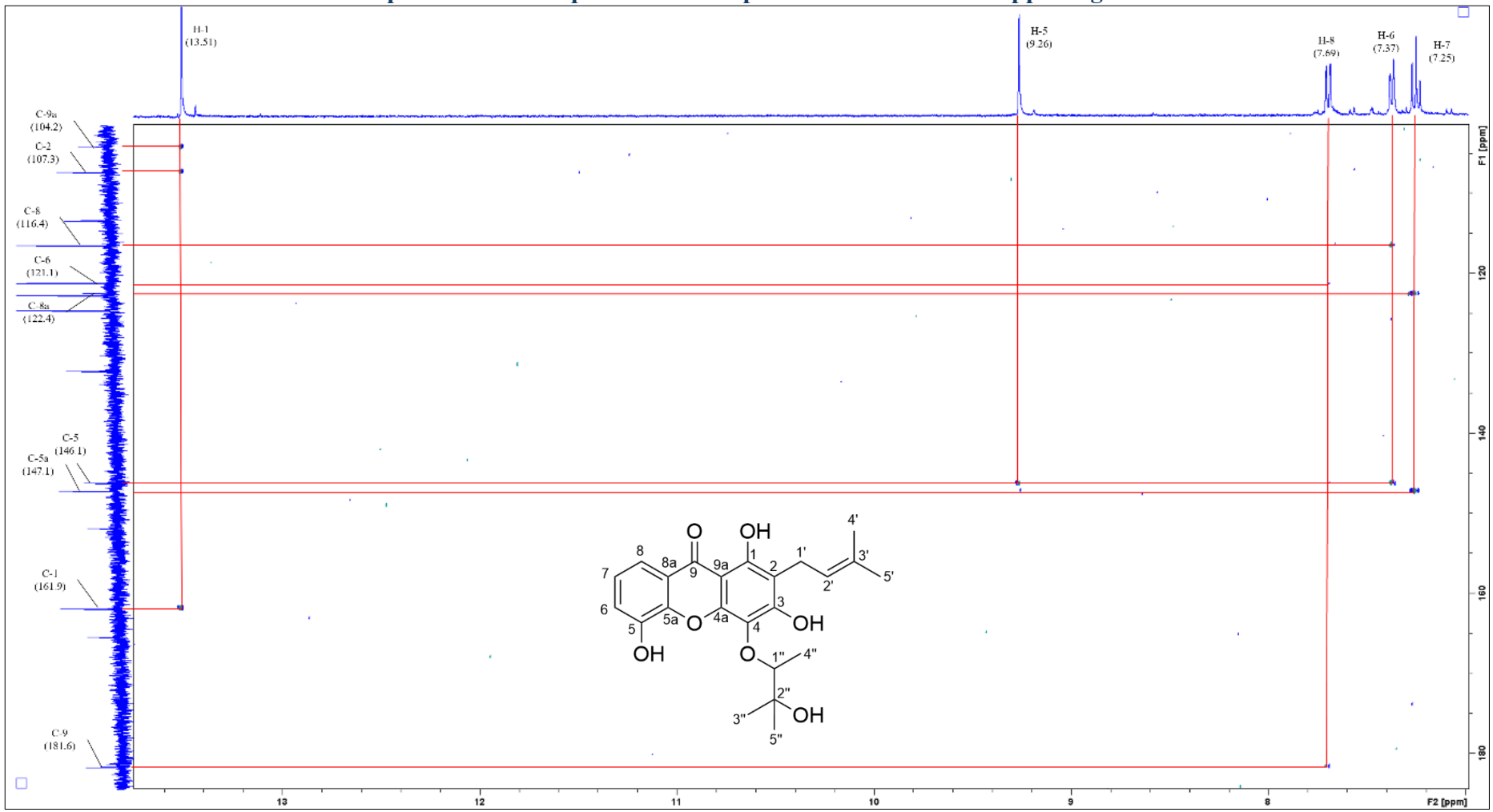

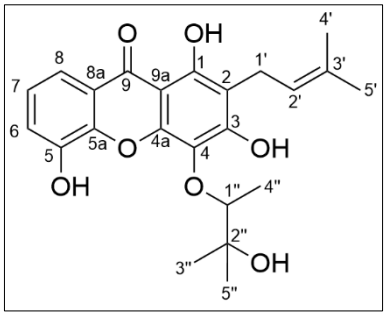

(**89**)

Table 4-1:
NMR assignment of nodosuxanthone (89)

No.	^{13}C (δ)	^{1}H (δ) (HSQC)	^{1}H-^{13}C HMBC	^{1}H-^{1}H COSY
1	161.9	13.51 (*s*, 1H, -OH)	C-1, C-2, C-9a	-
2	107.3	-	-	-
3	165.4	-	-	-
4	113.3	-	-	-
4a	151.8	-	-	-
5	146.1	9.26 (*s*, 1H, -OH)	C-5	-
5a	147.1	-	-	-
6	121.1	7.37 (*dd*, 1.5 Hz, 7.9 Hz, 1H)	C-8, C-5	H-7, H-8
7	124.6	7.25 (*t*, 7.9 Hz, 1H)	C-8a, C-5a	H-6, H-8
8	116.4	7.69 (*dd*, 1.5 Hz, 7.9 Hz, 1H)	C-6, C-5, C-9	H-7, H-6
8a	122.4	-	-	-
9	181.6	-	-	-
9a	104.2	-	-	-
1′	22.3	3.30 (*d*, 7.3 Hz, 2H)	C-2, C-2′, C-3′, C-1, C-3	H-5′, H-4′, H-2′
2′	122.7	5.29 (*t*, 7.3 Hz, 1H)	-	H-5′, H-4′, H-1′
3′	132.2	-	-	-
4′	17.9	1.78 (*s*, 3H)	C-5′, C-2′, C-3′	H-5′, H-1′, H-2′
5′	25.8	1.66 (*s*, 3H)	C-4′, C-2′, C-3′	H-4′, H-1′, H-2′
1″	91.6	4.61 (*q*, 6.6 Hz, 1H)	C-5″, C-3″	H-4″
2″	44.9	-	-	-
3″	25.9	1.64 (*s*, 3H)	C-5″, C-2″, C-1″, C-4	-
4″	14.7	1.44 (*d*, 6.6 Hz, 3H)	C-2″, C-1″	H-1″
5″	21.5	1.36 (*s*, 3H)	C-3″, C-2″, C-1″, C-4	-

4.2.2 Characterisation of Trapezifolixanthone (20)

Figure 4-16:
Structure of compound 20

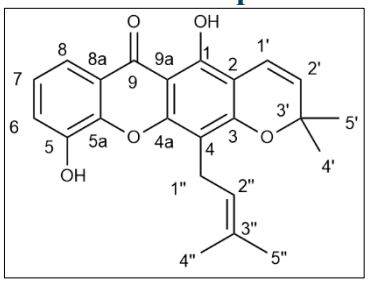

Compound **20** (Figure 4-16) was obtained as a yellow needle-like crystal (27.5 mg) from the fraction CnH17o2b1 and CnC3b6c3 of the *n*-hexane and chloroform extracts, respectively, with a melting point of 163-164 °C, like the reported value of 168-169 °C (Lizazman et al., 2023). The molecular formula of compound **20** was determined as $C_{23}H_{22}O_5$, deduced from the molecular peak at *m/z* 378 in the GC-MS spectrum (Figure 4-17).

Figure 4-17:
GC-MS for compound 20

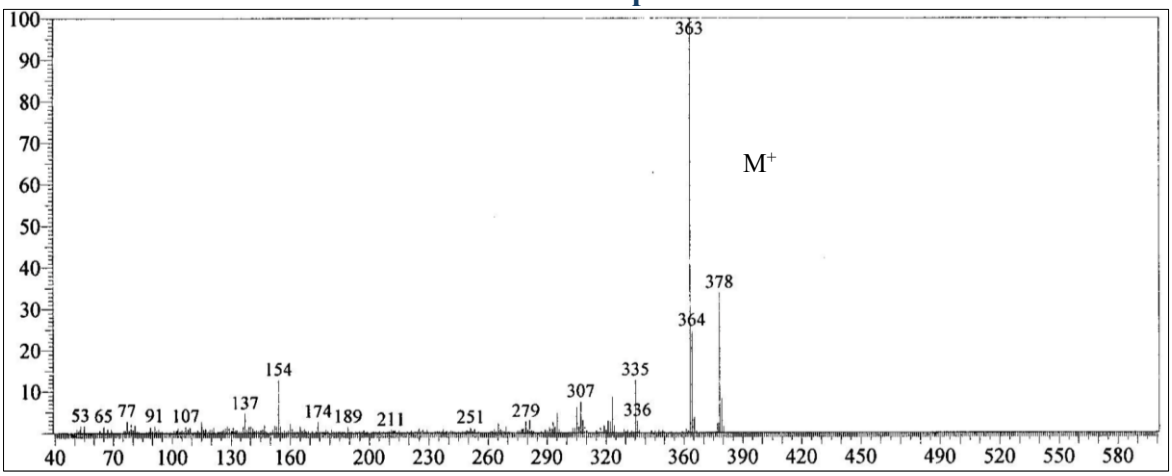

The UV-Vis spectrum of compound **20** displayed a maximum absorption at λ_{max} = 286 nm, indicating the presence of a conjugated system within the molecular structure. The FTIR spectrum demonstrated the presence of typical functional groups for the class of xanthone, such as a broad absorption band at 3323 cm^{-1}, which corresponded to the hydroxyl (-OH) groups, a weak 3030 – 3070 cm^{-1} absorption of aromatic C-H stretching, an aliphatic C-H stretching at 2928 cm^{-1} (Tejamukti et al., 2020) while an intense absorption at 1651 cm^{-1} was attributed to the conjugated carbonyl (C=O) stretching (Sun, 2005). An absorption at 1621 cm^{-1}, indicating presence of unsaturated alkene C=C stretching was observed.

Additionally, aromatic C=C stretching was observed at 1580 cm^{-1} and the absorption at 1286 cm^{-1} was attributed to C-O stretching (Abdel-Kerim & Shoeb, 1972).

The ^{1}H NMR spectrum of compound **20** (Figure 4-19) exhibited the most shifted singlet peak, chelated, which represented the chelated hydroxyl proton at δ_H 13.34, while another hydroxyl group appeared as a broad singlet in the downfield region at δ_H 9.24. The proton supported the presence of a 3-methylbut-2-enyl moiety signal at δ_H 3.57 (H-1″), 5.31 (H-2″), 1.66 (H-4 ″), and 1.87 (H-5″). A singlet resonance at δ_H 1.51 (6H, *s*, H-4′, H-5′), integrating for six protons, was indicative of two methyl groups on the pyrano ring, in addition to a pair of *ortho*-coupled doublets at δ_H 6.72 (1H, *d*, H-1′) and 5.77 (1H, *d*, H-2′) with a similar coupling constant of 10.0 Hz further confirmed the presence of the pyrano ring that fused to the xanthone core.

The ^{13}C NMR (Figure 4-20) and DEPT-135 spectra of compound **20** concluded one carbonyl carbon at δ_C 182.2 (C-9), eleven quaternary carbons (-C-), six methines (-CH), one methylene ($-CH_2$), and four methyl ($-CH_3$) carbons. Several carbon signals like the carbonyl carbon at δ_C 181.1 (C-9), the quaternary carbons at δ_C 159.1 (C-3), δ_C 156.6 (C-1), δ_C 154.8 (C-4a), δ_C 147.2 (C-5), and δ_C 146.4 (C-5a) exhibited significant deshielding effects due to the influence of an electro-withdrawing group, oxygen and the conjugation within the xanthone scaffold, shifting them more downfield.

The HSQC spectrum provided ^{1}J correlations, confirming the direct attachment of protons to their corresponding carbons (^{1}H-^{13}C). Meanwhile, the HMBC spectrum of compound **20**, as shown in Figure 4-18, exhibited ^{2}J to ^{3}J correlations, with cross-peaks observed between H-4′ and H-5′ (δ_H 1.51) with C-3′ (δ_C 79.0), indicating that both methyl groups were directly bonded to the same carbon. Additionally, the proton resonance of H-1′ (δ_H 6.72) correlated with C-2 (δ_C 104.0), confirming the attachment of the pyrano ring at carbons C-2 and C-3. The long-range coupling of H-1″ (δ_H 3.57) with C-4 (δ_C 108.5), C-4a (δ_C 154.8), and C-3 (δ_C 159.1) further supported the positioning of the prenyl moiety at C-4.

Figure 4-18:
HMBC (^{2}J and ^{3}J) ^{1}H-^{13}C correlations and ^{1}H-^{1}H COSY correlations of compound 20

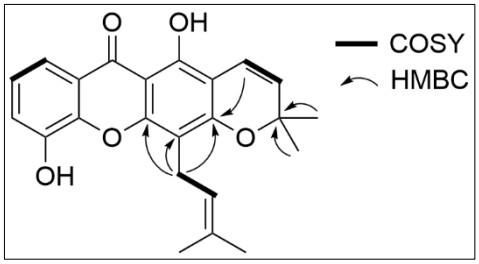

In addition, the COSY spectrum demonstrated couplings between benzylic proton H-1″ and olefinic proton H-2″, confirming an allylic coupling system within the prenyl moiety. Furthermore, an *ortho*-coupling was identified in the benzene ring between the triplet resonance (δ_H 7.28, H-7) and the doublet of doublets resonances (δ_H 7.69, H-8), whereby both exhibited a coupling constant of 8.0 Hz. Conversely, a *meta*-coupling was also observed between the triplet resonance (δ_H 7.28, H-7) and the doublet of doublets (δ_H 7.39, H-6), characterised by a coupling constant of 1.5 Hz. This suggested the trisubstituted aromatic ring present in the xanthone scaffold of compound **20**. The acquired spectroscopy data were compared with the published information in Table 4-2, and compound **20** was characterised as trapezifolixanthone (Figure 4-16). Other 2D-NMR data of compound **20**, such as DEPT-45, -90, -135, COSY, HSQC, and HMBC spectra, can be retrieved from Appendix 1-8.

Figure 4-19:
^{1}H NMR spectrum of compound 20

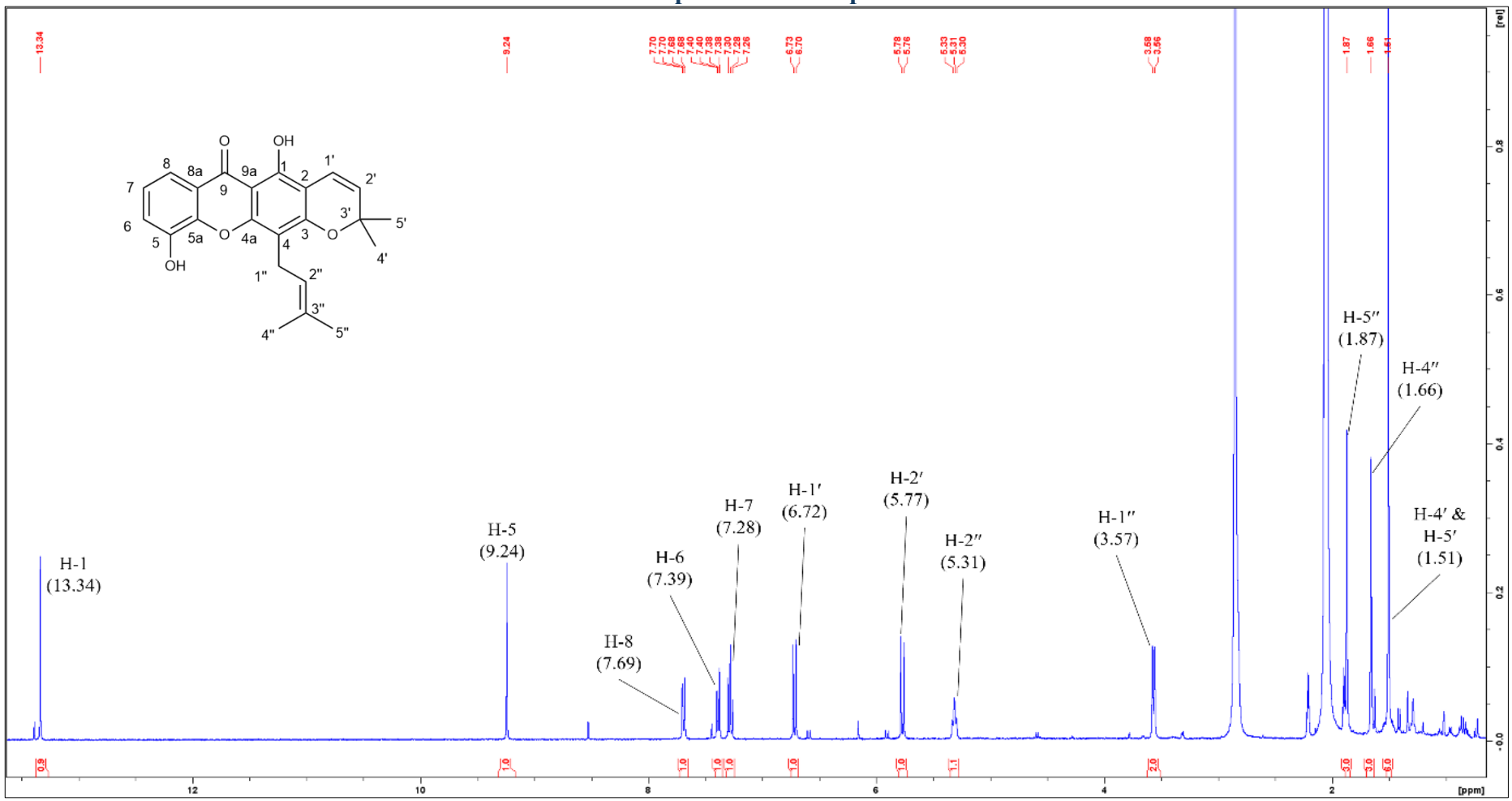

Figure 4-20:
^{13}C NMR spectrum of compound 20

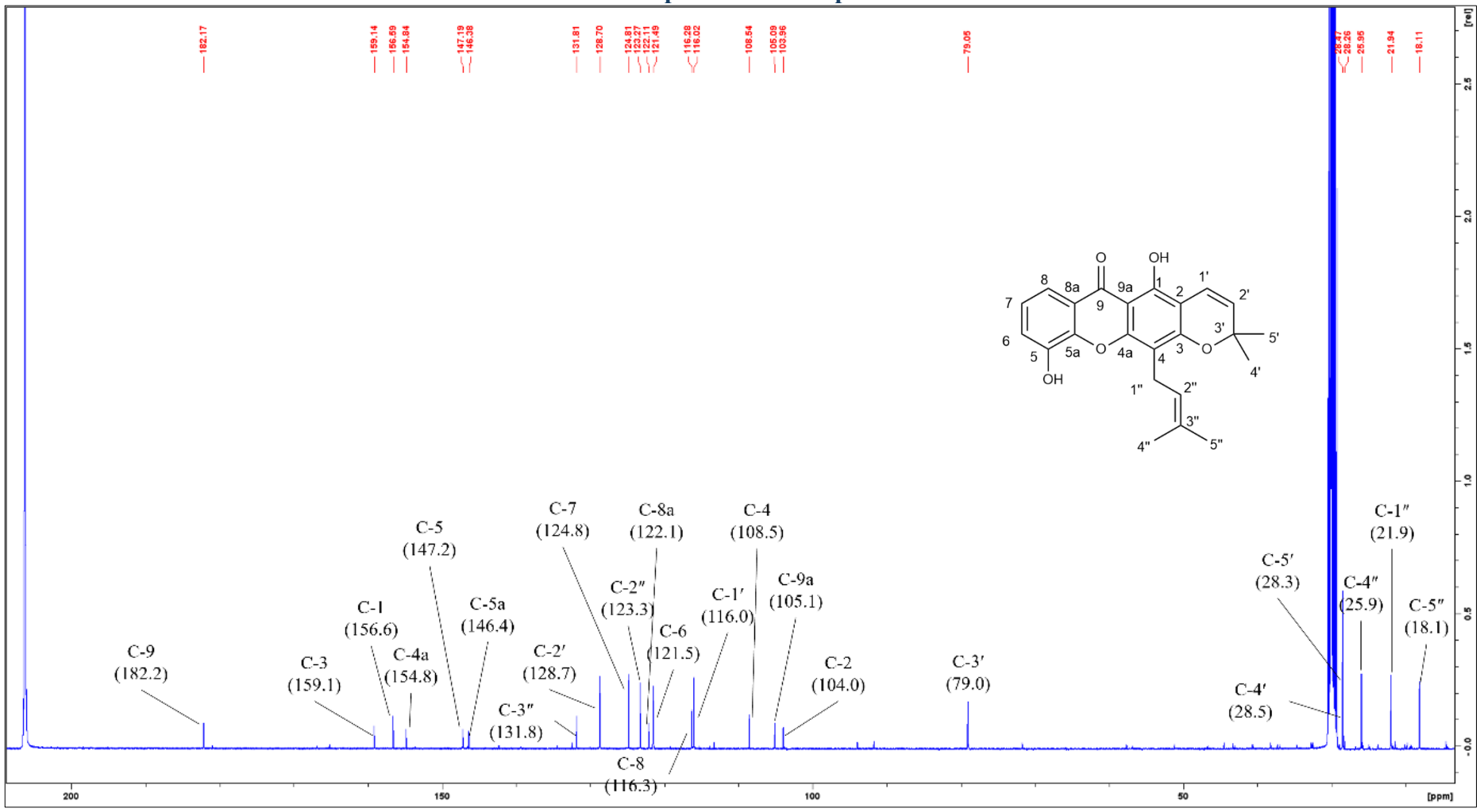

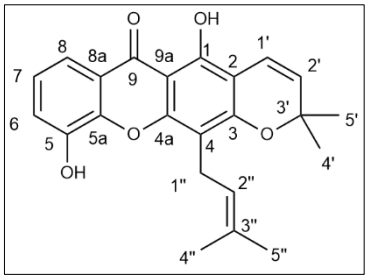

(**20**)

Table 4-2:
Spectral data comparison of compound 20 with previous literature

No.	^{13}C (δ)	^{13}C* (δ*)	^{1}H-^{13}C (δ) (HSQC)	^{1}H* (δ*)	^{1}H-^{13}C HMBC	^{1}H-^{1}H COSY
1	156.6	155.7	13.34 (*s*, 1-OH)	13.35 (*s*, 1-OH)	C-2, C-1, C-9a	-
2	104.0	104.2	-	-	-	-
3	159.1	158.3	-	-	-	-
4	108.5	107.7	-	-	-	-
4a	154.8	154.0	-	-	-	-
5	147.2	146.2	9.24 (*s*, 5-OH)	-	-	-
5a	146.4	145.5	-	-	-	-
6	121.5	120.6	7.39 (1H, *dd*, 7.9, 1.5, H-6)	7.39 (1H, *dd*, 7.8, 1.2, H-6)	C-5, C-8	H-7, H-8
7	124.8	123.9	7.28 (1H, *t*, 7.9, H-7)	7.29 (1H, *t*, 7.8, H-7)	C-5, C-8, C-8a	H-6, H-8
8	116.3	115.5	7.69 (1H, *dd*, 7.9, 1.5, H-8)	7.70 (1H, *dd*, 7.9, 1.2, H-8)	C-5, C-6	H-6, H-7
8a	122.1	121.2	-	-	-	-
9	182.2	181.3	-	-	-	-
9a	105.1	103.1	-	-	-	-
1′	116.0	115.1	6.72 (1H, *d*, 10.0, H-1′)	6.72 (1H, *d*, 9.9, H-10)	C-1, C-3, C-3′, C-4′, C-5′, C-9a	H-2′
2′	128.7	127.8	5.77 (1H, *d*, 10.0, H-2′)	5.78 (1H, *d*, 9.9, H-11)	C-3′, C-4′, C-5′, C-9a	H-1′
3′	79.0	78.2	-	-	-	-
4′	28.5	27.6	1.51 (3H, *s*, H-4′)	1.52 (3H, *s*, H-13)	C-1′, C-2′, C3′, C-5′	-
5′	28.3	27.6	1.51 (3H, *s*, H-5′)	1.52 (3H, *s*, H-14)	C-1′, C-2′, C-3′, C-4′	-
1″	21.9	21.1	3.57 (2H, *d*, 7.3, H-1″)	3.57 (2H, *d*, 7.4, H-1′)	C-3, C-4, C-4a, C-3″	H-2″
2″	123.3	122.4	5.31 (1H, *t*, 7.3, H-2″)	5.32 (1H, *t*, 7.4, H-2′)	-	H-1″
3″	131.8	130.9	-	-	-	-
4″	25.9	25.1	1.66 (3H, *s*, H-4″)	1.67 (3H, *s*, H-5′)	C-2″, C-3″, C-5″	-
5″	18.1	17.2	1.87 (3H, *s*, H-5″)	1.88 (3H, *s*, H-4′)	C-2″, C-3″, C-4″	-

*Karunakaran et al., 2022; measured in acetone-d_6, 700 MHz (^{1}H) and 175 MHz (^{13}C).

4.2.3 Characterisation of Caloxanthone C (5)

Figure 4-21:
Structure of compound 5

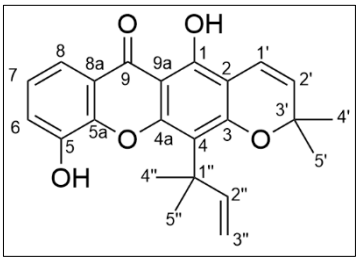

Compound **5** (Figure 4-21) was isolated as a yellow needle-like crystal (43.6 mg) from the fraction CnH3b6 in the *n*-hexane extract and fraction CnC3b6e2 in the chloroform extract, with a melting point of 214-215 °C, which closely aligns with the previously reported range of 211-213 °C (Zamakshshari et al., 2016). The molecular formula of compound **5** was determined to be $C_{23}H_{22}O_5$, based on the molecular ion peak observed at *m/z* 378 in the GC-MS spectrum (Figure 4-22). The molecular formula of compound **5** is identical to that of compound **20**, indicating that both compounds are structural isomers with different substitution patterns on the xanthone scaffold as confirmed by their distinct NMR spectral data.

Figure 4-22:
GC-MS for compound 5

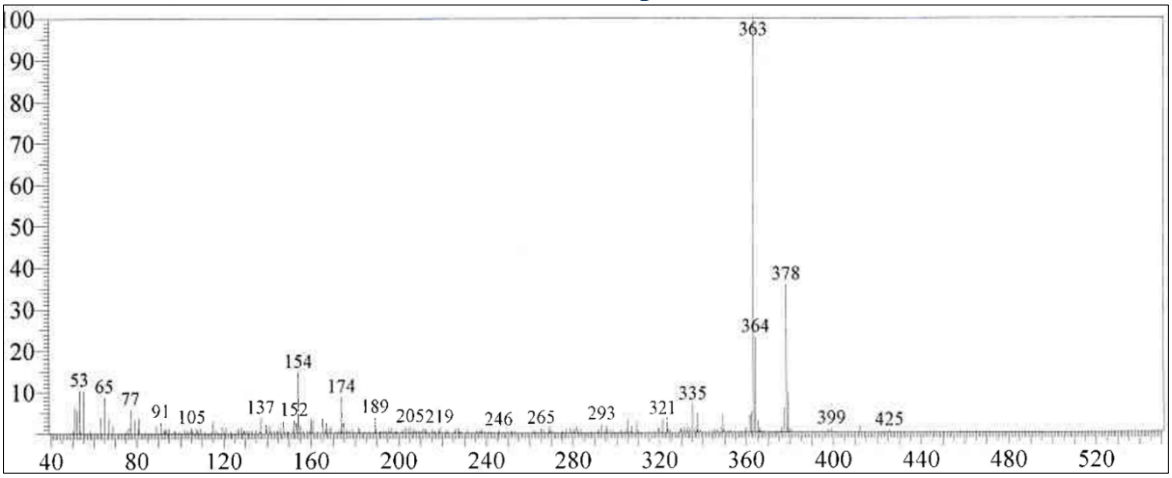

The IR spectrum exhibited absorptions characteristic of a xanthone derivative. A broad band at 3438 cm^{-1} was attributed to phenolic O–H stretching vibrations. A weak absorption at 3052 cm^{-1} corresponded to aromatic C–H stretching, while the band at 2931 cm^{-1} was assigned to aliphatic sp^3 C–H stretching vibrations. A strong absorption at 1649 cm^{-1} was attributed to the conjugated carbonyl (C=O) stretching of the xanthone nucleus

(Tejamukti et al., 2020). The band at 1616 cm^{-1} was assigned to alkene C=C stretching of the unsaturated side chain, whereas the absorption at 1498 cm^{-1} corresponded to aromatic C=C skeletal vibrations. The band observed at 1218 cm^{-1} was attributed to C–O stretching (Sun, 2005), consistent with hydroxyl substitution on the aromatic framework.

The ^{1}H NMR spectrum of compound **5** (Figure 4-24) revealed the presence of a chelated hydroxyl proton, which appeared as a singlet at δ_H 13.71, while another hydroxyl group attached to C-5 appeared as a broad singlet in the downfield region at δ_H 8.96. Three aromatic protons were observed at δ_H 7.37 (H-6), δ_H 7.28 (H-7), and δ_H 7.66 (H-8), indicating the presence of a xanthone skeleton. The COSY spectrum further confirmed that these aromatic protons were mutually coupled, providing additional evidence for the presence of a benzene ring within the molecular structure of compound **5**.

The presence of a pair of *ortho*-coupled doublets at δ_H 6.73 (10.0 Hz) and δ_H 5.80 (10.0 Hz) together with a singlet resonance at δ_H 1.52, integrating for six protons, suggested the presence of the 2,2-dimethyl-2H-pyrano ring. Additionally, the ^{13}C NMR (Figure 4-25) and DEPT-135 spectra of compound **5** confirmed the presence of 23 carbon resonances comprised of one carbonyl carbon at δ_C 182.4 (C-9), ten quaternary carbons (-C-), seven methines (-CH), one methylene ($-CH_2$), and four methyl ($-CH_3$) groups. The protons were assigned to their respective carbons based on the ^{1}J correlations from the HSQC spectrum. Meanwhile, the HMBC spectrum of compound **5** exhibited ^{3}J correlations as shown in Figure 4-23, with cross-peaks observed between δ_H 13.71 (1-OH) with δ_C 105.8 (C-2), δ_C 104.4 (C-9a), and δ_C 157.2 (C-1), indicating the positioning of the OH group at C-1.

Figure 4-23:
HMBC (^{2}J and ^{3}J) ^{1}H-^{13}C correlations and ^{1}H-^{1}H COSY correlations of compound 5

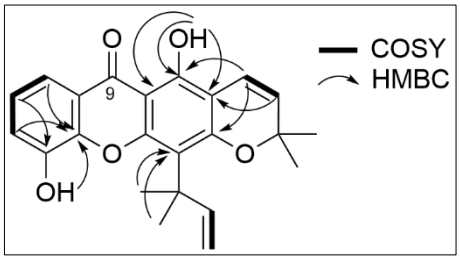

The fusion of the pyrano ring to the xanthone skeleton at C-2 and C-3 through an oxygen atom was supported by ^{3}J correlations of the olefinic proton δ_H 6.73 (H-1′) with δ_C 157.2 (C-1) and δ_C 160.2 (C-3). The COSY spectrum revealed the cis-trans coupling pattern between the olefinic proton resonances at δ_H 6.73 (H-2″), δ_H 4.89 (H-3″), and δ_H 5.01 (H-

3″), confirm vicinal coupling within an alkene system. The larger *J* value corresponds to trans coupling, while the smaller *J* value corresponds to cis coupling, a typical pattern for a terminal olefin (Wu & Cremer, 2003). The HMBC cross peaks of a singlet (δ_H 1.76, 6H) in the aliphatic region with δ_C 41.8 (C-1″) and δ_C 152.5 (C-2″) further confirm the presence of the 1,1-dimethylallyl group in compound **5**, which was also supported by the COSY experiment. The attachment of the 1,1-dimethylallyl group to δ_C 114.4 (C-4) was proposed based on its ^3J coupling with δ_H 1.76 (H-4″ and H-5″). The acquired spectroscopy data were compared with the published information in Table 4-3, and compound **5** was characterised as caloxanthone C (Figure 4-21). Other 2D-NMR data of compound **5**, such as DEPT-45, -90, -135, COSY, HSQC, and HMBC spectra, can be retrieved from Appendix 9-19.

Figure 4-24:
^{1}H NMR spectrum of compound 5

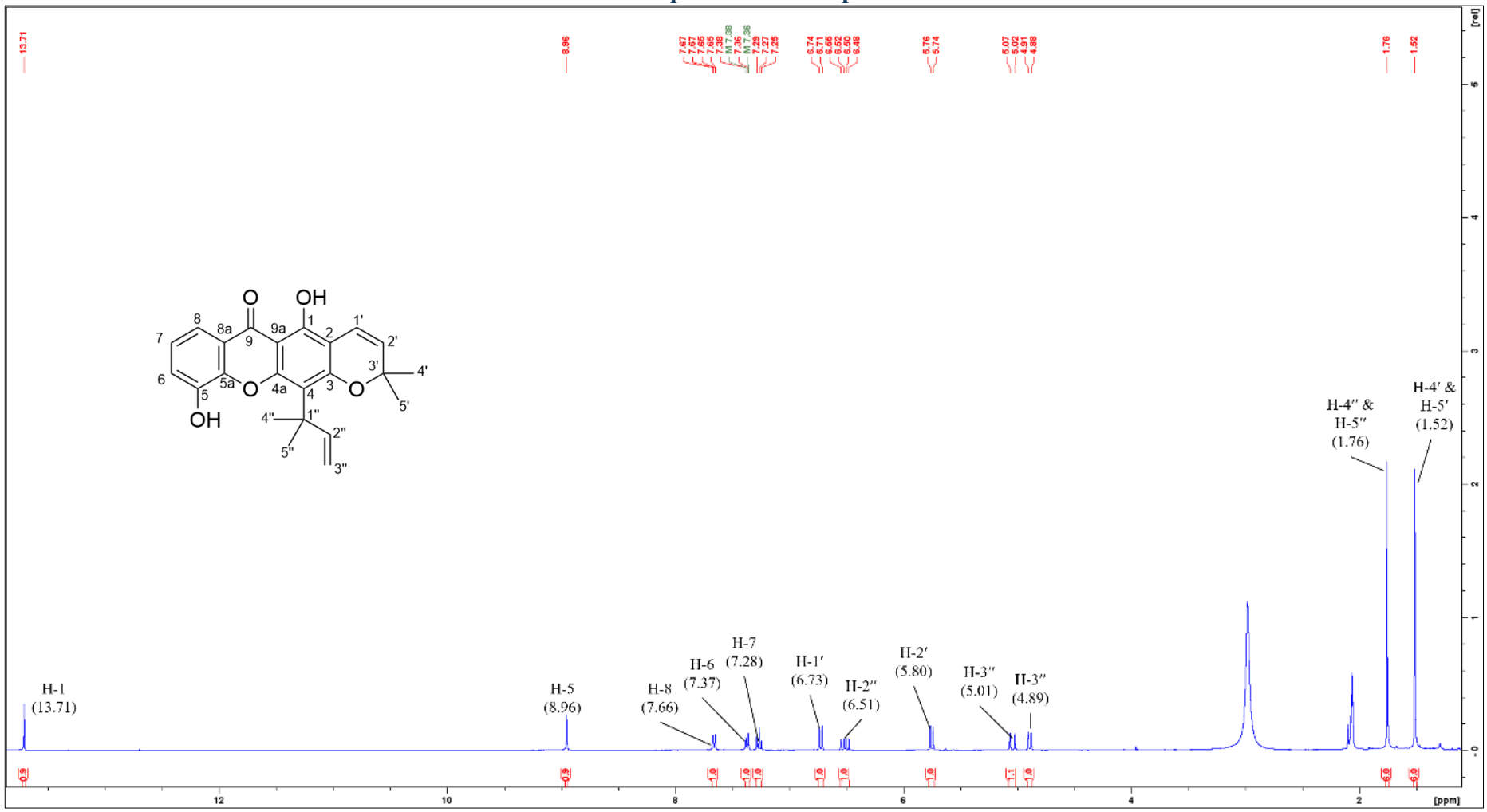

Figure 4-25:
^{13}C NMR spectrum of compound 5

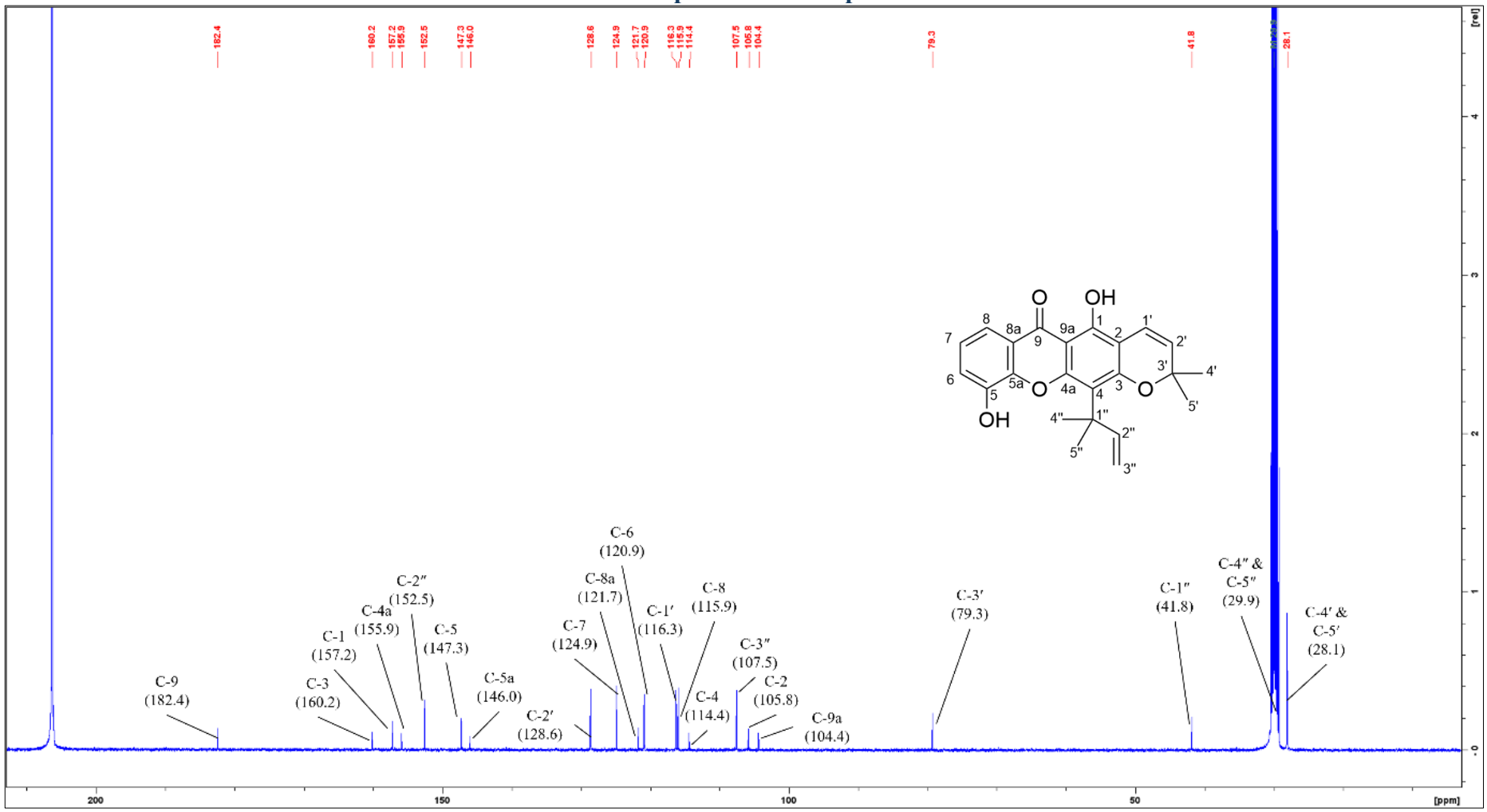

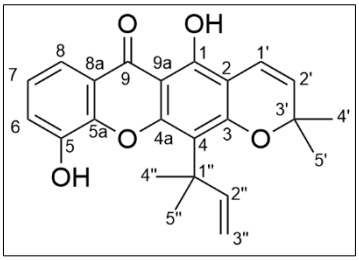

(**5**)

Table 4-3:
Spectral data comparison of compound 5 with previous literature

No.	^{13}C (δ)	^{13}C* (δ*)	^{1}H-^{13}C (δ) (HSQC)	^{1}H* (δ*)	^{1}H-^{13}C HMBC	^{1}H-^{1}H COSY
1	157.2	156.4	13.71(1H, *s*, 1-OH)	13.67 (1H, *s*, 1-OH)	C-1, C-2, C-9a	-
2	105.8	105.0	-	-	-	-
3	160.2	159.3	-	-	-	-
4	114.4	113.7	-	-	-	-
4a	155.9	155.1	-	-	-	-
5	147.3	145.1	8.96 (1H, *s*, 5-OH)	8.79 (1H, *s*, 5-OH)	C-5a	-
5a	146.0	146.4	-	-	-	-
6	120.9	120.1	7.37 (1H, *dd*, 0.9, 7.9, H-6)	7.34 (1H, *d*, 8.0, H-6)	C-5a, C-8	H-7
7	124.9	124.1	7.28 (1H, *d*, 7.9, H-7)	7.24 (1H, *t*, 8, H-7)	C-5, C-8a	H-6
8	115.9	115.2	7.66 (1H, *dd*, 0.9, 7.9, H-8)	7.63 (1H, *d*, 8, H-8)	C-5a. C-6	H-6, H-7
8a	121.7	120.9	-	-	-	-
9	182.4	181.6	-	-	-	-
9a	104.4	103.6	-	-	-	-
1′	116.3	115.4	6.73 (1H, *d*, 10.0, H-1′)	6.68 (1H, *d*, 10.3, H-1′)	C-1, C-3, C-3′	H-2′
2′	128.6	127.8	5.80 (1H, *d*, 10.0, H-2′)	5.72 (1H, *d*, 10.3, H-2′)	C-2, C-3′	H-1′
3′	79.3	78.5	-	-	-	-
4′	28.1	27.2	1.52 (3H, *s*, H-4′)	1.48 (3H, *s*, H-4′)	C-2′, C-3′, C-5′	-
5′	28.1	27.2	1.52 (3H, *s*, H-5′)	1.48 (3H, *s*, H-5′)	C-2′, C-3′, C-4′	-
1″	41.8	41.0	-	-	-	-
2″	152.5	151.8	6.51 (1H, *dd*, 10.6, 17.3, H-2″)	6.48 (1H, *dd*, 10.3, 17.2, H-2″)	C-4″, C-5″	H-3″
3″	107.5	106.7	4.89 (1H, *d*, 10.6, H-3″) 5.01 (1H, *d*, 17.3, H-3″)	4.85 (1H, *d*, 10.3, H-3″) 5.00 (1H, *d*, 17.2, H-3″)	C-1″, C-2″	H-2″
4″	29.9	29.2	1.76 (3H, *s*, H-4″)	1.71 (3H, *s*, H-4″)	C-4, C-1″, C-2″, C-5″	-
5″	29.9	29.2	1.76 (3H, *s*, H-5″)	1.71 (3H, *s*, H-5″)	C-4, C-1″, C-2″, C-4″	-

*Lee et al., 2017; measured in $CDCl_3$, 500 MHz (^{1}H) and 125 MHz (^{13}C).

4.2.4 Characterisation of 1-hydroxy-7-methoxyxanthone (27)

Figure 4-26:
Structure of compound 27

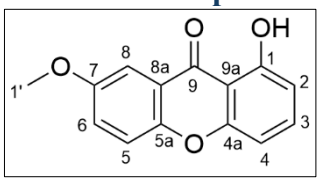

Compound **27** (Figure 4-26) was obtained as pale-yellow, needle-like crystals (22.7 mg) from the fraction CnH3b3 in the *n*-hexane extract and fraction CnC3b1b in the chloroform extract with a melting point of 121-124 °C, similar to the reported value of 124-126 °C (Gunatilaka et al., 1982). The IR spectrum of 1-hydroxy-7-methoxyxanthone exhibited characteristic absorptions consistent with a xanthone framework. A broad absorption band at 3428 cm^{-1} was attributed to phenolic O–H stretching vibrations. A weak band at 3087 cm^{-1} corresponded to aromatic C–H stretching (Tejamukti et al., 2020), while the absorption at 2930 cm^{-1} was assigned to aliphatic sp^3 C–H stretching vibrations associated with the methoxy substituent. A strong band observed at 1644 cm^{-1} was attributed to the conjugated carbonyl (C=O) stretching of the xanthone nucleus (Sun, 2005). The absorption at 1607 cm^{-1} was assigned to unsaturated C=C stretching within the aromatic framework, and the band at 1474 cm^{-1} corresponded to aromatic C=C skeletal vibrations. The absorption at 1238 cm^{-1} was attributed to C–O stretching (Abdel-Kerim & Shoeb, 1972), consistent with the presence of phenolic and methoxy functionalities.

The ^{1}H NMR of compound **27** (Figure 4-27) revealed that there are distinct functional groups present in the compound. A chelated hydroxyl proton was observed as a singlet at δ_H 12.71 (1-OH), while another functional group, the methoxy group, was attached to C-7. The ^{1}H NMR and COSY spectrum showed that six protons were mutually coupled in the aromatic regions in two distinctive ring systems as protons of δ_H 7.74, 7.04, 6.81 correlate with each other, confirming these protons were in the same ring system while protons of δ_H 7.64, 7.61, 7.53 correlate with each other, proving these protons were together in another ring system, hence confirming the presence of two benzene rings. This further proposes the xanthone skeleton structure to be available in the molecular structure of compound **27**. Furthermore, the proton δ_H 3.97 was in the alkoxy region as its integration showed three protons were present as a singlet in the spectrum, confirming it as a methoxy group.

Figure 4-27:
^{1}H NMR spectrum of compound 27

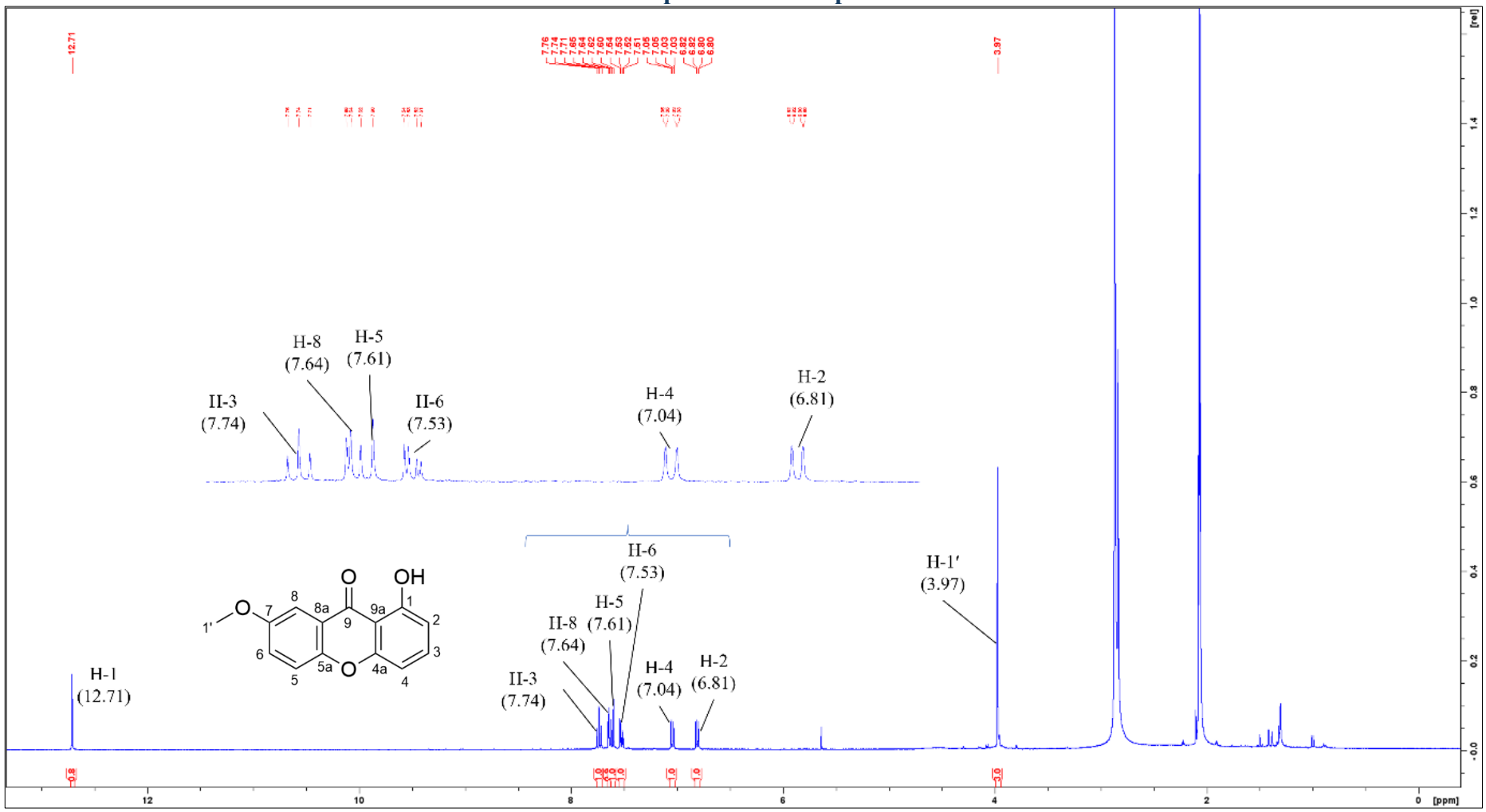

The ^{13}C NMR (Figure 4-29) and DEPT spectra of compound **27** confirmed the presence of 14 carbon resonances, which are consistent with its molecular formula. These resonances comprised one carbonyl carbon at δ_C 183.3 (C-9), a typical value for a carbonyl group in a xanthone skeleton, six quaternary carbons (-C-), six methines (-CH) and one methyl (-CH_3) group.

The HSQC spectrum provided ^1J correlations, confirming the direct attachment of protons to their respective carbons, as the HMBC correlation (Figure 4-28) confirmed the neighbouring attachment from 2J correlations, while within the protons and carbons. From the HMBC, there are cross-peaks observed between δ_H 12.71 (1-OH) with C-3 (δ_C138.4), C-4 (δ_C 111.2), and C-9a (δ_C 109.7), indicating the attachment of the hydroxyl group at the ring and towards the ring of the carbonyl group was present. Other than that, protons at H-1′ (δ_H 3.97) exhibited 3J correlation with C-7 (δ_C 157.8), and the proton at H-8 (δ_H 7.64) was coupled with carbons at C-6 (δ_C 127.0), C-9 (δ_C183.34) and C-7 (δ_C 157.8). The correlation between H-8 and C-9 proves the connection between the rings in compound **27**.

Figure 4-28:
HMBC (^2J and ^3J) ^1H-^{13}C correlations and ^1H-^1H COSY correlations of compound 27

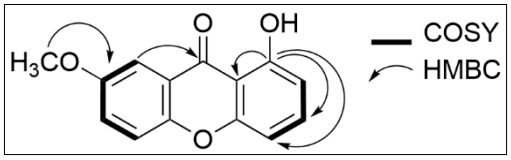

The acquired spectroscopy data were compared with the published information in Table 4-4, and compound **27** was characterised as 1-hydroxy-7-methoxyxanthone (Figure 4-26). Other 2D-NMR data of compound **27**, such as DEPT-45, -90, -135, COSY, HSQC, and HMBC spectra, can be retrieved from Appendix 20-24.

Figure 4-29:
^{13}C NMR spectrum of compound 27

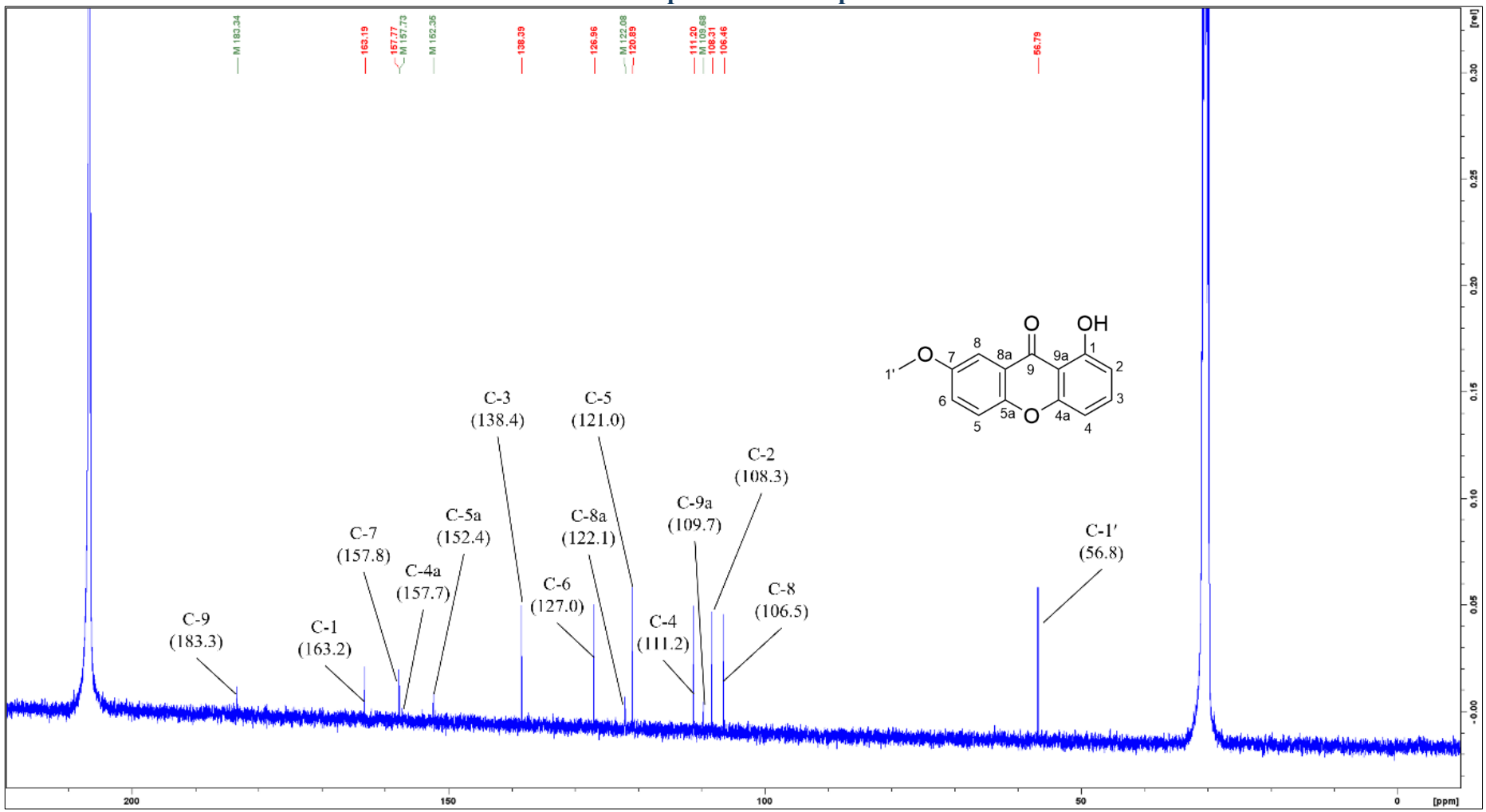

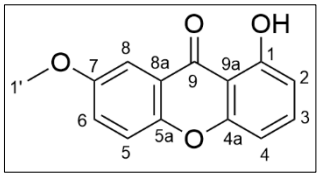

(**27**)

Table 4-4:
Spectral data comparison of compound 27 with previous literature

No.	^{13}C (δ)	^{13}C* (δ*)	^{1}H-^{13}C (δ) (HSQC)	^{1}H* (δ*)	^{1}H-^{13}C HMBC	^{1}H-^{1}H COSY
1	163.2	162.7	12.71 (1-OH, *s*)	12.69 (*s*, 1-OH)	C-4, C-3, C-9a	-
2	108.3	110.8	6.81 (1H, *dd*, 0.8, 8.3, H-2)	6.79 (1H, *dd*, *J* = 1.0 Hz, 8.2 Hz, H-2)	C-9a, C-1	H-3
3	138.4	137.9	7.74 (1H, *t*, 8.3, H-3)	7.72 (1H, *t*, *J* = 8.4 Hz, H-3)	C-4a, C-9a, C-1	H-4, H-2
4	111.2	107.9	7.04 (1H, *dd*, 0.8, 8.3, H-4)	7.02 (1H, *dd*, *J* = 1.0 Hz, 8.4 Hz, H-4)	C-9a, C-4a, C-1	H-3
4a	157.7	157.2	-	-	-	-
5	121.0	120.4	7.61 (1H, *d*, 9.1, H-5)	7.59 (1H, *d*, *J* = 9.1 Hz, H-5)	C-8a, C-7, C-5a	H-8
5a	152.4	151.9	-	-	-	-
6	127.0	126.5	7.53 (1H, *dd*, 3.1, 9.1, H-6)	7.50 (1H, *dd*, *J* = 3.1 Hz, 9.2 Hz, H-6)	C-8a, C-7, C-5a	H-5, H-8
7	157.8	157.3	-	-	-	-
8	106.5	106.1	7.64 (1H, *d*, 3.1, H-8)	7.62 (1H, *d*, *J* = 3.1 Hz, H-8)	C-6, C-9, C-7, C-5a	H-5
8a	122.1	121.6	-	-	-	-
9	183.3	182.9	-	-	-	-
9a	109.7	109.2	-	-	-	-
1′	56.8	56.3	3.97 (3H, *s*, 7-OCH_3)	3.96 (*s*, 7a-OCH_3)	C-7	-

*Lizazman et al. (2025) ; measured in acetone-d_6, 400 MHz (^{1}H) and 100 MHz (^{13}C).

4.2.5 Characterisation of Canumolactone (90)

Figure 4-30:
Structure of compound 90

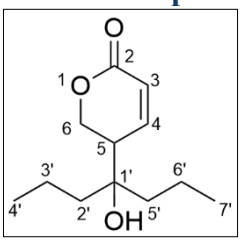

Compound **90** (Figure 4-30) was obtained as a yellowish-orange oil (110.8 mg) from the fraction CnH17o2a in the *n*-hexane extract with a molecular formula of $C_{12}H_{20}O_3$ as it is consistent with the LC-MS (ESI^-) spectrum exhibited a major ion peak at *m/z* 212.30 (Figure 4-31). The UV-Vis spectrum of compound **90** displayed absorption at λ_{max} = 250 and 280 nm, which indicates the *α*, *β*-unsaturated lactone system due to conjugation.

Figure 4-31:
LC-MS for compound 90

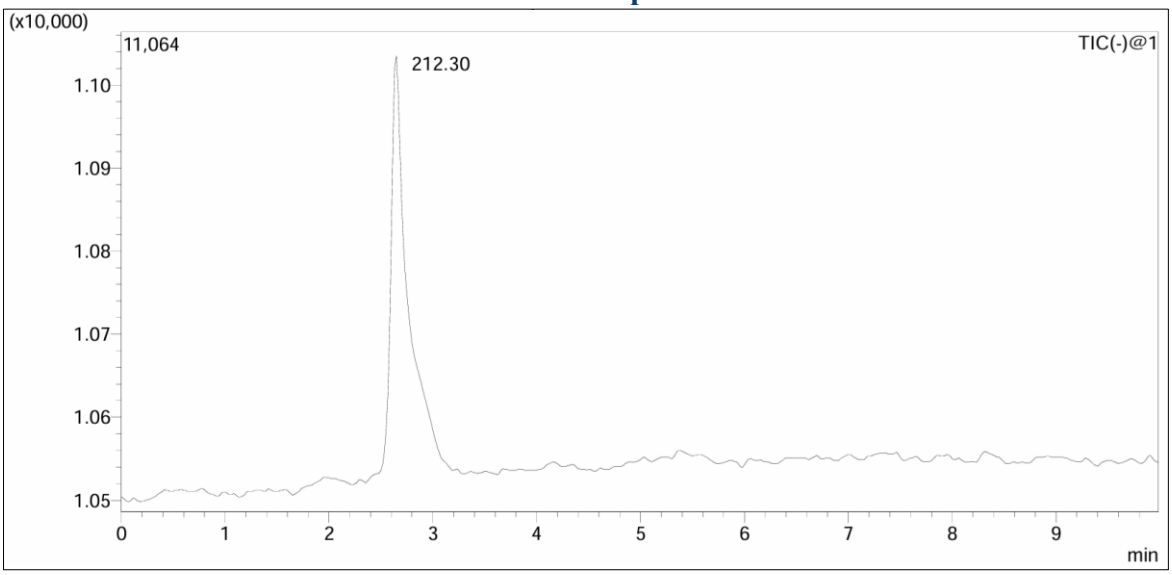

The IR spectrum exhibited a strong absorption at 1725 cm^{-1}, which is characteristic of the typical carbonyl group (C=O) stretching of a lactone ring (Sun, 2005). The presence of the bands at 2950 cm^{-1} and 1268 cm^{-1} suggested aliphatic C-H stretching and C-O-C stretching vibrations of the ester functionality (Abdel-Kerim & Shoeb, 1972), respectively. There is also the presence of an absorption band at 1603 cm^{-1} which is the alkene C=C vibration corresponds to the conjugated system adjacent to the lactone ring, further supporting the presence of a lactone ring system within the structure.

The ^{1}H NMR (Figure 4-33) and COSY spectra of compound **90** revealed that two sets of doublets of doublets resonating at δ_H 7.77 (H-3) and δ_H 7.67 (H-4) represent the olefinic protons, indicating an α, β-unsaturated lactone system. The correlation between the protons H-3 and H-4 was observed in the COSY spectrum. A downfield multiplet at δ_H 4.23 ppm was attributed to the oxygenated methylene proton (H-6), suggesting its attachment nearby to an electronegative atom, which is the oxygen atom. The proton resonance at δ_H 4.23 ppm (H-6) correlates with δ_H 1.71 (H-5), showing their connectivity within the lactone ring. A group of overlapping multiplet resonances at δ_H 1.33 (H-6′), 1.35 (H-5′), 1.39 (H-2′), and 1.42 (H-3′) stipulate the presence of aliphatic protons within the side chains of the lactone ring as methylene protons (CH_2). On the other hand, the presence of two terminal methyl groups exists as triplets at δ_H 0.92 (H-7′) and δ_H 0.95 (H-4′). The aliphatic protons of methylene and methyls showed correlations with each other, confirming the presence of the saturated alkyl side chain in compound **90**.

The ^{13}C NMR (Figure 4-34) and DEPT (135, 90, 45) spectra of compound **90** confirmed the presence of carbons consisting of two quaternary carbons (-C-), including a carbonyl carbon at δC 167.1 (C-2), three methines (-CH), five methylene (-CH_2-) and two methyl (-CH_3) groups. The olefinic carbons were displayed at δ_C 128.7 (C-3) and δ_C 131.1 (C-4), while the oxygenated methylene carbon was revealed at δ_C 67.4 (C-6). The remaining aliphatic carbons in methylene were observed within the range of 20 ppm to 30 ppm (δ_C 22.7 (C-6′), 23.6 (C-3′), 28.8 (C-5′), and 30.3 (C-2′)) while the terminal methyl carbons were identified at δ_C 13.4 (C-7′), and 10.4 (C-4′).

The HSQC spectrum provided ^{1}J correlations, confirming the direct attachment of each proton to the respective carbon. Meanwhile, the HMBC correlation (Figure 4-32) confirmed the neighboring attachment from ^{2}J correlations and above between the protons and carbons. From the HMBC spectrum, proton H-4 (δ_H 7.67) showed a long-range correlation with δ_C 132.6 (C-1′). The proton at δ_H 7.77 (H-3), which is adjacent to the carbonyl carbon, gave ^{2}J correlations to both C-2 (δ_C 167.1) and C-4 (δ_C 131.1). The proton at δ_H 4.23 (H-6) was correlated with δ_C 167.1 (C-2) and δ_C 38.8 (C-5), proving compound **90** is a closed-ring structure.

Figure 4-32:
HMBC (^{2}J and ^{3}J) ^{1}H-^{13}C correlations and ^{1}H-^{1}H COSY correlations of compound 90

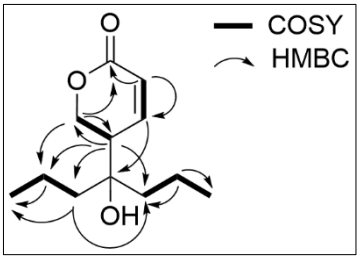

On the other hand, the aliphatic protons and carbons exhibited correlations with each other, such as H-3′ (δ_H 1.42) with C-2′ (δ_C 20.3), and C-4′ (δ_C 10.4), and H-6′ (δ_H 1.33) with C-5′ (δ_C 28.8), and C-7′ (δ_C 13.4), suggesting the presence of two identical aliphatic branches in the compound. Moreover, the cross-peaks between the proton resonance at δ_H 1.71 (H-5) and the methylene carbons resonating at δ_C 30.3 (C-2′), 23.6 (C-3′), and 28.8 (C-5′) suggest the attachment of the aliphatic chains on the lactone ring. Based on the spectral data, compound **90** was identified as canumolactone (Figure 4-30). The acquired spectroscopy data were compared with the published information in Table 4-5. Other 2D-NMR data of compound **90**, such as DEPT-45, -90, -135, COSY, HSQC, and HMBC spectra, can be retrieved from Appendix 25-30.

Figure 4-33:
^{1}H NMR spectrum of compound 90

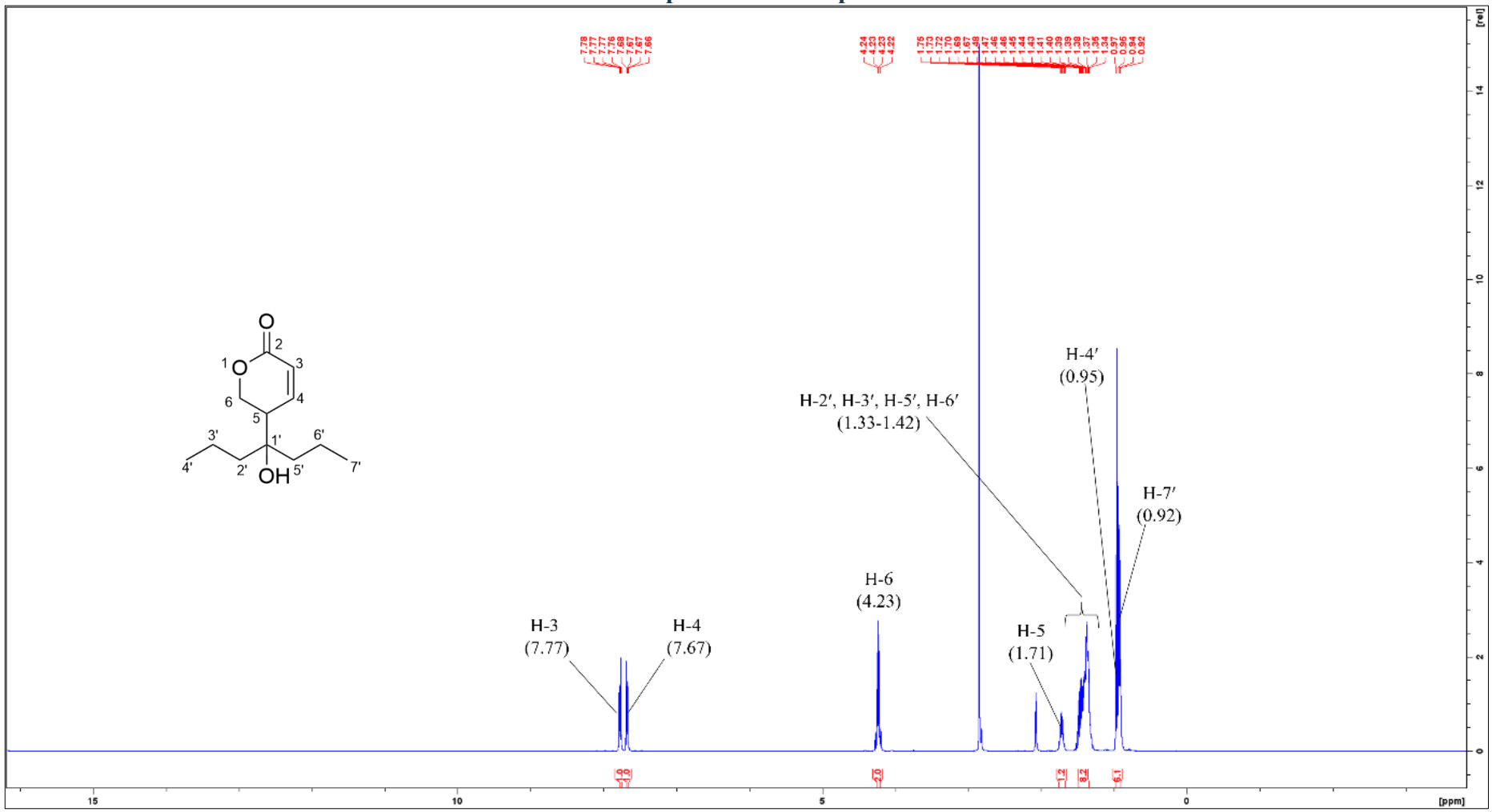

Figure 4-34:
^{13}C NMR spectrum of compound 90

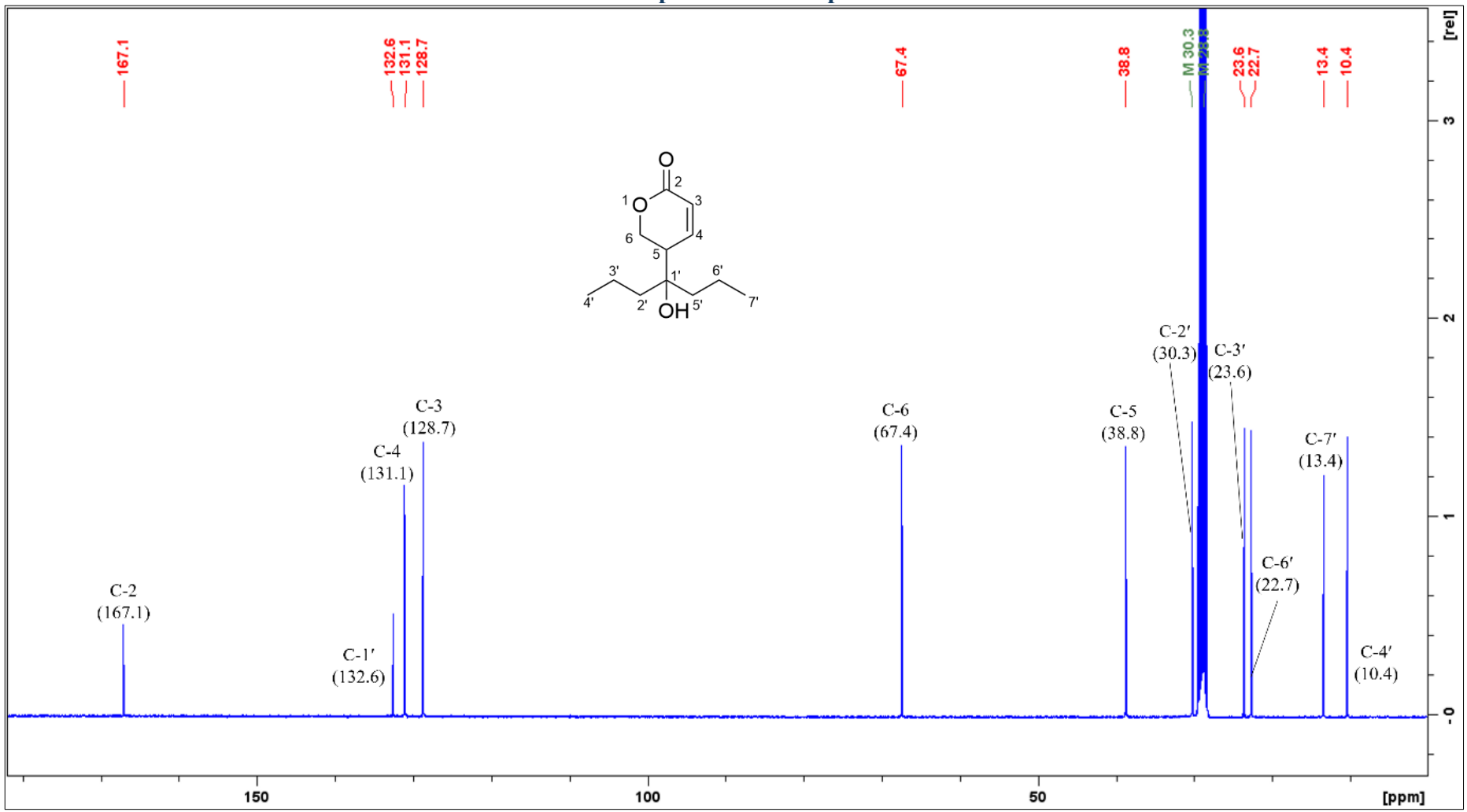

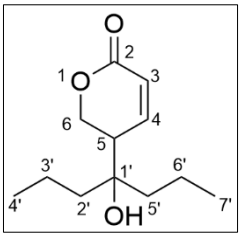

(90)

Table 4-5:
Spectral data comparison of compound 90 with previous literature

No.	δ ^{13}C (ppm)	δ ^{13}C (ppm) *	δ ^{1}H-^{13}C HSQC (^{1}J) (Mult. *J* Hz. int)	δ ^{1}H (Mult. *J* Hz. int) *	^{1}H-^{13}C HMBC	^{1}H-^{1}H COSY
2	167.1	168.0	-	-	-	-
3	128.7	129.6	7.77 (1H, *dd*, 3.4, 5.7, H-3)	7.75 (1H, *dd*, *J* = 3.3 Hz, 5.8 Hz, H-3)	C-4, C-2	H-4
4	131.1	132.0	7.67 (1H, *dd*, 3.4, 5.7, H-4)	7.65 (1H, *dd*, *J* = 3.3 Hz, 5.8 Hz, H-4)	C-3, C-1′	H-3
5	38.8	39.7	1.71 (1H, *m*, H-5)	1.70 (1H, *m*, H-5)	C-4′, C-3′, C-5′, C-2′, C-6′	H-6
6	67.4	68.4	4.23 (2H, *m*, H-6)	4.21 (2H, *m*, H-6)	C-2, C-3′, C-2′, C-5	H-5
1′	132.6	133.5	-	-	-	-
2′	30.3	31.2	1.39 (2H, *m*, H-2′)	1.39 (2H, *m*, H-2′)	C-5’, C-2′, C-5, C-6	H-4′
3′	23.6	24.5	1.42 (2H, *m*, H-3′)	1.44 (2H, *m*, H-3′)	C-4′, C-2′, C-5, C-6	H-4′
4′	10.4	11.3	0.95 (3H, *t*, H-4′)	0.94 (3H, *t*, H-4′)	C-3′, C-5	H-2′, H-3′
5′	28.8	29.7	1.35 (2H, *m*, H-5′)	1.35 (2H, *m*, H-5′)	C-4′, C-6′, C-5’, C-2′, C-5, C-6	H-7’
6′	22.7	23.6	1.33 (2H, *m*, H-6′)	1.33 (2H, *m*, H-6′)	C-7′, C-5′, C-2′	H-7′
7′	13.4	14.3	0.92 (3H, *t*, H-7′)	0.91 (3H, *t*, H-7′)	C-6′, C-5′	H-6′, H-5′

*Lizazman et al. (2026) ; measured in acetone-d_6, 400 MHz (^{1}H) and 100 MHz (^{13}C).

4.2.6 Characterisation of Friedelin (71)

Figure 4-35:
Structure of compound 71

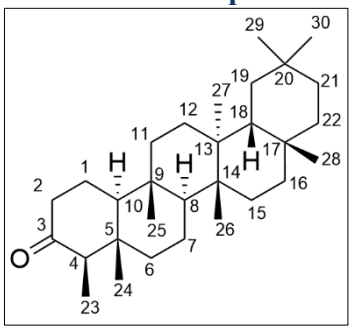

Compound **71** (Figure 4-35) was obtained as a white-needle crystal (54.2 mg) from CnH1 in the *n*-hexane extract with a melting point of 260-261 °C, similar to the reported value by Sunil et al. (2021): 263-265 °C. The GC-MS spectrum (Figure 4-36) yielded a molecular ion [M^+] at *m/z* 426, consistent with the molecular formula $C_{30}H_{50}O$.

Figure 4-36:
GC-MS for compound 71

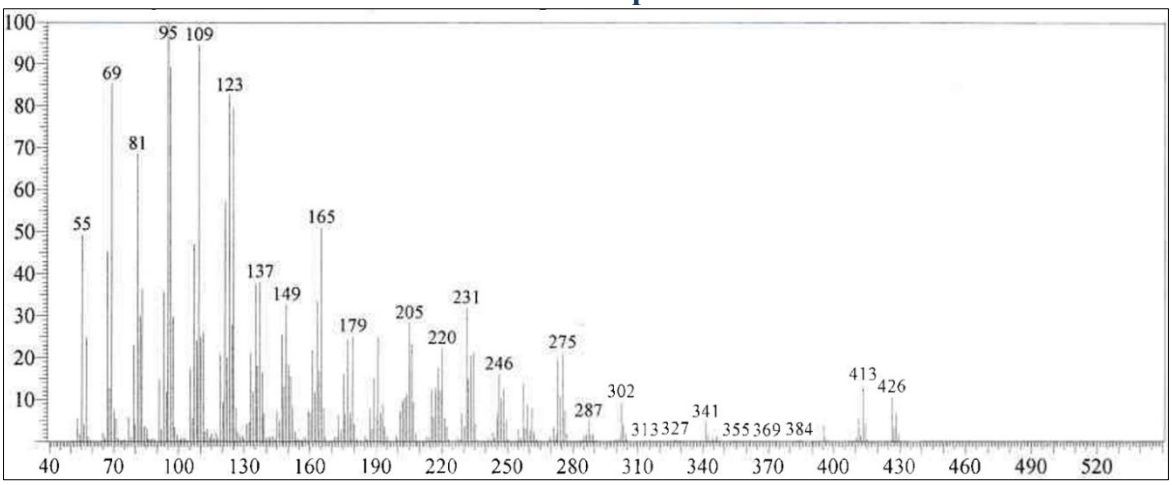

Compound **71** exhibited characteristic IR absorptions of a saturated triterpenoid ketone. Strong bands at 2925 and 2857 cm^{-1} were assigned to aliphatic C–H stretching vibrations of methyl and methylene groups. A sharp and intense absorption at 1714 cm^{-1} corresponded to a non-conjugated carbonyl (C=O) stretching vibration (Sun, 2005). Additional bands at 1460 and 1389 cm^{-1} were attributed to CH_3 bending (deformation) vibrations, consistent with a highly methylated pentacyclic triterpenoid framework. Meanwhile, the UV-Vis spectrum indicates the presence of the unsaturated bond at the maximum absorption of 288 nm.

The ^{1}H NMR spectrum of compound **71** (Figure 4-37) displayed characteristics of highly upfield signals due to its highly saturated structure. The proton singlets at δ_H 1.01 (C-29) and δ_H 0.97 (C-30), which integrated for three protons per singlet, confirmed the presence of methyl groups at C-20. However, the presence of a singlet at δ_H 2.22 (H-2) was more deshielded (downfield) due to its assignment at the C-2 position, adjacent to the C=O functional group.

The ^{1}C NMR spectrum (Figure 4-38) confirmed the presence of 30 carbon signals, which is consistent with the triterpenoid structure. A downfield signal at δ_C 213.4 corresponds to the carbon resonance in the carbonyl group (C=O). The comparison between C-13 and DEPT-135 spectra distinguished resonances of seven quaternary carbons, eleven methylene carbons, four methine carbons, and eight methyl carbons.

The assignments of the NMR spectra for compound **71** are tabulated in Table 4-6. Based on the comparison with previous literature, compound **71** was elucidated as friedelin (Figure 4-35). The 2D-NMR of compound **71** can be retrieved from Appendix 31.

Figure 4-37:
Expanded ^{1}H NMR spectrum of compound 71 in the 0-4 ppm region

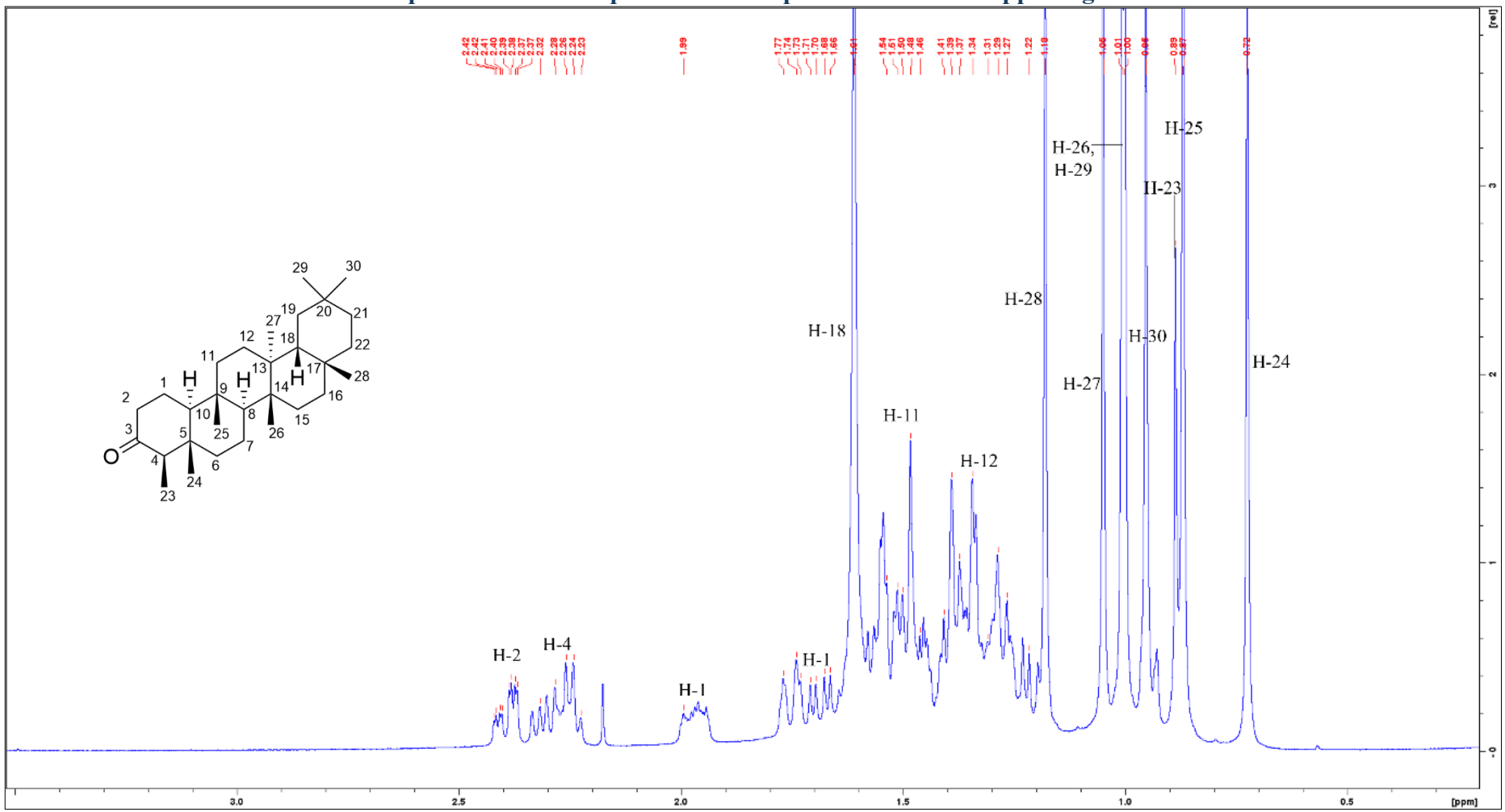

Figure 4-38:
^{13}C NMR spectrum of compound 71

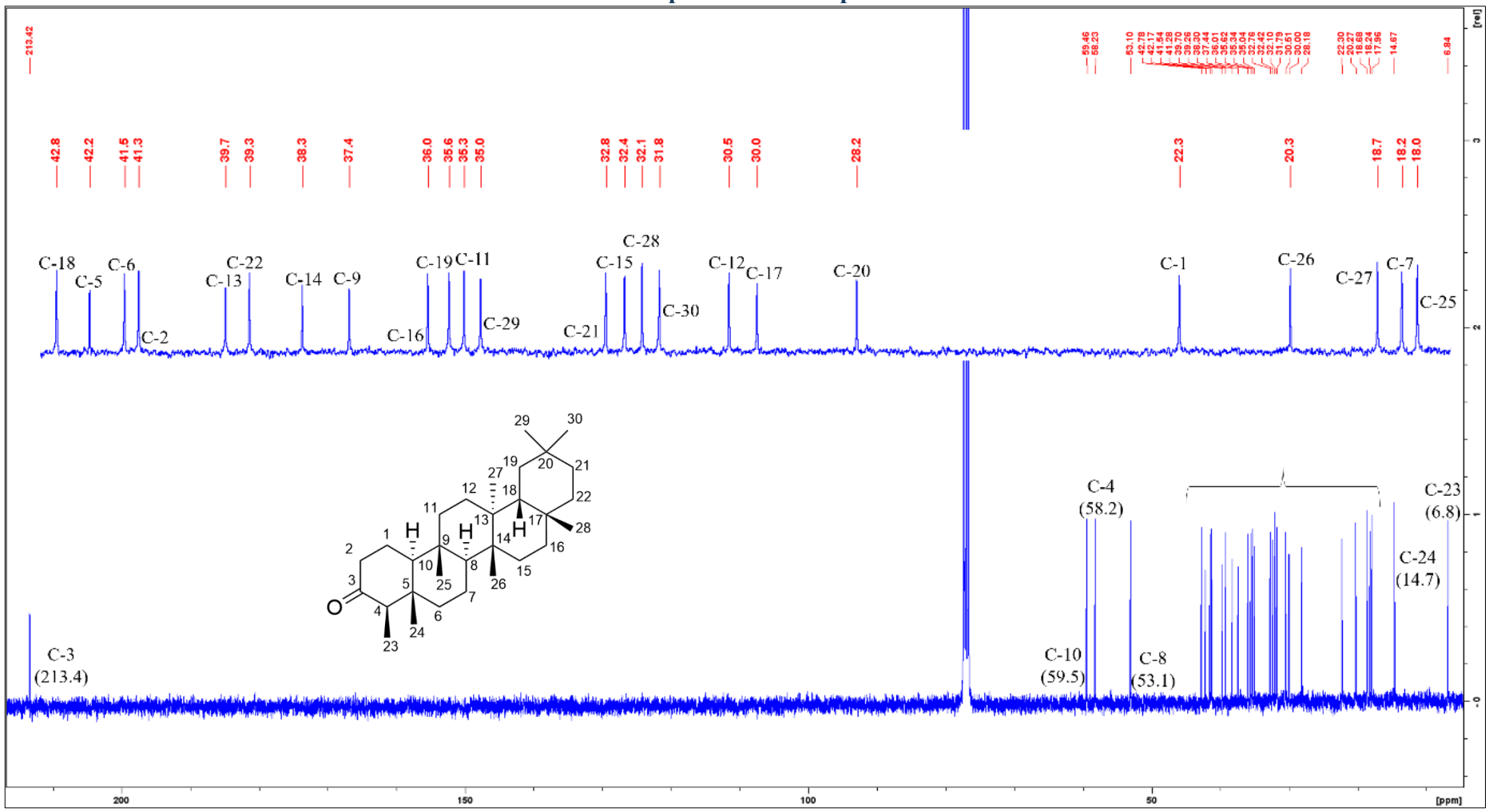

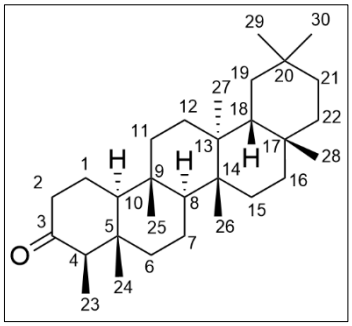

(**71**)

Table 4-6:
Spectral data comparison of compound 71 with previous literature

No.	δ ^{13}C (ppm)	δ ^{13}C * (ppm)	δ ^{1}H (Int. *J* Hz. Mult.)	δ ^{1}H * (Int. *J* Hz. Mult.)
1	22.3	22.4	1.71, 1.98 (2H, *m*)	1.72, 1.94, (1H, *m*)
2	41.3	41.4	2.26, 2.39 (2H, *m*)	2.26, 2.38, (2H, *m*)
3	213.4	213.3	-	-
4	58.2	58.3	2.26 (1H, 6.7, *q*)	2.23 (1H, 6.9, *q*)
5	42.2	42.2	-	-
6	41.5	41.6	1.28, 1.74 (2H, 11.9, *d*)	1.74, 1.26 (2H, 11.5, *d*)
7	18.2	18.3	1.41, 1.50 (2H, *m*)	1.37, 1.48 (2H, *m*)
8	53.1	53.2	1.41 (1H, 9.2, *t*)	1.37 (1H, 8.6, *t*)
9	37.4	37.5	-	-
10	59.5	59.6	1.53 (1H, *m*)	1.50 (1H, *m*)
11	35.3	35.4	1.28, 1.48 (2H, *m*)	1.46, 1.26 (2H, *m*)
12	30.5	30.6	1.34, 1.34 (2H, *m*)	1.32, 1.37 (2H, *m*)
13	39.7	39.8	-	-
14	38.3	38.4	-	-
15	32.4	32.5	1.27, 1.47 (2H, *m*)	1.45, 1.24 (2H, *m*)
16	36.0	36.1	1.37, 1.58 (2H, *m*)	1.52, 1.34 (2H, *m)*
17	30.0	30.1	-	-
18	42.8	42.9	1.58 (1H, *m*)	1.52 (1H, *m*)
19	36.0	35.7	1.22, 1.39 (2H, *m*)	1.19, 1.37 (2H, *m*)
20	28.2	28.2	-	-
21	32.8	32.8	1.31, 1.51 (2H, *m*)	1.30, 1.49 (2H, *m*)
22	39.3	39.3	0.94, 1.50 (2H, *m*)	1.49, 0.93 (2H, *m*)
23	6.8	6.9	0.90 (3H, 6.7, *d*)	0.86 (3H, 6.1, *d*)
24	14.7	14.7	0.74 (3H, *s*)	0.70 (3H, *s*)
25	18.0	18.0	0.88 (3H, *s*)	0.85 (3H, *s*)
26	20.3	20.3	1.02 (3H, *s*)	0.99 (3H, *s*)
27	18.7	18.7	1.06 (3H, *s*)	1.03 (3H, *s*)
28	32.1	32.2	1.19 (3H, *s*)	1.16 (3H, *s*)
29	35.0	35.1	1.01 (3H, *s*)	0.93 (3H, *s*)
30	31.8	31.9	0.97 (3H, *s*)	0.98 (3H, *s*)

*Heilman et al. (2024) ; measured in C_3D_6O, 500 MHz (^{1}H) and 125 MHz (^{13}C).

4.2.7 Characterisation of Stigmasterol (70)

Figure 4-39:
Structure of compound 70

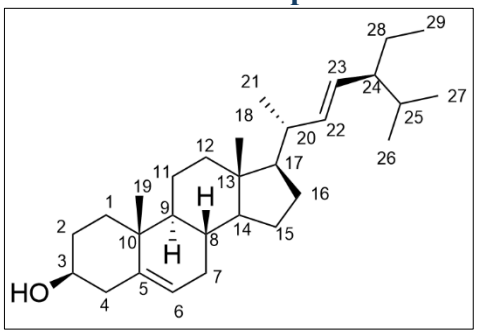

Compound **70** (Figure 4-39) was obtained as a white crystal (28.9 mg) from the fraction CnH17o2b1 in the *n*-hexane extract with a melting point of 174 - 175 °C, similar to the reported value of 175 °C (Zaine et al., 2024). The GC-MS spectrum (Figure 4-40) exhibited a molecular peak at m/z 412.70, which is aligned with the molecular formula $C_{29}H_{48}O$.

Figure 4-40:
GC-MS for compound 70

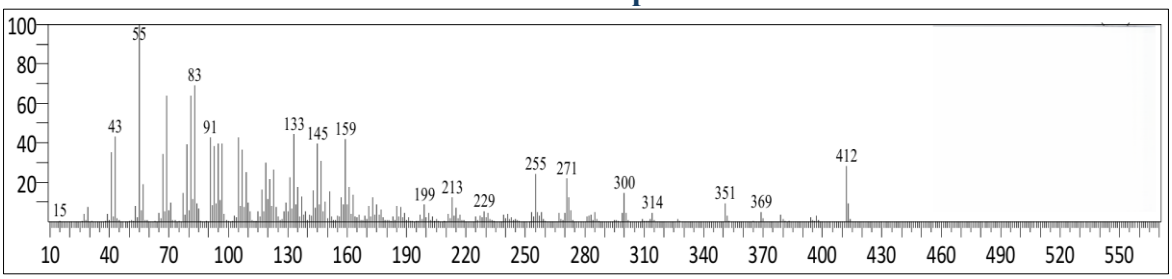

Compound **70** exhibited a broad absorption band at 3482 cm^{-1}, corresponding to O–H stretching of the hydroxyl group. A weak band at 3030 cm^{-1} was assigned to unsaturated (=C–H) stretching, while the strong absorptions at 2929 and 2868 cm^{-1} indicated aliphatic C–H stretching vibrations. The band at 1649 cm^{-1} was attributed to C=C stretching of the alkene functionalities. In addition, peaks at 1463 and 1382 cm^{-1} were consistent with CH_3 bending vibrations, and the absorption at 1052 cm^{-1} supported the presence of C–O stretching of the secondary alcohol group. Moreover, compound **70** displayed the UV maximum absorption at 279 nm, indicating the presence of the unsaturated bond.

The ^1H NMR spectrum (Figure 4-41) suggested the presence of a hydroxyl (-OH) group at position C-3 as the multiplet integrated for a proton resonating at δ_H 3.53 showed the characteristic of an axial proton adjacent to the hydroxyl group. Meanwhile, the olefinic

proton H-6 resonance at δ_H 5.36 indicates the presence of an unsaturated double bond between carbons 5 and 6 in the compound. The presence of methyl groups at C-18, C-19, C-26, C-27, and C-29 is evident from singlet and multiplet peaks in the range of 0.69 to 1.02 ppm. The multiplet at δ_H 5.16 (H-22) to δ_H 5.03 (H-23) corresponds to the C-22 and C-23 carbon positions, confirming the presence of a second double bond in the side branch.

The ^{13}C NMR spectrum (Figure 4-42) further supports the structure of compound **70** as the hydroxyl-bearing carbon, C-3, resonates at δ_C 71.9, due to the deshielding effect of the binding of electronegative oxygen to the carbon. The C-5 and C-6 double bond was confirmed by peaks at 140.9 ppm (C-5) and 121.8 ppm (C-6), while the C-22 and C-23 olefinic carbons resonate at δ_C 138.4 and 129.4, respectively, further supporting the unsaturation in the side chain. The aliphatic carbon resonances were observed within the range of δ_C 12.0 – 56.9, corresponding to the sterane skeleton.

The assignments of the NMR spectra for compound **70** were summarised in Table 4-7. Based on the comparison with previous literature, compound **70** was characterised as stigmasterol (Figure 4-39). The 2D-NMR of compound **71** can be retrieved from Appendix 32.

Figure 4-41:
^{1}H NMR spectrum of compound 70

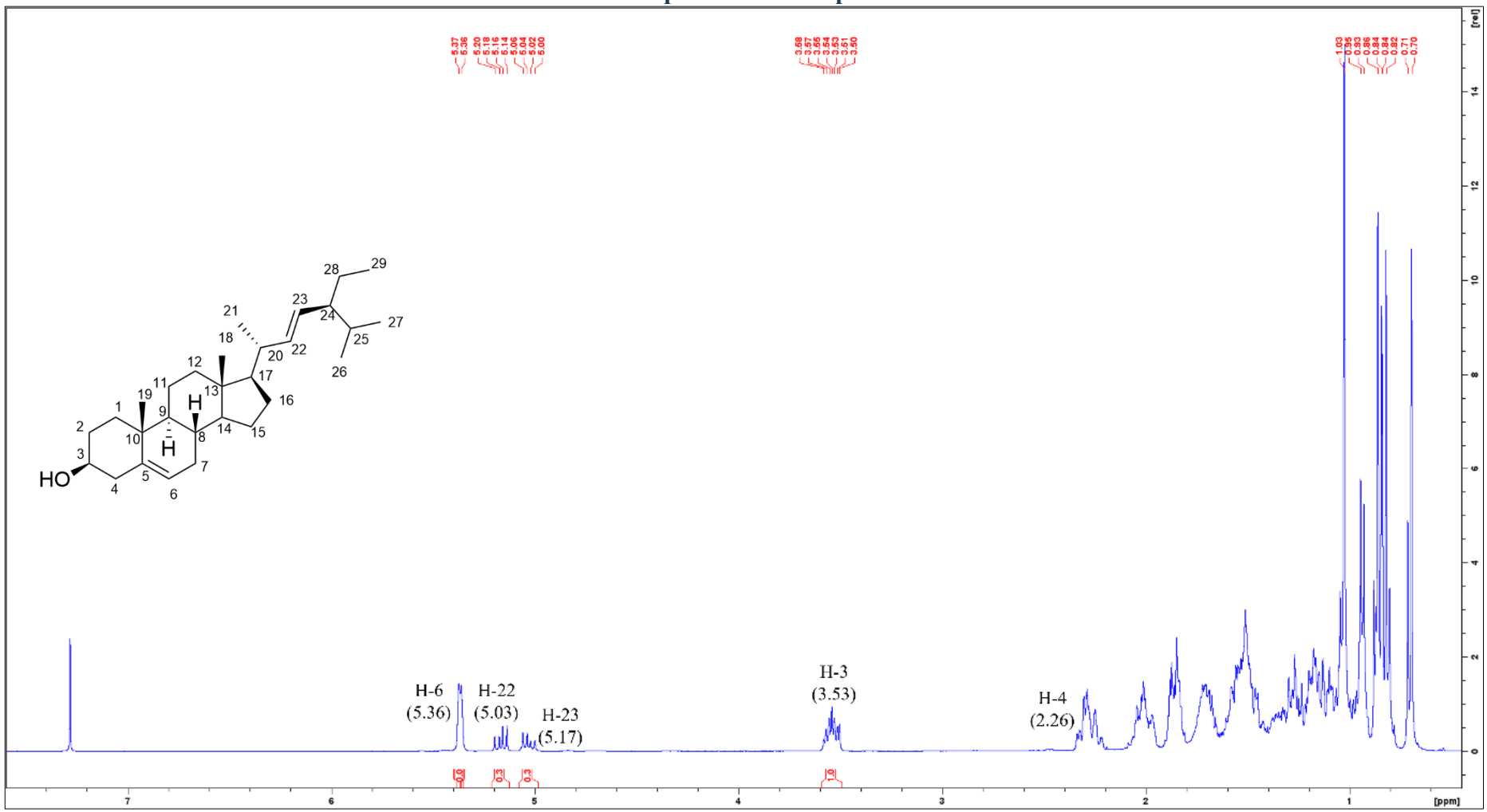

Figure 4-42:
^{13}C NMR spectrum of compound 70

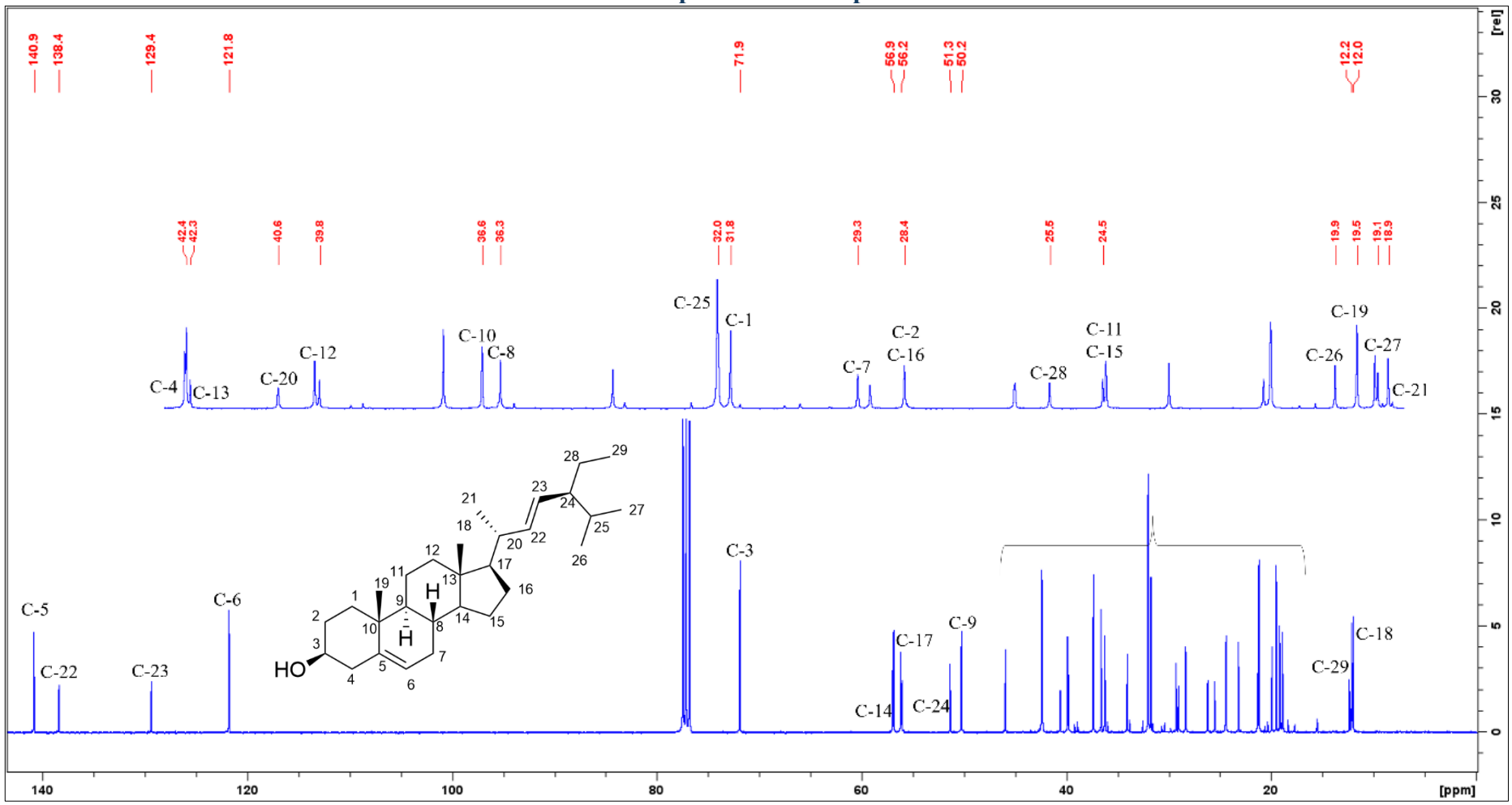

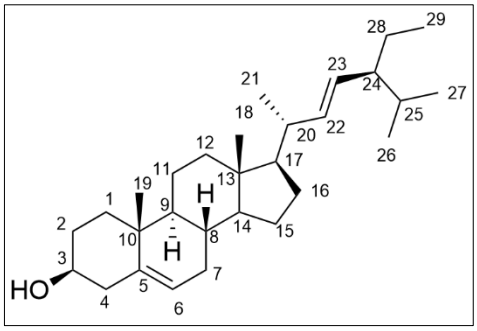

(70)

Table 4-7:
Spectral data comparison of compound 70 with previous literature

No.	δ ^{13}C (ppm)	δ ^{13}C (ppm) *	δ ^{1}H-^{13}C HSQC (^{1}J) (Mult. *J* Hz. Int)	δ ^{1}H (Mult. *J* Hz. int) *
1	31.8	36.6	1.52 (*m*)	1.84 (*m*)
2	28.4	29.3	1.85 (*m*)	1.83 (*m*)
3	71.9	71.9	3.53 (*m*, 1H)	3.52 (*m*)
4	42.4	42.3	2.26 (*m*)	2.30 (*m*)
5	140.9	140.9	-	-
6	121.8	121.8	5.35 (*m*, 1H)	5.35 (*m*)
7	29.3	31.8	1.67 (*m*)	1.97 (*m*)
8	36.3	29.0	1.37(*m*)	1.46 (*m*)
9	50.2	50.2	0.93 (*m*)	0.92 (*m*)
10	36.6	36.3		
11	24.5	24.4	1.56 (*m*)	1.50 (*m*)
12	39.8	39.8	2.00 (*m*)	2.00 (*m*)
13	42.3	40.6	-	-
14	56.9	56.9	1.02 (*m*)	1.01 (*m*)
15	24.5	24.5	1.58 (*m*)	1.56 (*m*)
16	28.4	28.4	1.26 (*m*)	1.72 (*m*)
17	56.2	56.1	1.13 (*m*)	1.15 (*m*)
18	12.0	12.0	0.69 (*m*)	0.69 (*m*)
19	19.5	19.1	1.02 (*m*)	1.01 (*m*)
20	40.6	39.9	2.05 (*m*)	2.06 (*m*)
21	18.9	23.2	0.93 (*m*)	1.02 (*m*)
22	138.4	138.4	5.16 (*dd*, 15.1, 8.6, 1H)	5.17 (*dd*, 15.2, 8.6)
23	129.4	129.4	5.03 (*dd*, 15.1, 8.6, 1H)	5.03 (*dd*, 15.2, 8.6)
24	51.3	51.3	1.54 (*m*)	1.54 (*m*)
25	32.0	34.1	1.45 (*m*)	1.55 (*m*)
26	19.9	21.2	0.85 (*m*)	0.85 (*m*)
27	19.1	21.3	0.82 (*m*)	0.80 (*m*)
28	25.5	25.5	1.43 (*m*)	1.44 (*m*)
29	12.2	12.1	0.82 (*m*)	0.81 (*m*)

*Marliyana et al. (2021); measured in $CDCl_3$, 500 MHz (^{1}H) and 125 MHz (^{13}C).

4.3 *C. nodosum* Antibacterial Activities

Secondary metabolites obtained from nature have been a valuable source of bioactive constituents with potential properties, providing new lead compound candidates for drug development. This study on *C. nodosum* has led to the identification of a new compound, nodosuxanthone (**89**), and the evaluation of both crude extracts and isolated compounds for antibacterial activity to assess their pharmaceutical potential. To achieve this, antibacterial assays were conducted on the crude extracts of *n*-hexane (CnH), chloroform (CnC), methanol (CnM) and all seven isolated compounds against different bacterial strains of Gram-positive (*S. aureus*) and Gram-negative bacteria (*A. baumannii, E. coli, P. aeruginosa*, and *K. pneumoniae*). In this study, one Gram-positive strain and four Gram-negative strains were selected to evaluate the antibacterial potential of the extracts and isolated compounds.

The inclusion of *S. aureus* as a common model Gram-positive pathogen allows comparison with previous studies that often report activity against this bacterial strain by extracts and isolated compounds from this genus, as shown in the literature review section (Abbas & Minarti, 2020; Alkhamaiseh et al., 2011, 2012; Aminudin et al., 2019; Kawamura et al., 2012; Ragasa et al., 2015; Yasunaka et al., 2005; Yimdjo et al., 2004). Meanwhile, this study emphasised Gram-negative bacteria because they are generally more challenging to treat due to their structural complexity and higher resistance mechanisms, like lipopolysaccharides (LPS), making them less susceptible to many conventional antibiotics (Breijyeh et al., 2020).

The difference in mechanism between the two Gram bacteria is that the Gram-positive bacteria generally have a thicker peptidoglycan cell wall layer compared to the Gram-negative bacteria, which can help protect them against some antibiotics by hindering the entry of the antibiotics (Kakoullis et al., 2021). While Gram-negative bacteria have a thin peptidoglycan layer (Reith & Mayer, 2011), they have an outer membrane layer with LPS, which often confers resistance to antibacterial agents (Miller, 2016).

In this study, the negative control used was dimethyl sulfoxide (DMSO), while the positive control used was ampicillin, a broad-spectrum antibiotic known for its efficacy against both types of bacteria (Sharma et al., 2013).

4.3.1 Well diffusion screening

The antibacterial activity of *C. nodosum* extracts (CnH, CnC, CnM) and all seven isolated compounds were initially screened using the agar well diffusion method. The zone of inhibition for each sample was evaluated by measuring the diameter of the clear inhibition zones around the wells after an incubation period with the bacteria. Each well was loaded with test samples at concentrations of 1 mg/mL and 0.1 mg/mL for crude extracts and isolated compounds, respectively. The screening was conducted in triplicate, and the results are summarised in Table 4-8.

One-way ANOVA revealed statistically significant differences among treatments for all five bacterial strains tested ($p < 0.05$). The homogeneity of variance was violated only for *S. aureus*, for which the Games-Howell post hoc analysis was applied. Tukey's HSD was used for the remaining strains. In this study, the threshold activity defined by Zamakshshari et al. (2024) was adopted as the reference standard, whereby antibacterial potency was categorized according to the diameter of the inhibition zone: weak (< 5 mm), moderate (5 – 10 mm), strong (10 – 20 mm), and very strong (20-30 mm) (Detha et al., 2018; Morales et al., 2003; Sanam et al., 2022).

In the preliminary screening stage, the *n*-hexane extract of *C. nodosum* (CnH) exhibited the most promising antibacterial activity, producing inhibition zones of 11.33 mm, 10.44 mm, and 11.67 mm against *A. baumannii*, *E. coli*, and *K. pneumoniae*, respectively. By contrast, the chloroform extract of *C. nodosum* (CnC) and the methanol extract of *C. nodosum* (CnM) exhibited inhibition zones below 10 mm across most strains and were therefore considered inactive in the preliminary screening Zamakshshari et al. (2024).

The strong inhibition of CnH suggests the enrichment of lipophilic bioactive constituents within the nonpolar fraction as several active compounds, like trapezifolixanthone (**20**), caloxanthone C (**5**), canumolactone (**90**), friedelin (**71**), and stigmasterol (**70**), were isolated from this extract and have individually displayed strong (> 10.00 mm) inhibitory effects. The better activity of CnH as compared to CnC and CnM is likely due to the higher proportion of membrane-active lipophilic compounds, especially the triterpenoid class compounds, like friedelin (**71**) and stigmasterol (**70**), which is known to disrupt bacterial membranes Yeap et al. (2017). The presence of these compounds was enough to make the antibacterial activity of CnH stand out, let alone the synergistic effect of all the compounds, as the synergistic interactions among multiple classes of constituents,

like xanthones, triterpenes, and lactones, may have also further enhanced the observed activity (Heilman et al., 2023).

Among the isolated compounds, all compounds demonstrated variable activities, as the newly undescribed xanthone, nodosuxanthone (**89**) shows weaker inhibition towards all bacterial strains tested, except for moderately inhibiting *P. aeruginosa* at 9.33 mm. Trapezifolixanthone (**20**) displayed a similar profile, being inactive against most strains but inhibiting *P. aeruginosa* with a diameter of 10.11 mm, suggesting that both compounds may share a related mechanism of action against this bacterial species for their similarity in chemical structure. The caloxanthone C (**5**) showed selective activity, inhibiting *E. coli* (10.33 mm) and *P. aeruginosa* (12.44 mm), while displaying minimal activity (<10.00 mm) against the remaining strains. Canumolactone (**90**) exhibited the broadest spectrum, producing inhibition zones of 12.56 mm against *A. baumannii* and 11.78 mm against both *E. coli* and *P. aeruginosa*. Similarly, stigmasterol (**70**) inhibited *K. pneumoniae* (12.00 mm) and *P. aeruginosa* (12.44 mm). Friedelin (**6**), a triterpenoid, demonstrated highly selective activity, inhibiting only *A. baumannii* (11.11 mm), while showing insufficient activity against the other strains. The 1-hydroxy-7-methoxyxanthone (**27**) was the only compound that was inactive across all bacterial species other than nodosuxanthone (**89**).

Although CnC had isolated some bioactive compounds as well, the active compounds isolated from CnC were not as many as in CnH, whereby the extract only successfully isolated the inactive, 1-hydroxy-7-methoxyxanthone (**27**), and two other xanthone class of compounds, trapezifolixanthone (**20**), and caloxanthone C (**5**). It could also be that the presence of the compounds that are active against the bacterial strains is present in smaller quantities in CnC and CnM as compared to CnH (Alawode et al., 2021).

Other than that, corresponding results were presented by Vittaya et al. (2023), as the *n*-hexane extract of another *Calophyllum* genus also exhibited better antibacterial activity in the study. Vittaya et al. (2023) stated that it could be due to the substituents within each of the compounds that are available in the extract, such as alkanes, alcohols, carboxylic acids, aromatics, esters, aliphatic amines, and alkyl halides (Gilbert, 2017). This has been mentioned in a study done by Kamdem et al. (2022) and Radi et al. (2023), that the predominatly polar substituents have a higher activity than nonpolar substituents according to the structure-activity relationship (SAR) reported.

Overall, the CnH extract appears enriched in compounds whose physicochemical properties are more effective against Gram-negative bacteria but less suited for Gram-positive targets. This can be seen as both the extract and isolated compounds exhibited limited efficacy against *S. aureus*. The results in this study are contradictory to previous studies, which have reported that the *Calophyllum* genus suggested greater susceptibility of Gram-positive bacteria compared to Gram-negative bacteria (Abbas & Minarti, 2020; Alkhamaiseh et al., 2011, 2012; Aminudin et al., 2019; Kawamura et al., 2012; Ragasa et al., 2015; Yasunaka et al., 2005; Yimdjo et al., 2004). This is likely due to its highly evolved and diverse mechanisms of antibiotic resistance. As detailed by Kakoullis et al. (2021), *S. aureus* can develop resistance toward the majority of antibiotic classes through various strategies like *β*-lactamase production, altered penicillin-binding proteins, efflux pumps, enzymatic inactivation, target site mutations, and thickened cell walls that impede antibiotic penetration (Nikolic & Mudgil, 2023). Another study done on the intraspecific variability in resistance genes has been documented across different isolates of *E. coli*, further emphasising that strain-to-strain differences can significantly influence susceptibility outcomes (Suarez & Martiny, 2024). Taken together, these explained the unexpected resistance even against compounds to which *S. aureus* strains are typically susceptible.

The lack of inhibition against *P. aeruginosa* by CnH at the extract level, despite certain compounds isolated from the extract being active, suggests that the permeability barriers and efflux mechanisms in this species of bacteria limit the efficacy of crude mixtures. This observation is consistent with previous studies on another *Calophyllum* extract, which also reported poor activity against *P. aeruginosa* due to the protective role of its outer membrane (Ha et al., 2009). The proportions of bioactive compounds present in the extract might affect activity in the preliminary screening stage, whereby some individual compounds may be synergistic or antagonistic among one another throughout the test (Budiyanto et al., 2022). The resulting crude extract is a mixture of tens to thousands, each ranging in quantity from trace to a major component of the mixture (Harris, 2002). Therefore, it is possible that the extract contained enough concentration of bioactive compounds such as friedelin (**71**) and stigmasterol (**70**) to inhibit the other Gram-negative bacterial strains but not *P. aeruginosa*.

The strong activity (> 10.00 mm) exhibited by stigmasterol (**70**) needs no introduction, as previous studies have evidenced its inhibition against Gram-negative bacteria (Ayele et al., 2022). This could be the same reason for its good activity towards

Gram-negative bacteria in this study, as stigmasterol (**70**) has been shown to exhibit very strong inhibition (24 mm) towards *E. coli* in another study (Yusuf et al., 2018). A study done by Alawode et al. (2021) also indicated that the antibacterial activity of stigmasterol is attributable to its ability to inhibit "sortase", which is an enzyme found in bacteria that participates in pathways involving secretion and anchoring of cell wall proteins. Another possible mechanism of action for stigmasterol against the bacteria is disrupting the bacterial cell membrane, altering its fluidity and causing leakage of cellular contents and thus affecting membrane-bound processes (de Dieu Tamokou et al., 2011). While the lack of antibacterial activity of friedelin (**71**) in this study was supported by Pretto et al. (2004), there is a review on the collection of data for previous research done for the antibacterial activity of friedelin, which shows contradictory results, as friedelin (**71**) shows inhibition toward bacterial strains across different studies (Radi et al., 2023).

On the other hand, the activity demonstrated by trapezifolixanthone (**20**) and caloxanthone C (**5**) are evidenced by literature, which has mentioned the good activity of this class of compounds, xanthone, particularly in antibacterial activity (Liu et al., 2021). This is especially true for the two compounds isolated, as another study has mentioned that the presence of hydrophobic prenyl groups attached to the aromatic ring of the xanthone, which in this case, is at the C-4 position of both trapezifolixanthone (**20**) and caloxanthone C (**5**), has increased the lipophilicity and membrane affinity of the compound to help penetrate bacterial membranes, allowing more interaction with bacterial phospholipid bilayers (Fu et al., 2025). Although 1-hydroxy-7-methoxyxanthone (**27**) also has a xanthone skeleton, the absence of a prenyl group within the structure causes the compound to lack antibacterial activity when compared with the other two xanthones, compounds (**20**) and (**5**). Other than that, there is a study that has been concluded by Liu et al. (2021), showing that the presence of simple methoxy and hydroxyl groups has little effect on antibacterial activity. This shows the reason why compound (**27**) did not show good inhibition, even though it is from the same class of compounds as compounds (**20**) and (**5**), since compound (**27**) is a simple xanthone with one hydroxyl and methoxy group only.

For the lactone isolated, there aren't many compounds of this class being isolated from the *Calophyllum* genus. However, the antibacterial activity of this class of compounds is well-known (Kowalczyk et al., 2021). This usually occurs in the smaller ring size (seven-membered and below) of the lactone (Mazur & Masłowiec, 2022). However, gamma (five-membered ring) and delta (six-membered ring) lactones are the ones that are most commonly

active and show antibacterial properties, as they form the most stable rings compared to the rest of them, which have a more constrained ring and have unfavourable interactions with the structure of the cyclic system (Kowalczyk et al., 2021).

This fits with canumolactone (**90**) description as the compound having six-membered cyclic esters, which is also known as the delta lactone. It is believed that the ability of canumolactone exhibits good activity towards the gram-negative bacteria specifically is due to it being an alpha-beta unsaturated lactone, having a conjugated double bond adjacent to the carbonyl group (Egbujor et al., 2022). This structure enables the compound to be more electrophilically active as the ring act as Michael acceptors (Mazur & Masłowiec, 2022), enabling them to form an irreversible covalent bond with the bacterial proteins through alkylation of enzymes to inhibit the key bacterial enzyme, disrupting cell membrane integrity, causing oxidative stress induction, and ultimately leading to cell death (Mayer et al., 2021). Refer to Appendix 33 for images showing the inhibition zone susceptibility of both isolated compounds and extracts derived from *C. nodosum*.

Statistical comparison with the positive standard revealed strain-dependent susceptibility patterns as canumolactone (**90**) was the only one that was statistically comparable to ampicillin ($p > 0.05$) against *S. aureus*, while all the other extracts and compounds were significantly lower inhibition. In contrast, ampicillin remained significantly superior to all tested samples against *E. coli* ($p < 0.05$), indicating limited comparability of the natural products for this strain. For *K. pneumoniae*, stigmasterol (**70**) showed significantly greater inhibition than ampicillin, while the CnH displayed statistically comparable activity. Interestingly, both caloxanthone C (**5**) and stigmasterol (**70**) significantly outperformed ampicillin, with canumolactone (**90**) also demonstrated superior inhibitory effects. A similar trend was observed for *A. baumannii*, as canumolactone (**90**) exhibited significantly higher activity than ampicillin, with CnH and friedelin (**71**) showing comparable inhibition. Collectively, these findings suggest that caloxanthone C (**5**), canumolactone (**90**) and stigmasterol (**70**) possess antibacterial activities comparable or exceeding the standard antibiotic against certain Gram-negative pathogens.

Table 4-8:
Inhibition zones (mm) of isolated compounds and extracts

	Diameter of inhibition zone (mm)				
	Gram-positive bacteria	Gram-negative bacteria			
Sample	*S. aureus*	*A. baumannii*	*E. coli*	*K. pneumoniae*	*P. aeruginosa*
CnH	7.56 ± 0.73^{b}	11.33 ± 1.22^{b}	10.44 ± 1.51^{b}	11.67 ± 1.00^{b}	8.22 ± 1.09^{e}
CnC	7.00 ± 0.00^{b}	8.00 ± 0.60^{d}	8.89 ± 0.78^{d}	8.00 ± 0.71^{d}	8.00 ± 0.71^{f}
CnM	7.44 ± 0.53^{b}	9.22 ± 0.83^{c}	9.44 ± 0.53^{c}	8.56 ± 0.88^{d}	7.66 ± 0.88^{f}
Nodosuxanthone (89)	7.22 ± 0.44^{b}	7.78 ± 0.67^{d}	8.33 ± 0.71^{d}	7.78 ± 0.67^{e}	9.33 ± 0.87^{d}
Trapezifolixanthone (20)	7.22 ± 0.44^{b}	7.78 ± 0.67^{d}	8.33 ± 0.71^{d}	8.67 ± 0.05^{d}	10.11 ± 0.60^{c}
Caloxanthone C (5)	7.67 ± 0.50^{b}	9.78 ± 0.83^{c}	10.33 ± 1.12^{b}	8.44 ± 0.88^{d}	12.44 ± 0.88^{a}
1-hydroxy-7-methoxyxanthone (27)	7.11 ± 0.33^{b}	8.78 ± 0.67^{c}	8.67 ± 0.71^{d}	8.78 ± 0.67^{d}	8.33 ± 0.50^{e}
Canumolactone (90)	8.11 ± 0.78^{a}	12.56 ± 0.53^{a}	11.78 ± 0.67^{b}	8.44 ± 0.53^{d}	11.78 ± 1.20^{b}
Friedelin (71)	7.67 ± 0.71^{b}	11.11 ± 1.05^{b}	9.89 ± 0.78^{c}	9.67 ± 1.32^{c}	8.67 ± 0.50^{e}
Stigmasterol (70)	7.00 ± 0.00^{b}	9.00 ± 1.22^{c}	9.78 ± 1.30^{c}	12.00 ± 1.00^{a}	12.44 ± 0.53^{a}
Ampicillin	8.67 ± 0.71^{a}	10.44 ± 1.74^{b}	14.22 ± 1.39^{a}	11.00 ± 0.50^{b}	8.67 ± 0.87^{e}
DMSO	NA	NA	NA	NA	NA

Different superscript letters within the same column indicate significant differences ($p < 0.05$) for respective bacterial strain only. Superscripts are not comparable across different bacteria. CnH: *Calophyllum nodosum n*-hexane extract; CnC: *Calophyllum nodosum* chloroform extract; CnM: *Calophyllum nodosum* methanol extract; DMSO: Dimethyl sulfoxide; NA: No Activity

4.3.2 Minimum inhibitory concentration (MIC) and minimum bactericidal concentration (MBC)

The minimum inhibitory concentration (MIC) stands for the lowest concentration of a sample at which no visible bacterial growth is observed, both before and following incubation (Parvekar et al., 2020). Only samples showing inhibition zones reaching or exceeding 10 mm are deemed as strong, suggesting such samples for further analysis using the MIC assay (Zamakshshari et al., 2023). Then, those showing no turbidity or visible bacterial growth within the tested concentration in the MIC test proceeded to the minimum bactericidal concentration (MBC) assay. Meanwhile, the MBC is defined as the lowest concentration of the sample that completely kills the bacterial cells, as confirmed by the absence of visible growth even after subculturing onto fresh agar plates following incubation (Parvekar et al., 2020). Following the criteria mentioned, CnH was brought forward to MIC and MBC against *A. baumanii*, *E. coli*, *K. pneumoniae*, and *P. aeruginosa*; trapezifolixanthone (**20**) against *P. aeruginosa*; caloxanthone C (**5**) against *E. coli* and *P. aeruginosa*; canumolactone (**90**) against *A. baumannii*, *E. coli*, and *P. aeruginosa*; Friedelin (**71**) against *A. baumanii*; stigmasterol (**70**) against *K. pneumoniae*, and *P. aeruginosa*.

In the MIC and MBC assay, the *n*-hexane extract (CnH) demonstrated moderate MIC values of 0.25 mg/mL against *E. coli*, *A. baumannii* and *K. pneumoniae*. The following MBC results for the *n*-hexane extract also indicated that it is bactericidal towards *A. baumannii* and *E. coli* at a concentration of 1.0 mg/mL, while it is bactericidal against *K. pneumoniae* at 0.5 mg/mL. This finding aligns with previous studies by (Abbas J, 2019; Vittaya et al., 2023), which showed that the *Calophyllum n*-hexane extract yielded the best results compared to the other extracts that are more polar at a concentration as low as < 0.098 mg/mL.

Among the isolated compounds, trapezifolixanthone (**20**) showed moderate activity towards *P. aeruginosa* at an MIC level of 0.025 mg/mL as well as 0.1 mg/mL in the MBC test against the same bacterial strain. On the other hand, caloxanthone C (**5**) inhibited *E. coli* and *P. aeruginosa*, each at an MIC value of 0.025 mg/mL, while exhibiting MBC values at 0.05 mg/mL and 0.1 mg/mL, respectively, towards the two strains. This shows that the xanthone skeleton structure of compounds **20** and **5** features a planar dibenzo-γ-pyrone core that, when decorated with hydrophobic prenyl side chains, gains high affinity for bacterial membranes (Gunter et al., 2020). This amphipathic balance lets these molecules insert into lipid bilayers, compromising membrane integrity and disrupting essential barrier functions,

leading to direct membrane targeting that causes their rapid bactericidal effects (Koh et al., 2018).

Canumolactone (**90**), on the other hand, exhibited moderate activity towards *A. baumannii*, *P. aeruginosa* and *E. coli* with MIC value at 0.025 mg/mL. Canumolactone (**90**) is also able to demonstrate bactericidal activity at 0.05 mg/mL for *A. baumannii* and 0.1 mg/mL for both *P. aeruginosa* and *E. coli*. This fits with the explanation above, mentioning the ability of canumolactone (**90**) in causing cell death, which features its bactericidal effect (Mayer et al., 2021). For the triterpenoids that were isolated, friedelin (**71**) was moderately active against *A. baumannii* at a concentration of 0.025 mg/mL, while having a bactericidal effect at a concentration of 0.1 mg/mL. The same applies to stigmasterol (**70**), as it displayed moderate activity towards *P. aeruginosa* and *K. pneumoniae* at a MIC value of 0.25 mg/mL and 0.05 mg/mL towards *K. pneumoniae* in the MBC test. However, stigmasterol (**70**) does not show bactericidal effect on *P. aeruginosa* at 0.1 mg/mL, which indicates that it might need a higher concentration to be bactericidal towards *P. aeruginosa*.

According to Akongwi et al. (2023), samples with an MBC: MIC ratio ≤ 4 are considered bactericidal against specific microbial strains. This method was used to determine the bactericidal potential of a sample. In this study, all samples that have been brought forward to MIC and MBC assays met this criterion, except for stigmasterol (**7**), which, when tested against *P. aeruginosa,* the bacteria still grew after incubation for another 18 hours. This matched with the previous report, indicating that stigmasterol does not kill the bacteria; instead, it only inhibits, giving bacteriostatic effects (Villarreal et al., 2022).

The MIC and MBC results tallied with the preliminary screening done, as strong correlations were seen that when the well diffusion method gives large inhibition zones, MIC results were shown, and even at a lower concentration. Most of the samples tested showed more killing of the bacteria instead of inhibiting the bacteria, except for stigmasterol (**70**). The results for MIC and MBC were tabulated as in Table 4-9.

Overall, integration of the well diffusion screening, statistical analysis, and MIC/MBC results identified canumolactone (**90**) as the most potent antibacterial compound, followed by caloxanthone C (**5**). Canumolactone consistently produced strong inhibition zones (> 10 mm), demonstrated statistical comparability or superiority to ampicillin against selected strains, and exhibited low MIC (0.025 mg/mL) with bactericidal MBC values of 0.05-0.1 mg/mL. Although caloxanthone C (**5**) displayed a comparatively narrower activity

spectrum, it demonstrated pronounced inhibition, particularly against *P. aeruginosa* and *E. coli*, with low MIC and bactericidal effects. In contrast, stigmasterol (**70**) exhibited higher MIC values and lacked bactericidal activity against *P. aeruginosa*, indicating comparatively lower killing efficiency. Collectively, these findings highlight canumolactone (**90**) and caloxanthone C (**5**) as the most promising antibacterial candidates identified in this study.

Table 4-9:
Minimum Inhibitory Concentration (MIC) and Minimum Bactericidal Concentration (MBC) of *Calophyllum nodosum* Extracts and Compounds

Sample	*A. baumannii*		*E. coli*		*K. pneumoniae*		*P. aeruginosa*	
	MIC	MBC	MIC	MBC	MIC	MBC	MIC	MBC
	mg/mL							
CnH	0.25	1.0	0.25	1.0	0.25	0.5	-	-
CnC	-	-	-	-	-	-	-	-
CnM	-	-	-	-	-	-	-	-
Nodosuxanthone (89)	-	-	-	-	-	-	-	-
Trapezifolixanthone (20)	-	-	-	-	-	-	0.025	0.1
Caloxanthone C (5)	-	-	0.025	0.05	-	-	0.025	0.1
1-hydroxy-7-methoxyxanthone (27)	-	-	-	-	-	-	-	-
Canumolactone (90)	0.025	0.05	0.025	0.1	-	-	0.025	0.1
Friedelin (71)	0.025	0.1	-	-	-	-	-	-
Stigmasterol (70)	-	-	-	-	0.025	0.05	0.025	> 0.1
Ampicillin	0.025	0.05	0.025	0.05	0.025	0.05	-	-
DMSO	-	-	-	-	-	-	-	-

CnH: *Calophyllum nodosum n*-hexane extract; CnC: *Calophyllum nodosum* chloroform extract; CnM: *Calophyllum nodosum* methanol extract; DMSO: Dimethyl sulfoxide; (-) = Not determined; MIC: Minimum inhibitory concentration; MBC: Minimum bactericidal concentration

CHAPTER 5:

CONCLUSION

5.1 Conclusion

In conclusion, the phytochemical analysis of the stem bark of *C. nodosum* has been done successfully, leading to the isolation and identification of seven compounds, including four xanthones, nodosuxanthone (**89**), trapezifolixanthone (**20**), caloxanthone C (**5**), 1-hydroxy-7-methoxyxanthone (**27**); a lactone, canumolactone (**90**); and two terpenes, friedelin (**71**) and stigmasterol (**70**). Significantly, this study marks the initial reporting of the undescribed naturally produced secondary metabolites, nodosuxanthone (**89**), further enriching the knowledge of bioactive compounds derived from the genus of *Calophyllum* and their future applications. The antibacterial results were conducted over a concentration range of 1.0 to 1.95 x 10^{-3} and 0.1 to 1.95 x 10^{-4} mg/mL, and the results indicated that both the *C. nodosum* crude extracts and its isolated compounds demonstrated promising activity towards bacterial strains at varying degrees, with the *n*-hexane extract showing moderate efficacy against *A. baumannii, E. coli,* and *K. pneumoniae*. Among the isolated compounds, caloxanthone C (**5**), and canumolactone (**90**) demonstrated notable antibacterial and bactericidal effects, particularly against Gram-negative bacteria. The enhanced activity observed in the *C. nodosum* extract may be due to the possible synergistic effects between these bioactive compounds, where the combined action of multiple phytoconstituents enhances the overall antibacterial activity. These findings suggest that the compounds in the nonpolar extract have the potential to become antibacterial agents, further proving that a lot of lead compounds can be derived from *Calophyllum* plants for medicinal findings and pharmaceutical development. The findings in this study suggest that *C. nodosum* is a promising source for identifying lead compound candidates as new antibacterial agents.

5.2 Recommendations

The isolated compounds were obtained in low yield, highlighting the need for a standardised isolation method to improve their recovery. This difficulty in separating compounds from each other resulted in low amounts after several purifications. Therefore, it is recommended to use Preparative High-Performance Liquid Chromatography (prep-HPLC) to separate the compounds. This technique is highly effective for the separation and purification of complex mixtures, allowing the compounds to be separated with greater precision. Once sufficient amounts are obtained, structural modifications should be explored to enhance their antibacterial potency and selectivity. In the antibacterial assay, a variety of bacterial strains consisting of Gram-positive and Gram-negative bacteria should be used to allow for a complete evaluation of antibacterial potential, revealing selective or broad activity, and ensuring relevance to real-world infections with varying resistance profiles. Additionally, integrating advanced analytical techniques such as computational modelling can optimise drug discovery by predicting bioactivity, improving compound-target interactions, and accelerating the development of lead compounds from *Calophyllum* species.

Specifically, molecular docking studies should be conducted to predict the binding interactions between the isolated compounds and key bacterial targets, such as DNA gyrase, topoisomerase IV, or penicillin-binding proteins, to elucidate possible mechanisms of antibacterial action at the molecular level. Furthermore, molecular dynamics (MD) simulations can be applied to evaluate the stability, conformational behavior, and interaction persistence of compound-target complexes under dynamic biological conditions, thereby strengthening the reliability of docking predictions. In addition, artificial intelligence (AI)-based activity prediction models, including quantitative structure-activity relationship (QSAR) analysis and machine learning algorithms, may be employed to predict antibacterial potency, identify key structural features responsible for activity, and guide rational lead optimization strategies. In future studies, a combination of two or more isolated compounds should be investigated to determine the potential of synergistic effects that could improve their antibacterial efficacy and broaden their biological activity.

Computational synergy modelling and in silico multi-target analysis may also be integrated to predict potential synergistic mechanisms prior to experimental validation. Moreover, the *in vivo* efficacy and toxicity profiles of these compounds should be assessed to explore their potential in pharmaceutical applications.

REFERENCES

Abbas J. (2019). Antioxidant and anti-bacterial activities of 11 *Calophyllum* species from Indonesia. *Journal of Microbial Systematics and Biotechnology*, *1*(2), 1–12.

Abbas, J., & Minarti. (2020). Antibacterial activity of isolated compounds from the stem bark of *Calophyllum euryphyllum*. *IOP Conference Series: Earth and Environmental Science*, *591*(1), 012019. https://doi.org/10.1088/1755-1315/591/1/012019

Abdel-Kerim, F. M., & Shoeb, H. A. (1972). Absorption Spectra of Xanthone and Dibenzoxanthones. *Zeitschrift Für Physikalische Chemie*, *251*(1), 209–216. https://doi.org/10.1515/zpch-1972-25123

Abdul Rahman, A., Wan Ngah, W. Z., Jamal, R., Makpol, S., Harun, R., & Mokhtar, N. (2022). Inhibitory Mechanism of Combined Hydroxychavicol with Epigallocatechin-3-Gallate Against Glioma Cancer Cell Lines: A Transcriptomic Analysis. *Frontiers in Pharmacology*, *13*, 844199. https://doi.org/10.3389/fphar.2022.844199

Abdullah, Khan, M. A., Ahmad, W., Ahmad, M., Adhikari, A., Ibrar, M., Rehman, M. ur, & Asif, M. (2022). Antioxidant, antinociceptive, anti-inflammatory, and hepatoprotective activities of pentacyclic triterpenes isolated from *Ziziphus oxyphylla* Edgew. *Drug and Chemical Toxicology*, *45*(4), 1796–1807. https://doi.org/10.1080/01480545.2021.1880427

Abe, I. (2007). Enzymatic synthesis of cyclic triterpenes. *Natural Product Reports*, *24*(6), 1311–1331. https://doi.org/10.1039/B616857B

Abe, I., Rohmer, M., & Prestwich, G. D. (1993). Enzymatic Cyclization of Squalene and Oxidosqualene to Sterols and Triterpenes. *Chemical Reviews*, *93*(6), 2189–2206. https://doi.org/10.1021/cr00022a009

Abegaz, B. M., & Kinfe, H. H. (2019). Secondary metabolites, their structural diversity, bioactivity, and ecological functions: An overview. *Physical Sciences Reviews*, *4*(6), 20180100. https://doi.org/10.1515/psr-2018-0100

Akongwi, M., Kwene, E. C., Awah, L. A., Tih, A. E., Ghogomu, R. T., Cho-Ngwa, F., & Ngemenya, M. N. (2023). Anti-Salmonella activity on multidrug-resistant strains and cytotoxicity of extracts and constituents of *Garcinia brevipedicellata* and *Garcinia epunctata*. *Scientific African*, *19*, e01465. https://doi.org/10.1016/j.sciaf.2022.e01465

Alamgir, A. N. M. (2018). Phytoconstituents—Active and Inert Constituents, Metabolic Pathways, Chemistry and Application of Phytoconstituents, Primary Metabolic Products, and Bioactive Compounds of Primary Metabolic Origin. *Progress in Drug Research*, *74*, 25–164. https://doi.org/10.1007/978-3-319-92387-1_2

Alawode, T. T., Lajide, L., Olaleye, M., & Owolabi, B. (2021). Stigmasterol and *β*-Sitosterol: Antimicrobial Compounds in the Leaves of *Icacina trichantha* identified by GC–MS. *Beni-Suef University Journal of Basic and Applied Sciences*, *10*(1), 1–8. https://doi.org/10.1186/s43088-021-00170-3

Aljeldah, M. M. (2022). Antimicrobial Resistance and Its Spread Is a Global Threat. *Antibiotics*, *11*(8). https://doi.org/10.3390/antibiotics11081082

Alkhamaiseh, S. I., Taher, M., & Ahmad, F. (2011). The Phytochemical Contents and Antimicrobial Activities of Malaysian *Calophyllum Rubiginosum*. *American Journal of Applied Sciences*, *8*(3), 201–205. https://doi.org/10.3844/ajassp.2011.201.205

Alkhamaiseh, S. I., Taher, M., Ahmad, F., Qaralleh, H., Althunibat, O. Y., Susanti, D., & Ichwan, S. J. A. (2012). The phytochemical content and antimicrobial activities of Malaysian *Calophyllum canum* (stem bark). *Pakistan Journal of Pharmaceutical Sciences*, *25*(3), 555–563.

Al-Mijalli, S. H., Mrabti, H. N., El Hachlafi, N., El Kamili, T., Elbouzidi, A., Abdallah, E. M., Flouchi, R., Assaggaf, H., Qasem, A., Zengin, G., Bouyahya, A., & Chahdi, F. O. (2023). Integrated analysis of antimicrobial, antioxidant, and phytochemical properties of *Cinnamomum verum*: A comprehensive *In vitro* and *In silico* study. *Biochemical Systematics and Ecology*, *110*, 104700. https://doi.org/10.1016/j.bse.2023.104700

Aminudin, N. I., Ahmad, F., & Taher, M. (2019). Antibacterial and antioxidant activities of extracts from *Calophyllum ferrugineum* and *Calophyllum incrassatum*. *Malaysian Journal of Analytical Sciences*, *23*, 637–647.

Aminudin, N. I., Ahmad, F., Taher, M., & Zulkifli, R. M. (2016a). Cytotoxic and antibacterial evaluation of coumarins and chromanone acid from *Calophyllum symingtonianum*. *Journal of Applied Pharmaceutical Science*, *6*(1), 23–27.

Aminudin, N. I., Ahmad, F., Taher, M., & Zulkifli, R. M. (2016b). Incrassamarin A–D: Four new 4-substituted coumarins from *Calophyllum incrassatum* and their biological activities. *Phytochemistry Letters*, *16*, 287–293. https://doi.org/10.1016/j.phytol.2016.05.008

Anjali, Kumar, S., Korra, T., Thakur, R., Arutselvan, R., Kashyap, A. S., Nehela, Y., Chaplygin, V., Minkina, T., & Keswani, C. (2023). Role of plant secondary metabolites in defence and transcriptional regulation in response to biotic stress. *Plant Stress*, *8*, 100154. https://doi.org/10.1016/j.stress.2023.100154

Aparamarta, H. W., Hapsari, S., Ismawan, R., Anggraeni, V., Widjaja, A., Widjaja, T., Ju, Y.-H., & Gunawan, S. (2018). Separation of xanthone and vitamin E from *Calophyllum inophyllum* leaf. *Malaysian Journal of Fundamental and Applied Sciences*, *14*(4), 484–489. https://doi.org/10.11113/mjfas.v14n4.933

Araya-Maturana, R., Pessoa-Mahana, H., & Weiss-López, B. (2008). Very Long-Range Correlations ($^{n}J_{C,H}$ n > 3) in HMBC Spectra. *3*(3), 445–450. https://doi.org/10.1177/1934578X0800300321

Awuchi, C. G. (2019). The biochemistry, toxicology, and uses of the pharmacologically active phytochemicals: Alkaloids, terpenes, polyphenols, and glycosides. *Journal of Food and Pharmaceutical Sciences*, *7*(1), 2.

Ayele, T. T., Gurmessa, G. T., Abdissa, Z., Kenasa, G., & Abdissa, N. (2022). Oleanane and Stigmasterol-Type Triterpenoid Derivatives from the Stem Bark of *Albizia gummifera* and Their Antibacterial Activities. *Journal of Chemistry*, *2022*(1), 9003143. https://doi.org/10.1155/2022/9003143

Badiali, C., Petruccelli, V., Brasili, E., & Pasqua, G. (2023). Xanthones: Biosynthesis and Trafficking in Plants, Fungi and Lichens. Plants, *12*(4), 694. https://doi.org/10.3390/plants12040694

Bakar, F. I. A., Bakar, M. F. A., Abdullah, N., Endrini, S., & Rahmat, A. (2018). A Review of Malaysian Medicinal Plants with Potential Anti-Inflammatory Activity. *Advances in Pharmacological and Pharmaceutical Sciences*, *2018*(1), 8603602. https://doi.org/10.1155/2018/8603602

Beacham, I. R. (1979). Periplasmic enzymes in gram-negative bacteria. *International Journal of Biochemistry*, *10*(11), 877–883. https://doi.org/10.1016/0020-711X(79)90117-4

Biagi, G. L., Guerra, M. C., Barbaro, A. M., & Gamba, M. F. (1970). Influence of lipophilic character on the antibacterial activity of cephalosporins and penicillins. *Journal of Medicinal Chemistry*, *13*(3), 511–516. https://doi.org/10.1021/jm00297a038

Bolagun, O. S., Ajayi, O. S., & Kolawole, R. F. (2019). Chemical constituents and cytotoxic activity of stem bark extract of *Calophyllum inophyllum*. *Ife Journal of Science*, *21*(2), 411–416. https://doi.org/10.4314/ijs.v21i2.14

Breijyeh, Z., Jubeh, B., & Karaman, R. (2020). Resistance of Gram-Negative Bacteria to Current Antibacterial Agents and Approaches to Resolve It. *Molecules*, *25*(6), 1340. https://doi.org/10.3390/molecules25061340

Budiyanto, F., Ghandourah, M. A., Bawakid, N. O., Alorfi, H. S., Abdel-Lateff, A., & Alarif, W. M. (2022). Threat and gain: The metabolites of the red algae genus *Acanthophora*. *Algal Research*, *65*, 102751. https://doi.org/10.1016/j.algal.2022.102751

Cabral, F. N., Trad, R. J., Amorim, B. S., Maciel, J. R., do Carmo Estanislau do Amaral, M., & Stevens, P. (2021). Phylogeny, divergence times, and diversification in Calophyllaceae: Linking key characters and habitat changes to the evolution of Neotropical Calophylleae. *Molecular Phylogenetics and Evolution*, *157*(5), 107041. https://doi.org/10.1016/j.ympev.2020.107041

Calophyllum nodosum Vesque | Calophyllaceae | Malaysia Biodiversity Information System (MyBIS). (n.d.). Retrieved 11 June 2024, from https://www.mybis.gov.my/sp/64981

Chase, M. W., Christenhusz, M. J. M., Fay, M. F., Byng, J. W., Judd, W. S., Soltis, D. E., Mabberley, D. J., Sennikov, A. N., Soltis, P. S., Stevens, P. F. (2016). An update of the Angiosperm Phylogeny Group classification for the orders and families of flowering plants: APG IV. *Botanical Journal of the Linnean Society*, *181*(1), 1–20. https://doi.org/10.1111/boj.12385

Chinthu, R. V., Raveendran, P. B., & Raveendran, M. (2023). A review on the genus *Calophyllum* (Clusiaceae): a potential medicinal tree species. *Plant Science Today*, *10*(3), 01–05. https://doi.org/10.14719/pst.1818

Christaki, E., Marcou, M., & Tofarides, A. (2020). Antimicrobial Resistance in Bacteria: Mechanisms, Evolution, and Persistence. *Journal of Molecular Evolution*, *88*(1), 26–40. https://doi.org/10.1007/s00239-019-09914-3

Claridge, T. D. W. (2016). High-Resolution NMR Techniques in Organic Chemistry. In *High-Resolution NMR Techniques in Organic Chemistry: Third Edition* (3rd ed.). Elsevier. https://doi.org/10.1016/C2015-0-04654-8

Cottiglia, F., Dhanapal, B., Sticher, O., & Heilmann, J. (2004). New chromanone acids with antibacterial activity from *Calophyllum brasiliense*. *Journal of Natural Products*, *67*(4), 537–541. https://doi.org/10.1021/np030438n

Damit, A., Matusin, Dg Ku Rozianah, Sugau, J., & Pereira, J. T. (2024, September 7). *Calophyllum nodosum*. IUCN Red List of Threatened Species. https://dx.doi.org/10.2305/IUCN.UK.2024-2.RLTS.T37663A227979285.en

Daud, S., Karunakaran, T., Santhanam, R., Nagaratnam, S. R., Jong, V. Y. M., & Ee, G. C. L. (2021). Cytotoxicity and nitric oxide inhibitory activities of Xanthones isolated from

Calophyllum hosei Ridl. *Natural Product Research*, *35*(24), 6067–6072. https://doi.org/10.1080/14786419.2020.1819273

de Dieu Tamokou, J., Kuiate, J. R., Tene, M., Nwemeguela, T. J. K., & Tane, P. (2011). The Antimicrobial Activities of Extract and Compounds Isolated from *Brillantaisia lamium*. *Iranian Journal of Medical Sciences*, *36*(1), 24. https://pmc.ncbi.nlm.nih.gov/articles/PMC3559120/

Detha, A. I. R., Datta, F. U., Beribe, E., Foeh, N. D. F. K., & Ndaong, N. (2018). Efektivitas bakteri asam laktat yang diisolasi dari susu kuda sumba terhadap kualitas silase Jerami padi. *Jurnal Kajian Veteriner*, *6*(1), 31–37. https://doi.org/10.35508/jkv.v6i1.1053

Diana, E. J., Kanchana, U. S., & Mathew, T. V. (2021). Current developments in the synthesis of 4-chromanone-derived compounds. *Organic & Biomolecular Chemistry*, *19*(37), 7995–8008. https://doi.org/10.1039/D1OB01352A

Dweck, A. C., & Meadows, T. (2002). Tamanu (*Calophyllum inophyllum*) – the African, Asian, Polynesian and Pacific Panacea. *International Journal of Cosmetic Science*, *24*(6), 341-348.

Ee, G. C. L., Mah, S. H., Teh, S. S., Rahmani, M., Go, R., & Taufiq-Yap, Y. H. (2011). Soulamarin, a new coumarin from stem bark of *Calophyllum soulattri*. *Molecules*, *16*(11), 9721–9727. https://doi.org/10.3390/molecules16119721

Egbujor, M. C., Buttari, B., Profumo, E., Telkoparan-Akillilar, P., & Saso, L. (2022). An Overview of NRF2-Activating Compounds Bearing *α,β*-Unsaturated Moiety and Their Antioxidant Effects. *International Journal of Molecular Sciences 2022, Vol. 23, Page 8466*, *23*(15), 8466. https://doi.org/10.3390/ijms23158466

Elateeq, Z.-H. ;, Khan, A. A. ;, Khan, Y. ;, Khan, J. ;, Ali, A. ;, Plant, S., Hanada, K., Barna, B., Salam, U., Ullah, S., Tang, Z.-H., Elateeq, A. A., Khan, Y., Khan, J., Khan, A., & Ali, S. (2023). Plant Metabolomics: An Overview of the Role of Primary and Secondary Metabolites against Different Environmental Stress Factors. *Life 2023, Vol. 13, Page 706*, *13*(3), 706. https://doi.org/10.3390/life13030706

Elsaman, T., Mohamed, M. S., Eltayib, E. M., Abdalla, A. E., & Mohamed, M. A. (2020). Xanthone: A Promising Antimycobacterial Scaffold. *Medicinal Chemistry*, *17*(4), 310–331. https://doi.org/10.2174/1573406416666200619114124

Emami, S., & Ghanbarimasir, Z. (2015). Recent advances of chroman-4-one derivatives: Synthetic approaches and bioactivities. *European Journal of Medicinal Chemistry*, *93*, 539–563. https://doi.org/10.1016/j.ejmech.2015.02.048

Fleming, I., & Williams, D. (2020). Spectroscopic Methods in Organic Chemistry, Seventh Edition. In *Spectroscopic Methods in Organic Chemistry, Seventh Edition* (7th ed.). Springer International Publishing. https://doi.org/10.1007/978-3-030-18252-6

Fu, X., Mah, S. H., & Liu, M. (2025). Xanthones as Promising Anti-Infective Agents: Mechanisms and Therapeutic Potential. *American Journal of Biomedical Science & Research*, *26*(5). https://biomedgrid.com/pdf/AJBSR.MS.ID.003479.pdf

Genovese, S., Fiorito, S., Taddeo, V. A., & Epifano, F. (2016). Recent developments in the pharmacology of prenylated xanthones. *Drug Discovery Today*, *21*(11), 1814–1819. https://doi.org/10.1016/j.drudis.2016.06.033

Gilbert, A. S. (2017). IR Spectral Group Frequencies of Organic Compounds. *Encyclopedia of Spectroscopy and Spectrometry*, 408–418. https://doi.org/10.1016/B978-0-12-803224-4.00337-X

Gunter, N. V., Teh, S. S., Lim, Y. M., & Mah, S. H. (2020). Natural Xanthones and Skin Inflammatory Diseases: Multitargeting Mechanisms of Action and Potential Application. *Frontiers in Pharmacology*, *11*, 594202. https://doi.org/10.3389/fphar.2020.594202

Gupta, S., & Gupta, P. (2020). The Genus *Calophyllum*: Review of Ethnomedicinal Uses, Phytochemistry and Pharmacology. *Bioactive Natural Products in Drug Discovery*, 215. https://doi.org/10.1007/978-981-15-1394-7_5

Ha, M. H., Nguyen, V. T., Quynh, K., Nguyen, C., Cheah, E. L., & Heng, P. W. (2009). Antimicrobial activity of *Calophyllum inophyllum* crude extracts obtained by pressurized liquid extraction. *Asian Journal of Traditional Medicines*, *4*(4).

Hakim, A., Jufri, A. W., & Jamaluddin. (2021). Isolation of artelasticine for student practice in low-resource laboratory settings. *IOP Conference Series: Earth and Environmental Science*, *712*(1), 012050. https://doi.org/10.1088/1755-1315/712/1/012050

Hamza, M., Nadir, M., Mehmood, N., & Farooq, A. (2016). In vitro effectiveness of triterpenoids and their synergistic effect with antibiotics against *Staphylococcus aureus* strains. *Indian Journal of Pharmacology*, *48*(6), 714. https://doi.org/10.4103/0253-7613.194851

Harris, G. H. (2002). The use of CCC in the pharmaceutical industry. *Comprehensive Analytical Chemistry*, *38*, 301–330. https://doi.org/10.1016/S0166-526X(02)80013-7

Hasanah, U., Tjahjandarie, T. S., & Tanjung, M. (2019). Chromanone acid derivatives from the stem bark of *Calophyllum incrassatum*. *IOP Conference Series: Earth and Environmental Science*, *217*(1), 12010. https://doi.org/10.1088/1755-1315/217/1/012010

Heilman, D. N. A. A., Hui, A. Y. C., Mian, V. J. Y., Ahmad, F. B., Cee, L. P., Stanslas, J., & Zamakshshari, N. H. (2023). Unlocking the Antibacterial Potential of Xanthone from *Calophyllum* Species: Inhibition of Nucleic Acid Synthesis. *ChemistrySelect*, *8*(46), e202302737. https://doi.org/10.1002/slct.202302737

Heilman, D. N. A. A., Zamakshshari, N. H., Yi Mian, V. J., Chee Hui, A. Y., Lizazman, M. A., & Ahmad, F. B. (2024). Soulaxanthone, a new xanthone derivative from *Calophyllum soulattri*. *Natural Product Research*, *39*(19), 5502-5508. https://doi.org/10.1080/14786419.2024.2345752

Herawati, Z., & Rakhmawati, R. (2025). A review of calophyllolide from *Calophyllum inophyllum* L.: isolation, quantification, analytical method, and burn wound healing potential. *Jurnal Ilmiah Farmasi*, *21*(1), 105–119. https://journal.uii.ac.id/JIF/article/view/22921

Hogarth, P. (2004). Ecology and Silviculture of Tropical Wetland Forests. *Encyclopedia of Forest Sciences*, 1094–1100. https://doi.org/10.1016/B0-12-145160-7/00234-9

Ito, C., Matsui, T., Kobayashi, T., Tokuda, H., Shanmugam, S., & Itoigawa, M. (2018). Cancer chemopreventive activity of xanthones from *Calophyllum elatum*. *Natural Product Communications*, *13*(4), 447–449. https://doi.org/10.1177/1934578x1801300417

Joshi, P. P. (2021). A review on biological activities of linear pyranocoumarins. *International Journal of Advance Study and Research Work*, *4*(1), 2581–5997. https://doi.org/10.5281/zenodo.4478566

Kakoullis, L., Papachristodoulou, E., Chra, P., & Panos, G. (2021). Mechanisms of Antibiotic Resistance in Important Gram-Positive and Gram-Negative Pathogens and Novel Antibiotic Solutions. *Antibiotics, 10*(4), 415. https://doi.org/10.3390/antibiotics10040415

Kamboj, S., & Singh, R. (2021). Chromanone-A prerogative therapeutic scaffold: An overview. *Arabian Journal for Science and Engineering*, 47(1), 75-111. https://doi.org/10.1007/s13369-021-05858-3

Kamdem, M. H. K., Ojo, O., Kemkuignou, B. M., Talla, R. M., Fonkui, T. Y., Silihe, K. K., Tata, C. M., Fotsing, M. C. D., Mmutlane, E. M., Ndinteh, D. T., Kamdem, M. H. K., Ojo, O., Kemkuignou, B. M., Talla, R. M., Fonkui, T. Y., Silihe, K. K., Tata, C. M., Fotsing, M. C. D., Mmutlane, E. M., & Ndinteh, D. T. (2022). Pentacyclic Triterpenoids, Phytosteroids and Fatty Acid Isolated from the Stem-bark of *Cola lateritia* K. Schum. (Sterculiaceae) of Cameroon origin; Evaluation of Their Antibacterial Activity. *Arabian Journal of Chemistry*, *15*(1). https://doi.org/10.1016/j.arabjc.2021.103506

Karunakaran, T., Firouz, N. S., Santhanam, R., & Jong, V. Y. M. (2022). Phytochemicals from *Calophyllum macrocarpum* Hook.f. and its cytotoxic activities. *Natural Product Research*, *36*(2), 654–659. https://doi.org/10.1080/14786419.2020.1795658

Kashman, Y., Gustafson, K. R., Fuller, R. W., II, J. H. C., McMahon, J. B., Currens, M. J., Buckheit, R. W. Jr., Hughes, S. H., Cragg, G. M., & Boyd, M. R. (1992). The calanolides, a novel HIV-inhibitory class of coumarin derivatives from the tropical rainforest tree, *Calophyllum lanigerum*. *Journal of Medicinal Chemistry*, *35*(15), 2735–2743. https://doi.org/10.1021/jm00093a004

Kawamura, F., Muhamud, A., Hashim, R., Sulaiman, O., & Ohara, S. (2012). Two antifungal xanthones from the heartwood of *Calophyllum symingtonianum*. *Japan Agricultural Research Quarterly*, *46*(2), 181–185. https://doi.org/10.6090/jarq.46.181

Khan, U. A., Rahman, H., Niaz, Z., Qasim, M., Khan, J., Tayyaba, & Rehman, B. (2013). Antibacterial activity of some medicinal plants against selected human pathogenic bacteria. *European Journal of Microbiology & Immunology*, *3*(4), 272–274. https://doi.org/10.1556/eujmi.3.2013.4.6

Kilari, V. B., Oroszi, T., Kilari, V. B., & Oroszi, T. (2024). The Misuse of Antibiotics and the Rise of Bacterial Resistance: A Global Concern. *Pharmacology & Pharmacy*, *15*(12), 508–523. https://doi.org/10.4236/pp.2024.1512028

Klein-Júnior, L. C., Campos, A., Niero, R., Corrêa, R., Heyden, Y. Vander, & Filho, V. C. (2020). Xanthones and cancer: From natural sources to mechanisms of action. *Chemistry and Biodiversity*, *17*(2), e1900499. https://doi.org/10.1002/cbdv.201900499

Koh, J. J., Lin, S., Bai, Y., Sin, W. W. L., Aung, T. T., Li, J., Chandra, V., Pervushin, K., Beuerman, R. W., & Liu, S. (2018). Antimicrobial activity profiles of Amphiphilic Xanthone derivatives are a function of their molecular oligomerization. *Biochimica et Biophysica Acta (BBA) - Biomembranes*, *1860*(11), 2281–2298. https://doi.org/10.1016/j.bbamem.2018.05.006

Kowalczyk, P., Gawdzik, B., Trzepizur, D., Szymczak, M., Skiba, G., Raj, S., Kramkowski, K., Lizut, R., & Ostaszewski, R. (2021). *δ*-Lactones—A New Class of Compounds That Are Toxic to *E. Coli* K12 and R2–R4 Strains. *Materials*, *14*(11), 2956. https://doi.org/10.3390/ma14112956

Krysa, M., Szymańska-Chargot, M., & Zdunek, A. (2022). FT-IR and FT-Raman fingerprints of flavonoids – A review. *Food Chemistry*, *393*, 133430. https://doi.org/10.1016/j.foodchem.2022.133430

Kudera, T., Rondevaldova, J., Kant, R., Umar, M., Skrivanova, E., & Kokoska, L. (2017). *In vitro* growth-inhibitory activity of *Calophyllum inophyllum* ethanol leaf extract against diarrhoea-causing bacteria. *Tropical Journal of Pharmaceutical Research*, *16*(9), 2207–2213. https://doi.org/10.4314/tjpr.v16i9.23

Kumar, A., & Garg, Y. (2020). In-vitro evaluation of antibacterial, antifungal and anti-HIV effects of *Calophyllum inophyllum* leaf extract. *Biomedical and Pharmacology Journal*, *13*(4), 2003–2014. https://dx.doi.org/10.13005/bpj/2079

Kurniawan, Y. S., Priyangga, K. T. A., Jumina, Pranowo, H. D., Sholikhah, E. N., Zulkarnain, A. K., Fatimi, H. A., & Julianus, J. (2021). An Update on the Anticancer Activity of Xanthone Derivatives: A Review. *Pharmaceuticals*, *14*(11), 1144. https://doi.org/10.3390/ph14111144

Lee, K. W., Ee, G. C. L., Daud, S., & Karunakaran, T. (2017). Xanthones from *Calophyllum inophyllum*. *Pertanika J. Trop. Agric. Sci*, *40*(1), 111–118. https://ptsldigital.ukm.my/jspui/handle/123456789/579006

Lee, K. W., Zamakshshari, N. H., Ee, G. C. L., Mah, S. H., & Mohd Nor, S. M. (2018). Isolation and structural modifications of ananixanthone from *Calophyllum teysmannii* and their cytotoxic activities. *Natural Product Research*, *32*(18), 2147–2151. https://doi.org/10.1080/14786419.2017.1367781

Léguillier, T., Lecsö-Bornet, M., Lémus, C., Rousseau-Ralliard, D., Lebouvier, N., Hnawia, E., Nour, M., Aalbersberg, W., Ghazi, K., Raharivelomanana, P., & Rat, P. (2015). The Wound Healing and Antibacterial Activity of Five Ethnomedical *Calophyllum inophyllum* Oils: An Alternative Therapeutic Strategy to Treat Infected Wounds. *PLOS ONE*, *10*(9), e0138602. https://doi.org/10.1371/journal.pone.0138602

Lemos, L. M. S., Martins, T. B., Tanajura, G. H., Gazoni, V. F., Bonaldo, J., Strada, C. L., Silva, M. G. Da, Dall'Oglio, E. L., De Sousa Júnior, P. T., & Martins, D. T. D. O. (2012). Evaluation of antiulcer activity of chromanone fraction from *Calophyllum brasiliesnse* Camb. *Journal of Ethnopharmacology*, *141*(1), 432–439. https://doi.org/10.1016/j.jep.2012.03.006

Leslie Gunatilaka, A. A., Jasmin De Silva, A. M. Y., & Sotheeswaran, S. (1982). Minor xanthones of *Hypericum mysorense*. *Phytochemistry*, *21*(7), 1751–1753. https://doi.org/10.1016/S0031-9422(82)85053-X

Li, X., Li, J., & Stevens, P. (2007). *Calophyllum* Linnaeus, Sp. P1. 1:513.1753. *Flora of China*, *13*, 38–40. http://www.efloras.org/florataxon.aspx?flora_id=2&taxon_id=105209

Li, Y., Kong, D., Fu, Y., Sussman, M. R., & Wu, H. (2020). The effect of developmental and environmental factors on secondary metabolites in medicinal plants. *Plant Physiology and Biochemistry*, *148*, 80–89. https://doi.org/10.1016/j.plaphy.2020.01.006

Li, Y. Z., Li, Z. L., Yin, S. L., Shi, G., Liu, M. S., Jing, Y. K., & Hua, H. M. (2010). Triterpenoids from *Calophyllum inophyllum* and their growth inhibitory effects on human leukemia HL-60 cells. *Fitoterapia*, *81*(6), 586-589. https://doi.org/10.1016/j.fitote.2010.02.005

Lim, C. K., Gan, S. Y., Jong, V. Y. M., Leong, C. O., Mai, C. W., & Chee, C. F. (2019). Cytotoxic activity of phytochemicals from the stem bark of *Calophyllum castaneum*. *Pakistan Journal of Pharmaceutical Sciences*, *32*(5), 2183–2187.

Liu, X., Shen, J., & Zhu, K. (2021). Antibacterial activities of plant-derived xanthones. *RSC Medicinal Chemistry*, *13*(2), 107. https://doi.org/10.1039/D1MD00351H

Lizazman, M. A., Jong, V. Y. M., Zamakshshari, N. H., Suffian, Y., Ismail, M. I. B., Md Yusof, E. N., & Seruji, N. M. U. B. (2026). Phytochemical investigation of *Calophyllum sundaicum* P.F. Stevens: isolation, structure elucidation, and biological potential. *Natural product research*, 1–11. Advance online publication. https://doi.org/10.1080/14786419.2026.2613276

Lizazman, M. A., Jong, V. Y. M., Karunakaran, T., Suffian, Y., Zamakshshari, N. H., Nazeri, A. M., Nik Mohd Nazri, N. Z. H., Ismail, M. I., & Banga Singh, K. K. (2026). Phytochemical composition, antioxidant and antibacterial activities of *Calophyllum canum* Hook. f. ex T. Anderson extracts: Molecular docking insights. *Chemistry & biodiversity*. https://doi.org/10.1002/cbdv.202500773

Lizazman, M. A., Jong, V. Y. M., Chua, P. F., Lim, W. K., & Karunakaran, T. (2023). Phytochemicals from *Calophyllum canum* Hook f. ex T. Anderson and their neuroprotective effects. *Natural Product Research*, *37*(12), 2043–2048. https://doi.org/10.1080/14786419.2022.2116021

Lizazman, M. A., Karunakaran, T., & Jong, Vi. Y. M. (2022). Trapezifolixanthone as a common constituent in the genus *Calophyllum*: An insight Review. *Biocatalysis and Agricultural Biotechnology*, *44*, 102471. https://doi.org/10.1016/j.bcab.2022.102471

Ma, N., Li, J. C. B., An, F., Ding, Y., & Xue, X. (2024). Medicinal Chemistry Strategies for the Modification of Bioactive Natural Products. *Molecules, 29*(3), 689. https://doi.org/10.3390/molecules29030689

Mah, S. H., Teh, S. S., & Ee, G. C. L. (2019). Comparative studies of selected *Calophyllum* plants for their anti-inflammatory properties. *Pharmacognosy Magazine*, *15*(60), 135–140. http://dx.doi.org/10.4103/pm.pm_212_18

Marliyana, S. D., Wibowo, F. R., Handayani, D. S., Kusumaningsih, T., Suryanti, V., Firdaus, M., & Annisa, E. N. (2021). Stigmasterol and stigmasterone from methanol extract of *Calophyllum soulattri* Burm. F. Stem Bark. *Jurnal Kimia Sains Dan Aplikasi*, *24*(4), 108–113. https://doi.org/10.14710/jksa.24.4.108-113

Mayer, R. J., Allihn, P. W. A., Hampel, N., Mayer, P., Sieber, S. A., & Ofial, A. R. (2021). Electrophilic reactivities of cyclic enones and *α,β*-unsaturated lactones. *Chemical Science*, *12*(13), 4850–4865. https://doi.org/10.1039/D0SC06628A

Mazur, M., & Masłowiec, D. (2022). Antimicrobial Activity of Lactones. *Antibiotics 2022, Vol. 11, Page 1327*, *11*(10), 1327. https://doi.org/10.3390/antibiotics11101327

Miller, S. I. (2016). Antibiotic resistance and regulation of the Gram-negative bacterial outer membrane barrier by host innate immune molecules. *MBio*, *7*(5), 10-1128. https://doi.org/10.1128/mbio.01541-16

Miller, S. I., & Salama, N. R. (2018). The gram-negative bacterial periplasm: Size matters. *PLOS Biology*, *16*(1), e2004935. https://doi.org/10.1371/journal.pbio.2004935

Mishra, S., Pandey, A., & Manvati, S. (2020). Coumarin: An emerging antiviral agent. *Heliyon*, *6*(1), e03217. https://doi.org/10.1016/j.heliyon.2020.e03217

Mishra, U. S., Murthy, P. N., Choudhury, K., Panigrahi, G., Mohapatra, S., & Pradhan, D. (2010). Antibacterial and Analgesic Effects of the Stem Barks of *Calophyllum inophyllum*. *International Journal of ChemTech Research*, *2*(2), 973–979.

Moghal, N. E., Hegde, S., & Eastham, K. M. (2004). Ibuprofen and acute renal failure in a toddler. *Archives of Disease in Childhood*, *89*(3), 276–277. https://doi.org/10.1136/adc.2002.024141

Molyneux, R. J., Lee, S. T., Gardner, D. R., Panter, K. E., & James, L. F. (2007). Phytochemicals: The good, the bad and the ugly? *Phytochemistry*, *68*(22–24), 2973–2985. https://doi.org/10.1016/j.phytochem.2007.09.004

Morales, G., Sierra, P., Mancilla, A., Paredes, A., Loyola, L. A., Gallardo, O., & Borquez, J. (2003). Secondary metabolites from four medicinal plants from Northern Chile: Antimicrobial activity and biotoxicity against *Artemia salina*. *Journal of the Chilean Chemical Society*, *48*(2), 13–18. https://doi.org/10.4067/s0717-97072003000200002

Newman, D. J., & Cragg, G. M. (2020). Natural products as sources of new drugs over the nearly four decades from 01/1981 to 09/2019. *Journal of Natural Products*, *83*(3), 770–803. https://doi.org/10.1021/acs.jnatprod.9b01285

Nikolic, P., & Mudgil, P. (2023). The Cell Wall, Cell Membrane and Virulence Factors of *Staphylococcus aureus* and Their Role in Antibiotic Resistance. *Microorganisms, 11*(2), 259. https://doi.org/10.3390/microorganisms11020259

Nisar, B., Sultan, A., & Rubab, S. L. (2018). Comparison of Medicinally Important Natural Products versus Synthetic Drugs-A Short Commentary. *Natural Products Chemistry & Research*, *6*(2). https://doi.org/10.4172/2329-6836.1000308

Noh, I. A., & Jong, V. Y. M. (2020). Phytochemicals, Antimicrobials and Antioxidants Studies of the Stem Bark Extract from *Calophyllum ferrugineum*. *Scientific Research Journal*, *17*(2), 1. https://doi.org/10.24191/srj.v17i2.6917

NParks | Calophyllum inophyllum. (n.d.). Retrieved 17 November 2025, from https://www.nparks.gov.sg/florafaunaweb/flora/2/7/2774

Nugroho, A. E., Sasaki, T., Kaneda, T., Hadi, A. H. A., & Morita, H. (2017). Calofolic acids A – F, chromanones from the bark of *Calophyllum scriblitifolium* with vasorelaxation activity. *Bioorganic & Medicinal Chemistry Letters*, *27*(10), 2124–2128. https://doi.org/10.1016/j.bmcl.2017.03.071

Parvekar, P., Palaskar, J., Metgud, S., Maria, R., & Dutta, S. (2020). The minimum inhibitory concentration (MIC) and minimum bactericidal concentration (MBC) of silver nanoparticles against *Staphylococcus aureus*. *Biomaterial Investigations in Dentistry*, *7*(1), 105–109. https://doi.org/10.1080/26415275.2020.1796674

Pavela, R., Maggi, F., & Benelli, G. (2021). Coumarin (2H-1-benzopyran-2-one): a novel and eco-friendly aphicide. *Natural Product Research*, *35*(9), 1566–1571. https://doi.org/10.1080/14786419.2019.1660334

Pavia, D. L.., Lampman, G. M.., Kriz, G. S.., & Vyvyan, J. R.. (2015). *Introduction to spectroscopy* (5th ed.). Cengage Learning.

Pessoa, M. J. G., Pireda, S., Simioni, P., Bautz, N., & Cunha, M. Da. (2021). Structural and histochemical attributes of secretory ducts and cavities in leaves of four species of Calophyllaceae J. Agardh in Amazonian savannas. *Plant Biology*, *23*(6), 1128–1140. https://doi.org/10.1111/plb.13321

Pinto, M. M. M., Palmeira, A., Fernandes, C., Resende, D. I. S. P., Sousa, E., Cidade, H., Tiritan, M. E., Correia-da-Silva, M., & Cravo, S. (2021). From natural products to new synthetic small molecules: A journey through the world of xanthones. *Molecules*, *26*(2), 431. https://doi.org/10.3390/molecules26020431

Ponguschariyagul, S., Sichaem, J., Khumkratok, S., Siripong, P., Lugsanangarm, K., & Tippyang, S. (2018). Caloinophyllin A, a new chromanone derivative from *Calophyllum inophyllum* roots. *Natural Product Research*, *32*(21), 2535–2541. https://doi.org/10.1080/14786419.2018.1425845

Pretto, J. B., Cechinel-Filho, V., Noldin, V. F., Sartori, M. R. K., Isaias, D. E. B., & Cruz, A. B. (2004). Antimicrobial activity of fractions and compounds *from Calophyllum brasiliense* (Clusiaceae/Guttiferae). *Zeitschrift Fur Naturforschung - Section C Journal of Biosciences*, *59*(9–10), 657–662. https://doi.org/10.1515/znc-2004-9-1009

Proshkina, E., Plyusnin, S., Babak, T., Lashmanova, E., Maganova, F., Koval, L., Platonova, E., Shaposhnikov, M., & Moskalev, A. (2020). Terpenoids as potential geroprotectors. *Antioxidants*, *9*(6), 1–51. https://doi.org/10.3390/antiox9060529

Quintans, J. S. S., Costa, E. V., Tavares, J. F., Souza, T. T., Araújo, S. S., Estevam, C. S., Barison, A., Cabral, A. G. S., Silva, M. S., Serafini, M. R., & Quintans-Júnior, L. J. (2014). Phytochemical study and antinociceptive effect of the hexanic extract of leaves from *Combretum duarteanum* and friedelin, a triterpene isolated from the hexanic extract, in orofacial nociceptive protocols. *Revista Brasileira de Farmacognosia*, *24*(1), 60–66. https://doi.org/10.1590/0102-695X20142413347

Radi, M. H., El-Shiekh, R. A., El-Halawany, A. M., & Abdel-Sattar, E. (2023). Friedelin and 3*β*-Friedelinol: Pharmacological Activities. *Revista Brasileira de Farmacognosia*, *33*(5), 886–900. https://doi.org/10.1007/s43450-023-00415-5

Ragasa, C. Y., Ebajo, V., Reyes, M. M. D. L., Mandia, E. H., Brkljača, R., & Urban, S. (2015). Triterpenes from *Calophyllum inophyllum* Linn. *International Journal of Pharmacognosy and Phytochemical Research*, *7*(4), 718–722. https://doi.org/10.1016/S0040-4020(01)82592-8

Rahman, M. N. A., Nafiah, M. A., Salleh, W. M. N. H. W., Hashim, N. M., Zamakshshari, N. H., Abdul Rahman, M. N., Nafiah, M. A., Wan Salleh, W. M. N. H., Tan, S. P., Hashim, N. M., Zamakshshari, N. H., Rahman, M. N. A., Nafiah, M. A., Salleh, W. M. N. H. W., Hashim, N. M., & Zamakshshari, N. H. (2022). Antioxidant, Antimicrobial, and Cytotoxic Activities of the Hexane and Dichloromethane Extracts of Malaysian *Mitragyna spesioca* Korth. Leaves. *Malaysian Journal of Chemistry*, *24*(2), 191–198. https://doi.org/10.55373/mjchem.v24i2.191

Rahmatullah, A. A., Ratnaningtyas, N., Sugihartuti, R., Susilowati, S., Safitri, E., & Mulyati, S. (2024). Protective effect of the extract of Dayak Onions (*Eleutherine palmifolia*) on sertoli and leydig cell necrosis in mice (*Mus Musculus*) induced with monosodium glutamate. *Media Kedokteran Hewan*, *35*(2), 87–96. https://doi.org/10.20473/mkh.v35i2.2024.87-96

Raj, S. P., Solomon, P. R., & Thangaraj, B. (2022). Clusiaceae. *Biodiesel from Flowering Plants*, 141–157. https://doi.org/10.1007/978-981-16-4775-8_11

Rascón-Valenzuela, L., Moreno, H. T., Velazquez, C., Garibay-Escobar, A., & Robles-Zepeda, R. (2016). Triterpenoids: Synthesis, Uses in Cancer Treatment and other Biological Activities. In *Advances in Medicine and Biology* (Vol. 106). Nova Science Publishers, Inc. https://novapublishers.com/shop/advances-in-medicine-and-biology-volume-106/

Reith, J., & Mayer, C. (2011). Peptidoglycan turnover and recycling in Gram-Positive bacteria. *Applied Microbiology and Biotechnology*, *92*(1), 1–11. https://doi.org/10.1007/s00253-011-3486-x

Ren, Y., & Kinghorn, A. D. (2019). Natural product triterpenoids and their semi-synthetic derivatives with potential anticancer activity. *Planta Medica*, *85*(11–12), 802–814. https://doi.org/10.1055/a-0832-2383

Ribeiro, P. R., Ferraz, C. G., & Cruz, F. G. (2019). New steroid and other compounds from non-polar extracts of *Clusia burle-marxii* and their chemotaxonomic significance. *Biochemical Systematics and Ecology*, *82*, 31–34. https://doi.org/10.1016/j.bse.2018.12.001

Rojas-Sandoval, J. (2023). *Calophyllum inophyllum* (Alexandrian laurel). *CABI Compendium*. https://doi.org/10.1079/cabicompendium.14124

Roy, A., & Saraf, S. (2006). Limonoids: Overview of Significant Bioactive Triterpenes Distributed in Plants Kingdom. *Biological and Pharmaceutical Bulletin*, *29*(2), 191–201. https://doi.org/10.1248/bpb.29.191

Salman, Z., Yu-Qing, J., Bin, L., Cai-Yun, P., Iqbal, C. M., Atta-ur, R., & Wei, W. (2019). Antioxidant Nature Adds Further Therapeutic Value: An Updated Review on Natural Xanthones and Their Glycosides. *Digital Chinese Medicine*, *2*(3), 166–192. https://doi.org/10.1016/j.dcmed.2019.12.005

Sanam, M. U. E., Detha, A. I. R., & Rohi, N. K. (2022). Detection of antibacterial activity of lactic acid bacteria, isolated from Sumba mare's milk, against *Bacillus cereus*, *Staphylococcus aureus*, and *Escherichia coli*. *Journal of Advanced Veterinary and Animal Research*, *9*(1), 53. https://doi.org/10.5455/javar.2022.i568

Sezer, F., Deniz, S., Sevim, D., Chaachouay, N., & Zidane, L. (2024). Plant-Derived Natural Products: A Source for Drug Discovery and Development. *Drugs and Drug Candidates 2024, Vol. 3, Pages 184-207*, *3*(1), 184–207. https://doi.org/10.3390/ddc3010011

Sharma, S. K., Singh, L., & Singh, S. (2013). Review Article Comparative Study between Penicillin and Ampicillin. *Scholars Journal of Applied Medical Sciences (SJAMS) (P) Sch. J. App. Med. Sci*, *1*(4), 291–294. https://doi.org/10.36347/sjams.2013.v01i04.019

Sichaem, J., Tip-Pyang, S., & Siripong, P. (2018). Chemical constituents from the root bark of *Calophyllum inophyllum*. *Natural Product Communications*, *13*(6), 727–729. https://doi.org/10.1177/1934578x1801300618

Silverstein, R. M.., Webster, F. X.., Kiemle, D. J.., & Bryce, D. L.. (2015). *Spectrometric identification of organic compounds* (8th ed.). Wiley.

Stevens, P. F. (1980). A revision of the Old World species of *Calophyllum* (Guttiferae). *Journal of the Arnold Arboretum*, *61*(2), 117–424. https://www.jstor.org/stable/43782071

Su, C. R., Kuo, P. C., Wang, M. L., Liou, M. J., Damu, A. G., & Wu, T. S. (2003). Acetophenone derivatives from *Acronychia pedunculata*. *Journal of Natural Products*, *66*(7), 990–993. https://doi.org/10.1021/np030054x

Suarez, S. A., & Martiny, A. C. (2024). Intraspecific variation in antibiotic resistance potential within *E. coli*. *Microbiology Spectrum*, *12*(6). https://doi.org/10.1128/spectrum.03162-23

Sun, X. (2005). The investigation of chemical structure of coal macerals via transmitted-light FT-IR microspectroscopy. *Spectrochimica Acta Part A: Molecular and Biomolecular Spectroscopy*, *62*(1–3), 557–564. https://doi.org/10.1016/j.saa.2005.01.020

Sunil, C., Irudayaraj, S. S., Duraipandiyan, V., Alrashood, S. T., Alharbi, S. A., & Ignacimuthu, S. (2021). Friedelin exhibits antidiabetic effect in diabetic rats via modulation of glucose metabolism in liver and muscle. *Journal of Ethnopharmacology*, *268*, 113659. https://doi.org/10.1016/j.jep.2020.113659

Taher, M., Salleh, W. M. N. H. W., Alkhamaiseh, S. I., Ahmad, F., Rezali, M. F., Susanti, D., & Hasan, C. M. (2021). A new xanthone dimer and cytotoxicity from the stem bark of *Calophyllum canum*. *Zeitschrift Für Naturforschung C*, *76*(1–2), 87–91. https://doi.org/10.1515/znc-2020-0089

Tanjung, M., Tjahjandarie, T. S., Saputri, R. D., Aldin, M. F., & Purnobasuki, H. (2022). Two new pyranoxanthones from the stem bark of *Calophyllum pseudomolle* P.F. Stevens. *Natural Product Research*, *36*(3), 822–827. https://doi.org/10.1080/14786419.2020.1808638

Tanjung, M., Tjahjandarie, T. S., Saputri, R. D., Kurnia, B. D., Rachman, M. F., & Syah, Y. M. (2021). Calotetrapterins A-C, three new pyranoxanthones and their cytotoxicity from the stem bark of *Calophyllum tetrapterum* Miq. *Natural Product Research*, *35*(3), 407–412. https://doi.org/10.1080/14786419.2019.1634714

Tanne, J. (2006). Paracetamol causes most liver failure in UK and US. *BMJ*, *332*(7542), 628. https://doi.org/10.1136/bmj.332.7542.628-a

Tantapakul, C., Maneerat, W., Sripisut, T., Ritthiwigrom, T., Andersen, R. J., Cheng, P., Cheenpracha, S., Raksat, A., & Laphookhieo, S. (2016). New benzophenones and xanthones from *Cratoxylum sumatranum* ssp. neriifolium and their antibacterial and antioxidant activities. *Journal of Agricultural and Food Chemistry*, *64*(46), 8755–8762. https://doi.org/10.1021/acs.jafc.6b03643

Tee, K. H., Ee, G. C. L., Ismail, I. S., Karunakaran, T., Teh, S. S., Jong, V. Y. M., & Mohd Nor, S. M. (2018). A new coumarin from stem bark of *Calophyllum wallichianum*. *Natural Product Research*, *32*(21), 2565–2570. https://doi.org/10.1080/14786419.2018.1428588

Tee, K. H., Ee, G. C. L., Wong, K. W., Karunakaran, T., Jong, V. Y. M., & Teh, S. S. (2018). Natural products from stem bark of *Calophyllum andersonii*. *Pertanika Journal of Tropical Agricultural Science*, *41*(2), 759–768.

Tejamukti, E. P., Setyaningsih, W., Irnawati, Yasir, B., Alam, G., & Rohman, A. (2020). Application of FTIR Spectroscopy and HPLC Combined with Multivariate Calibration for Analysis of Xanthones in Mangosteen Extracts. *Scientia Pharmaceutica 2020, Vol. 88, Page 35*, *88*(3), 35. https://doi.org/10.3390/scipharm88030035

Thanh, N. Van, Jang, H. J., Vinh, L. B., Linh, K. T. P., Huong, P. T. T., Cuong, N. X., Nam, N. H., Minh, C. Van, Kim, Y. H., & Yang, S. Y. (2019). Chemical constituents from Vietnamese mangrove *Calophyllum inophyllum* and their anti-inflammatory effects. *Bioorganic Chemistry*, *88*, 102921. https://doi.org/10.1016/j.bioorg.2019.102921

Thiagarajan, S., Yong, F. L., Subramaniam, H., Jong, V. Y. M., Lim, C. K., & Say, Y. H. (2017). Anti-obesity effect of phenylcoumarins from two *Calophyllum* spp in 3t3-l1 adipocytes. *Tropical Journal of Pharmaceutical Research*, *16*(3), 563–572. https://doi.org/10.4314/tjpr.v16i3.9

Tjahjandarie, T. S., Tanjung, M., Rahmania, D. F., Rhidoma, C. I., & Saputri, R. D. (2021). Calodioscurins A and B, two new isoprenylated xanthones from the stem bark of *Calophyllum dioscurii* P.F. Stevens. *Natural Product Research*, *35*(7), 1153–1158. https://doi.org/10.1080/14786419.2019.1643864

Trad, R. J., Cabral, F. N., Bittrich, V., da Silva, S. R., & do Carmo Estanislau do Amaral, M. (2021). Calophyllaceae plastomes, their structure and insights in relationships within the clusioids. *Scientific Reports*, *11*(1), 1–15. https://doi.org/10.1038/s41598-021-99178-z

Vanegas, A. M. M., Trujillo, S. B., Jaramillo, C. P., & Carda, M. (2019). Antiplasmodials soulattrolide derivatives from *Calophyllum brasiliense* and its mechanism of activity. *Journal of King Saud University - Science*, *31*(4), 1208–1214. https://doi.org/10.1016/j.jksus.2019.03.005

Villarreal, F., Bakrim, S., Benkhaira, N., Bourais, I., Benali, T., Lee, L.-H., El Omari, N., Sheikh, R. A., Wen Goh, K., Chiau Ming, L., & Bouyahya, A. (2022). Health Benefits and Pharmacological Properties of Stigmasterol. *Antioxidants*, *11*(10), 1912. https://doi.org/10.3390/antiox11101912

Vittaya, L., Chalad, C., Ratsameepakai, W., & Leesakul, N. (2023). Phytochemical characterization of bioactive compounds extracted with different solvents from *Calophyllum inophyllum* flower and activity against pathogenic bacteria. *South African Journal of Botany*, *154*, 346–355. https://doi.org/10.1016/j.sajb.2023.01.052

Wang, Y., Yan, F., Xu, D. Q., Liu, M., Liu, Z. F., & Tang, Y. P. (2025). Traditional uses, botany, phytochemistry, pharmacology and applications of *Labisia pumila*: A comprehensive review. *Journal of Ethnopharmacology*, *336*, 118522. https://doi.org/10.1016/j.jep.2024.118522

World Flora Online. (2025). *Calophyllum nodosum Vesque*. Published on Internet. https://www.worldfloraonline.org/taxon/wfo-0000581249

Wu, A., & Cremer, D. (2003). Extension of the Karplus Relationship for NMR Spin-Spin Coupling Constants to Nonplanar Ring Systems: Pseudorotation of Tetrahydrofuran. *International Journal of Molecular Sciences 2003, Vol. 4, Pages 158-192*, *4*(4), 158–192. https://doi.org/10.3390/i4040158

Xu, G. B., Xiao, Y. H., Zhang, Q. Y., Zhou, M., & Liao, S. G. (2018). Hepatoprotective natural triterpenoids. *European Journal of Medicinal Chemistry*, *145*, 691–716. https://doi.org/10.1016/j.ejmech.2018.01.011

Yasunaka, K., Abe, F., Nagayama, A., Okabe, H., Lozada-Pérez, L., López-Villafranco, E., Muñiz, E. E., Aguilar, A., & Reyes-Chilpa, R. (2005). Antibacterial activity of crude extracts from Mexican medicinal plants and purified coumarins and xanthones. *Journal of Ethnopharmacology*, *97*(2), 293–299. https://doi.org/10.1016/j.jep.2004.11.014

Yeap, B. Y. R., Ran, Y., Tunku, U., & Rahman, A. (2017). *Preliminary Screening of Crude Extracts of Calophyllum species for Cytotoxicity, Antibacterial and Antioxidant Activities*. Universiti Tunku Abdul Rahman.

Yimdjo, M. C., Azebaze, A. G., Nkengfack, A. E., Meyer, A. M., Bodo, B., & Fomum, Z. T. (2004). Antimicrobial and cytotoxic agents from *Calophyllum inophyllum*. *Phytochemistry*, *65*(20), 2789–2795. https://doi.org/10.1016/j.phytochem.2004.08.024

Yusuf, A. J., Abdullahi, M. I., Aleku, G. A., Ibrahim, I. A. A., Alebiosu, C. O., Yahaya, M., Adamu, H. W., Sanusi, A., Mailafiya, M. M., Abubakar, H., & Yusuf, A. (2018). Antimicrobial activity of stigmasterol from the stem bark of *Neocarya macrophylla*. *Journal of Medicinal Plants for Economic Development*, *2*(1), 5. https://doi.org/10.4102/JOMPED.V2I1.38

Zailan, A. A. D., Karunakaran, T., Abu Bakar, M. H., & Mian, V. J. Y. (2022). The Malaysian genus *Calophyllum* (Calophyllaceae): a review on its phytochemistry and pharmacological activities. *Natural Product Research*, *36*(17), 4575–4585. https://doi.org/10.1080/14786419.2021.1982936

Zaine, N. F. Z., Zamakshshari, N. H., Abd Halim, A. N., Yi Mian, V. J., & Ngui Sing, N. (2024). Isolation, derivatization, and anti-microbial evaluation of secondary metabolites from *Garcinia dryobalanoides*. *Natural Product Research*. https://doi.org/10.1080/14786419.2024.2371109

Zamakshshari, H. N., Zaine, N. F. Z., Heilman. D. N. A., Abd Halim, A. N., Phornvillay, S., Yeo, K. W., Mian, V. J. Y., & Ahmad, & F. B. (2024). Phytochemical Profiling of *Garcinia rostrata*, *Garcinia dryobalanosides* and *Garcinia cuneifolia* and Their Antibacterial Activity. *Borneo Journal of Resource Science and Technology*, *14*(1), 80–87. https://doi.org/10.33736/bjrst.5672.2024

Zamakshshari, N., Ahmed, I. A., Nasharuddin, M. N. A., Mohd Hashim, N., Mustafa, M. R., Othman, R., & Noordin, M. I. (2021). Effect of extraction procedure on the yield and biological activities of hydroxychavicol from *Piper betle* L. leaves. *Journal of Applied Research on Medicinal and Aromatic Plants*, *24*, 100320. https://doi.org/10.1016/j.jarmap.2021.100320

Zamakshshari, N. H., Ee, G. C. L., Ismail, I. S., Ibrahim, Z., & Mah, S. H. (2019). Cytotoxic xanthones isolated from *Calophyllum depressinervosum* and *Calophyllum buxifolium* with antioxidant and cytotoxic activities. *Food and Chemical Toxicology*, *133*, 110800. https://doi.org/10.1016/j.fct.2019.110800

Zamakshshari, N. H., Ee, G. C. L., Teh, S. S., Daud, S., Karunakaran, T., & Safinar, I. (2016). Natural product compounds from *Calophyllum depressinervosum*. *Pertanika Journal of Tropical Agricultural Science*, *39*(2), 249–255.

Zein, N., Aziz, S. W., El-Sayed, A. S., & Sitohy, B. (2019). Comparative cytotoxic and anticancer effect of Taxol derived from *Aspergillus terreus* and *Taxus brevifolia*. *Bioscience Research*, *16*(2), 1500–1509. https://urn.kb.se/resolve?urn=urn:nbn:se:umu:diva-162350

Appendix 1:
DEPT spectra of compound 20

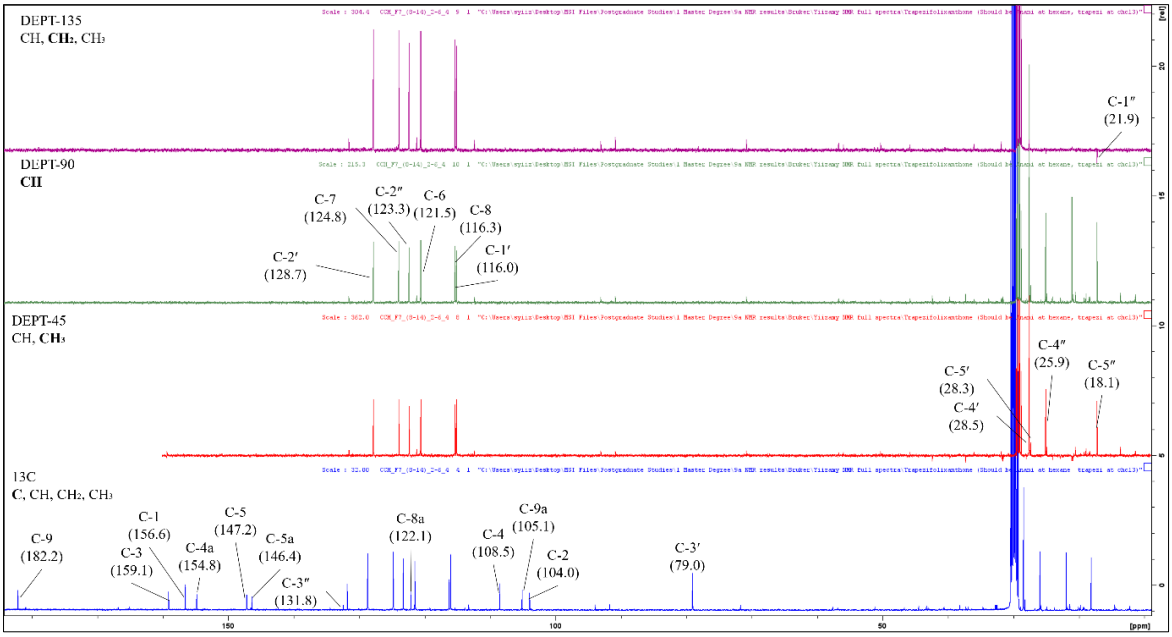

Appendix 2:
COSY spectrum of compound 20

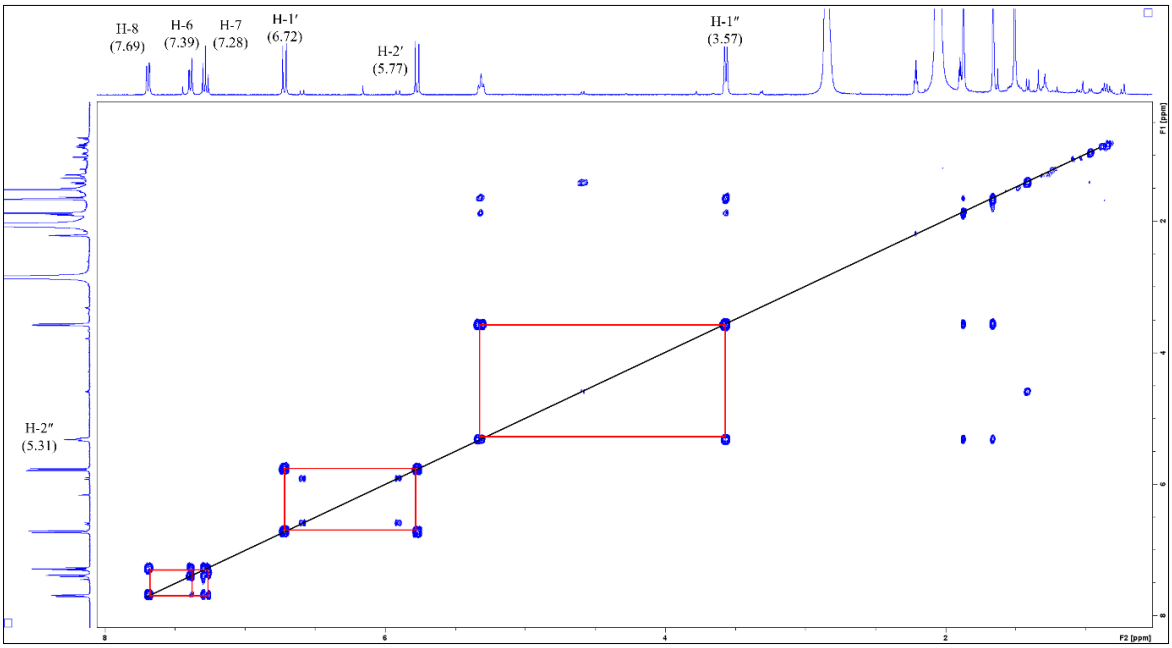

Appendix 3:
HSQC spectrum of compound 20

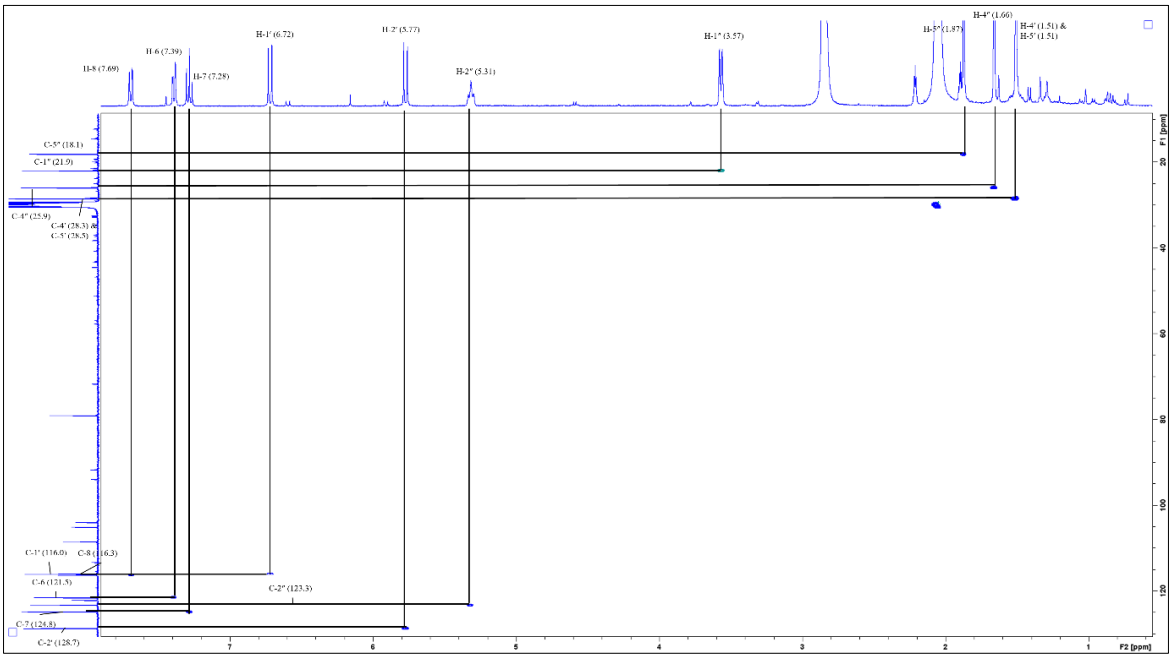

Appendix 4:
Expanded HSQC spectrum of compound 20 in the 1.0-4.0 ppm region

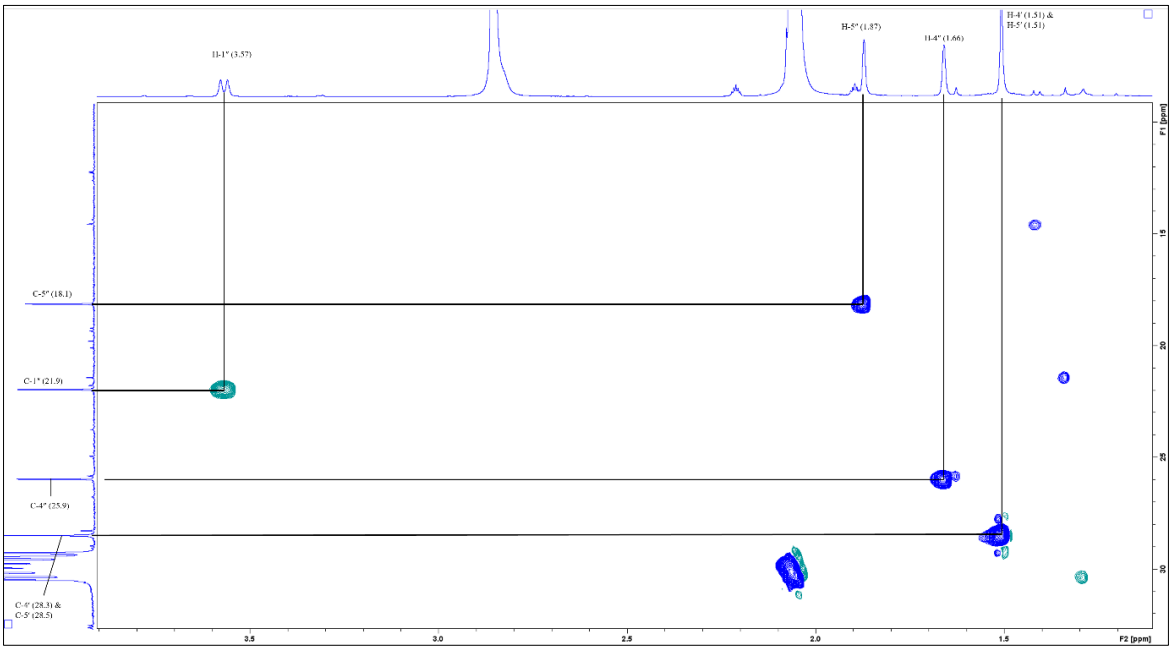

Appendix 5:
Expanded HSQC spectrum of compound 20 in the 5.0-8.0 ppm region

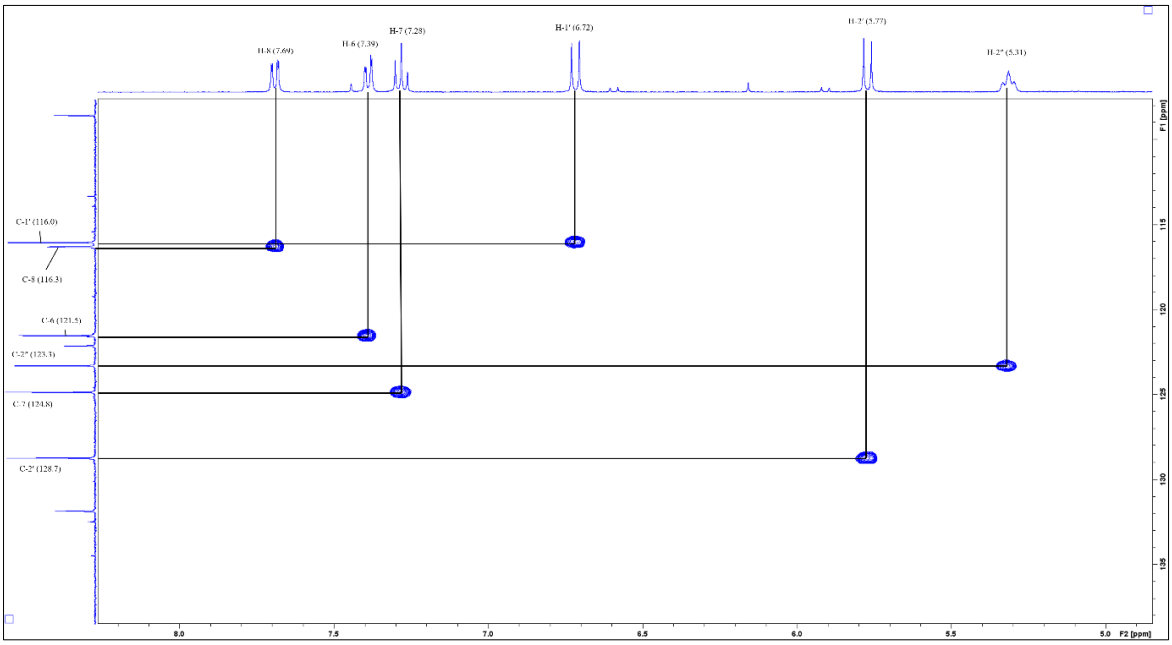

Appendix 6:
HMBC spectrum of compound 20

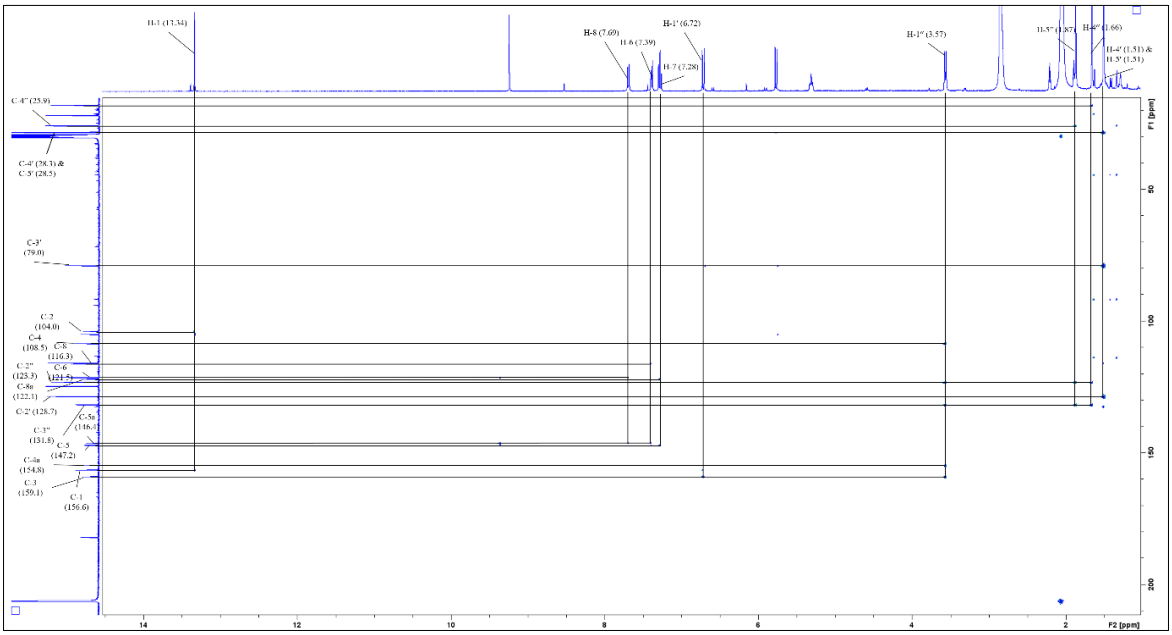

Appendix 7:
Expanded HMBC spectrum of compound 20 in the 1.0-4.0 ppm region

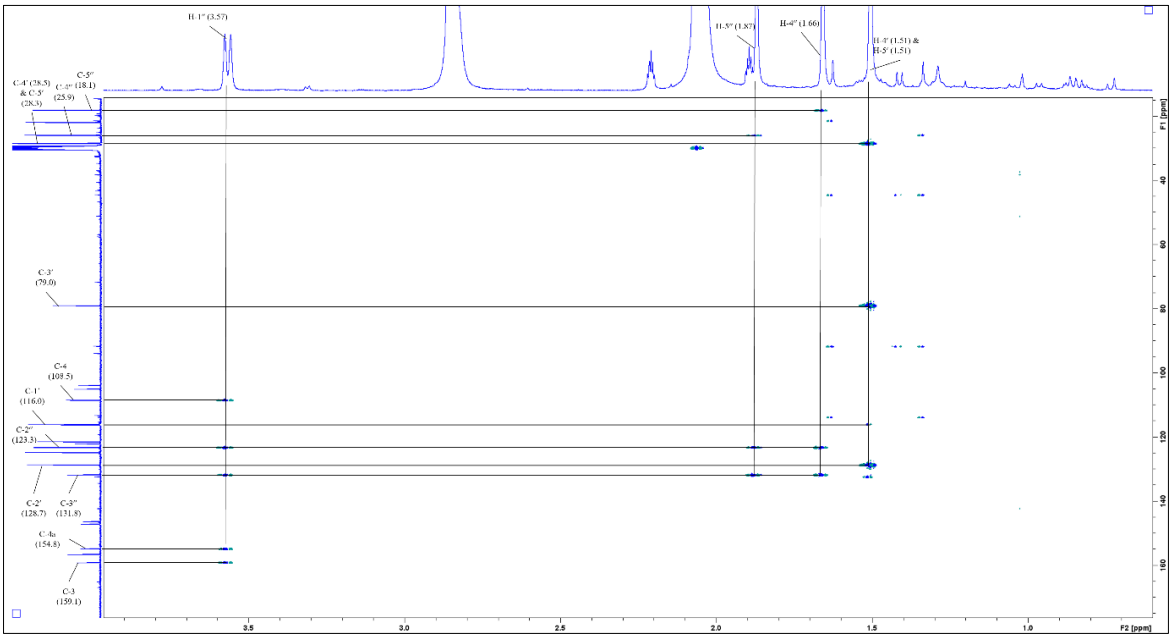

Appendix 8:
Expanded HMBC spectrum of compound 20 in the 5.0-8.0 ppm region

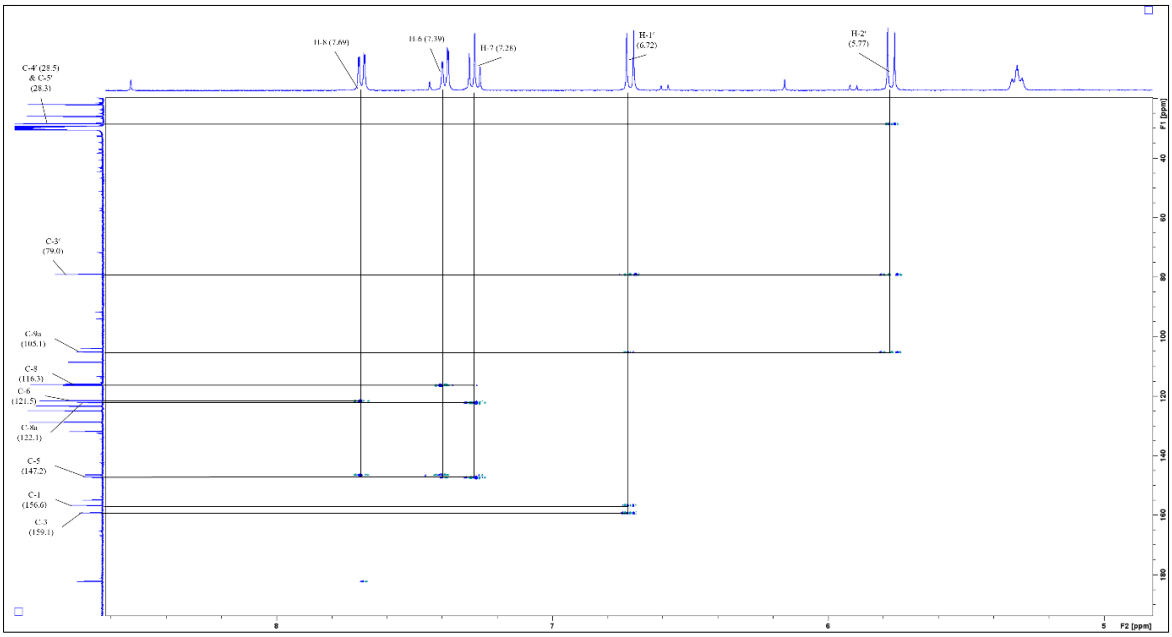

Appendix 9:
DEPT spectra of compound 5

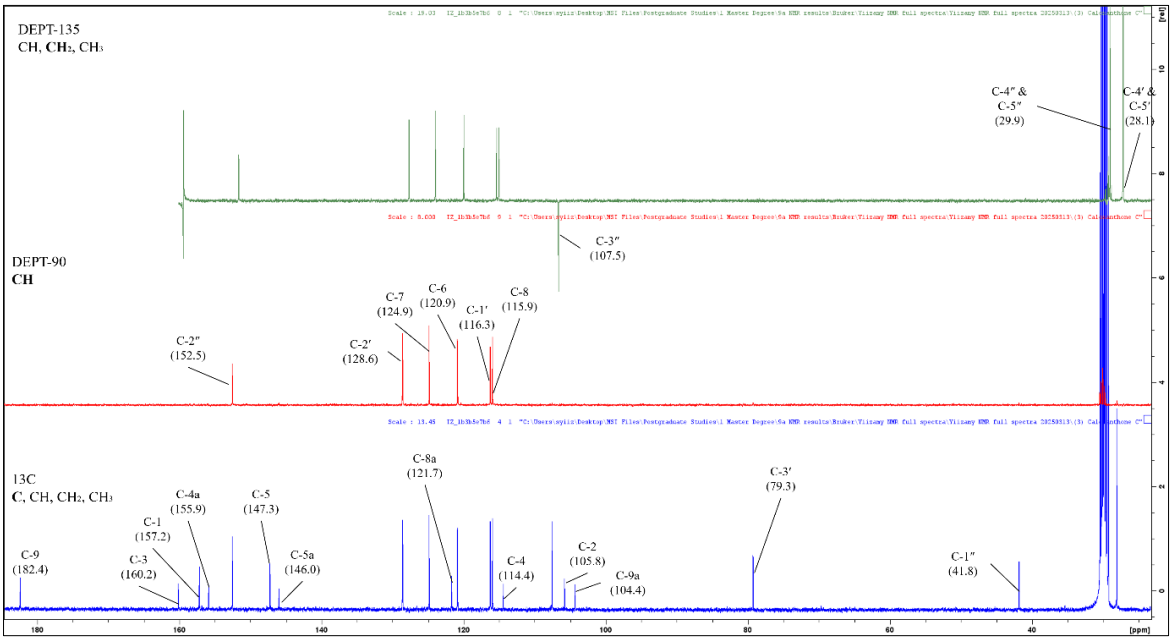

Appendix 10:
COSY spectrum of compound 5

Appendix 11:
Expanded COSY spectrum of compound 5 in the 4.0-8.0 ppm region

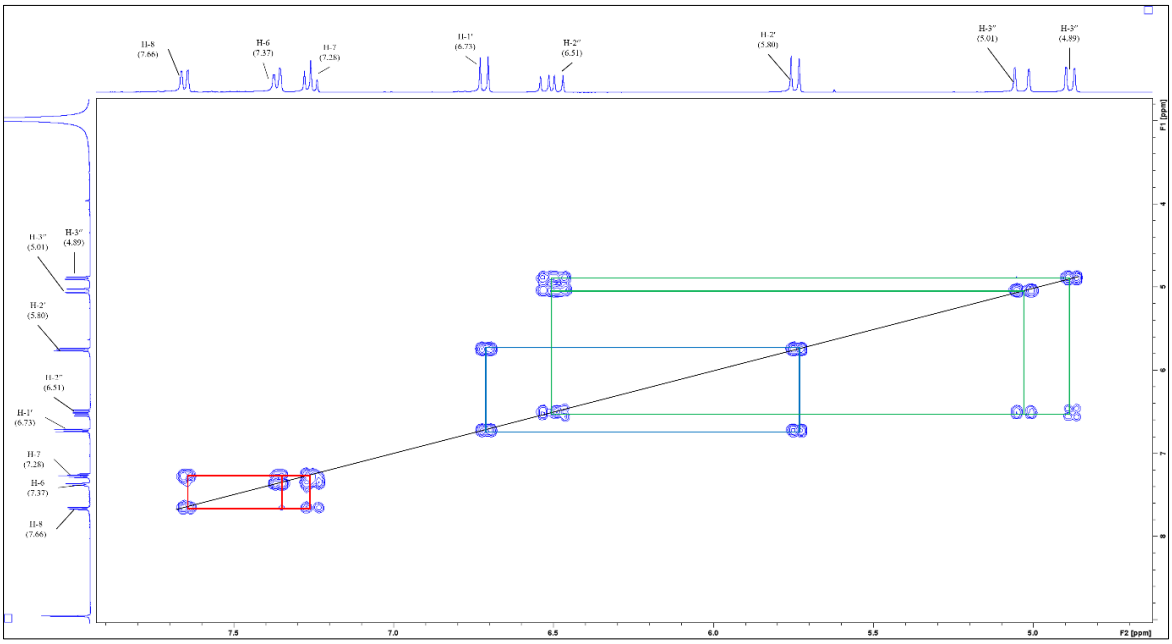

Appendix 12:
HSQC spectrum of compound 5

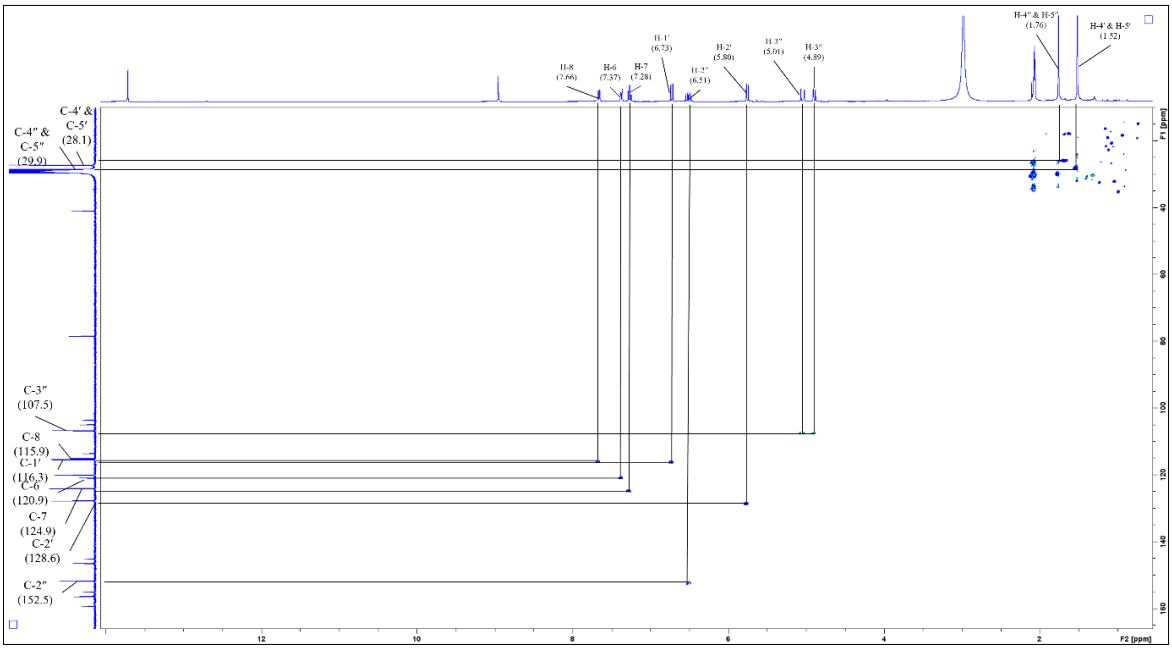

Appendix 13:
Expanded HSQC spectrum of compound 5 in the 0.0-3.0 ppm region

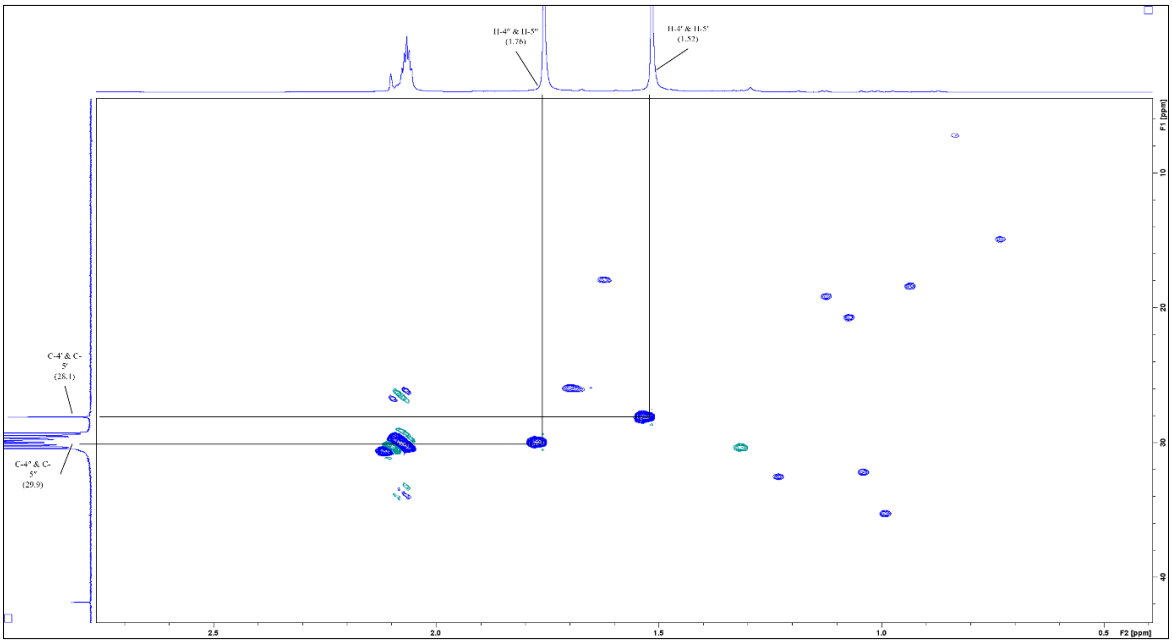

Appendix 14:
Expanded HSQC spectrum of compound 5 in the 4.0-8.0 ppm region

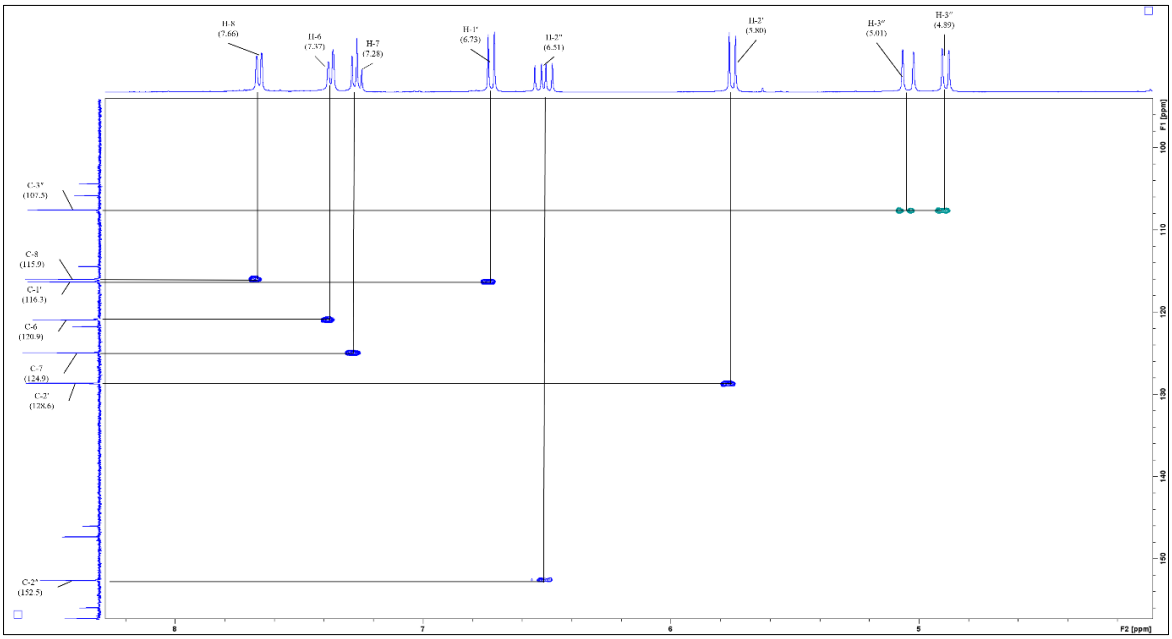

Appendix 15:
HMBC spectrum of compound 5 in the 1.0-14.0 ppm region

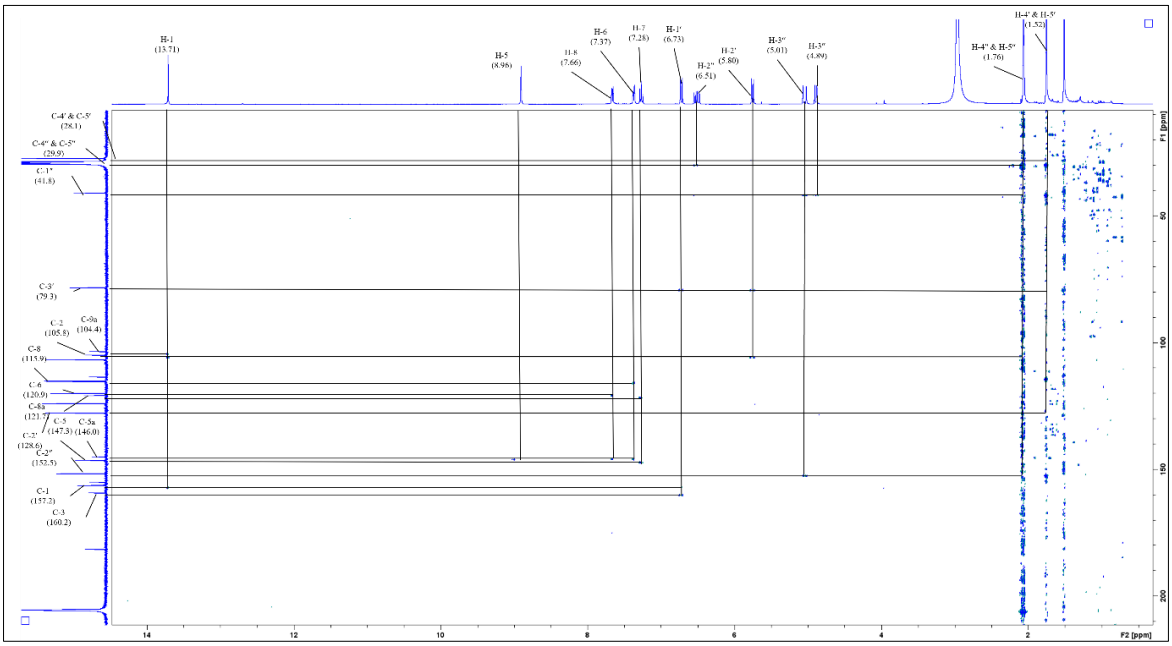

Appendix 16:
Expanded HMBC spectrum of compound 5 in the 1.5-2.5 ppm region

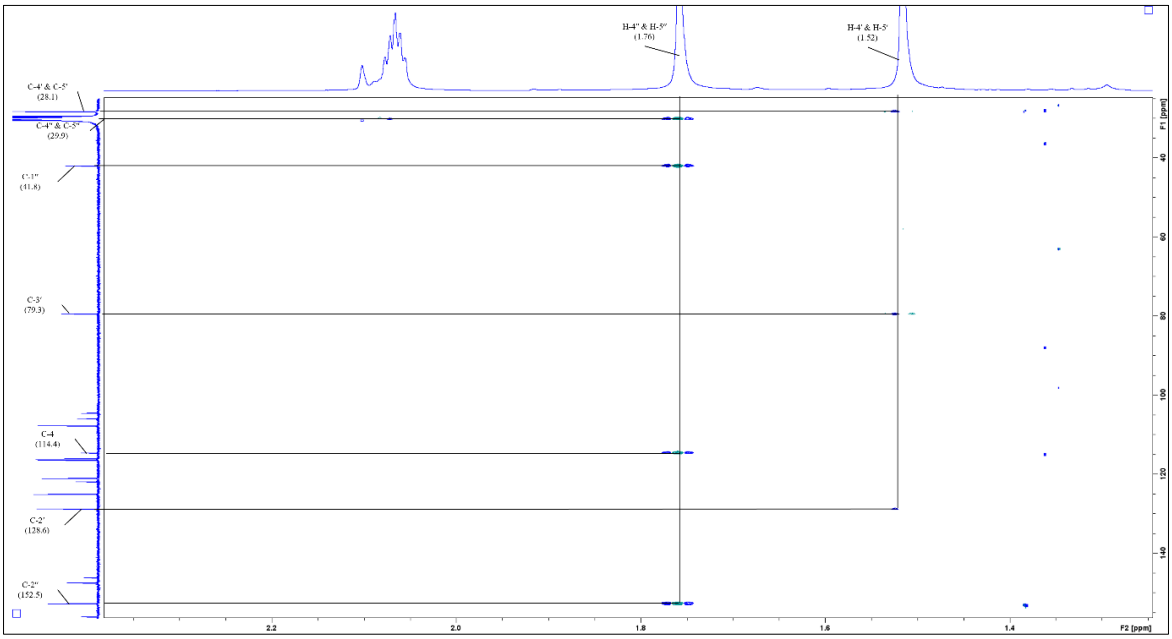

Appendix 17:
Expanded HMBC spectrum of compound 5 in the 4.0-7.0 ppm region

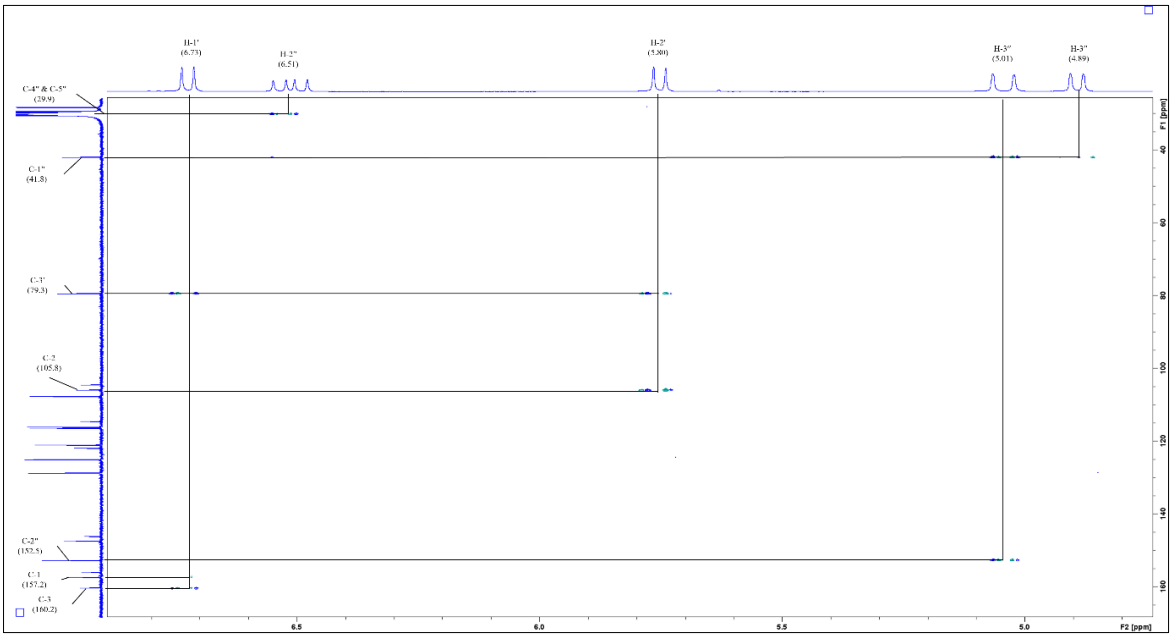

Appendix 18:
Expanded HMBC spectrum of compound 5 in the 7.0-9.0 ppm region

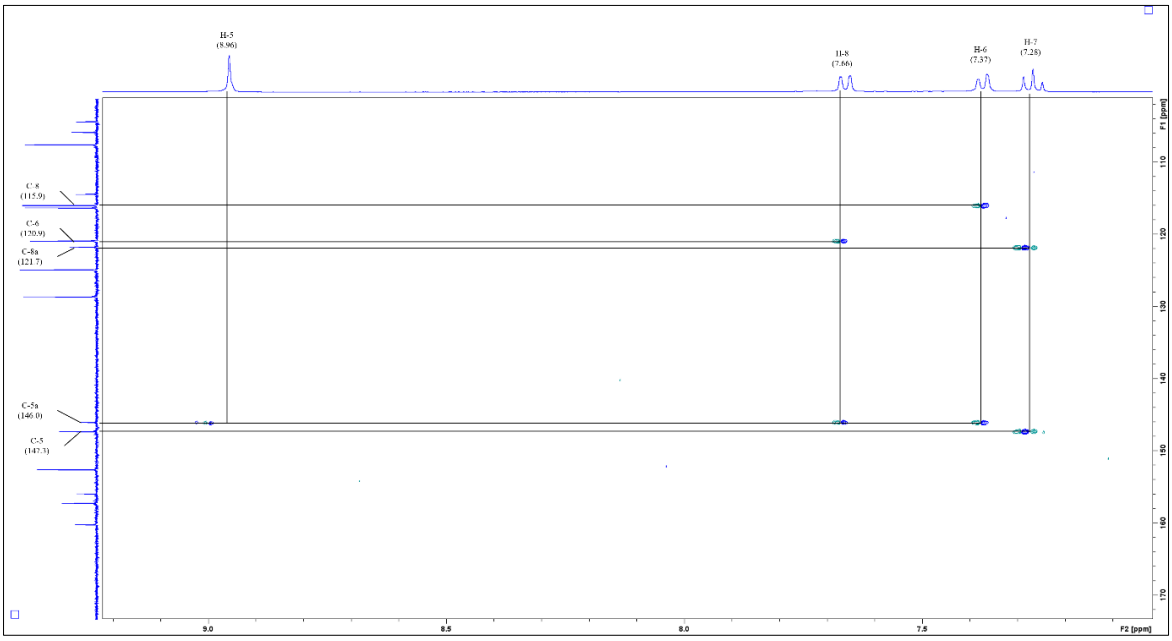

Appendix 19:
Expanded HMBC spectrum of compound 5 in the 13.0-14.0 ppm region

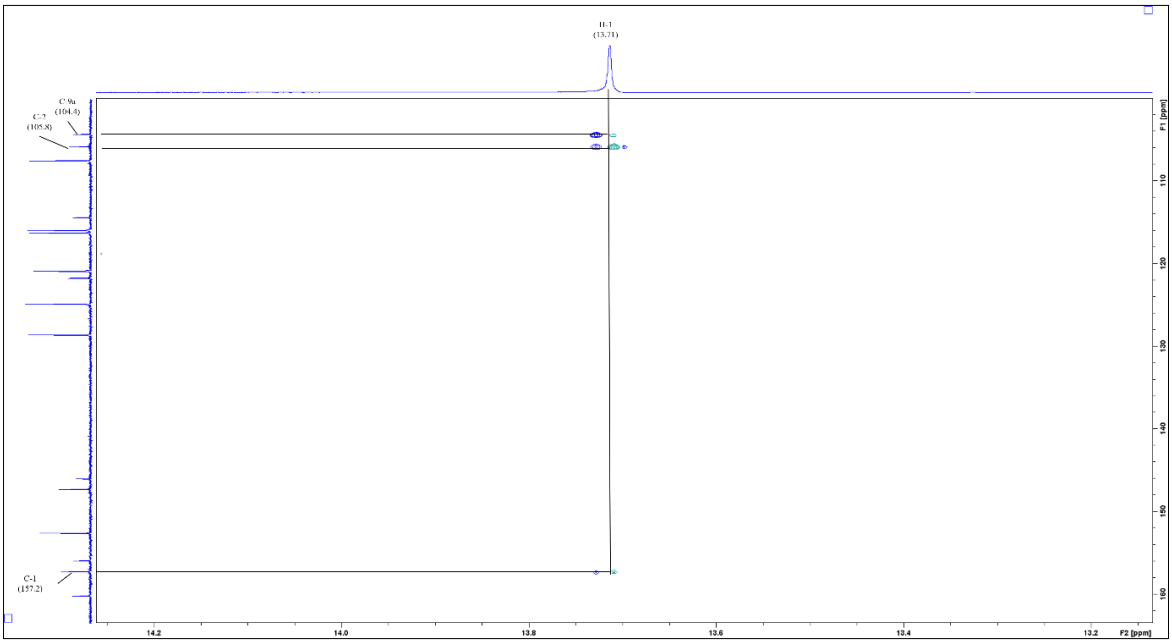

Appendix 20:
DEPT spectra of compound 27

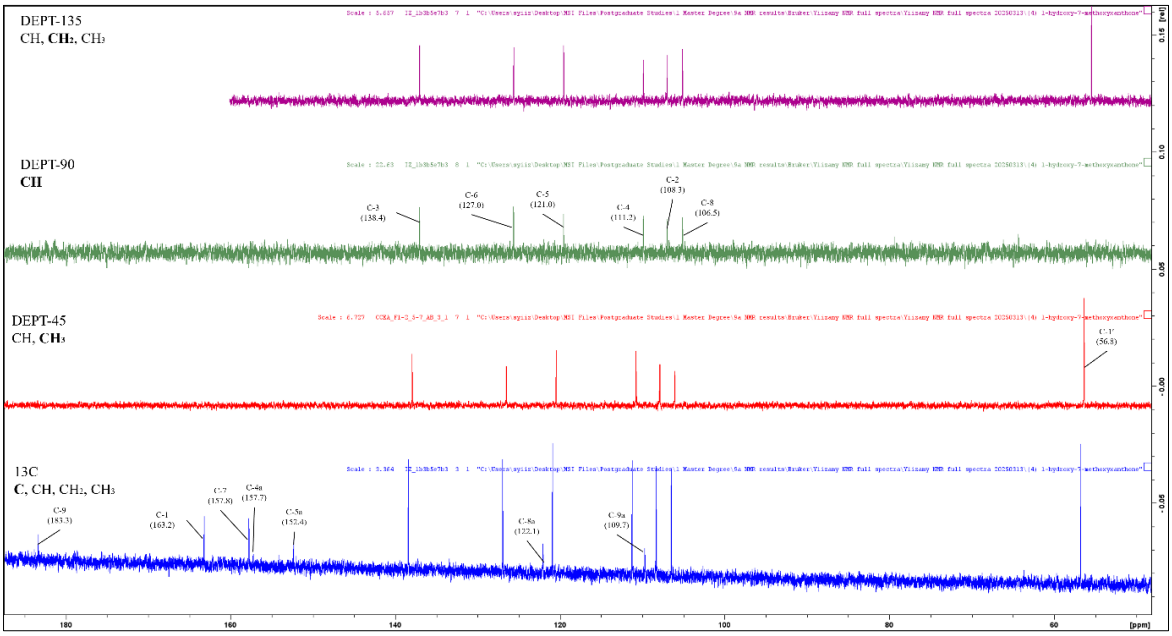

Appendix 21:
COSY spectrum of compound 27

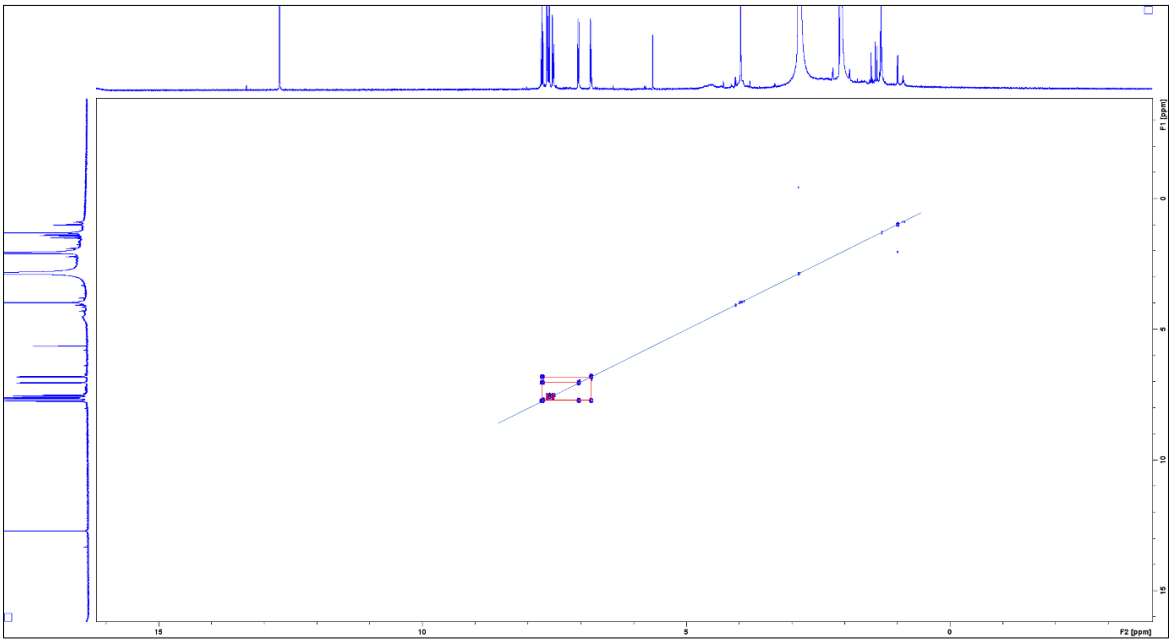

Appendix 22:
Expanded COSY spectrum of compound 27 in the 6.0-8.0 ppm region

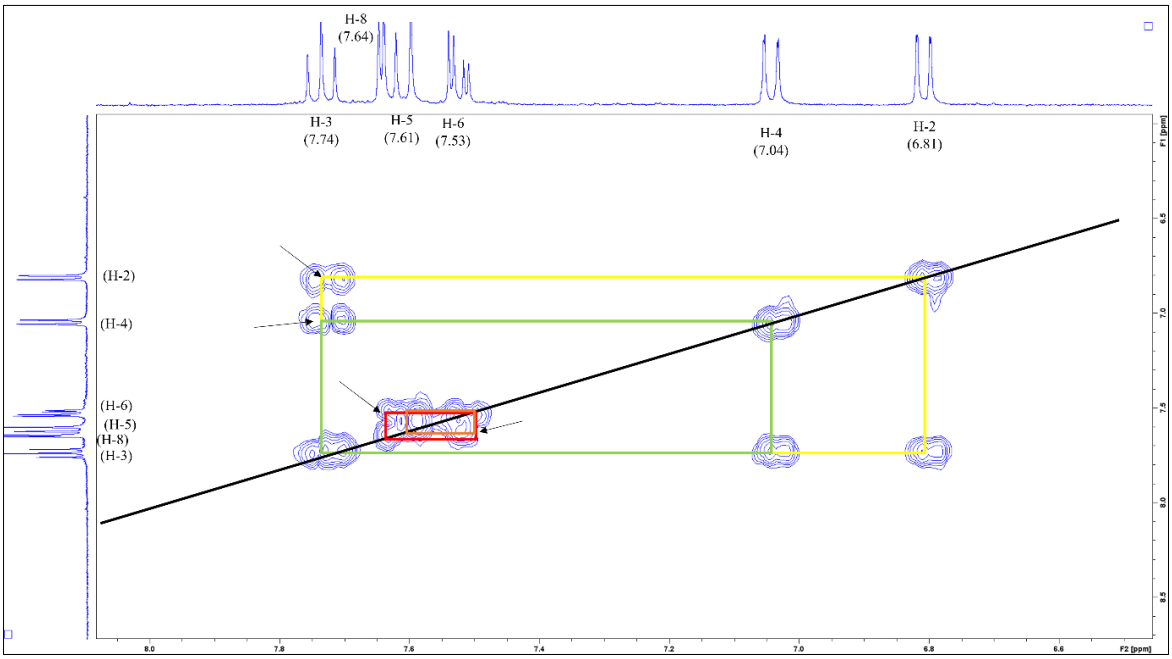

Appendix 23:
HSQC spectrum of compound 27

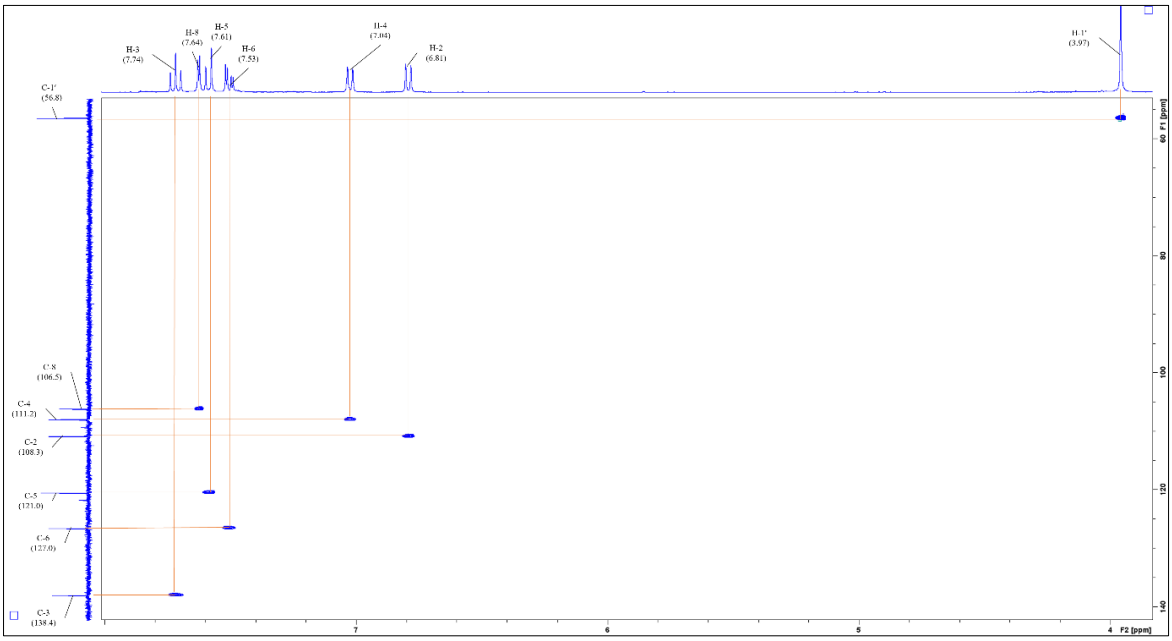

Appendix 24:
HMBC spectrum of compound 27

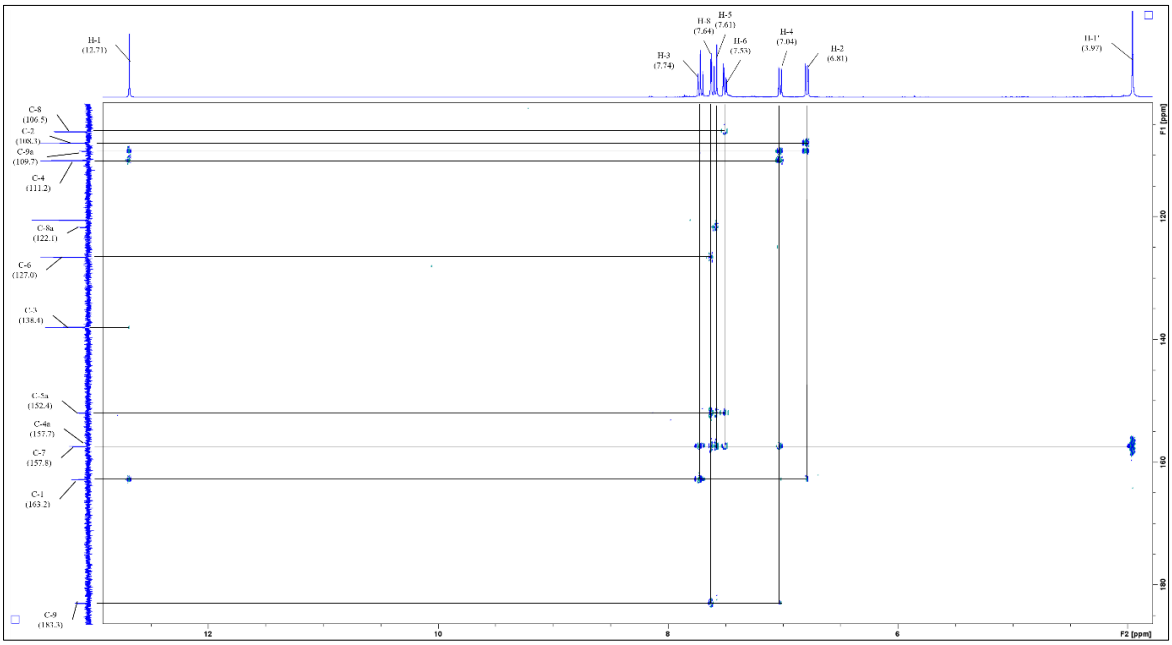

Appendix 25:
DEPT spectra of compound 90

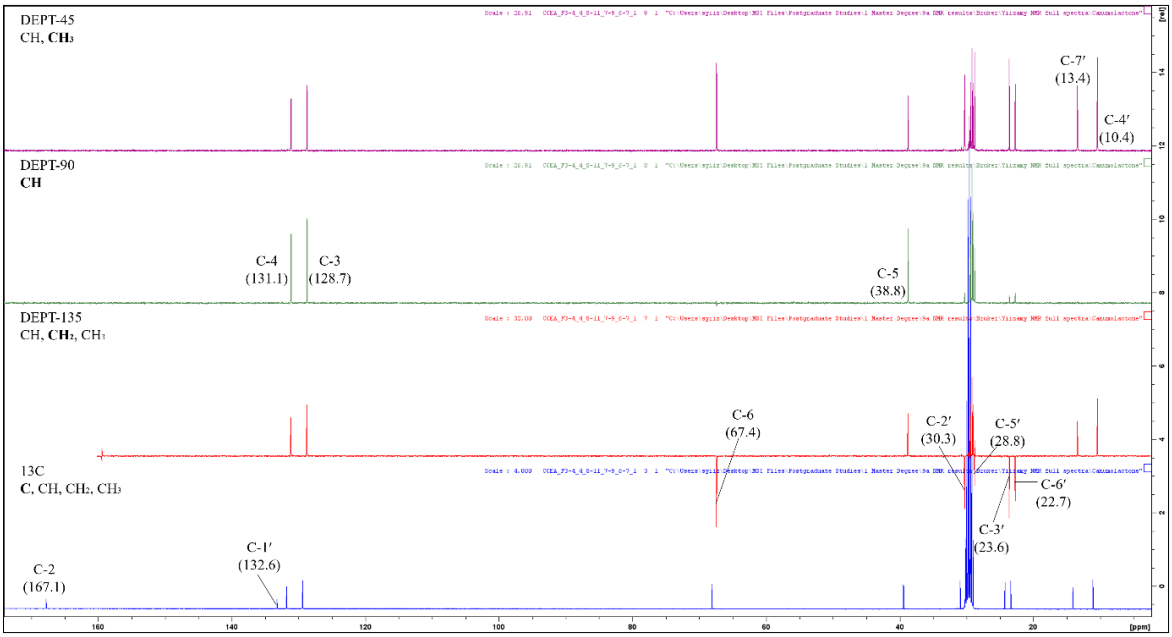

Appendix 26:
COSY spectrum of compound 90

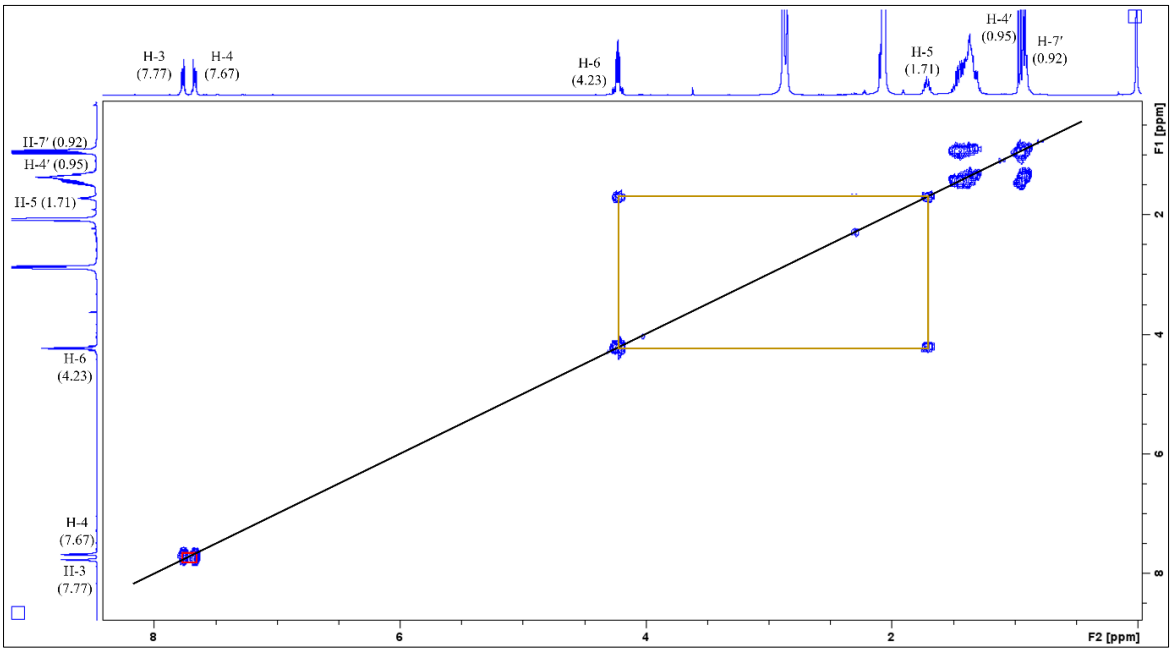

Appendix 27:
Expanded COSY spectrum of compound 90 in the 0-1.5 ppm region

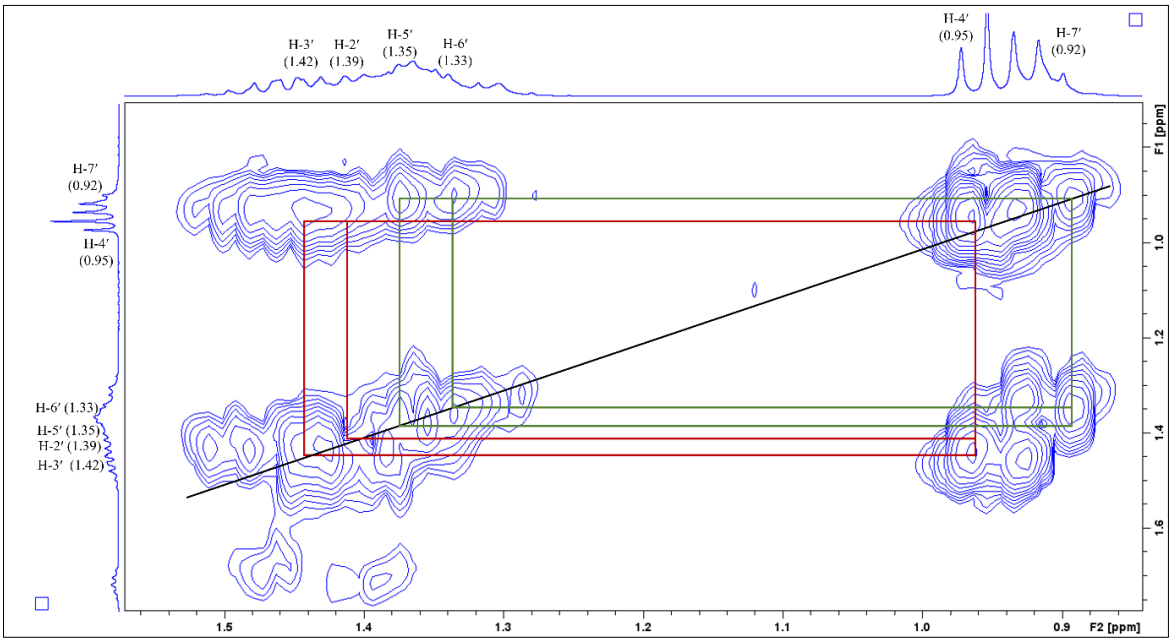

Appendix 28:
HSQC spectrum of compound 90

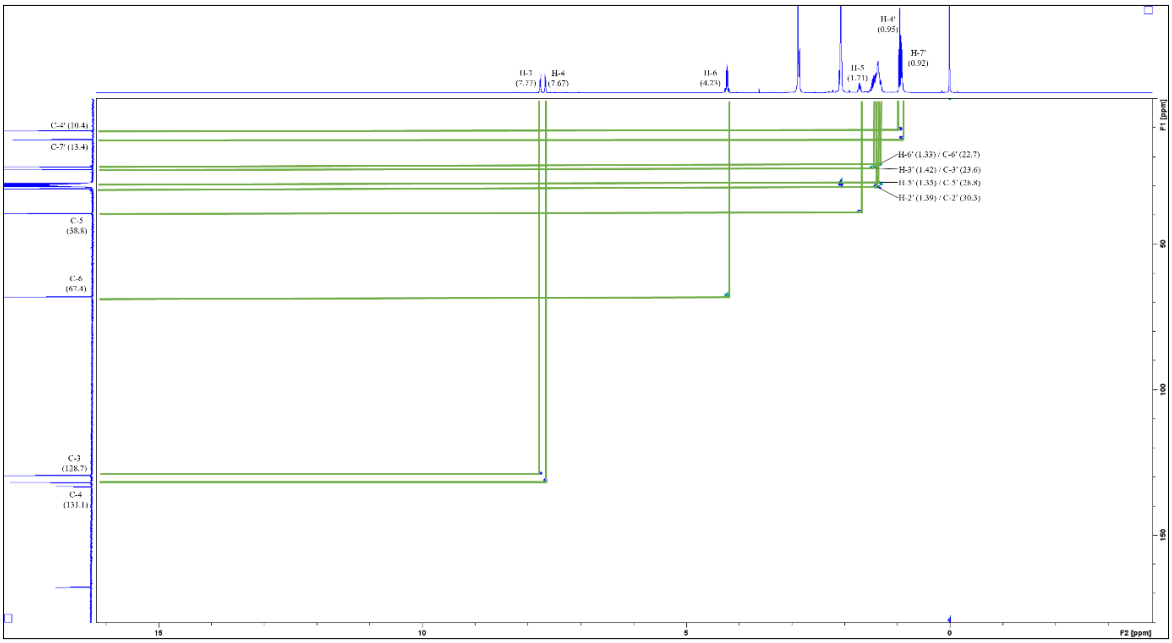

Appendix 29:
HMBC spectrum of compound 90

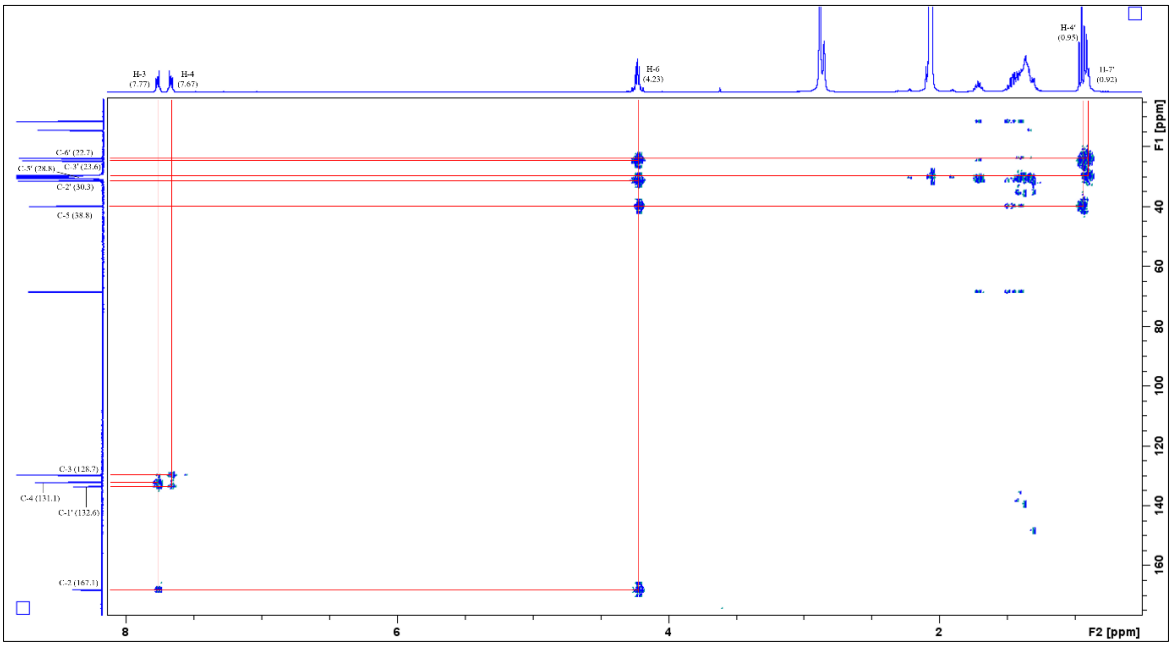

Appendix 30:
Expanded HMBC spectrum of compound 90 in the 1.3-1.8 ppm region

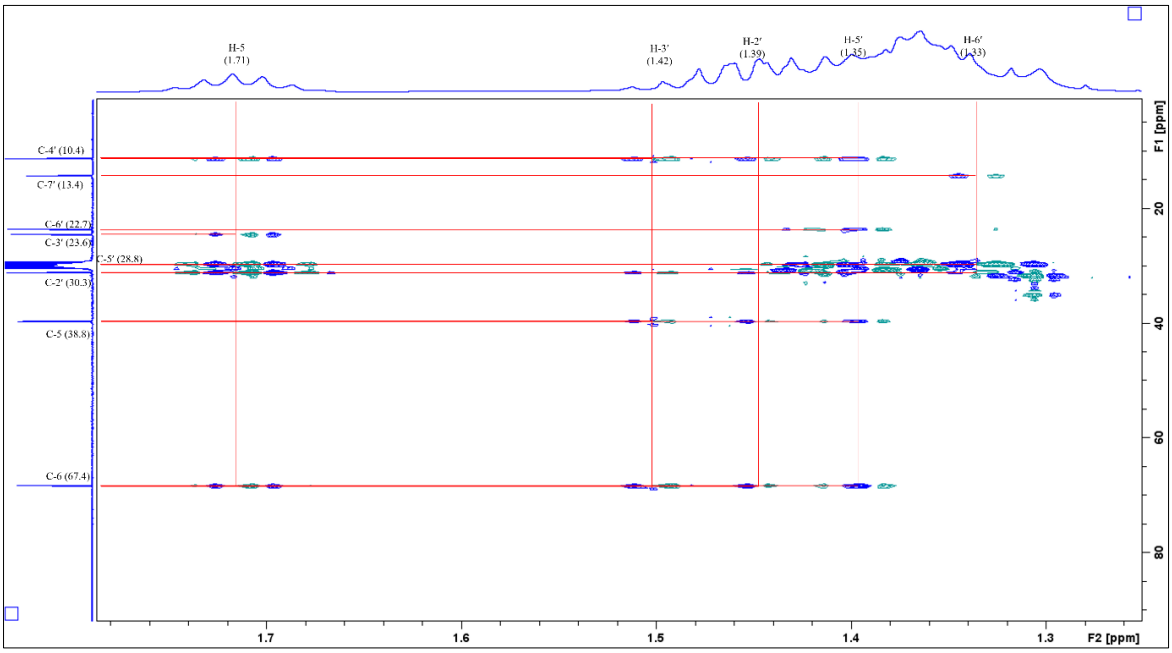

Appendix 31:
DEPT spectra of compound 71

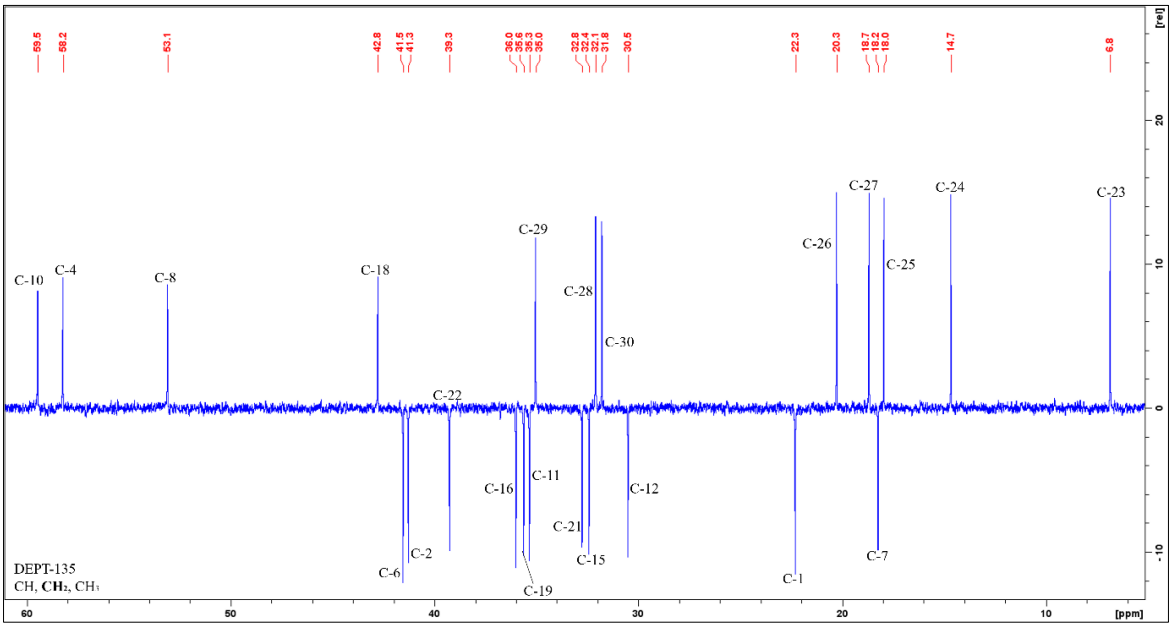

Appendix 32:
DEPT spectra of compound 70

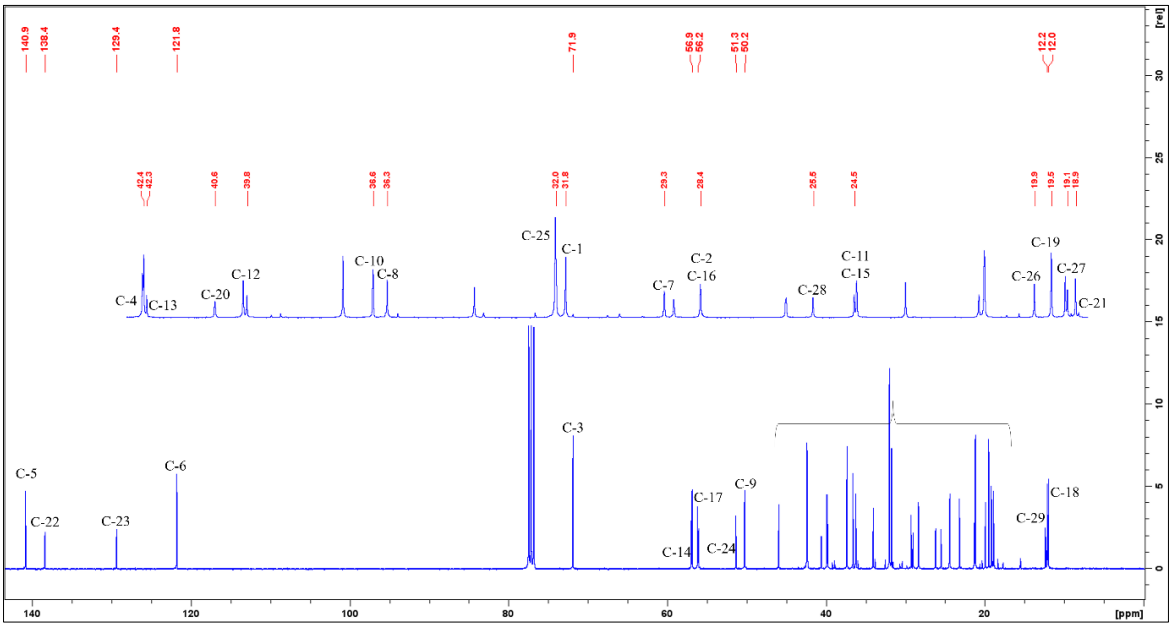

Appendix 33:
Inhibition zone by *C. nodosum* extracts and isolated compounds

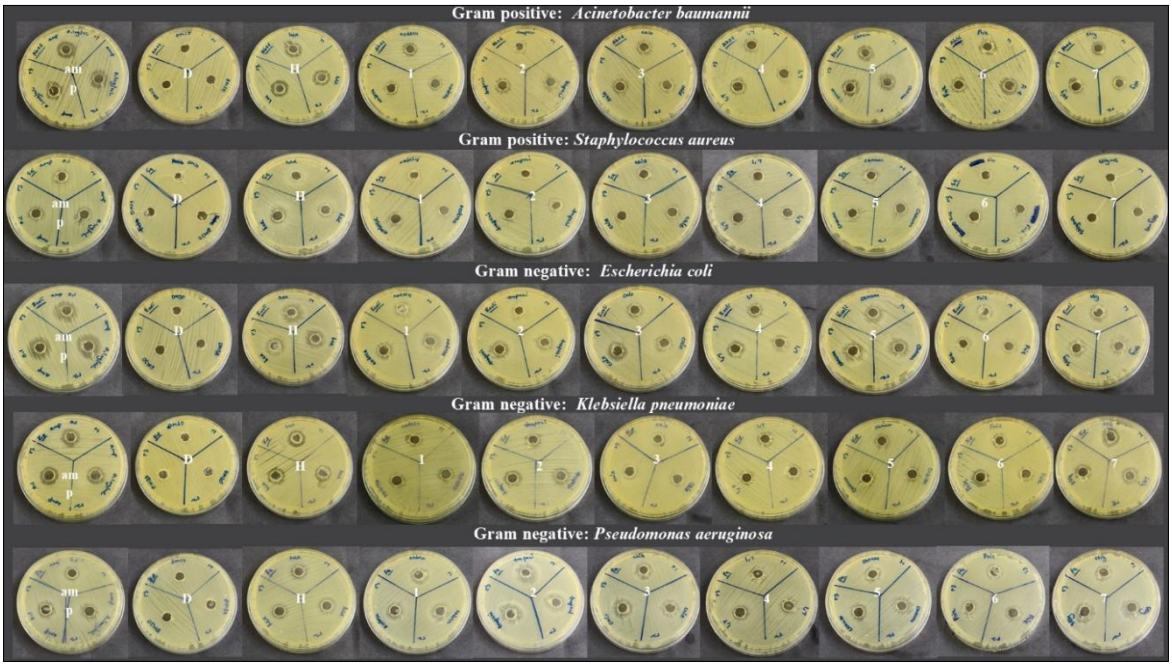

Appendix 34:
SPSS output of statistic descriptives against *S. aureus*

Descriptives

Zone_mm

	N	Mean	Std. Deviation	Std. Error	95% Confidence Interval for Mean		Minimum	Maximum
					Lower Bound	Upper Bound		
Ampicillin_0.1	9	8.6667	.70711	.23570	8.1231	9.2102	8.00	10.00
Hex	9	7.5556	.72648	.24216	6.9971	8.1140	7.00	9.00
Chloroform	9	7.0000	.00000	.00000	7.0000	7.0000	7.00	7.00
Methanol	9	7.4444	.52705	.17568	7.0393	7.8496	7.00	8.00
Nodosuxanthone	9	7.2222	.44096	.14699	6.8833	7.5612	7.00	8.00
Trapezifolixanthone	9	7.2222	.44096	.14699	6.8833	7.5612	7.00	8.00
1-hydroxy-7-methoxyxanthone	9	7.1111	.33333	.11111	6.8549	7.3673	7.00	8.00
Caloxanthone C	9	7.6667	.50000	.16667	7.2823	8.0510	7.00	8.00
Canumolactone	9	8.1111	.78174	.26058	7.5102	8.7120	7.00	9.00
Friedelin	9	7.6667	.70711	.23570	7.1231	8.2102	7.00	9.00
Stigmasterol	9	7.0000	.00000	.00000	7.0000	7.0000	7.00	7.00
Total	99	7.5152	.70514	.07087	7.3745	7.6558	7.00	10.00

Appendix 35:
SPSS output of homogeneity of variances test against *S. aureus*

Tests of Homogeneity of Variances

		Levene Statistic	df1	df2	Sig.
Zone_mm	Based on Mean	7.101	10	88	<.001
	Based on Median	2.093	10	88	.033
	Based on Median and with adjusted df	2.093	10	61.891	.038
	Based on trimmed mean	6.896	10	88	<.001

Appendix 36:
SPSS output of one-way ANOVA against *S. aureus*

ANOVA

Zone_mm

	Sum of Squares	df	Mean Square	F	Sig.
Between Groups	23.394	10	2.339	8.126	<.001
Within Groups	25.333	88	.288		
Total	48.727	98			

Appendix 37:
SPSS output of Games-Howell post hoc analysis against *S. aureus*

Multiple Comparisons

Dependent Variable: Zone_mm

Games-Howell

(I) Sample	(J) Sample	Mean Difference (I-J)	Std. Error	Sig.	95% Confidence Interval	
					Lower Bound	Upper Bound
Ampicillin_0.1	Hex	1.11111	.33793	.108	-.1449	2.3672
	Chloroform	1.66667*	.23570	.002	.6578	2.6756
	Methanol	1.22222*	.29397	.024	.1169	2.3275
	Nodosuxanthone	1.44444*	.27778	.005	.3833	2.5056
	Trapezifolixanthone	1.44444*	.27778	.005	.3833	2.5056
	1-hydroxy-7-methoxyxanthone	1.55556*	.26058	.002	.5299	2.5812
	Caloxanthone C	1.00000	.28868	.086	-.0899	2.0899
	Canumolactone	.55556	.35136	.869	-.7521	1.8633
	Friedelin	1.00000	.33333	.175	-.2388	2.2388
	Stigmasterol	1.66667*	.23570	.002	.6578	2.6756
Hex	Ampicillin_0.1	-1.11111	.33793	.108	-2.3672	.1449
	Chloroform	.55556	.24216	.508	-.4810	1.5921
	Methanol	.11111	.29918	1.000	-1.0161	1.2383
	Nodosuxanthone	.33333	.28328	.975	-.7518	1.4184
	Trapezifolixanthone	.33333	.28328	.975	-.7518	1.4184
	1-hydroxy-7-methoxyxanthone	.44444	.26644	.825	-.6073	1.4961
	Caloxanthone C	-.11111	.29397	1.000	-1.2236	1.0014
	Canumolactone	-.55556	.35573	.877	-1.8786	.7675
	Friedelin	-.11111	.33793	1.000	-1.3672	1.1449
	Stigmasterol	.55556	.24216	.508	-.4810	1.5921
Chloroform	Ampicillin_0.1	-1.66667*	.23570	.002	-2.6756	-.6578
	Hex	-.55556	.24216	.508	-1.5921	.4810
	Methanol	-.44444	.17568	.401	-1.1964	.3075
	Nodosuxanthone	-.22222	.14699	.881	-.8514	.4069
	Trapezifolixanthone	-.22222	.14699	.881	-.8514	.4069
	1-hydroxy-7-methoxyxanthone	-.11111	.11111	.989	-.5867	.3645
	Caloxanthone C	-.66667	.16667	.070	-1.3801	.0467
	Canumolactone	-1.11111	.26058	.051	-2.2265	.0043
	Friedelin	-.66667	.23570	.289	-1.6756	.3422
	Stigmasterol	.00000	.00000	.	.0000	.0000
Methanol	Ampicillin_0.1	-1.22222*	.29397	.024	-2.3275	-.1169
	Hex	-.11111	.29918	1.000	-1.2383	1.0161
	Chloroform	.44444	.17568	.401	-.3075	1.1964
	Nodosuxanthone	.22222	.22906	.994	-.6329	1.0773
	Trapezifolixanthone	.22222	.22906	.994	-.6329	1.0773
	1-hydroxy-7-methoxyxanthone	.33333	.20787	.857	-.4596	1.1263
	Caloxanthone C	-.22222	.24216	.996	-1.1226	.6781
	Canumolactone	-.66667	.31427	.582	-1.8582	.5249
	Friedelin	-.22222	.29397	.999	-1.3275	.8831
	Stigmasterol	.44444	.17568	.401	-.3075	1.1964

Nodosuxanthone	Ampicillin_0.1	-1.44444*	.27778	.005	-2.5056	-.3833
	Hex	-.33333	.28328	.975	-1.4184	.7518
	Chloroform	.22222	.14699	.881	-.4069	.8514
	Methanol	-.22222	.22906	.994	-1.0773	.6329
	Trapezifolixanthone	.00000	.20787	1.000	-.7725	.7725
	1-hydroxy-7-methoxyxanthone	.11111	.18426	1.000	-.5809	.8032
	Caloxanthone C	-.44444	.22222	.652	-1.2722	.3833
	Canumolactone	-.88889	.29918	.202	-2.0438	.2660
	Friedelin	-.44444	.27778	.858	-1.5056	.6167
	Stigmasterol	.22222	.14699	.881	-.4069	.8514
Trapezifolixanthone	Ampicillin_0.1	-1.44444*	.27778	.005	-2.5056	-.3833
	Hex	-.33333	.28328	.975	-1.4184	.7518
	Chloroform	.22222	.14699	.881	-.4069	.8514
	Methanol	-.22222	.22906	.994	-1.0773	.6329
	Nodosuxanthone	.00000	.20787	1.000	-.7725	.7725
	1-hydroxy-7-methoxyxanthone	.11111	.18426	1.000	-.5809	.8032
	Caloxanthone C	-.44444	.22222	.652	-1.2722	.3833
	Canumolactone	-.88889	.29918	.202	-2.0438	.2660
	Friedelin	-.44444	.27778	.858	-1.5056	.6167
	Stigmasterol	.22222	.14699	.881	-.4069	.8514
1-hydroxy-7-methoxyxanthone	Ampicillin_0.1	-1.55556*	.26058	.002	-2.5812	-.5299
	Hex	-.44444	.26644	.825	-1.4961	.6073
	Chloroform	.11111	.11111	.989	-.3645	.5867
	Methanol	-.33333	.20787	.857	-1.1263	.4596
	Nodosuxanthone	-.11111	.18426	1.000	-.8032	.5809
	Trapezifolixanthone	-.11111	.18426	1.000	-.8032	.5809
	Caloxanthone C	-.55556	.20031	.260	-1.3158	.2047
	Canumolactone	-1.00000	.28328	.097	-2.1267	.1267
	Friedelin	-.55556	.26058	.580	-1.5812	.4701
	Stigmasterol	.11111	.11111	.989	-.3645	.5867
Caloxanthone C	Ampicillin_0.1	-1.00000	.28868	.086	-2.0899	.0899
	Hex	.11111	.29397	1.000	-1.0014	1.2236
	Chloroform	.66667	.16667	.070	-.0467	1.3801
	Methanol	.22222	.24216	.996	-.6781	1.1226
	Nodosuxanthone	.44444	.22222	.652	-.3833	1.2722
	Trapezifolixanthone	.44444	.22222	.652	-.3833	1.2722
	1-hydroxy-7-methoxyxanthone	.55556	.20031	.260	-.2047	1.3158
	Canumolactone	-.44444	.30932	.918	-1.6231	.7342
	Friedelin	.00000	.28868	1.000	-1.0899	1.0899
	Stigmasterol	.66667	.16667	.070	-.0467	1.3801

Canumolactone	Ampicillin_0.1	-.55556	.35136	.869	-1.8633	.7521
	Hex	.55556	.35573	.877	-.7675	1.8786
	Chloroform	1.11111	.26058	.051	-.0043	2.2265
	Methanol	.66667	.31427	.582	-.5249	1.8582
	Nodosuxanthone	.88889	.29918	.202	-.2660	2.0438
	Trapezifolixanthone	.88889	.29918	.202	-.2660	2.0438
	1-hydroxy-7-methoxyxanthone	1.00000	.28328	.097	-.1267	2.1267
	Caloxanthone C	.44444	.30932	.918	-.7342	1.6231
	Friedelin	.44444	.35136	.963	-.8633	1.7521
	Stigmasterol	1.11111	.26058	.051	-.0043	2.2265
Friedelin	Ampicillin_0.1	-1.00000	.33333	.175	-2.2388	.2388
	Hex	.11111	.33793	1.000	-1.1449	1.3672
	Chloroform	.66667	.23570	.289	-.3422	1.6756
	Methanol	.22222	.29397	.999	-.8831	1.3275
	Nodosuxanthone	.44444	.27778	.858	-.6167	1.5056
	Trapezifolixanthone	.44444	.27778	.858	-.6167	1.5056
	1-hydroxy-7-methoxyxanthone	.55556	.26058	.580	-.4701	1.5812
	Caloxanthone C	.00000	.28868	1.000	-1.0899	1.0899
	Canumolactone	-.44444	.35136	.963	-1.7521	.8633
	Stigmasterol	.66667	.23570	.289	-.3422	1.6756
Stigmasterol	Ampicillin_0.1	-1.66667*	.23570	.002	-2.6756	-.6578
	Hex	-.55556	.24216	.508	-1.5921	.4810
	Chloroform	.00000	.00000	.	.0000	.0000
	Methanol	-.44444	.17568	.401	-1.1964	.3075
	Nodosuxanthone	-.22222	.14699	.881	-.8514	.4069
	Trapezifolixanthone	-.22222	.14699	.881	-.8514	.4069
	1-hydroxy-7-methoxyxanthone	-.11111	.11111	.989	-.5867	.3645
	Caloxanthone C	-.66667	.16667	.070	-1.3801	.0467
	Canumolactone	-1.11111	.26058	.051	-2.2265	.0043
	Friedelin	-.66667	.23570	.289	-1.6756	.3422

*. The mean difference is significant at the 0.05 level.

Appendix 38:
SPSS output of statistic descriptives against *A. baumannii*

Descriptives

Zone_mm

	N	Mean	Std. Deviation	Std. Error	95% Confidence Interval for Mean		Minimum	Maximum
					Lower Bound	Upper Bound		
Ampicillin_0.1	9	10.4444	1.74005	.58002	9.1069	11.7820	8.00	13.00
Hex	9	11.3333	1.22474	.40825	10.3919	12.2748	10.00	14.00
Chloroform	9	8.0000	1.00000	.33333	7.2313	8.7687	7.00	10.00
Methanol	9	9.2222	.83333	.27778	8.5817	9.8628	8.00	11.00
Nodosuxanthone	9	7.7778	.66667	.22222	7.2653	8.2902	7.00	9.00
Trapezifolixanthone	9	7.7778	.66667	.22222	7.2653	8.2902	7.00	9.00
1-hydroxy-7-methoxyxanthone	9	8.7778	.66667	.22222	8.2653	9.2902	8.00	10.00
Caloxanthone C	9	9.7778	.83333	.27778	9.1372	10.4183	9.00	11.00
Canumolactone	9	12.5556	.52705	.17568	12.1504	12.9607	12.00	13.00
Friedelin	9	11.1111	1.05409	.35136	10.3009	11.9214	10.00	13.00
Stigmasterol	9	9.0000	1.22474	.40825	8.0586	9.9414	8.00	12.00
Total	99	9.6162	1.79402	.18031	9.2584	9.9740	7.00	14.00

Appendix 39:
SPSS output of homogeneity of variances test against *A. baumannii*

Tests of Homogeneity of Variances

		Levene Statistic	df1	df2	Sig.
Zone_mm	Based on Mean	1.677	10	88	.099
	Based on Median	.872	10	88	.562
	Based on Median and with adjusted df	.872	10	57.184	.564
	Based on trimmed mean	1.641	10	88	.108

Appendix 40:
SPSS output of one-way ANOVA against *A. baumannii*

ANOVA

Zone_mm

	Sum of Squares	df	Mean Square	F	Sig.
Between Groups	226.303	10	22.630	22.348	<.001
Within Groups	89.111	88	1.013		
Total	315.414	98			

Appendix 41:
SPSS output of Tukey HSD post hoc analysis against *A. baumannii*

Multiple Comparisons

Dependent Variable: Zone_mm

Tukey HSD

(I) Sample	(J) Sample	Mean Difference (I-J)	Std. Error	Sig.	95% Confidence Interval	
					Lower Bound	Upper Bound
Ampicillin_0.1	Hex	-.88889	.47437	.732	-2.4566	.6789
	Chloroform	2.44444*	.47437	<.001	.8767	4.0122
	Methanol	1.22222	.47437	.277	-.3455	2.7900
	Nodosuxanthone	2.66667*	.47437	<.001	1.0989	4.2344
	Trapezifolixanthone	2.66667*	.47437	<.001	1.0989	4.2344
	1-hydroxy-7-methoxyxanthone	1.66667*	.47437	.028	.0989	3.2344
	Caloxanthone C	.66667	.47437	.944	-.9011	2.2344
	Canumolactone	-2.11111*	.47437	.001	-3.6789	-.5434
	Friedelin	-.66667	.47437	.944	-2.2344	.9011
	Stigmasterol	1.44444	.47437	.099	-.1233	3.0122
Hex	Ampicillin_0.1	.88889	.47437	.732	-.6789	2.4566
	Chloroform	3.33333*	.47437	<.001	1.7656	4.9011
	Methanol	2.11111*	.47437	.001	.5434	3.6789
	Nodosuxanthone	3.55556*	.47437	<.001	1.9878	5.1233
	Trapezifolixanthone	3.55556*	.47437	<.001	1.9878	5.1233
	1-hydroxy-7-methoxyxanthone	2.55556*	.47437	<.001	.9878	4.1233
	Caloxanthone C	1.55556	.47437	.054	-.0122	3.1233
	Canumolactone	-1.22222	.47437	.277	-2.7900	.3455
	Friedelin	.22222	.47437	1.000	-1.3455	1.7900
	Stigmasterol	2.33333*	.47437	<.001	.7656	3.9011
Chloroform	Ampicillin_0.1	-2.44444*	.47437	<.001	-4.0122	-.8767
	Hex	-3.33333*	.47437	<.001	-4.9011	-1.7656
	Methanol	-1.22222	.47437	.277	-2.7900	.3455
	Nodosuxanthone	.22222	.47437	1.000	-1.3455	1.7900
	Trapezifolixanthone	.22222	.47437	1.000	-1.3455	1.7900
	1-hydroxy-7-methoxyxanthone	-.77778	.47437	.861	-2.3455	.7900
	Caloxanthone C	-1.77778*	.47437	.013	-3.3455	-.2100
	Canumolactone	-4.55556*	.47437	<.001	-6.1233	-2.9878
	Friedelin	-3.11111*	.47437	<.001	-4.6789	-1.5434
	Stigmasterol	-1.00000	.47437	.575	-2.5678	.5678
Methanol	Ampicillin_0.1	-1.22222	.47437	.277	-2.7900	.3455
	Hex	-2.11111*	.47437	.001	-3.6789	-.5434
	Chloroform	1.22222	.47437	.277	-.3455	2.7900
	Nodosuxanthone	1.44444	.47437	.099	-.1233	3.0122
	Trapezifolixanthone	1.44444	.47437	.099	-.1233	3.0122
	1-hydroxy-7-methoxyxanthone	.44444	.47437	.997	-1.1233	2.0122
	Caloxanthone C	-.55556	.47437	.984	-2.1233	1.0122
	Canumolactone	-3.33333*	.47437	<.001	-4.9011	-1.7656
	Friedelin	-1.88889*	.47437	.006	-3.4566	-.3211
	Stigmasterol	.22222	.47437	1.000	-1.3455	1.7900

Nodosuxanthone	Ampicillin_0.1	-2.66667*	.47437	<.001	-4.2344	-1.0989
	Hex	-3.55556*	.47437	<.001	-5.1233	-1.9878
	Chloroform	-.22222	.47437	1.000	-1.7900	1.3455
	Methanol	-1.44444	.47437	.099	-3.0122	.1233
	Trapezifolixanthone	.00000	.47437	1.000	-1.5678	1.5678
	1-hydroxy-7-methoxyxanthone	-1.00000	.47437	.575	-2.5678	.5678
	Caloxanthone C	-2.00000*	.47437	.003	-3.5678	-.4322
	Canumolactone	-4.77778*	.47437	<.001	-6.3455	-3.2100
	Friedelin	-3.33333*	.47437	<.001	-4.9011	-1.7656
	Stigmasterol	-1.22222	.47437	.277	-2.7900	.3455
Trapezifolixanthone	Ampicillin_0.1	-2.66667*	.47437	<.001	-4.2344	-1.0989
	Hex	-3.55556*	.47437	<.001	-5.1233	-1.9878
	Chloroform	-.22222	.47437	1.000	-1.7900	1.3455
	Methanol	-1.44444	.47437	.099	-3.0122	.1233
	Nodosuxanthone	.00000	.47437	1.000	-1.5678	1.5678
	1-hydroxy-7-methoxyxanthone	-1.00000	.47437	.575	-2.5678	.5678
	Caloxanthone C	-2.00000*	.47437	.003	-3.5678	-.4322
	Canumolactone	-4.77778*	.47437	<.001	-6.3455	-3.2100
	Friedelin	-3.33333*	.47437	<.001	-4.9011	-1.7656
	Stigmasterol	-1.22222	.47437	.277	-2.7900	.3455
1-hydroxy-7-methoxyxanthone	Ampicillin_0.1	-1.66667*	.47437	.028	-3.2344	-.0989
	Hex	-2.55556*	.47437	<.001	-4.1233	-.9878
	Chloroform	.77778	.47437	.861	-.7900	2.3455
	Methanol	-.44444	.47437	.997	-2.0122	1.1233
	Nodosuxanthone	1.00000	.47437	.575	-.5678	2.5678
	Trapezifolixanthone	1.00000	.47437	.575	-.5678	2.5678
	Caloxanthone C	-1.00000	.47437	.575	-2.5678	.5678
	Canumolactone	-3.77778*	.47437	<.001	-5.3455	-2.2100
	Friedelin	-2.33333*	.47437	<.001	-3.9011	-.7656
	Stigmasterol	-.22222	.47437	1.000	-1.7900	1.3455
Caloxanthone C	Ampicillin_0.1	-.66667	.47437	.944	-2.2344	.9011
	Hex	-1.55556	.47437	.054	-3.1233	.0122
	Chloroform	1.77778*	.47437	.013	.2100	3.3455
	Methanol	.55556	.47437	.984	-1.0122	2.1233
	Nodosuxanthone	2.00000*	.47437	.003	.4322	3.5678
	Trapezifolixanthone	2.00000*	.47437	.003	.4322	3.5678
	1-hydroxy-7-methoxyxanthone	1.00000	.47437	.575	-.5678	2.5678
	Canumolactone	-2.77778*	.47437	<.001	-4.3455	-1.2100
	Friedelin	-1.33333	.47437	.171	-2.9011	.2344
	Stigmasterol	.77778	.47437	.861	-.7900	2.3455

Canumolactone	Ampicillin_0.1	2.11111*	.47437	.001	.5434	3.6789
	Hex	1.22222	.47437	.277	-.3455	2.7900
	Chloroform	4.55556*	.47437	<.001	2.9878	6.1233
	Methanol	3.33333*	.47437	<.001	1.7656	4.9011
	Nodosuxanthone	4.77778*	.47437	<.001	3.2100	6.3455
	Trapezifolixanthone	4.77778*	.47437	<.001	3.2100	6.3455
	1-hydroxy-7-methoxyxanthone	3.77778*	.47437	<.001	2.2100	5.3455
	Caloxanthone C	2.77778*	.47437	<.001	1.2100	4.3455
	Friedelin	1.44444	.47437	.099	-.1233	3.0122
	Stigmasterol	3.55556*	.47437	<.001	1.9878	5.1233
Friedelin	Ampicillin_0.1	.66667	.47437	.944	-.9011	2.2344
	Hex	-.22222	.47437	1.000	-1.7900	1.3455
	Chloroform	3.11111*	.47437	<.001	1.5434	4.6789
	Methanol	1.88889*	.47437	.006	.3211	3.4566
	Nodosuxanthone	3.33333*	.47437	<.001	1.7656	4.9011
	Trapezifolixanthone	3.33333*	.47437	<.001	1.7656	4.9011
	1-hydroxy-7-methoxyxanthone	2.33333*	.47437	<.001	.7656	3.9011
	Caloxanthone C	1.33333	.47437	.171	-.2344	2.9011
	Canumolactone	-1.44444	.47437	.099	-3.0122	.1233
	Stigmasterol	2.11111*	.47437	.001	.5434	3.6789
Stigmasterol	Ampicillin_0.1	-1.44444	.47437	.099	-3.0122	.1233
	Hex	-2.33333*	.47437	<.001	-3.9011	-.7656
	Chloroform	1.00000	.47437	.575	-.5678	2.5678
	Methanol	-.22222	.47437	1.000	-1.7900	1.3455
	Nodosuxanthone	1.22222	.47437	.277	-.3455	2.7900
	Trapezifolixanthone	1.22222	.47437	.277	-.3455	2.7900
	1-hydroxy-7-methoxyxanthone	.22222	.47437	1.000	-1.3455	1.7900
	Caloxanthone C	-.77778	.47437	.861	-2.3455	.7900
	Canumolactone	-3.55556*	.47437	<.001	-5.1233	-1.9878
	Friedelin	-2.11111*	.47437	.001	-3.6789	-.5434

*. The mean difference is significant at the 0.05 level.

Appendix 42:
SPSS output of statistic descriptives against *E. coli*

Descriptives

Zone_mm

	N	Mean	Std. Deviation	Std. Error	95% Confidence Interval for Mean		Minimum	Maximum
					Lower Bound	Upper Bound		
Ampicillin_0.1	9	14.2222	1.39443	.46481	13.1504	15.2941	13.00	17.00
Hex	9	10.4444	1.50923	.50308	9.2843	11.6045	8.00	13.00
Chloroform	9	8.8889	.78174	.26058	8.2880	9.4898	8.00	10.00
Methanol	9	9.4444	.52705	.17568	9.0393	9.8496	9.00	10.00
Nodosuxanthone	9	8.3333	.70711	.23570	7.7898	8.8769	7.00	9.00
Trapezifolixanthone	9	8.3333	1.00000	.33333	7.5647	9.1020	7.00	10.00
1-hydroxy-7-methoxyxanthone	9	8.6667	.70711	.23570	8.1231	9.2102	8.00	10.00
Caloxanthone C	9	10.3333	1.11803	.37268	9.4739	11.1927	9.00	12.00
Canumolactone	9	11.7778	.66667	.22222	11.2653	12.2902	11.00	13.00
Friedelin	9	9.8889	.78174	.26058	9.2880	10.4898	9.00	11.00
Stigmasterol	9	9.7778	1.30171	.43390	8.7772	10.7784	8.00	11.00
Total	99	10.0101	1.91926	.19289	9.6273	10.3929	7.00	17.00

Appendix 43:
SPSS output of homogeneity of variances test against *E. coli*

Tests of Homogeneity of Variances

		Levene Statistic	df1	df2	Sig.
Zone_mm	Based on Mean	1.938	10	88	.050
	Based on Median	1.101	10	88	.370
	Based on Median and with adjusted df	1.101	10	62.080	.376
	Based on trimmed mean	1.763	10	88	.079

Appendix 44:
SPSS output of one-way ANOVA against *E. coli*

ANOVA

Zone_mm

	Sum of Squares	df	Mean Square	F	Sig.
Between Groups	272.101	10	27.210	26.938	<.001
Within Groups	88.889	88	1.010		
Total	360.990	98			

Appendix 45:
SPSS output of Tukey HSD post hoc analysis against *E. coli*

Multiple Comparisons

Dependent Variable: Zone_mm

Tukey HSD

(I) Sample	(J) Sample	Mean Difference (I-J)	Std. Error	Sig.	95% Confidence Interval	
					Lower Bound	Upper Bound
Ampicillin_0.1	Hex	3.77778*	.47378	<.001	2.2120	5.3436
	Chloroform	5.33333*	.47378	<.001	3.7675	6.8991
	Methanol	4.77778*	.47378	<.001	3.2120	6.3436
	Nodosuxanthone	5.88889*	.47378	<.001	4.3231	7.4547
	Trapezifolixanthone	5.88889*	.47378	<.001	4.3231	7.4547
	1-hydroxy-7-methoxyxanthone	5.55556*	.47378	<.001	3.9898	7.1214
	Caloxanthone C	3.88889*	.47378	<.001	2.3231	5.4547
	Canumolactone	2.44444*	.47378	<.001	.8786	4.0102
	Friedelin	4.33333*	.47378	<.001	2.7675	5.8991
	Stigmasterol	4.44444*	.47378	<.001	2.8786	6.0102
Hex	Ampicillin_0.1	-3.77778*	.47378	<.001	-5.3436	-2.2120
	Chloroform	1.55556	.47378	.053	-.0102	3.1214
	Methanol	1.00000	.47378	.573	-.5658	2.5658
	Nodosuxanthone	2.11111*	.47378	.001	.5453	3.6769
	Trapezifolixanthone	2.11111*	.47378	.001	.5453	3.6769
	1-hydroxy-7-methoxyxanthone	1.77778*	.47378	.013	.2120	3.3436
	Caloxanthone C	.11111	.47378	1.000	-1.4547	1.6769
	Canumolactone	-1.33333	.47378	.170	-2.8991	.2325
	Friedelin	.55556	.47378	.984	-1.0102	2.1214
	Stigmasterol	.66667	.47378	.943	-.8991	2.2325
Chloroform	Ampicillin_0.1	-5.33333*	.47378	<.001	-6.8991	-3.7675
	Hex	-1.55556	.47378	.053	-3.1214	.0102
	Methanol	-.55556	.47378	.984	-2.1214	1.0102
	Nodosuxanthone	.55556	.47378	.984	-1.0102	2.1214
	Trapezifolixanthone	.55556	.47378	.984	-1.0102	2.1214
	1-hydroxy-7-methoxyxanthone	.22222	.47378	1.000	-1.3436	1.7880
	Caloxanthone C	-1.44444	.47378	.098	-3.0102	.1214
	Canumolactone	-2.88889*	.47378	<.001	-4.4547	-1.3231
	Friedelin	-1.00000	.47378	.573	-2.5658	.5658
	Stigmasterol	-.88889	.47378	.731	-2.4547	.6769
Methanol	Ampicillin_0.1	-4.77778*	.47378	<.001	-6.3436	-3.2120
	Hex	-1.00000	.47378	.573	-2.5658	.5658
	Chloroform	.55556	.47378	.984	-1.0102	2.1214
	Nodosuxanthone	1.11111	.47378	.414	-.4547	2.6769
	Trapezifolixanthone	1.11111	.47378	.414	-.4547	2.6769
	1-hydroxy-7-methoxyxanthone	.77778	.47378	.860	-.7880	2.3436
	Caloxanthone C	-.88889	.47378	.731	-2.4547	.6769
	Canumolactone	-2.33333*	.47378	<.001	-3.8991	-.7675
	Friedelin	-.44444	.47378	.997	-2.0102	1.1214
	Stigmasterol	-.33333	.47378	1.000	-1.8991	1.2325

Nodosuxanthone	Ampicillin_0.1	-5.88889*	.47378	<.001	-7.4547	-4.3231
	Hex	-2.11111*	.47378	.001	-3.6769	-.5453
	Chloroform	-.55556	.47378	.984	-2.1214	1.0102
	Methanol	-1.11111	.47378	.414	-2.6769	.4547
	Trapezifolixanthone	.00000	.47378	1.000	-1.5658	1.5658
	1-hydroxy-7-methoxyxanthone	-.33333	.47378	1.000	-1.8991	1.2325
	Caloxanthone C	-2.00000*	.47378	.003	-3.5658	-.4342
	Canumolactone	-3.44444*	.47378	<.001	-5.0102	-1.8786
	Friedelin	-1.55556	.47378	.053	-3.1214	.0102
	Stigmasterol	-1.44444	.47378	.098	-3.0102	.1214
Trapezifolixanthone	Ampicillin_0.1	-5.88889*	.47378	<.001	-7.4547	-4.3231
	Hex	-2.11111*	.47378	.001	-3.6769	-.5453
	Chloroform	-.55556	.47378	.984	-2.1214	1.0102
	Methanol	-1.11111	.47378	.414	-2.6769	.4547
	Nodosuxanthone	.00000	.47378	1.000	-1.5658	1.5658
	1-hydroxy-7-methoxyxanthone	-.33333	.47378	1.000	-1.8991	1.2325
	Caloxanthone C	-2.00000*	.47378	.003	-3.5658	-.4342
	Canumolactone	-3.44444*	.47378	<.001	-5.0102	-1.8786
	Friedelin	-1.55556	.47378	.053	-3.1214	.0102
	Stigmasterol	-1.44444	.47378	.098	-3.0102	.1214
1-hydroxy-7-methoxyxanthone	Ampicillin_0.1	-5.55556*	.47378	<.001	-7.1214	-3.9898
	Hex	-1.77778*	.47378	.013	-3.3436	-.2120
	Chloroform	-.22222	.47378	1.000	-1.7880	1.3436
	Methanol	-.77778	.47378	.860	-2.3436	.7880
	Nodosuxanthone	.33333	.47378	1.000	-1.2325	1.8991
	Trapezifolixanthone	.33333	.47378	1.000	-1.2325	1.8991
	Caloxanthone C	-1.66667*	.47378	.027	-3.2325	-.1009
	Canumolactone	-3.11111*	.47378	<.001	-4.6769	-1.5453
	Friedelin	-1.22222	.47378	.275	-2.7880	.3436
	Stigmasterol	-1.11111	.47378	.414	-2.6769	.4547
Caloxanthone C	Ampicillin_0.1	-3.88889*	.47378	<.001	-5.4547	-2.3231
	Hex	-.11111	.47378	1.000	-1.6769	1.4547
	Chloroform	1.44444	.47378	.098	-.1214	3.0102
	Methanol	.88889	.47378	.731	-.6769	2.4547
	Nodosuxanthone	2.00000*	.47378	.003	.4342	3.5658
	Trapezifolixanthone	2.00000*	.47378	.003	.4342	3.5658
	1-hydroxy-7-methoxyxanthone	1.66667*	.47378	.027	.1009	3.2325
	Canumolactone	-1.44444	.47378	.098	-3.0102	.1214
	Friedelin	.44444	.47378	.997	-1.1214	2.0102
	Stigmasterol	.55556	.47378	.984	-1.0102	2.1214

Canumolactone	Ampicillin_0.1	-2.44444*	.47378	<.001	-4.0102	-.8786
	Hex	1.33333	.47378	.170	-.2325	2.8991
	Chloroform	2.88889*	.47378	<.001	1.3231	4.4547
	Methanol	2.33333*	.47378	<.001	.7675	3.8991
	Nodosuxanthone	3.44444*	.47378	<.001	1.8786	5.0102
	Trapezifolixanthone	3.44444*	.47378	<.001	1.8786	5.0102
	1-hydroxy-7-methoxyxanthone	3.11111*	.47378	<.001	1.5453	4.6769
	Caloxanthone C	1.44444	.47378	.098	-.1214	3.0102
	Friedelin	1.88889*	.47378	.006	.3231	3.4547
	Stigmasterol	2.00000*	.47378	.003	.4342	3.5658
Friedelin	Ampicillin_0.1	-4.33333*	.47378	<.001	-5.8991	-2.7675
	Hex	-.55556	.47378	.984	-2.1214	1.0102
	Chloroform	1.00000	.47378	.573	-.5658	2.5658
	Methanol	.44444	.47378	.997	-1.1214	2.0102
	Nodosuxanthone	1.55556	.47378	.053	-.0102	3.1214
	Trapezifolixanthone	1.55556	.47378	.053	-.0102	3.1214
	1-hydroxy-7-methoxyxanthone	1.22222	.47378	.275	-.3436	2.7880
	Caloxanthone C	-.44444	.47378	.997	-2.0102	1.1214
	Canumolactone	-1.88889*	.47378	.006	-3.4547	-.3231
	Stigmasterol	.11111	.47378	1.000	-1.4547	1.6769
Stigmasterol	Ampicillin_0.1	-4.44444*	.47378	<.001	-6.0102	-2.8786
	Hex	-.66667	.47378	.943	-2.2325	.8991
	Chloroform	.88889	.47378	.731	-.6769	2.4547
	Methanol	.33333	.47378	1.000	-1.2325	1.8991
	Nodosuxanthone	1.44444	.47378	.098	-.1214	3.0102
	Trapezifolixanthone	1.44444	.47378	.098	-.1214	3.0102
	1-hydroxy-7-methoxyxanthone	1.11111	.47378	.414	-.4547	2.6769
	Caloxanthone C	-.55556	.47378	.984	-2.1214	1.0102
	Canumolactone	-2.00000*	.47378	.003	-3.5658	-.4342
	Friedelin	-.11111	.47378	1.000	-1.6769	1.4547

*. The mean difference is significant at the 0.05 level.

Appendix 46:
SPSS output of statistic descriptives against *K. pneumoniae*

Descriptives

Zone_mm

	N	Mean	Std. Deviation	Std. Error	95% Confidence Interval for Mean		Minimum	Maximum
					Lower Bound	Upper Bound		
Ampicillin_0.1	9	11.0000	.50000	.16667	10.6157	11.3843	10.00	12.00
Hex	9	11.6667	1.00000	.33333	10.8980	12.4353	10.00	13.00
Chloroform	9	8.7778	.83333	.27778	8.1372	9.4183	8.00	10.00
Methanol	9	8.5556	.88192	.29397	7.8777	9.2335	7.00	10.00
Nodosuxanthone	9	7.7778	.66667	.22222	7.2653	8.2902	7.00	9.00
Trapezifolixanthone	9	8.6667	.50000	.16667	8.2823	9.0510	8.00	9.00
1-hydroxy-7-methoxyxanthone	9	8.7778	.66667	.22222	8.2653	9.2902	8.00	10.00
Caloxanthone C	9	8.4444	.88192	.29397	7.7665	9.1223	7.00	10.00
Canumolactone	9	8.4444	.52705	.17568	8.0393	8.8496	8.00	9.00
Friedelin	9	9.6667	1.32288	.44096	8.6498	10.6835	8.00	12.00
Stigmasterol	9	12.0000	1.00000	.33333	11.2313	12.7687	10.00	13.00
Total	99	9.4343	1.59822	.16063	9.1156	9.7531	7.00	13.00

Appendix 47:
SPSS output of homogeneity of variances test against *K. pneumoniae*

Tests of Homogeneity of Variances

		Levene Statistic	df1	df2	Sig.
Zone_mm	Based on Mean	1.942	10	88	.050
	Based on Median	1.147	10	88	.337
	Based on Median and with adjusted df	1.147	10	74.891	.340
	Based on trimmed mean	1.992	10	88	.044

Appendix 48:
SPSS output of one-way ANOVA against *K. pneumoniae*

ANOVA

Zone_mm

	Sum of Squares	df	Mean Square	F	Sig.
Between Groups	188.990	10	18.899	27.116	<.001
Within Groups	61.333	88	.697		
Total	250.323	98			

Appendix 49:
SPSS output of Tukey HSD post hoc analysis against *K. pneumoniae*

Multiple Comparisons

Dependent Variable: Zone_mm

Tukey HSD

(I) Sample	(J) Sample	Mean Difference (I-J)	Std. Error	Sig.	95% Confidence Interval	
					Lower Bound	Upper Bound
Ampicillin_0.1	Hex	-.66667	.39355	.835	-1.9673	.6340
	Chloroform	2.22222*	.39355	<.001	.9216	3.5229
	Methanol	2.44444*	.39355	<.001	1.1438	3.7451
	Nodosuxanthone	3.22222*	.39355	<.001	1.9216	4.5229
	Trapezifolixanthone	2.33333*	.39355	<.001	1.0327	3.6340
	1-hydroxy-7-methoxyxanthone	2.22222*	.39355	<.001	.9216	3.5229
	Caloxanthone C	2.55556*	.39355	<.001	1.2549	3.8562
	Canumolactone	2.55556*	.39355	<.001	1.2549	3.8562
	Friedelin	1.33333*	.39355	.040	.0327	2.6340
	Stigmasterol	-1.00000	.39355	.296	-2.3007	.3007
Hex	Ampicillin_0.1	.66667	.39355	.835	-.6340	1.9673
	Chloroform	2.88889*	.39355	<.001	1.5882	4.1895
	Methanol	3.11111*	.39355	<.001	1.8105	4.4118
	Nodosuxanthone	3.88889*	.39355	<.001	2.5882	5.1895
	Trapezifolixanthone	3.00000*	.39355	<.001	1.6993	4.3007
	1-hydroxy-7-methoxyxanthone	2.88889*	.39355	<.001	1.5882	4.1895
	Caloxanthone C	3.22222*	.39355	<.001	1.9216	4.5229
	Canumolactone	3.22222*	.39355	<.001	1.9216	4.5229
	Friedelin	2.00000*	.39355	<.001	.6993	3.3007
	Stigmasterol	-.33333	.39355	.999	-1.6340	.9673
Chloroform	Ampicillin_0.1	-2.22222*	.39355	<.001	-3.5229	-.9216
	Hex	-2.88889*	.39355	<.001	-4.1895	-1.5882
	Methanol	.22222	.39355	1.000	-1.0784	1.5229
	Nodosuxanthone	1.00000	.39355	.296	-.3007	2.3007
	Trapezifolixanthone	.11111	.39355	1.000	-1.1895	1.4118
	1-hydroxy-7-methoxyxanthone	.00000	.39355	1.000	-1.3007	1.3007
	Caloxanthone C	.33333	.39355	.999	-.9673	1.6340
	Canumolactone	.33333	.39355	.999	-.9673	1.6340
	Friedelin	-.88889	.39355	.471	-2.1895	.4118
	Stigmasterol	-3.22222*	.39355	<.001	-4.5229	-1.9216
Methanol	Ampicillin_0.1	-2.44444*	.39355	<.001	-3.7451	-1.1438
	Hex	-3.11111*	.39355	<.001	-4.4118	-1.8105
	Chloroform	-.22222	.39355	1.000	-1.5229	1.0784
	Nodosuxanthone	.77778	.39355	.665	-.5229	2.0784
	Trapezifolixanthone	-.11111	.39355	1.000	-1.4118	1.1895
	1-hydroxy-7-methoxyxanthone	-.22222	.39355	1.000	-1.5229	1.0784
	Caloxanthone C	.11111	.39355	1.000	-1.1895	1.4118
	Canumolactone	.11111	.39355	1.000	-1.1895	1.4118
	Friedelin	-1.11111	.39355	.167	-2.4118	.1895
	Stigmasterol	-3.44444*	.39355	<.001	-4.7451	-2.1438

Nodosuxanthone	Ampicillin_0.1	-3.22222*	.39355	<.001	-4.5229	-1.9216
	Hex	-3.88889*	.39355	<.001	-5.1895	-2.5882
	Chloroform	-1.00000	.39355	.296	-2.3007	.3007
	Methanol	-.77778	.39355	.665	-2.0784	.5229
	Trapezifolixanthone	-.88889	.39355	.471	-2.1895	.4118
	1-hydroxy-7-methoxyxanthone	-1.00000	.39355	.296	-2.3007	.3007
	Caloxanthone C	-.66667	.39355	.835	-1.9673	.6340
	Canumolactone	-.66667	.39355	.835	-1.9673	.6340
	Friedelin	-1.88889*	.39355	<.001	-3.1895	-.5882
	Stigmasterol	-4.22222*	.39355	<.001	-5.5229	-2.9216
Trapezifolixanthone	Ampicillin_0.1	-2.33333*	.39355	<.001	-3.6340	-1.0327
	Hex	-3.00000*	.39355	<.001	-4.3007	-1.6993
	Chloroform	-.11111	.39355	1.000	-1.4118	1.1895
	Methanol	.11111	.39355	1.000	-1.1895	1.4118
	Nodosuxanthone	.88889	.39355	.471	-.4118	2.1895
	1-hydroxy-7-methoxyxanthone	-.11111	.39355	1.000	-1.4118	1.1895
	Caloxanthone C	.22222	.39355	1.000	-1.0784	1.5229
	Canumolactone	.22222	.39355	1.000	-1.0784	1.5229
	Friedelin	-1.00000	.39355	.296	-2.3007	.3007
	Stigmasterol	-3.33333*	.39355	<.001	-4.6340	-2.0327
1-hydroxy-7-methoxyxanthone	Ampicillin_0.1	-2.22222*	.39355	<.001	-3.5229	-.9216
	Hex	-2.88889*	.39355	<.001	-4.1895	-1.5882
	Chloroform	.00000	.39355	1.000	-1.3007	1.3007
	Methanol	.22222	.39355	1.000	-1.0784	1.5229
	Nodosuxanthone	1.00000	.39355	.296	-.3007	2.3007
	Trapezifolixanthone	.11111	.39355	1.000	-1.1895	1.4118
	Caloxanthone C	.33333	.39355	.999	-.9673	1.6340
	Canumolactone	.33333	.39355	.999	-.9673	1.6340
	Friedelin	-.88889	.39355	.471	-2.1895	.4118
	Stigmasterol	-3.22222*	.39355	<.001	-4.5229	-1.9216
Caloxanthone C	Ampicillin_0.1	-2.55556*	.39355	<.001	-3.8562	-1.2549
	Hex	-3.22222*	.39355	<.001	-4.5229	-1.9216
	Chloroform	-.33333	.39355	.999	-1.6340	.9673
	Methanol	-.11111	.39355	1.000	-1.4118	1.1895
	Nodosuxanthone	.66667	.39355	.835	-.6340	1.9673
	Trapezifolixanthone	-.22222	.39355	1.000	-1.5229	1.0784
	1-hydroxy-7-methoxyxanthone	-.33333	.39355	.999	-1.6340	.9673
	Canumolactone	.00000	.39355	1.000	-1.3007	1.3007
	Friedelin	-1.22222	.39355	.085	-2.5229	.0784
	Stigmasterol	-3.55556*	.39355	<.001	-4.8562	-2.2549

Canumolactone	Ampicillin_0.1	-2.55556*	.39355	<.001	-3.8562	-1.2549
	Hex	-3.22222*	.39355	<.001	-4.5229	-1.9216
	Chloroform	-.33333	.39355	.999	-1.6340	.9673
	Methanol	-.11111	.39355	1.000	-1.4118	1.1895
	Nodosuxanthone	.66667	.39355	.835	-.6340	1.9673
	Trapezifolixanthone	-.22222	.39355	1.000	-1.5229	1.0784
	1-hydroxy-7-methoxyxanthone	-.33333	.39355	.999	-1.6340	.9673
	Caloxanthone C	.00000	.39355	1.000	-1.3007	1.3007
	Friedelin	-1.22222	.39355	.085	-2.5229	.0784
	Stigmasterol	-3.55556*	.39355	<.001	-4.8562	-2.2549
Friedelin	Ampicillin_0.1	-1.33333*	.39355	.040	-2.6340	-.0327
	Hex	-2.00000*	.39355	<.001	-3.3007	-.6993
	Chloroform	.88889	.39355	.471	-.4118	2.1895
	Methanol	1.11111	.39355	.167	-.1895	2.4118
	Nodosuxanthone	1.88889*	.39355	<.001	.5882	3.1895
	Trapezifolixanthone	1.00000	.39355	.296	-.3007	2.3007
	1-hydroxy-7-methoxyxanthone	.88889	.39355	.471	-.4118	2.1895
	Caloxanthone C	1.22222	.39355	.085	-.0784	2.5229
	Canumolactone	1.22222	.39355	.085	-.0784	2.5229
	Stigmasterol	-2.33333*	.39355	<.001	-3.6340	-1.0327
Stigmasterol	Ampicillin_0.1	1.00000	.39355	.296	-.3007	2.3007
	Hex	.33333	.39355	.999	-.9673	1.6340
	Chloroform	3.22222*	.39355	<.001	1.9216	4.5229
	Methanol	3.44444*	.39355	<.001	2.1438	4.7451
	Nodosuxanthone	4.22222*	.39355	<.001	2.9216	5.5229
	Trapezifolixanthone	3.33333*	.39355	<.001	2.0327	4.6340
	1-hydroxy-7-methoxyxanthone	3.22222*	.39355	<.001	1.9216	4.5229
	Caloxanthone C	3.55556*	.39355	<.001	2.2549	4.8562
	Canumolactone	3.55556*	.39355	<.001	2.2549	4.8562
	Friedelin	2.33333*	.39355	<.001	1.0327	3.6340

*. The mean difference is significant at the 0.05 level.

Appendix 50:
SPSS output of statistic descriptives against *P. aeruginosa*

Descriptives

Zone_mm

	N	Mean	Std. Deviation	Std. Error	95% Confidence Interval for Mean		Minimum	Maximum
					Lower Bound	Upper Bound		
Ampicillin_0.1	9	8.6667	.86603	.28868	8.0010	9.3324	8.00	10.00
Hex	9	8.2222	1.09291	.36430	7.3821	9.0623	7.00	10.00
Chloroform	9	8.0000	.70711	.23570	7.4565	8.5435	7.00	9.00
Methanol	9	7.6667	.70711	.23570	7.1231	8.2102	7.00	9.00
Nodosuxanthone	9	9.3333	.86603	.28868	8.6676	9.9990	8.00	11.00
Trapezifolixanthone	9	10.1111	.60093	.20031	9.6492	10.5730	9.00	11.00
1-hydroxy-7-methoxyxanthone	9	8.3333	.50000	.16667	7.9490	8.7177	8.00	9.00
Caloxanthone C	9	12.4444	.88192	.29397	11.7665	13.1223	11.00	14.00
Canumolactone	9	11.7778	1.20185	.40062	10.8540	12.7016	10.00	14.00
Friedelin	9	8.6667	.50000	.16667	8.2823	9.0510	8.00	9.00
Stigmasterol	9	12.4444	.52705	.17568	12.0393	12.8496	12.00	13.00
Total	99	9.6061	1.89423	.19038	9.2283	9.9839	7.00	14.00

Appendix 51:
SPSS output of homogeneity of variances test against *P. aeruginosa*

Tests of Homogeneity of Variances

		Levene Statistic	df1	df2	Sig.
Zone_mm	Based on Mean	1.796	10	88	.073
	Based on Median	.959	10	88	.485
	Based on Median and with adjusted df	.959	10	74.593	.486
	Based on trimmed mean	1.769	10	88	.078

Appendix 52:
SPSS output of one-way ANOVA against *P. aeruginosa*

ANOVA

Zone_mm

	Sum of Squares	df	Mean Square	F	Sig.
Between Groups	295.192	10	29.519	46.022	<.001
Within Groups	56.444	88	.641		
Total	351.636	98			

Appendix 53:
SPSS output of Tukey HSD post hoc analysis against *P. aeruginosa*

Multiple Comparisons

Dependent Variable: Zone_mm

Tukey HSD

(I) Sample	(J) Sample	Mean Difference (I-J)	Std. Error	Sig.	95% Confidence Interval	
					Lower Bound	Upper Bound
Ampicillin_0.1	Hex	.44444	.37754	.983	-.8033	1.6922
	Chloroform	.66667	.37754	.796	-.5811	1.9144
	Methanol	1.00000	.37754	.241	-.2477	2.2477
	Nodosuxanthone	-.66667	.37754	.796	-1.9144	.5811
	Trapezifolixanthone	-1.44444*	.37754	.010	-2.6922	-.1967
	1-hydroxy-7-methoxyxanthone	.33333	.37754	.998	-.9144	1.5811
	Caloxanthone C	-3.77778*	.37754	<.001	-5.0255	-2.5300
	Canumolactone	-3.11111*	.37754	<.001	-4.3589	-1.8634
	Friedelin	.00000	.37754	1.000	-1.2477	1.2477
	Stigmasterol	-3.77778*	.37754	<.001	-5.0255	-2.5300
Hex	Ampicillin_0.1	-.44444	.37754	.983	-1.6922	.8033
	Chloroform	.22222	.37754	1.000	-1.0255	1.4700
	Methanol	.55556	.37754	.925	-.6922	1.8033
	Nodosuxanthone	-1.11111	.37754	.127	-2.3589	.1366
	Trapezifolixanthone	-1.88889*	.37754	<.001	-3.1366	-.6411
	1-hydroxy-7-methoxyxanthone	-.11111	.37754	1.000	-1.3589	1.1366
	Caloxanthone C	-4.22222*	.37754	<.001	-5.4700	-2.9745
	Canumolactone	-3.55556*	.37754	<.001	-4.8033	-2.3078
	Friedelin	-.44444	.37754	.983	-1.6922	.8033
	Stigmasterol	-4.22222*	.37754	<.001	-5.4700	-2.9745
Chloroform	Ampicillin_0.1	-.66667	.37754	.796	-1.9144	.5811
	Hex	-.22222	.37754	1.000	-1.4700	1.0255
	Methanol	.33333	.37754	.998	-.9144	1.5811
	Nodosuxanthone	-1.33333*	.37754	.026	-2.5811	-.0856
	Trapezifolixanthone	-2.11111*	.37754	<.001	-3.3589	-.8634
	1-hydroxy-7-methoxyxanthone	-.33333	.37754	.998	-1.5811	.9144
	Caloxanthone C	-4.44444*	.37754	<.001	-5.6922	-3.1967
	Canumolactone	-3.77778*	.37754	<.001	-5.0255	-2.5300
	Friedelin	-.66667	.37754	.796	-1.9144	.5811
	Stigmasterol	-4.44444*	.37754	<.001	-5.6922	-3.1967
Methanol	Ampicillin_0.1	-1.00000	.37754	.241	-2.2477	.2477
	Hex	-.55556	.37754	.925	-1.8033	.6922
	Chloroform	-.33333	.37754	.998	-1.5811	.9144
	Nodosuxanthone	-1.66667*	.37754	.001	-2.9144	-.4189
	Trapezifolixanthone	-2.44444*	.37754	<.001	-3.6922	-1.1967
	1-hydroxy-7-methoxyxanthone	-.66667	.37754	.796	-1.9144	.5811
	Caloxanthone C	-4.77778*	.37754	<.001	-6.0255	-3.5300
	Canumolactone	-4.11111*	.37754	<.001	-5.3589	-2.8634
	Friedelin	-1.00000	.37754	.241	-2.2477	.2477
	Stigmasterol	-4.77778*	.37754	<.001	-6.0255	-3.5300

Nodosuxanthone	Ampicillin_0.1	.66667	.37754	.796	-.5811	1.9144
	Hex	1.11111	.37754	.127	-.1366	2.3589
	Chloroform	1.33333*	.37754	.026	.0856	2.5811
	Methanol	1.66667*	.37754	.001	.4189	2.9144
	Trapezifolixanthone	-.77778	.37754	.608	-2.0255	.4700
	1-hydroxy-7-methoxyxanthone	1.00000	.37754	.241	-.2477	2.2477
	Caloxanthone C	-3.11111*	.37754	<.001	-4.3589	-1.8634
	Canumolactone	-2.44444*	.37754	<.001	-3.6922	-1.1967
	Friedelin	.66667	.37754	.796	-.5811	1.9144
	Stigmasterol	-3.11111*	.37754	<.001	-4.3589	-1.8634
Trapezifolixanthone	Ampicillin_0.1	1.44444*	.37754	.010	.1967	2.6922
	Hex	1.88889*	.37754	<.001	.6411	3.1366
	Chloroform	2.11111*	.37754	<.001	.8634	3.3589
	Methanol	2.44444*	.37754	<.001	1.1967	3.6922
	Nodosuxanthone	.77778	.37754	.608	-.4700	2.0255
	1-hydroxy-7-methoxyxanthone	1.77778*	.37754	<.001	.5300	3.0255
	Caloxanthone C	-2.33333*	.37754	<.001	-3.5811	-1.0856
	Canumolactone	-1.66667*	.37754	.001	-2.9144	-.4189
	Friedelin	1.44444*	.37754	.010	.1967	2.6922
	Stigmasterol	-2.33333*	.37754	<.001	-3.5811	-1.0856
1-hydroxy-7-methoxyxanthone	Ampicillin_0.1	-.33333	.37754	.998	-1.5811	.9144
	Hex	.11111	.37754	1.000	-1.1366	1.3589
	Chloroform	.33333	.37754	.998	-.9144	1.5811
	Methanol	.66667	.37754	.796	-.5811	1.9144
	Nodosuxanthone	-1.00000	.37754	.241	-2.2477	.2477
	Trapezifolixanthone	-1.77778*	.37754	<.001	-3.0255	-.5300
	Caloxanthone C	-4.11111*	.37754	<.001	-5.3589	-2.8634
	Canumolactone	-3.44444*	.37754	<.001	-4.6922	-2.1967
	Friedelin	-.33333	.37754	.998	-1.5811	.9144
	Stigmasterol	-4.11111*	.37754	<.001	-5.3589	-2.8634
Caloxanthone C	Ampicillin_0.1	3.77778*	.37754	<.001	2.5300	5.0255
	Hex	4.22222*	.37754	<.001	2.9745	5.4700
	Chloroform	4.44444*	.37754	<.001	3.1967	5.6922
	Methanol	4.77778*	.37754	<.001	3.5300	6.0255
	Nodosuxanthone	3.11111*	.37754	<.001	1.8634	4.3589
	Trapezifolixanthone	2.33333*	.37754	<.001	1.0856	3.5811
	1-hydroxy-7-methoxyxanthone	4.11111*	.37754	<.001	2.8634	5.3589
	Canumolactone	.66667	.37754	.796	-.5811	1.9144
	Friedelin	3.77778*	.37754	<.001	2.5300	5.0255
	Stigmasterol	.00000	.37754	1.000	-1.2477	1.2477

Canumolactone	Ampicillin_0.1	3.11111*	.37754	<.001	1.8634	4.3589
	Hex	3.55556*	.37754	<.001	2.3078	4.8033
	Chloroform	3.77778*	.37754	<.001	2.5300	5.0255
	Methanol	4.11111*	.37754	<.001	2.8634	5.3589
	Nodosuxanthone	2.44444*	.37754	<.001	1.1967	3.6922
	Trapezifolixanthone	1.66667*	.37754	.001	.4189	2.9144
	1-hydroxy-7-methoxyxanthone	3.44444*	.37754	<.001	2.1967	4.6922
	Caloxanthone C	-.66667	.37754	.796	-1.9144	.5811
	Friedelin	3.11111*	.37754	<.001	1.8634	4.3589
	Stigmasterol	-.66667	.37754	.796	-1.9144	.5811
Friedelin	Ampicillin_0.1	.00000	.37754	1.000	-1.2477	1.2477
	Hex	.44444	.37754	.983	-.8033	1.6922
	Chloroform	.66667	.37754	.796	-.5811	1.9144
	Methanol	1.00000	.37754	.241	-.2477	2.2477
	Nodosuxanthone	-.66667	.37754	.796	-1.9144	.5811
	Trapezifolixanthone	-1.44444*	.37754	.010	-2.6922	-.1967
	1-hydroxy-7-methoxyxanthone	.33333	.37754	.998	-.9144	1.5811
	Caloxanthone C	-3.77778*	.37754	<.001	-5.0255	-2.5300
	Canumolactone	-3.11111*	.37754	<.001	-4.3589	-1.8634
	Stigmasterol	-3.77778*	.37754	<.001	-5.0255	-2.5300
Stigmasterol	Ampicillin_0.1	3.77778*	.37754	<.001	2.5300	5.0255
	Hex	4.22222*	.37754	<.001	2.9745	5.4700
	Chloroform	4.44444*	.37754	<.001	3.1967	5.6922
	Methanol	4.77778*	.37754	<.001	3.5300	6.0255
	Nodosuxanthone	3.11111*	.37754	<.001	1.8634	4.3589
	Trapezifolixanthone	2.33333*	.37754	<.001	1.0856	3.5811
	1-hydroxy-7-methoxyxanthone	4.11111*	.37754	<.001	2.8634	5.3589
	Caloxanthone C	.00000	.37754	1.000	-1.2477	1.2477
	Canumolactone	.66667	.37754	.796	-.5811	1.9144
	Friedelin	3.77778*	.37754	<.001	2.5300	5.0255

*. The mean difference is significant at the 0.05 level.